

**LANDSLIDE PREDICTION MODEL USING REMOTE
SENSING, GIS AND FIELD GEOLOGY : A CASE STUDY
OF WANG CHIN DISTRICT, PHRAE PROVINCE,
NORTHERN THAILAND**



**A Thesis submitted in Partial Fulfillment of the requirements for the
Degree of Doctor of Philosophy in Geotechnology
Suranaree University of Technology**

Academic Year 2006

ISBN 974-533-584-3

**แบบจำลองการทำนายดินถล่มโดยใช้ เทคนิคการรับรู้ระยะไกล
ระบบสารสนเทศภูมิศาสตร์ และการสำรวจธรณีวิทยาภาคสนาม:
กรณีศึกษาพื้นที่อำเภอวังชิ้น จังหวัดแพร่ ภาคเหนือ ประเทศไทย**



นางสุรีย์ ชีระรังสิกุล

วิทยานิพนธ์นี้เป็นส่วนหนึ่งของการศึกษาตามหลักสูตรปริญญาวิศวกรรมศาสตรดุษฎีบัณฑิต

สาขาวิชาเทคโนโลยีธรณี

มหาวิทยาลัยเทคโนโลยีสุรนารี

ปีการศึกษา 2549

ISBN 974-533-584-3

**LANDSLIDE PREDICTION MODEL USING REMOTE SENSING,
GIS AND FIELD GEOLOGY: A CASE STUDY OF WANG CHIN
DISTRICT, PHRAE PROVINCE, NORTHERN THAILAND**

Suranaree University of Technology has approved this thesis submitted in partial fulfillment of the requirements for the Degree of Doctor of Philosophy.

Thesis Examining Committee



(Asst. Prof. Thara Lekuthai)

Chairperson



(Dr. Chongpan Chonglakmani)

Member (Thesis Advisor)



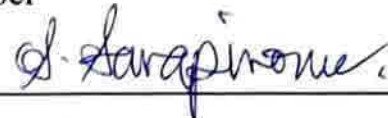
(Dr. Friedrich Kuehn)

Member



(Dr. Tawisak Silakul)

Member



(Dr. Sunya Sarapirome)

Member



(Assoc. Prof. Dr. Saowanee Rattanaphani)

Vice Rector for Academic Affairs



(Assoc. Prof. Dr. Vorapot Khompis)

Dean of Institute of Engineering

สุริย์ ชีระรังสิกุล : แบบจำลองการทำนายดินถล่มโดยใช้เทคนิคการรับรู้ระยะไกล ระบบสารสนเทศภูมิศาสตร์ และการสำรวจธรณีวิทยาภาคสนาม : กรณีศึกษาพื้นที่อำเภอวังชิ้น จังหวัดแพร่ ภาคเหนือ ประเทศไทย (LANDSLIDE PREDICTION MODEL USING REMOTE SENSING, GIS AND FIELD GEOLOGY : A CASE STUDY OF WANG CHIN DISTRICT, PHRAE PROVINCE, NORTHERN THAILAND) อาจารย์ที่ปรึกษา : ดร.จงพันธ์ จงลักษณ์ณี, 220 หน้า. ISBN 974-533-584-3

การประเมินประเมินพิบัติภัยดินถล่มหมายความรวมถึงการทำนายและกำหนดความเป็นไปได้ของการเกิดดินถล่ม การศึกษาในครั้งนี้ได้ทำการประเมินศักยภาพและแบบจำลองทำนายพิบัติภัยดินถล่ม มาตราส่วนระดับภูมิภาค (1 :50,000 ถึง 1 :100,000) โดยใช้การรับรู้ระยะไกล ระบบสารสนเทศภูมิศาสตร์ และการสำรวจธรณีวิทยาภาคสนาม กรณีศึกษาพื้นที่ อำเภอวังชิ้น จังหวัดแพร่ ภาคเหนือ ประเทศไทย บทบาทหลักของการใช้ข้อมูลการรับรู้ระยะไกล คือ ทำแผนที่การแผ่กระจายตัวของตำแหน่งดินถล่มที่เกิดขึ้นแล้ว และทำแผนที่ปัจจัยที่มีผลต่อการเกิดดินถล่ม ขณะที่ระบบสารสนเทศภูมิศาสตร์นำมาใช้ในการสร้างและจัดการฐานข้อมูล แสดงข้อมูล วิเคราะห์ข้อมูล เพื่อให้ได้มาซึ่งแผนที่พิบัติภัยดินถล่ม

วิธีการศึกษาที่ใช้ในการประเมินพิบัติภัยดินถล่ม คือ การวิเคราะห์ความน่าจะเป็นแบบคู่ และการให้ค่าน้ำหนัก (Bivariate probability and weighting analysis) ซึ่งการวิเคราะห์จะอยู่บนพื้นฐานของการหาความสัมพันธ์ระหว่างปัจจัยที่มีผลต่อการเกิดดินถล่ม และเหตุการณ์ดินถล่มที่เกิดขึ้นมาแล้วในอดีต โดยใช้เทคนิคทางระบบสารสนเทศภูมิศาสตร์ ความเป็นไปได้ของการเกิดดินถล่มซึ่งบ่งชี้ถึงพื้นที่พิบัติภัยได้มาจากการวิเคราะห์ด้วยวิธีความน่าจะเป็นแบบคู่และการจำแนกพื้นที่แสดงศักยภาพดินถล่มนั้นควรมีการให้ค่าน้ำหนักของความสัมพันธ์ของปัจจัยที่จะก่อให้เกิดดินถล่ม ซึ่งวิธีการที่จะให้ค่าน้ำหนักนั้นประกอบด้วย วิธีความน่าจะเป็นแบบเชื่อถือได้ (Reliability probability) วิธีความน่าจะเป็นแบบความรับผิดชอบ (Accountability probability) และวิธีประสมประสานระหว่างความน่าจะเป็นแบบเชื่อถือได้และความน่าจะเป็นแบบความรับผิดชอบ สำหรับ วิธีความน่าจะเป็นแบบเชื่อถือได้มีวิธีการคำนวณ โดยใช้ร้อยละของพื้นที่ในแต่ละปัจจัยที่มีค่าความเป็นไปได้ของการเกิดดินถล่มสูงกว่า 1 เทียบกับผลบวกของค่าความเป็นไปได้ของการเกิดดินถล่มสูงกว่า 1 วิธีความน่าจะเป็นแบบความรับผิดชอบ มีวิธีการคำนวณ โดยใช้ร้อยละของพื้นที่ในแต่ละปัจจัยที่มีค่าความเป็นไปได้ของการเกิดดินถล่มสูงกว่า 1 เทียบกับผลบวกของจำนวนจุดของการเกิดดินถล่มที่อยู่ในพื้นที่ที่ค่าความเป็นไปได้ของการเกิดดินถล่มสูงกว่า 1 สุดท้ายแล้วแผนที่พิบัติภัยดินถล่มได้

จากแบบจำลองที่แตกต่างกัน คือ แผนที่พิบัติภัยดินถล่มจากการให้ค่าน้ำหนักแบบเชื่อได้ แผนที่พิบัติภัยดินถล่มจากการให้ค่าน้ำหนักแบบความรับผิดชอบ และ แผนที่พิบัติภัยดินถล่มจากการประสมประสานของให้ค่าน้ำหนักแบบเชื่อได้และความรับผิดชอบ และได้แบ่งระดับของพิบัติภัยดินถล่มออกเป็นระดับต่ำมาก ระดับต่ำ ระดับปานกลาง ระดับสูง และระดับสูงมาก ซึ่งสามารถบ่งบอกถึงการเป็นพื้นที่พิบัติภัยดินถล่มในอนาคตด้วย

นอกจากนี้ข้อมูลที่ได้จากวิธีดังกล่าวข้างต้นยังถูกนำไปสร้างแบบจำลองทำนายดินถล่มโดยใช้ Band Math Function Tool ของโปรแกรม ENVI ซึ่งเป็นการประเมินพิบัติภัยดินถล่มแบบอัตโนมัติ เพื่อแสดงพื้นที่ที่มีโอกาสเกิดดินถล่มในอนาคตในพื้นที่ที่มีปัจจัยหรือเงื่อนไขคล้ายคลึงกับพื้นที่วังซัน ในการศึกษาครั้งนี้เมื่อวิเคราะห์ด้วยวิธีการวิเคราะห์ความมั่นคงของความลาดชัน ในรูปแบบของระบบผู้เชี่ยวชาญของระบบสารสนเทศภูมิศาสตร์ (Guenther, 2003) ซึ่งข้อมูลที่นำมาใช้ในการวิเคราะห์ ได้แก่ ข้อมูลความสูงเชิงตัวเลขและคุณสมบัติทางวิศวกรรมของหิน ผลที่ได้คือแผนที่ความมั่นคงของความลาดชันพื้นที่วังซัน และนำมาเปรียบเทียบกับแผนที่พิบัติภัยดินถล่มจากการวิเคราะห์ความน่าจะเป็น และการให้ค่าน้ำหนักให้ค่าน้ำหนัก

แผนที่พิบัติภัยดินถล่มทั้งหมดที่ได้ เมื่อนำมาตรวจสอบความถูกต้องด้วยวิธีการวิเคราะห์ความน่าจะเป็นระหว่าง แผนที่พิบัติภัยดินถล่มและแผนที่การกระจายตัวของตำแหน่งดินถล่มแล้วพบว่า แผนที่พิบัติภัยดินถล่มจากการประสมประสานของให้ค่าน้ำหนักแบบเชื่อได้และความรับผิดชอบ มีความเชื่อได้สูงสุด รวมถึงการเปรียบเทียบกับผลที่ได้จากการวิเคราะห์ความมั่นคงของความลาดชันแล้วพบว่าไปในทิศทางเดียวกัน จึงสามารถสรุปได้ว่า วิธีการวิเคราะห์เพื่อทำแผนที่พิบัติภัยดินถล่มจากการศึกษาในครั้งนี้ สามารถนำไปใช้ประโยชน์ในการทำนายถึงพื้นที่พื้นที่พิบัติภัยดินถล่มป้องกันและบรรเทาการเสี่ยงภัย และเพื่อการวางแผนการใช้พื้นที่ในอนาคต

สาขาวิชาเทคโนโลยีธรณี

ปีการศึกษา 2549

ลายมือชื่อนักศึกษา _____

ลายมือชื่ออาจารย์ที่ปรึกษา _____

ลายมือชื่ออาจารย์ที่ปรึกษาร่วม _____

SUREE TEERARUNGSIGUL : LANDSLIDE PREDICTION MODEL
USING REMOTE SENSING, GIS AND FIELD GEOLOGY : A CASE
STUDY OF WANG CHIN DISTRICT, PHRAE PROVINCE, NORTHERN
THAILAND. THESIS ADVISOR : CHONGPAN CHONGLAKMANI, Ph.D.
220 PP. ISBN xxx-xxx-xxx-x

LANDSLIDE PREDICTION MODEL/LANDSLIDE HAZARD ASSESSMENT/
LANDSLIDE HAZARD/REMOTE SENSING/GIS/FIELD GEOLOGY/
PROBABILITY

Landslide hazard assessment usually involves in predicting and expressing the probability of landslide occurrences. This study, landslide hazard potential and prediction model were assessed at regional scale (1:50,000 to 1: 100,000) using remote sensing, geographic information systems (GIS) and field geology. The case study area is at Wang Chin District, Phrae Province, Northern Thailand. The role of remote sensing is mainly to map the distribution of existing landslides location and to map some factors those are affected on landslide occurrences. While, the GIS is used for database construction and management, data displays, data analysis and produce landslide hazard map.

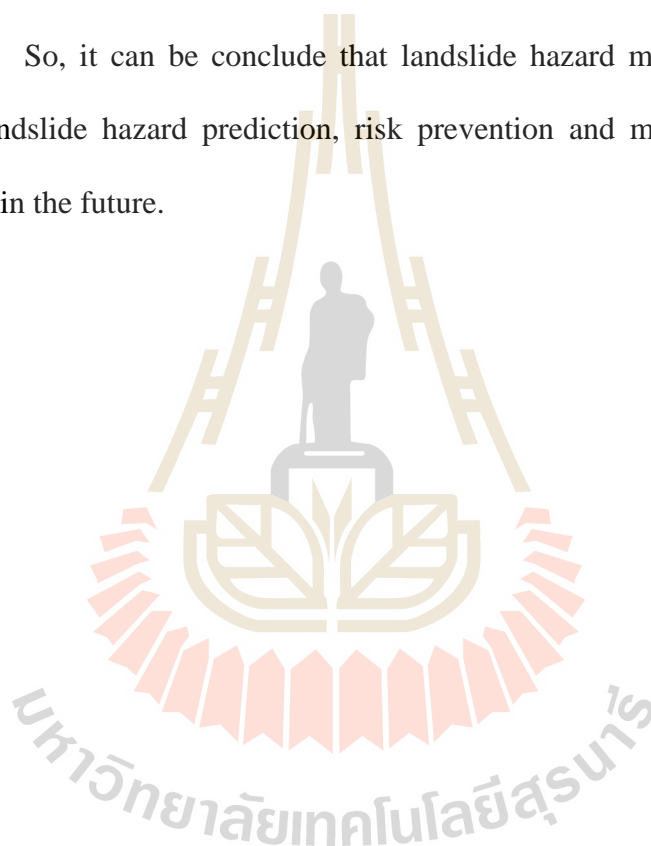
In this study, the methodology for landslide hazard assessment is bivariate probability and weighting analysis using GIS technique. It is based on the observed relationship between each instability factor and the past landslide distribution. The bivariate probability analysis was applied to the task of assessing the probability of landslide occurrence which is indicated the hazard areas. In addition, the relative

weighting of importance of factors to landslide occurrence is required for the identification of landslide potential areas. Weighting methods are based on reliability probability (RP), accountability probability (AP), and combination of reliability and accountability probability method. The RP was calculated by the percentage area of factors corresponding to landslides. The AP was calculated by the total landslide population accounted for each factor. In both performance measures, only probability values of attributes ≥ 1 (i.e. mean and above mean landslide incidence) are considered. The results of RP and AP of each factor were used to ranking and weighting the relative importance of each factor on landslide occurrences. Finally, landslide hazard maps were produced in different three models. These are 1) landslide hazard map based on reliability weighted; 2) landslide hazard map based on accountability weighted; 3) landslide hazard map based on combination of reliability and accountability weighted. The degree of landslide hazard is expressed in relative term from very low to very high hazard level, and represents the expectation of future landslide occurrence based on the conditions of that particular area.

Beside these, data obtained from the probability analysis and combination weighted of reliability and accountability in the study area was used to produce the landslide prediction model using Band Math Tool in ENVI software, which can be used as an automatic assessment for future landslide prone ground of another area that has similar condition factors with the Wang Chin area. In this study, the expert system of the Rock Slope Stability GIS (Guenther, 2003) was used to produce the landslide hazard map for Wang Chin area. DEM and engineering properties of rock were used as a database for the analysis. The result of this analysis referred the slope stabilities of the Wang Chin area, and it was compared to the landslide susceptibility

map using probability and weighting analysis.

Landslide hazard maps (all of three models) are verified using existing landslide data and landslide hazard maps using probability method. The validation result shows satisfactory agreement between the landslide hazard map based on combination weighted of reliability and accountability. Also the comparison between landslide hazard maps based and slope stability map of Wang Chin area are conformably. So, it can be conclude that landslide hazard map from this study is useful for landslide hazard prediction, risk prevention and mitigation, and project development in the future.



School of Geotechnology

Academic Year 2006

Student's Signature_____

Advisor's Signature_____

Co-advisor's Signature_____

ACKNOWLEDGEMENTS

Grateful acknowledgements and deep appreciation are expressed to Dr. Chongpan Chonglukmani, thesis advisor and Dr. Friedrich Kuehn, thesis co-advisor for their guidance, encouragement, valuable discussion, and reading of the manuscript.

I would also like to thank Dr. Assanee Meesook for his help in reading and correction grammatically of the manuscript. Many thanks are extended to Dr. Andreas Guenther from BGR for his support in slope stability analysis for this study.

Thanks are extended to Mrs. Piyathida Thonnarat and Miss. Namphon Khampilang for the preparation of maps and assistance during the field investigation.

Thanks are also extended to Mrs. Benjavan Jarukalat, Director, and Mr. Verapong Tansuwan, Chief of Geological Section 5, Bureau of Geological Survey, Department of Mineral Resources for providing permission and facilities during the course of study.

Grateful appreciation is due to the Remote Sensing Section, Federal Institute for Geosciences and Natural Resources (BGR) and their staffs for providing permission and facilities during the course of study in Hannover, Germany.

I would like to thank both of my parents and my son for their patience during the long time of my study. Finally, the author is indebted to my husband, Mr. Naramase Teerarungsigul, who has continuously given so much helpful guidance in all aspects and tolerance during the writing of this thesis.

Suree Teerarungsigul

TABLE OF CONTENTS

	PAGE
ABSTRACT (THAI).....	I
ABSTRACT (ENGLISH).....	III
ACKNOWLEDGEMENTS.....	VI
TABLE OF CONTENTS.....	VII
LIST OF TABLES.....	XIII
LIST OF FIGURES.....	XVI
CHAPTER	
I INTRODUCTION.....	1
1.1 Introduction to this Study.....	1
1.2 Characterization of the Problem.....	2
1.3 Objective of Research.....	6
1.4 Scope and Limitation of Research.....	6
1.5 Expected Results.....	7
1.6 Characterization of the Study Area.....	7
1.6.1 Location.....	7
1.6.2 Topography.....	9
1.6.3 Climate.....	11
1.7 Geological Setting.....	11

TABLE OF CONTENTS (Continued)

	PAGE
1.7.1 Paleozoic rocks (Donchai Group; CP, Pm1, Pm2, and Pm3).....	14
1.7.2 Permo-Triassic rocks (PTr).....	15
1.7.3 Triassic rocks (Wang Chin Formation, Tr3, Tr3-1, Tr3-2, and TR3-3; Lampang Group).....	15
1.7.4 Quaternary.....	16
1.7.5 Geological Structures.....	16
II LITERATURE REVIEW	18
2.1 The Classification of Landslide.....	18
2.1.1 Material Types Involved in Landslide.....	18
2.1.2 Type of Landslides.....	20
2.2 Landslide Causes.....	26
2.2.1 Landslides and Water.....	26
2.2.2 Landslides and Seismic Activity.....	27
2.2.3 Landslides and Volcanic Activity.....	27
2.3 Landslide Hazards.....	28
2.4 Technical Aspects of Remote Sensing.....	30
2.5 Technical Aspects of Geographic Information System.....	34
2.5.1 Data Input.....	34
2.5.2 Data Structures.....	34

TABLE OF CONTENTS (Continued)

	PAGE
2.5.3 Data Manipulation and Analysis.....	38
2.5.4 Data Output.....	38
2.6 Integration Remote Sensing and GIS for Geo-Spatial Analysis.....	38
2.7 Methods of Approaches to Landslide Hazard Assessment.....	39
2.7.1 Qualitative Methodologies.....	42
2.7.2 Quantitative Methodologies.....	46
2.8 Landslide Assessments.....	49
2.8.1 Factors Related to Landslide.....	50
2.8.2 Application of GIS and Remote Sensing on Landslide Assessment.....	51
2.8.3 Landslide Assessment based on Slope Stability Method of Guenther.....	55
III METHODOLOGY.....	59
3.1 Data Acquired and Used.....	61
3.1.1 Remote Sensing Data.....	61
3.1.2 Non-Remote Sensing Data.....	61
3.2 Method of Remote Sensing Data Processing and Interpretation.....	64

TABLE OF CONTENTS (Continued)

	PAGE
3.2.1 Image Processing.....	64
3.2.2 Data Interpretation.....	78
3.2.3 Digital Elevation Model Extraction.....	81
3.3 Fieldwork.....	88
3.4 GIS Grids Preparation.....	88
3.4.1 GIS Technique.....	88
3.4.2 Database construction.....	91
3.5 Spatial Data Analysis and Data Integration.....	97
3.5.1 Overlay the Landslide Inventory Map on Each Factor Map.....	97
3.5.2 Landslide Assessment Analysis.....	99
3.5.3 Producing Landslide Hazard Map.....	105
3.6 Band Math Approach for Landslide Prediction Model.....	106
3.6.1 Introduction.....	106
3.6.2 Basic Concept of the Band Math.....	108
3.6.3 Landslide Prediction Model Construction.....	111
3.7 Comparison with Slope Stability Model.....	115
3.8 Verification of the Result and Reporting.....	116
IV RESULTS.....	118
4.1 Landslides Information Construction (LSIC).....	119

TABLE OF CONTENTS (Continued)

	PAGE
4.1.1 Landslides in Wang Chin Area.....	119
4.1.2 Factors Map Related to Landslide and Database Construction.....	128
4.2 Landslide Assessment Analysis.....	153
4.2.1 Relationship between Landslide Occurrence and the Factors.....	153
4.2.2 Probability Analysis.....	156
4.2.3 Weighting for the Importance of Factors on Landsliding.....	158
4.3 Landslide Hazard Zonation Map.....	166
4.4 Landslide Prediction Model based on Band Math Tool in ENVI.....	179
4.5 Verification of the Result.....	183
V DISCUSION AND CONCLUSION.....	186
5.1 Discussions.....	186
5.2 Conclusions.....	189
REFERENCES.....	191
APPENDICES	
APPENDIX A. RELATIONSHIP BETWEEN LANDSLIDE OCCURRENCES AND FACTORS.....	205

APPENDIX B. PROBABILITY RATIO OF LANDSLIDE OCCURRENCE WITHIN FACTORS.....	210
APPENDIX C. RELIABILITY AND ACCOUNTABILITY PROBABILITY OF IMPORTANCE OF FACTORS ON LANDSLIDING.....	215
BIOGRAPHY.....	220



LIST OF TABLES

TABLE	PAGE
1.1 Stratigraphy of the study area (modified from Piyasin (1971, 1974), Bunopas (1981), Charoenpavat (1968), and Chaodamrong (1992)).....	13
2.1 Type of landslides is classified based on the types of movements and materials (from Varnes, 1978).....	21
2.2 Example of relative terms and ranges of annual probability of occurrence (from Resources Inventory Committee Government of British Columbia, 1996).....	22
2.3 Summary of Landslide susceptibility mapping methods in the landslide occurrence zone (from Resources Inventory Committee Government of British Columbia, 1996).....	40
2.4 Summary of the feasibility of usefulness of applying remote sensing techniques for landslide hazard zonation in three working scales (Montavani <i>et al.</i> , 1996).....	52
2.5 The method of landslide susceptibility analysis of this study compared with Lee (2001) and Greenbaum (1995) studies.....	57
3.1 Overview of satellites data of the study area.....	60
3.2 Technical parameters of the satellite remote sensing systems used.....	63
3.3 Overview of non-remote sensing data types and sources for the study.....	64

LIST OF TABLES (Continued)

TABLE	PAGE
3.4 Factors map for landslide assessment of Wang Chin area.....	93
3.5 The Band Math's basic arithmetic and relational operators (from ENVI user's manual online, 2006).....	109
3.6 The operator precedence (from ENVI user's manual online, 2006).....	110
3.7 Band names of the nine factors used in landslide prediction model construction.....	113
3.8 Engineering properties of geological material (After Guenther, 2005).....	117
4.1 Reliability probability and rank order of factors related to landslide.....	160
4.2 Accountability probability and rank order of factors related to landslide.....	163
4.3 Combination weights and rank of reliability and accountability probability....	164
4.4 The importance of factors on landslide occurrence.....	165
4.5 Landslide probability index value and hazard level of the Wang Chin area based on reliability probability.....	168
4.6 Landslide probability index value and hazard level of the Wang Chin area based on accountability probability.....	171
4.7 Landslide probability index value and hazard level of the Wang Chin area based on combination of reliability and accountability probability.....	174
4.8 Band math expressions to evaluated the landslide probability index of each factor image.....	182

LIST OF TABLES (Continued)

TABLE	PAGE
4.9 Comparison of landslide occurrence and landslide hazard map based on combination of reliability and accountability weighted using probability method.....	184
4.10 Comparison of landslide occurrence and landslide hazard map based on accountability weighted using probability method.....	185
4.11 Comparison of landslide occurrence and landslide hazard map based on reliability weighted using probability method.	185

LIST OF FIGURES

FIGURE		PAGE
1.1	Landslide occurrences are shown as a bare ground on the mountainous area at Wang Chin District, Phrae Province.	3
1.2	Inundation and deposition due to up stream debris flow at Muang Kham Village.....	4
1.3	Location map of the study area with initial scale 1:250,000 (from Royal Thai Survey Department, 1969).....	8
1.4	Elevation and shaded relief map showing the topography and streams of the study area (from Aster DEM, taken on 28/11/2001, and topographic map, scale 1:50,000 of Royal Thai Survey, 1995).....	10
1.5	Geological map of the study area of initial scale 1:50,000 (modified from Department of Mineral Resources ,1981-1991).....	12
2.1	The graphic illustration shows common terminology of landslide features (from http://nationalatlas.gov/article/geology/a_landslide.html ,2005).....	21
2.2	The most common types of landslide (from http://www.em.gov.bc.ca/mining/Geolsurv/Surficial/landslide/ls2.htm , 2005)	
	(a) Fall	
	(b) Topple	
	(c) Rotational slide	
	(d) Transitional slide.....	22

LIST OF FIGURES (Continued)

FIGURE	PAGE
<p>2.2 The most common types of landslide (from http://www.em.gov.bc.ca/mining/Geolsurv/Surficial/landslide/ls2.htm, 2005), (continued)</p> <p style="padding-left: 40px;">(e) Transitional rock slide (f) Debris flow</p> <p style="padding-left: 40px;">(g) Creep (h) Lateral spread.....</p>	23
<p>2.3 Vector data of points with x, y coordinates (modified from Rolf et al.; 2000).....</p>	36
<p>2.4 The data structure of line data model (modified from Rolf <i>et al.</i>, 2000).....</p>	36
<p>2.5 The data structure of an area data model (Polygon) (modified from Rolf et al., 2000).....</p>	37
<p>2.6 Typical file coordinate with resolution and information attribute of raster data model (modified from Rolf et al., 2000).....</p>	37
<p>3.1 Flow chart of thesis methodology.....</p>	60
<p>3.2 Flow chart shows the method applied of remote sensing.....</p>	66
<p>3.3 (a), concept of the image-to-map registration using ground control points, which are uniquely located on the image and on the 1:50,000 scale of topographic map. (b), Geocoded IRS-1D satellite image.....</p>	67
<p>3.4 (a) image without stretching; (b) Example for linear contrast stretching enhancement applied to each of the three Landsat 7 bands 4, 5, 7 before coding with the colors Red/Green/Blue: land cover units can be distinguished more reliability in the stretched image.....</p>	69

LIST OF FIGURES (Continued)

FIGURE	PAGE
3.5	Histogram showing the limited dynamic range as it is typical for original image data (a), and the dynamic range of the same image after application of linear stretching (b).....70
3.6	RGB composite images showing the terrain in natural- like colour based on band 3/Red, band 2/Green and band 1/blue of Landsat 7.....73
3.7	RGB in false colour composite image showing the terrain based on band 4/Red, band 5/Green and band 7/Blue of Landsat 7.....74
3.8	A 3x3 convolution kernel being applied to a pixel in the third column, third row of sample data (the pixel that corresponds to the center of the kernel) (modified from Yamakawa <i>et. al.</i> , 1998).....75
3.9	The edge-enhanced image is the result of 3 x 3 kernel high pass filtering and highlights linear arrangements of small topographic features that can be interpret as lineaments (white color lines) (Landsat 7, Path 130/Row 48, taken on 28/11/2001).....76
3.10	Example of the use of principal components analysis, a six-band Thematic Mapper (TM) data set may be transformed such that the first three principal components contain over 90 percent of the information in the original six bands.....82

LIST OF FIGURES (Continued)

FIGURE	PAGE
3.11 RGB color composite based on PC1/Red, PC2/Green and PC3/Blue, area of landslide and alluvium deposit (pink color) can be separated from the other area.....	83
3.12 A Clustering algorithm of unsupervised classification dividing the pixel into statistically defined classes (modified from Alfoldi, 2000).....	84
3.13 Supervised classifications; the analyst identifies in imagery homogeneous representative samples (training areas) of the different surface cover types (information classes) of interest (modified from Alfoldi, 2000).....	84
3.14 Training sites, which were selected for supervised classification on Landsat 7, Path 130/Row 48, taken on 28/11/2001 (colored rectangles).....	85
3.15 Result of the supervised classification for some part of the Wang Chin area (Landsat 7, part 130/Row 48, taken on 28/11/2001).....	86
3.16 Digital elevation model (DEM) data generated from Aster satellite data (band 3N and 3B) taken on 28/11/2001(white colour is high elevation, black colour is low elevation).....	87
3.17 Flow chart shows the database construction into GIS.....	89
3.18 Concept of cross-tabulate area aggregation (modified from Alfoldi, 2000).....	92
3.19 Concept of reclassification function (modified from Alfoldi, 2000).....	92

LIST OF FIGURES (Continued)

FIGURE	PAGE
3.20	Flow chart shows the procedure of spatial data analysis and integration for landslide hazard assessment.....98
3.21	This example shows that the slope factor contained probability ratio of landslide occurrence is multiplied by its importance weight.....104
3.22	Band Math processes – Additional of three bands.....109
3.23	Exported data of nine factors to text file format and ENVI-readable files.....113
3.24	Band math dialog.....114
3.25	Variables to bands pairings dialog.....114
4.1	Shallow landslide of weathered surfaced in the study area.....121
4.2	The initiation zone of landslide occurrence is closed to the mountainous ridge and first order stream in the study area.....122
4.3	The masses of weathered surface rocks and wood fragments moved down from the mountain slopes and stream to the low land area.....123
4.4	The debris flow moved quickly downward along the channel and pour out at the valley floor at Hong Village as a special flood, which is a mixture of water, mud, sand, rock, and wood fragments.....124
4.5	Debris flow sediment at Muang Kham Village, Wang Chin District.....125
4.6	Landslide damaged the house at Pa Sak Village.....126
4.7	The human activities in form of deforestation and agricultural has also influenced landslide occurrences (in white circles).....127

LIST OF FIGURES (Continued)

FIGURE	PAGE
4.8 False color combinations of Landsat 7, B4, B5 and B 7 shows characteristic of the study area such as alluvium deposit, flow path, slide scar, forest, deforestation and bare soil (Landsat 7, path 148 / row 48, taken on 28/11/2001).....	130
4.9 False color combinations of Landsat 7, B5, B4 and B 2 shows characteristic of the study area such as alluvium deposit, flow path, slide scar, forest, deforestation and bare soil (Landsat 7, path 138/row 48, taken on 28/11/2001).....	131
4.10 RGB color composite based on PC1/Red, PC2/Green and PC3/Blue, area of landslide and alluvium deposit and bare soil appeared almost pink (Landsat 7, path 130 / row 48, taken on 28/11/2001).....	135
4.11 Comparative images of the same area for landslide detection between (a) Landsat ETM, B4, B5 and B7 false color composites with 30 x 30 metres resolutions for clarifying the characteristics of the study (light blue color = alluvial fan deposit, blue color = resident area, white color = bare soil or slide scar, orange color = vegetation), (b) Aster data B1, B2 and B3 false color composites with 15x15 metres resolutions, which show more clearly landslide location than Landsat image (Landsat 7, path 130 / row 48, taken on 28/11/2001, and Aster, taken on 28/11/2001).....	136

LIST OF FIGURES (Continued)

FIGURE	PAGE
4.12 IRS-1 D panchromatic band with resolution 5 m x 5 m shows very clear landslide scar as white color on the mountainous area (IRS-1D, path 126 / row 026, taken on 27/12/2000).....	137
4.13 Merging IRS-1D PAN (5 m x 5 m) and Aster (15 m x 15 m) B1, B2, and B3 shows very clear landslide scar as white color on the mountainous area (IRS-1D, taken on 27/12/2000, and Aster, taken on 28/11/2001).....	138
4.14 Landslide distribution map based on satellite imagery interpretation (Landsat 7, path 130/row 48, taken 28/11/2001; Aster, taken on 28/11/2001, and IRS-1D Pan, path 126/row 026, taken on 27/12/2001).....	139
4.15 Lithologic map based on DMR, 1981-1991, and modified using satellite image data interpretation and fieldwork (Aster, taken, path 126/row 026 taken on 27/12/2001 and Landsat 7, path 130/ row 48 taken on 28/11/2001).....	140
4.16 Merging IRS-1D PAN (5 m x 5 m, taken on 27/12/2001) and Landsat 7 (30 m x 30 m, , path130/row 48, taken on 28/11/2001) B4, B5, and B7 with filter enhancement shows clear lineament structure.....	141
4.17 Lineament buffer zones map having distance 100 to 100 metres from the lineaments.....	142

LIST OF FIGURES (Continued)

FIGURE	PAGE
4.18 Land use map modified from LDD, 1996, and based on supervised classification using Landsat 7 image (path 130/row 48, taken on 28/11/ 2001) and fieldwork.....	146
4.19 Normalized vegetation index (NDVI) map based on Landsat 7 image (path 130/row 48, taken on 28/11/2001) using NDVI function of ENVI.....	147
4.20 Elevation map based on DEM, which is derived from Aster data (taken on 28/11/2001).....	148
4.21 Slope angle map derived from DEM, which is derived from Aster data (taken on 28/11/2001).....	149
4.22 Slope aspect map based on DEM, which is derived from Aster data (taken on 28/11/2001).....	150
4.23 Flow direction map based on DEM, which is derived from Aster data (taken on 28/11/2001).....	151
4.24 Soil type map based on Land Development Department, 1996.....	152
4.25 The input data layers were multiplied by their corresponding reliability weighted, and were summed up together to obtain the Landslide Probability Index (LPI) for each 30 by 30 metres (Soilunit.Ratiox2_r = Soil unit map layer contained probability ratio of landslide occurrence x reliability weighted of its layer (2)).....	168

LIST OF FIGURES (Continued)

FIGURE	PAGE
4.26	Landslide hazard map based on reliability probability.....169
4.27	The input data layers were multiplied by their corresponding accountability weighted, and were summed up together to obtain the Landslide Probability Index (LPI) for each 30 by 30 metres (eg. Soilunit.Ratiox20_a = Soil unit map layer contained probability ratio of landslide occurrence x accountability weighted of its layer (20)).....171
4.28	Landslide hazard map based on accountability probability.....172
4.29	The input data layers were multiplied by their corresponding combination of reliability and accountability weighted, and were summed up together to obtain the Landslide Potential Index (LPI) for each 30 by 30 metres (e.g. Soilunit.Ratiox11_a = Soil unit map layer contained probability ratio of landslide occurrence x combination weighted of its layer (11)).....174
4.30	Landslide susceptibility map based on reliability and accountability probability.....175
4.31	Landslide hazard zonation with flow path and deposit area.....177
4.32	Slope stability map shows the stability of the Wang Chin area, which is derived from RSS model (from Guenther, 2005).....178
4.33	Landslide susceptibility map based on Band Math prediction model.....181

CHAPTER I

INTRODUCTION

Landslide is world-wide occurring natural hazards, which most cases of landslide occurrence are debris flow and caused by intense and continuous rainfall. Debris flows are commonly mixed of water, mud, sand, rock, and wood fragments and resulted in severe risks to people, farmlands, buildings and urban infrastructures. In many cases, such as the disastrous February 2006 debris flow in the Philippines, the disastrous in Thailand, for example 2001 Petchabun and Phrae debris flow disaster and the disastrous May 2006 debris flow in Uttaradit, and Sukhothai, hundreds of people lost their life or be came injured. In Thailand, many parts of the mountainous areas are exposed to landslide hazard occurrences, which are damaged to people and properties, and infrastructures. Consequently, it is necessary to study on landslide hazard assessment, to assess the hazards, and to reduce the risks as in this study.

1.1 Introduction to this Study

This study was initiated in order to contribute to improving the methodology for landslide hazard assessment, and is focused on landslides triggered by intense rainfall. The aim is to assess landslide hazard or susceptibility at a regional scale (1:50,000 to 1:100,000). It is based on an inventory of existing landslides and physical factors related to landsliding. The factors considered for this study include geologic, topographic, hydrologic, and vegetation condition. The study area is

located at the Wang Chin District, Phrae Province, Northern Thailand.

In this study, existing landslides location and physical factors related to landslide occurrences were collected from available sources, and derived from remote sensing data. Remote sensing data were used to map existing landslide locations and factors that are important in landslide initiation, such as slope, slope aspect, elevation, land use/land cover, vegetation mass (NDVI), lithology, and lineaments. The results from the remote sensing interpretation were verified by field investigation. All data related to landslide occurrences in the study area were transformed to digital formats and stored in the database of the GIS.

The methodology used for landslide hazard assessment in this study is the “bivariate probability and weighting analysis”. The probability and weighting of landslide occurrence on each factor were analysed using geographic information systems (GIS) technique. Landslide hazard map and landslide prediction model were produced based on probability and weighted value of landslide occurrence of each factor, which shows the degree of landslide occurring in the study area and . A landslide prediction model of the study area is able to use as a prediction for future landslide-prone ground. Landslide hazard map was compared with a slope stability model derived by Guenther (2003) and verified using the probability method.

1.2 Characterization of the Problem

On 4 May 2001, a disastrous landslide was initiated in Wang Chin District, Phrae Province after three days of the heavy and continuous rainfall in the form of debris flow (Figure 1.1). The debris flow moved extremely and travelled rapidly for several kilometres along the channel, and inundated the low land area. Sixty houses

and one bridge were completely destroyed, forty people died, three people are still missing, and approximately eighty percent of agriculture farms in the study area were damaged, specially at Hong, Pa Sak, Kham Muak, Song Kwae and Muang Kham Villages seriously (Figure 1.2).

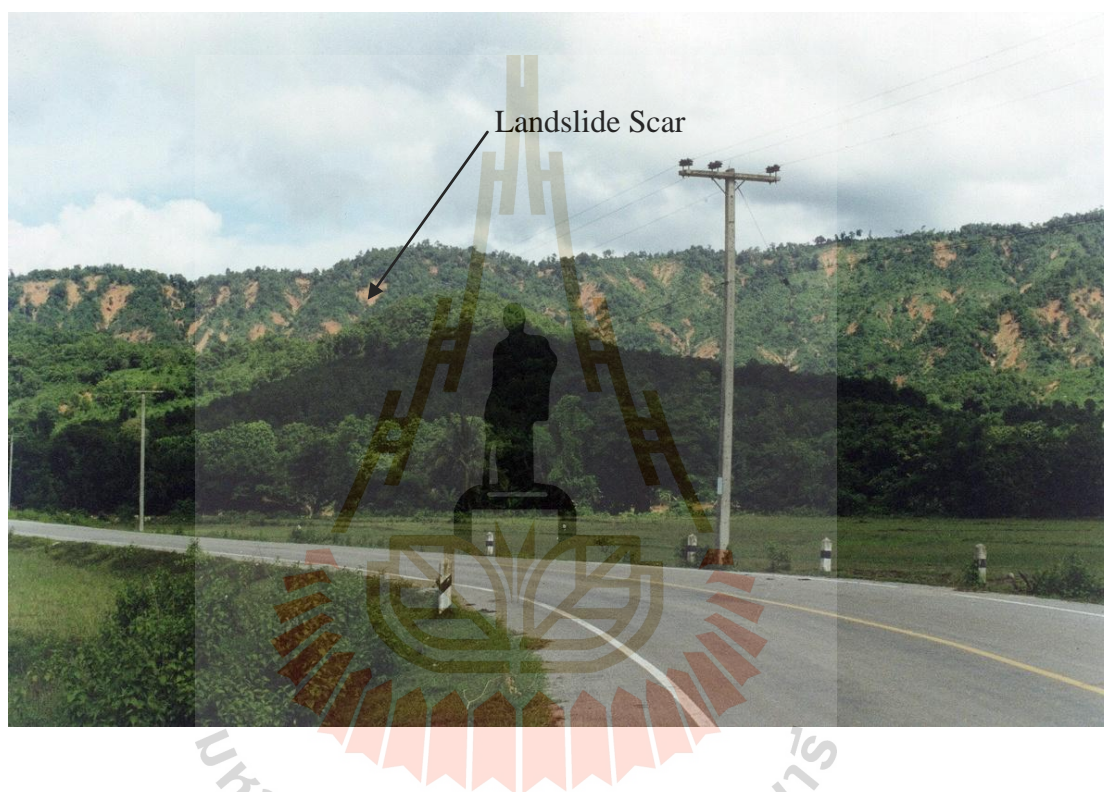


Figure 1.1 Landslide occurrences are shown as a bare ground on the mountainous area at Wang Chin District, Phrae Province.

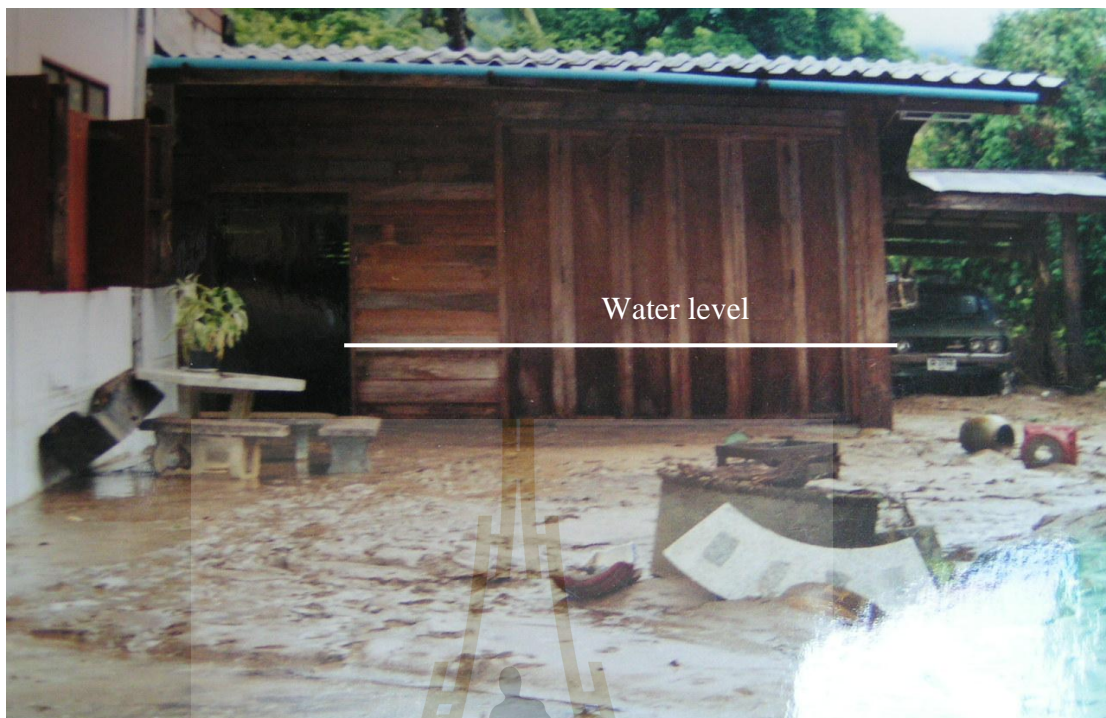


Figure 1.2 Inundation and deposition due to up stream debris flow at Muang Kham Village.

มหาวิทยาลัยเทคโนโลยีสุรนารี

The serious problem in landslide hazards assessment is to find out where and when landsliding will be occurred. The answers will be able to help the planner to plan for protection against landslide hazards and risk. Consequently, it is necessary to study on landslide hazard assessment for delineate area that will be affected by probable landslide hazards occurring in the future.

At present, remote sensing and GIS are the most important application for landslide assessment analysis. There are many landslide prediction models using remote sensing and GIS to identifying hazard areas affected by landslide-prone ground (e.g., Wang and Unwin, 1992; Greenbaum *et al.*, 1995; Chang *et al.*, 1998; Lee, 2001). Most of them are different in terms of methodology and type of factors that are used for landslide hazard analysis. These differences are depended on experience of researchers, geographic location, and type of landslides. Most of these methods, GIS were used to compile and manipulate data, and to produce final landslide hazard maps, which are used remotely sensed data as 1) to spatially detect and classify landslides; 2) to monitor the activity of existing landslides, and 3) to analyse and to predict slope failure in both space and time (Mantavani, 1995). Landslide hazard map was produced based on mathematical algorithms, such as regression and probability functions.

In this study, the methodology and causative factors used in landslide hazard analysis are depended on the experience of researcher, environment of the study area, and type of landslide. Therefore, it is a need to justify the methodology for landslide hazard analysis and landslide prediction models, on the basis this study. The methodology used was improved and modified from the method of Lee (2001) and Greenbaum *et al.* (1995). In addition, ranking and weighting of importance of

causative factors, which control landslide occurrences were analysed.

The goal of landslide hazard or susceptibility analysis is to assess the landslide hazards in order to reduce the risks to people, urban areas, infrastructures and farmlands. An essential part of this landslide hazard mapping is to validate the significance of the prediction result, so that it can be used to predict landslide-prone ground in further areas with similar physical factors related to landsliding.

1.3 Objective of Research

The main objective of research is to generate a landslide prediction model for landslide hazard mapping. The following sub-goals are formulated:

- 1) To develop probability and weighting method used as a prediction model for outlining the landslide hazard areas.
- 2) To derive GIS database for the landslide prediction model with the aim at identifying the areas that are likely affected by future landslides-prone ground.
- 3) To validate the results of 1) and 2) by compare with the results of a slope stability model, and cross checking using probability method with existing landslide location.

1.4 Scope and Limitation of Research

This research integrates remote sensing and GIS techniques with field mapping and verification for landslide hazard assessment. The analysis focuses on the relationship between existing landslide distributions and physical factors affected to landslide occurrences. These physical factors comprise lithology, lineaments,

elevation, slope angle, slope aspect, NDVI, land use/land cover, soil units, and flow direction. The landslide hazard or susceptibility analysis was based on the bivariate probability and weighting methods. Landslide hazard or susceptibility map was derived by incorporating physical factors related to landing in term of probability on landslide occurrences using GIS technique.

1.5 Expected Results

The following results will be expected by this study.

- 1) General improvement of methodology for landslide hazards detection.
- 2) Landslide hazard or susceptibility maps for Wang Chin study area.
- 3) Landslide prediction model based on Band Math technique of ENVI software, which shall be serving as an improved method to identify areas those are affected by future landslide events.

1.6 Characterization of the Study Area

1.6.1 Location

The Wang Chin area is located in the south-western part of Phrae Province and the northern part of Thailand between 17°30' to 18° North and 99° to 99°45' East (Figure 1.3). This study area is situated in the catchments of Mae Nam Yom River. It is called Mae Nam Yom Valley of which surface accounts are approximately 540 square kilometres. The Mae Nam Yom Valley extends from Wang Chin District to Muang Kham Village, which located at the south-western portion of Wang Chin District.

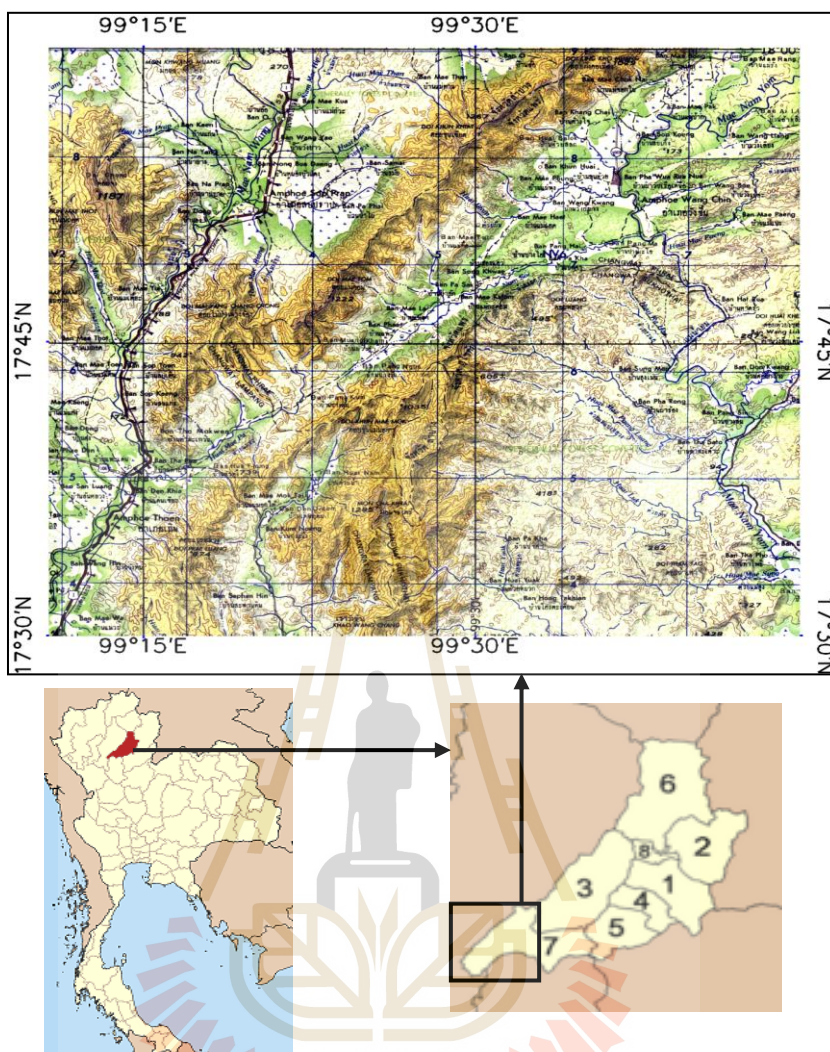


Figure 1.3 Location map of the study area with initial scale 1:250,000 (from Royal Thai Survey Department, 1969).

1.6.2 Topography

The topography of the area is characterized by mountains, terraces, and flood Plains (Figure 1.4). The elevation of the study area is approximately 1,267 metres above mean sea level at Khun Khiat range and less than 100 metres above mean sea level at the Mae Nam Yom Valley floor in the southern portion of Wang Chin District.

There are two mountain ranges in the western and eastern parts of the study area, and show a general orientation from northeast to southwest. Elevation of the western mountainous range is between 250 and 1,267 metres above mean sea level, where as elevation of the eastern mountainous range is between 200 and 900 metres high above mean sea level. Both mountainous ranges are covered by moderate to dense natural forests, which is partly deforested. The central part of the study area shows an undulated terrain with elongated shape trending in approximately NE-SW direction. The terrain consists of small and low hills, lying closely to high mountain range. The teak plantation dominates the land use in this area. The lowest portion of the terrain is floodplain, where many important rivers flow through, namely Mae Nam Yom River, Mae Nam Suai River, Huai Mae Kham Muak, and Huai Mae Kra Tom. Mae Nam Yom River, the main river in the study area, flows from the north to southwest. Mae Nam Suai River is a tributary of Mae Nam Yom River and flows from Muang Kham Village to Pak Huai Suai Village in the south-west to the north-east direction of the study area. Paddy field, mixed orchards, and crops are the main land use units of this flood plain.

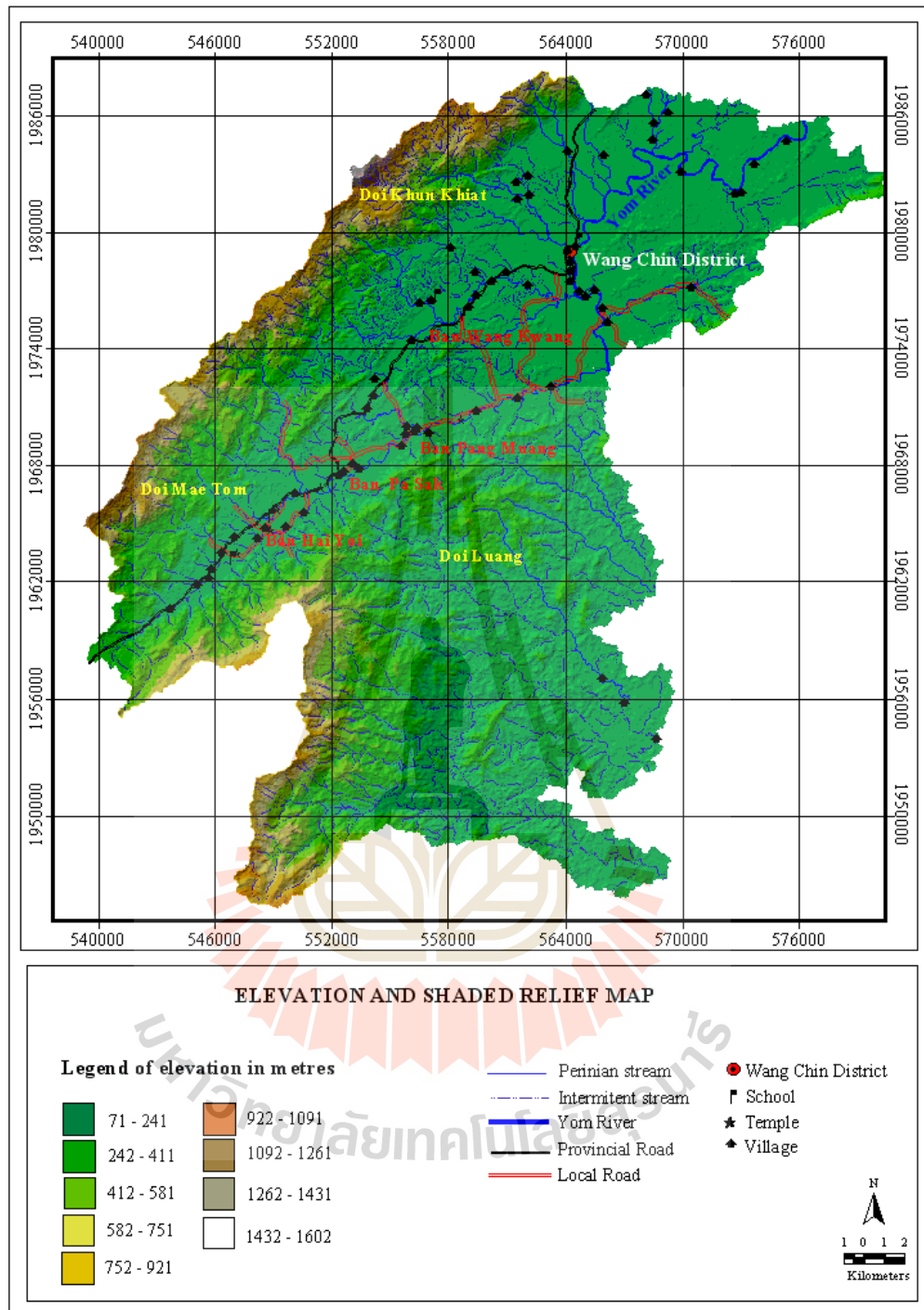


Figure 1.4 Elevation and shaded relief map showing topography and streams of the study area (from Aster DEM, taken on 28/11/2001, and topographic map, scale 1:50,000 of Royal Thai Survey, 1995).

1.6.3 Climate

The climate is typical of tropical rain forest region. The rainy period starts from mid of May to mid of October, and is mainly influenced by the southwest monsoon season. The average annual rainfall is about 1,500 to 2,000 millimetres within the warm temperature periods. The winter season is during mid of October to mid of February, and mainly influenced by the northeast monsoon. The temperature is between 10° and 30° Celsius. The summer period starts from mid of February to mid of May between the winter and rainy season. The temperature is between 28° and 38° Celsius, and rainy storms may appear.

1.7 Geological Setting

The study area is underlain by rocks ranging in age from Permian to Recent (Figure 1.5). The geology of the region has been previously described by various workers, i.e. Heim and Hirschi (1939), Charoenpravat (1968), Piyasin (1972, 1974) etc. Geological maps at scales of 1:250,000 and 1:50,000 of the study area were issued by Department of Mineral Resources (Charoenpravat, 1968; Piyasin, 1972 and 1974; and Charoenpravat *et al.*, 1987). The stratigraphic sequences of the eastern part consist mainly of low-grade metamorphic rocks known as the Donchai Group. The western and central parts are mainly rhyolitic and volcanic rocks represented by tuff, agglomerate, other extrusive material, shale, calcareous shale, and sandstone. The description of those rock units are given below from the oldest to the youngest (Table 1.1).

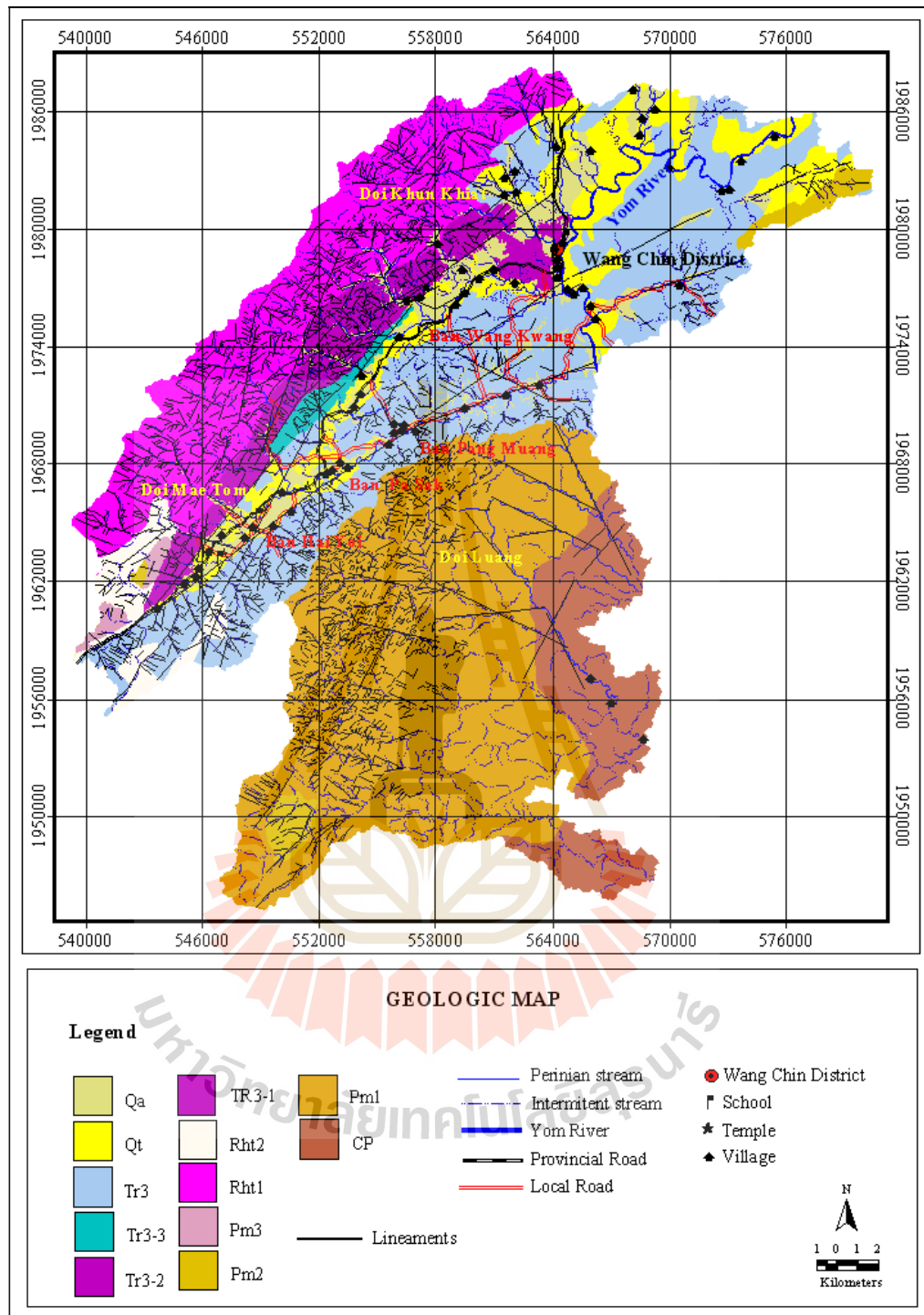


Figure 1.5 Geological map of the study area of initial scale 1:50,000 (modified from Department of Mineral Resources, 1981-1991).

Table 1.1 Stratigraphy of the study area (modified from Piyasin (1971, 1974), Bunopas (1981), Charoenpavat (1968), and Chaodamrong (1992)).

Age	Group	Formation	Rock Unit (this study)	Lithology	Remark
QUATERNARY			Alluvium channel (Qa)	Gravel, sand, silt, and clay	
			Terrace deposit (Qt)	Gravel, sand, and laterite layers	
TRIASSIC	Lampang	Wang Chin	Unconformity		500-800 metres thick
			Tr3-3	Clastic rocks with limestone lenses	
			Tr3-2	Sandstone	
			Tr3-1	Shale	
			Tr3	Shale intercalated with sandstone	
PERMIAN-TRIASSIC		Pha Thang	Unconformity		
			Rht2	Rhyolitic rocks	
			Rht1	Andesitic rocks	
PERMIAN-CARBONIFEROUS	Donchai		Pm3	Quartzite, schist, chert, tuff and agglomerate, 300-400 m thick	
			Pm2	Limestone and marble, 30 m thick	
			Pm1	Phyllite and chorite-sericite schist, 300-400 m thick	
			CP	Pebbly shale, sandstone, and mudstone, 1,000 m thick	

1.7.1 Paleozoic Rocks (Donchai Group; CP, Pm 1, Pm2, and Pm3)

Charoenpravat *et al.* (1987) proposed the subdivision of the Donchai Group into four units, namely, CP, Pm 1, Pm2, and Pm3, respectively in ascending order.

CP rock: The Permo-Carboniferous rocks (CP) in this area are mainly undifferentiated shale, pebbly shale, chert, sandstone, and tuff (Piyasin, 1972 and 1974), which commonly show moderately mountainous topography. The Permo-Carboniferous rocks (CP) are widely distributed in the south-eastern part i.e. Doi Mae Paeng. The thickness of this formation is approximately up to more than 1,000 metres (Charoenpravat *et al.*, 1987).

Pm1 rock: The unit is mainly composed of black to greyish black phyllite and chlorite-sericite schist of low grade metamorphic rocks and the various lithologies are often repeated by folding in different sections. This unit is exposed along the northeast-southwest trend at Doi Luang, and Doi Pong. The thickness of this sequence is approximately 300-400 metres.

Pm2 rock: The Pm2 rock unit mostly consists of white to greyish black limestone, marble, and well bedded to very thick-bedded. Fossils and crystalline limestones are locally presented. This unit is exposed in north-eastern and south-western parts of the study area. The thickness of this unit is approximately 30 metres.

Pm3 rock: This unit mainly consists of greenish grey to reddish brown quartzite, quartz-feldspathic schist, chert, tuff, and agglomerate. The unit is exposed quartzite, quartz-feldspathic schist, chert, tuff, and agglomerate. The unit is exposed along the south-western trend at Huai Hia. The thickness of this unit is approximately 300-400 metres.

According to Bunopas (1983), the total thickness of the Donchai Group is more than 1,500 metres. Fossil have not yet been found in the clastic rocks of the Don Chai Group. In 1970, the geologist of the Department of Mineral Resources found rugose coral, *Yatsengia* sp., which usually occurs in the Artinskian Stage of the Early Permian. Bunopas (1981) proposed that the Donchai Group is represented to the foreland basin deposit of quartzofeldspathic composition, the detritus components having been derived from a craton to the west.

1.7.2 Permo-Triassic Rocks (PTr)

According to Charoenpravat (1968), the Permo - Triassic rocks (PTr, Pha Thang Formation) is composed of greenish grey andesitic rocks (andesite, agglomerate, and tuff) which slightly metamorphosed, and to minor rhyolitic rocks.

Based on this study, these units are divided into 2 rock types, greenish grey andesitic (Rht1) and rhyolitic rocks (Rht2), respectively in ascending order. This formation is exposed as a high mountainous terrain in the western to south-western part of the study area. The extrusive rocks and shallow intrusive rocks related to the tectonic events of the Doi Chong Group indicate the Late Permian age. Piyasin (1972, 1974) considered the bulk of the acidic volcanic rocks to be Permo Triassic in age.

1.7.3 Triassic Rocks (Wang Chin Formation, Tr3, Tr3-1, Tr3-2, and Tr3-3; Lampang Group)

The Triassic clastic sequence represented in the northern portion of Thailand as the Lampang Group (Piyasin, 1971, 1974; Bunopas, 1981; Charoenpravat, 1968; and Chaodamrong, 1992), is well exposed in the central part trending NE-SW direction. The unit unconformable overlies the Permo-Triassic rocks with basal conglomerate in many localities of these areas. The formation mainly consists of grey

to light brown shale intercalated with fine-grained, thin-bedded sandstone, limestone lenses and calcareous shale. The total thickness of this formation is between 500 and 800 metres. Charoenpravat (1968) noted the various occurrences of *Halobia*, *Daonella*, *Posidonia*, ammonites, and coral. Based on these fossils and succession, this formation was assigned as Anisian age. This study divided the clastic rocks of the Wang Chin Formation (Lampang Group) into 4 units in ascending order as follows: shale intercalated with sandstone (Tr3), shale (Tr3-1), sandstone (Tr3-2), and clastic rocks with limestone lenses (Tr3-3).

1.7.4 Quaternary

Quaternary sediments are widespread in the central part of the study area. The Pleistocene fluviatile sediments (Qt) are characterized by gravel, sand and laterite layers unconformable overlying older basements. Along the low-lying area, the Holocene unit (Qa) is well exposed and characterized by gravel, sand, silt, and clay. Quaternary unit is the most important factor on landslide occurrence as well as weathered surface of shale and sandstone on the mountainous area.

1.7.5 Geological Structures

The Wang Chin area is a structurally complex area with folding and overthrusting towards the east (Bunopas, 1981). The belt extends from northern Thailand through the Gulf of Thailand. The area is characterized by strong volcanism (calc-alkaline volcanic) during the Late Permian to Middle Triassic. It is interpreted as a collision belt along the sutured zone between the Shan Thai and Indochina blocks (Bunopas, 1981; Mitchell, 1981; and Hahn *et al.*, 1986).

Three major different fault systems in northern Thailand were distinguished: NE-SW, NW-SE strike-slip faults and N-S normal faults. The N-S

normal faults are predominant in the isolated mountainous basins. There are two major anticlines and synclines in the NE-SW and NW-SE directions in the study area. These faults lie along the Nam Yom valley and dip direction face to the valley floor. These are the major cause of discontinuities of bedrock, and rock weathering according to the tropical rain forest climate, which play important roles for slope instability in the study area.



CHAPTER II

LITERATURE REVIEW

Landsliding is a general term used to describe the down slope mass movement of rock and soil under gravitational influence (Varnes, 1984). According to Cruden (1991), a landslide is defined as “the mass movement of rock, debris, or earth down a slope”. Other terms used to refer to landslide are mass movement, slope failure, slope instability, and terrain instability. Landslide events are complex geological and geomorphological processes. Hence it is very difficult to classify the characteristic of landslide. Most of landslides are classified based on material types, type, and velocity of movements.

2.1 The Classification of Landslides

The systems for the classification of landslides are based on the parameter as shown in Table 2.1. According to Cruden and Varnes (1996), the various types of landslides can be differentiated by the kind of material and the mode of movement as follows:

2.1.1 Material Types Involved in Landslide

The material types involved in landslide were classified into two groups; bedrock and soil. Soil is generally unconsolidated surficial material. It is further subdivided into debris and earth depending upon its textures.

Table 2.1 Type of landslides is classified based on the types of movements and materials (from Varnes, 1978).

Type of Movement		Type of Material		
		Bed Rock	Engineering Soils	
			Predominately Coarse	Predominantly Fine
	FALLS	Rock fall	Debris fall	Earth fall
	TOPPLES	Rock topple	Debris slide	Earth slide
SLIDES	ROTATIONAL	Rock slide	Debris slide	Earth slide
	TRANSLASTIONAL			
	LATERAL SPREADS	Rock spread	Debris spread	Earth spread
	FLOWS	Rock flow	Debris flow	Earth flow
		(Deep creep)	(soil creep)	
	COMPLEX	Combination of two or more principle types of movement		

Bedrock: Bedrock refers to earth materials that have been created by rock forming processes. Its strength depends on the rock type, degree of weathering, density and orientation of discontinuities, which are generally the planes of weakness in the rock mass. For instance, if a dense and hard granite rock contains many fractures, the rock mass may be less strong than a coarse-grained soil.

Debris: Debris is composed of predominantly coarse-grained soil including boulder to gravel and sandy materials. It can also include pieces of highly fractured bedrock. The strength of coarse-grained soil generally depends on the friction between the grains. Woody debris such as tree or logs, or other organic material, is sometime mixed with the inorganic debris.

Earth: Earth refers to predominantly fine-grained soil (silt and clay size materials). The strength of fine-grained soil generally depends on cohesion, chemical and electrical bonding between small particles.

2.1.2 Type of Landslides

The term “landslide” describes a wide variety of processes that result in the downward and outward movement of slope forming materials, including rock, soil, artificial fill or a combination of these. The material may move by sliding, falling, toppling, spreading, or flowing. Figure 2.1 shows a graphic illustration of a landslide, with the commonly accepted terminology describing its features (http://nationalatlas.gov/article/geology/a_landslide.html, 2005).

The very common types of landslide are fall, topple, rotational slide, translational slide, translation rock slide, creep, debris flow and lateral spread as described follows (Figures 2.2a-2.2h):

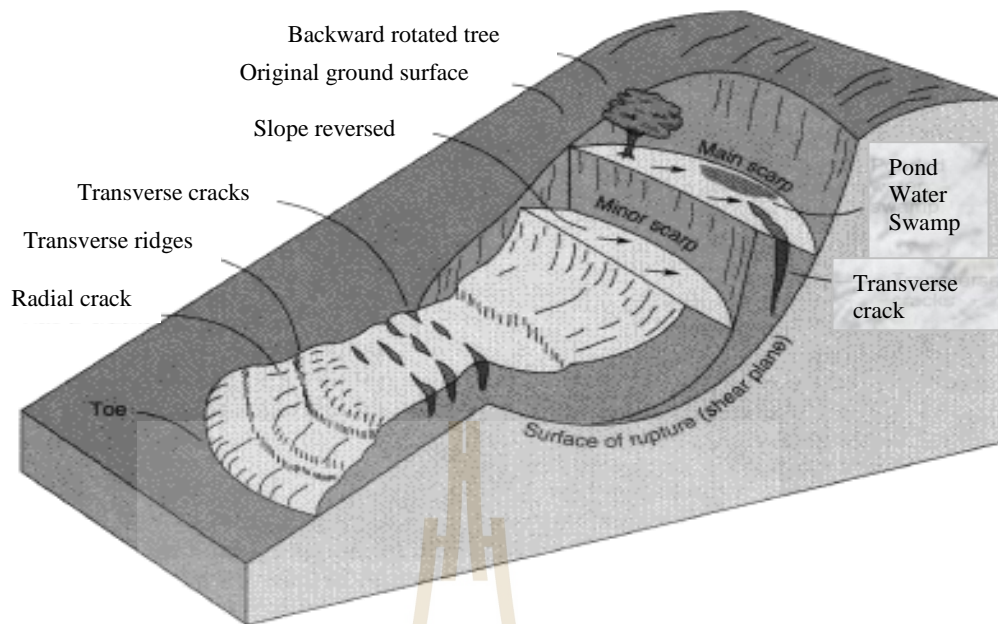


Figure 2.1 The graphic illustration shows common terminology of landslide features (from http://nationalatlas.gov/article/geology/a_landslide.html, 2005).



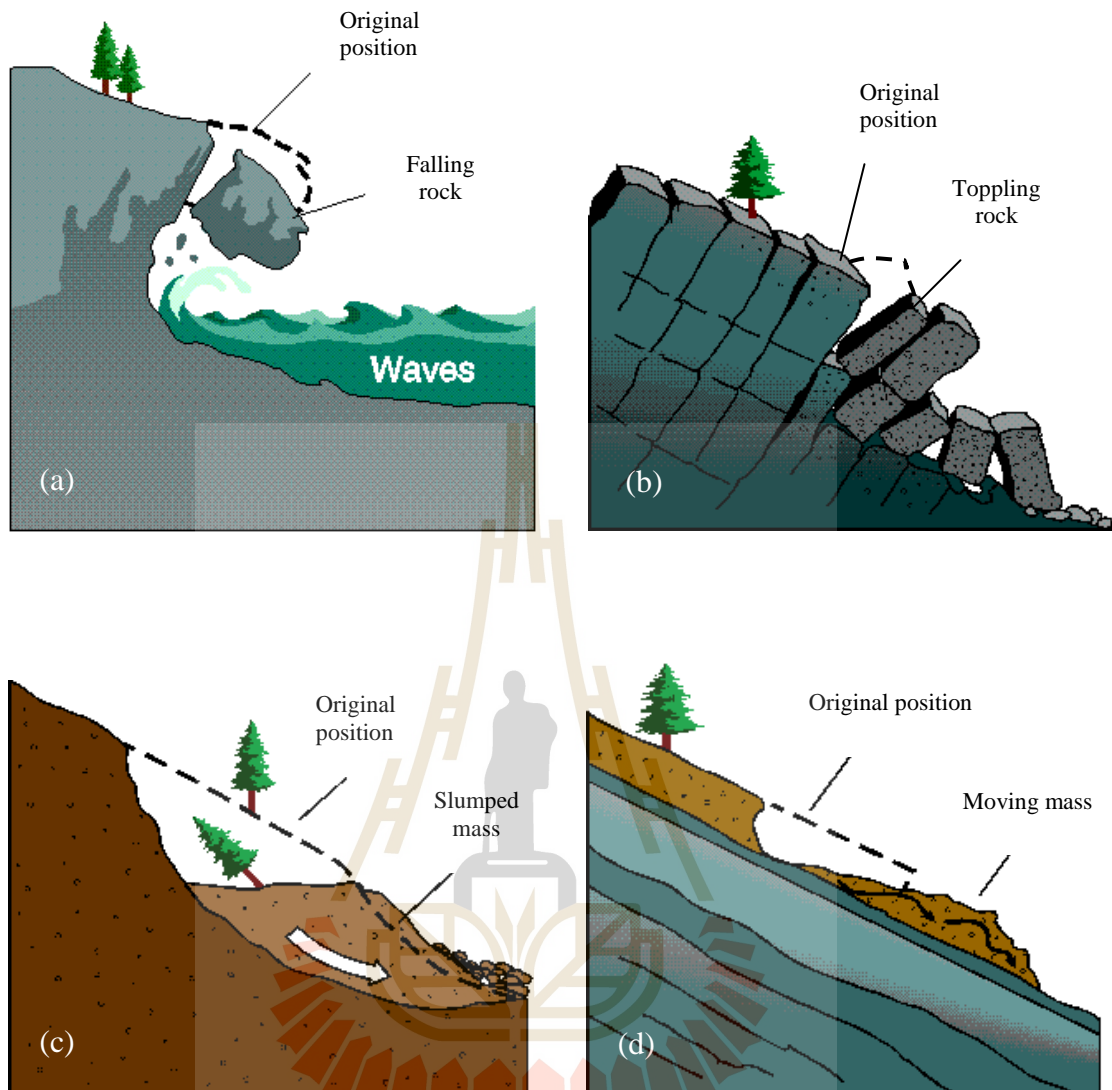


Figure 2.2 The most common types of landslide (from <http://www.em.gov.bc.ca/Mining/Geolsurv/Surficial/landslide/ls2.htm>, 2005).

(a) Fall

(b) Topple

(c) Rotational slide

(d) Transitional slide

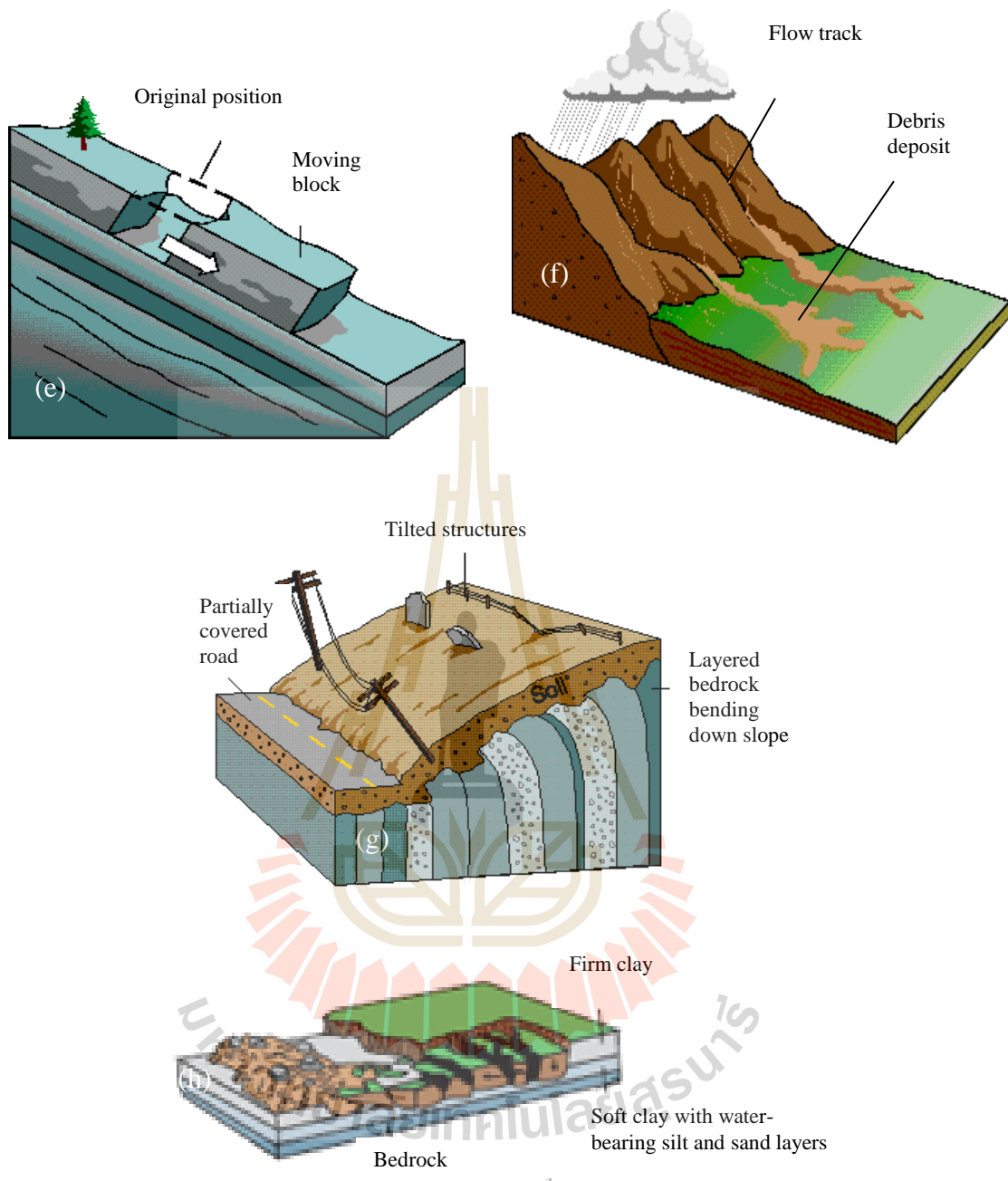


Figure 2.2 The most common types of landslide (from <http://www.em.gov.bc.ca/Mining/Geosurv/Surficial/landslide/l2.htm>, 2005), (continued).

- (e) Transitional rock slide
- (f) Debris flow
- (g) Creep
- (h) Lateral spread

Falls: Falls are abrupt movements of masses of geological material, such as separated rocks and boulders from steep slope or cliff by free-fall, bouncing and rolling. Separations of rocks occur along fractures, joints and bedding planes. The fall is strongly influenced by gravity, mechanical weathering, and the presence of interstitial water.

Topples: Topples are characterized by the forward rotation of units of rock or soil about some pivot points, under the actions of gravity and forces exerted by adjacent units or by fluids in cracks.

Slides: Slides are referring to the movement along one or more distinct surfaces. Slides can be subdivided into rotational and translational slides, depending on the shape of the failure plane.

1) Rotational slide is a slide that has the concavely upward curved surface of rupture. The slide movement is roughly rotational. The axis of slide movement is parallel to the ground surface and transverse across the slide. Rotational slides refer to slumps, involve movement along a curve failure planes.

2) Translational slide is a slide, which the landslide mass moves along roughly planar surface. The failure planes often exist before the occurrence of movement.

Lateral spreads: Lateral spreads are distinctive because they usually occur on very gentle slopes or flat terrains. The dominant mode of movement is lateral extension accompanied by shear and tensile fractures. The failure is caused by liquefaction, and usually triggered by earthquake.

Flows: Flows refer to movement as viscous fluid. There are five basic categories of flows that differ from one another in fundamental ways.

1) Debris flow is a form of rapid mass movement in which a combination of loose soil, rock, organic matter, air, and water flows down slope as a slurry. Intense surface-water flow, due to heavy rainfall or rapid snowmelt commonly caused debris flow. They are also commonly transformed from other types of landslides that occur on steep slope and nearly saturated and consist of large proportion of silt and sand sized material. The source areas of debris flow are often associated with steep gullies. The presence of debris fans at the mouths of gullies usually indicates debris flow deposits.

2) Debris avalanche is a variety of very rapid to extremely rapid debris flows.

3) Earth flow is elongate flow and usually occurs in fine-grained materials or clay bearing rocks on moderate slope and under saturated conditions. The slope material liquefies and run out, forming a bowl or depression at the head. However, dry flows of granular material are also possible to occur.

4) Mud flow is an earth flow consisting of material that is wet enough to flow rapidly and that contains at least 50 percent sand, silt, and clay sized particles.

5) Creep is the very slow movement of slope forming soil or rocks. The movement is caused by shear stress sufficient to produce permanent deformation, but too small to produce shear failure. Curved tree trunks, bent fences or retaining walls, tilted poles or fences, and small soil ripples or bridges indicate it.

Complex landslides: In general, complex landslides are involving the combination of two or more types of movement. Commonly one type of movement starts the materials moving, such as debris slide, and once underway the materials take

on the character of another type of movement such as a debris flow. For example, the combination of the type of movement between debris slide and debris flow called as a debris slide-debris flow. The rate of movement depends on the types of movements in addition, material.

2.2 Landslide Causes

According to Greenbaum (1995), the causes of landslide occurrence at a given location depend on a number of conditions, which may be considered as controlling factors and triggering events.

Controlling factors can be broadly divided into material properties (rock and soil type, and insitu and post movement strength, etc.), and terrain conditions (slope, aspect, fracturing and cultivation, and land use/land cover, etc.). Triggering events of landslide can be divided into natural events and human activities. These are included earthquakes, intense rainfall and possibly new construction and development.

The three following are the most important causes of landslide around the world (http://nationalatlas.gov/article/geology/a_landslide.html, 2005).

2.2.1 Landslide and Water

A primary cause of landslides is slope saturation by water. This effect can occur through intense rainfall, snowmelt, changes in ground water levels, and water-level changes along shorelines, earth dams, bank of lakes, reservoirs, canals, and rivers. Rainfall triggering action in mountainous region is caused landslides in the Wang Chin area.

Landslide and flooding are closely affiliated because both are related to precipitation, runoff, and the saturation of the ground by water. In addition, debris

flows and mudflows usually occur in small, steep stream channels that cause a special flood as a mixture of water and debris in the lowland areas.

Landslide may be a cause of flooding by forming landslide dams that block valleys and stream channels, trapping large amounts of water to back up. This causes backwater flooding and, if the dam fails, subsequent downstream flooding. Solid landslide debris can be increasing volume and density to normal stream flow, or cause channel blockages and diversions flow direction of stream, which is creating flood or localized erosion. Landslide can also cause overtopping of reservoirs and/or reduce capacity of reservoirs to store water.

2.2.2 Landslides and Seismic Activity

Many mountainous areas that are vulnerable to landslides have also experienced at least moderate rates of earthquakes occurrence in records times. The occurrence of earthquakes in steep landslide prone areas greatly increases the likelihood that landslide will occur, due to ground shaking alone or shaking-caused dilation of soil materials, which allows rapid infiltration of water. Moreover, ground shaking caused widespread rock falls of loosens rocks.

2.2.3 Landslides and Volcanic Activity

Landslide due to volcanic activity belongs to one of the most devastating types. Volcanic lava may melt snow at rapid rate, causing a torrent of rock, soil, ash, and water that accelerates rapidly on the steep slopes of volcanoes, devastating anything in its path. These volume debris flows are also known as lahars. In many cases, not only lava based snowmelt may cause lahars but also rainfall leads to liquefaction of thick ash layers causing lahars. These lahars reach great distances, once they leave the flanks of the volcano, and can damage structures in lowland areas surrounding the

volcanoes.

In Thailand, most of landslides occurrence depend on the material and terrain conditions combined with human activities, and rainfall triggering actions such as Katoon area in Nakorn Sri Thammarat Province, Nam Ko area in Petchaboon Province as well as the Wang Chin area in Phrae Province.

2.3 Landslide Hazards

The United Nations definition of natural hazard is “the probability of occurrence of a potentially damaging natural phenomenon” (Varnes, 1984). In reference to landslides, Fell (1994) defined hazard as “the magnitude of the event times the probability of its occurrence”. However, hazard is also often used to describe the damaging phenomenon called natural, geological, and landslide hazards, or a specific type of landslide hazard.

Landslide hazard is represented by susceptibility, which the probability of a potentially disastrous landslide is occurring within the given area. Probability of landsliding is the chance or probability that a landslide hazard will occur. It can be expressed in relative (Qualitative) terms or probabilistic (Quantitative) terms. Examples of relative terms are very high, high, moderate, and low, or very frequent, frequent, infrequent, and seldom. The results of probabilistic are often presented in ranges of value such as $>1/20$, $1/100 - 1/20$, $1/500 - 1/100$ and $1/2,500 - 1/500$ (Table 2.2).

Table 2.2 Example of relative terms and ranges of annual probability of occurrence

(from Resources Inventory Committee Government of British Columbia, 1996).

Relative term of probability	Range of probability of occurrence (Pa)	Comments
Very high	$>1/20$	Pa of 1/20 indicates the hazard is imminent, and well within the lifetime of a person. Landslides occurring with a return interval of 1/20 or less generally have clear and relatively fresh signs of disturbance.
High	1/100 to 1/20	Pa of 1/100 indicates that the hazard can happen within the approximate lifetime of a person. Landslides are clearly identifiable from deposits and vegetation, but may appear fresh.
Moderate	1/500 to 1/100	Pa of 1/500 indicates that the hazard within a given lifetime is not likely, but possible. Signs of previous landslides, such as vegetation damage may not be easily noted.
Low	1/2,500 to 1/500	Pa of 1/2,500 indicates the hazard is of uncertain significance. A similar probability was at one time used to define the Maximum Credible Earthquake for dams, but this definition has been dropped.

2.4 Technical Aspects of Remote Sensing

Remote sensing refers to specific methods used for obtaining information about the Earth's surface, which sense electromagnetic (EM) radiation. Remotely sensed has no direct contact between the sensors carried by either aircraft or satellite and the objects being observed. Remote sensing utilizes EM radiation principally in the ultraviolet, visible light, infrared, and microwave portions of the EM spectrum. Single (e.g. IRS-1D Pan) and multi-band (Landsat TM, Landsat 7) data acquisition systems are used as tools for gathering remotely sensed data.

Interaction of EM radiation with the Earth's surface provided information about the reflecting or absorbing surface. Due to the short wave length of the EM radiation (centimeter to nanometer range), there is limited penetration of the target objects. Therefore, data and images are obtained only from the earth surface. Consequently, remote sensing information on conditions and structures underlying a natural or artificial terrain surface can be derived only by interpretation. Thus, the reliability of an interpretation depends on the knowledge and experience of the interpreter.

In recent years, remote sensing has been increasingly recognized as a means of obtaining geo-scientific data for regional and site-specific investigations. Remotely sensed data provides a synoptic perspective view, and covers large areas in a relative short time, which is unachievable with traditional field studies. Remote sensing is an excellent tool for site characterization because it is not limited by extremes in terrain or hazardous conditions, which may be encountered during an on-site appraisal. These are effective for basic and applied research covering a wide range of subject, including mineral exploration, geo-environmental and geo-hazard evaluation.

Remote sensing data should be acquired and integrated into early stages of an investigation and used in conjunction with traditional mapping techniques. It is the best suited method for the following purposes.

- Preliminary assessment and site characterization of an area prior to the application of more costly and time-consuming traditional assessment techniques, such as field mapping, drilling, and geophysical surveys.

- Clarification of geo-scientific problems using the broad perspective provided by an aircraft or satellite image.

- Geo-scientific assessment of regions with limited or no access, such as rugged terrain, hazardous sites, and disaster areas.

Most of remote sensing data from satellite based systems are best suited for regional studies at scales of 1:100,000 to 1:50,000 (e.g. general site characterization, topographical and land use/cover mapping, structural mapping). The high resolution satellite image data, such as IKONOS, QUICK BIRD can be used for the scale of 1:50,000 to 1:10,000. These data are commonly used to characterize natural resources that have a wide distribution (e.g. tropical rain forests), to monitor flooding, ice cover of polar waters, as well as detect and monitor environmental problems (e.g. impacts on soil and ground water, land subsidence, collapse-prone ground, hazard due to landslides, forest fires and soil spills). Satellite images have also been shown to be an effective tool for characterizing and assessing areas of human activity, such as deforestation, open-pit mines and extension of land development areas.

Aerial remote sensing systems are also provided useful data for integrated development planning and natural hazard assessments. Airborne remote sensing is the process of recording information from sensors on aircraft. Available airborne systems

include aerial cameras, multispectral scanners, thermal infrared (IR) scanners, passive microwave imaging radiometers, and side-looking airborne radars (SLAR). The most useful scales for airborne photographs and images range from regional scale to large scale. Availability and acquiescing of airborne data are limited and costly. Due to the specialized systems and operators required to produce airborne imagery. These data are usually available only from a limited number of organizations which either own or lease the systems (<http://www.oas/dsd/publications/Units/oea66e/ch04.htm>, 2006).

Consequently, remotely sensed data can be used to effectively detect and to assess factors related to landslide occurrence (Franco *et al.*, 1995). The interpreter should have a working knowledge of remote sensing techniques and capability to assess the reliability of an interpretation, as well as the ability to use the derived information. For instance, the interpreter of remote sensing for landslide assessments should be having a knowledge and experience of the characteristics of landscape of landslide and factors related to landslide, and how these factors interact and affect the resulting information.

The factors that determine the utility of remote sensing in landslide hazard assessments are scale, resolution, and tonal or color contrast of the data. Other factors include area of coverage, repetition cycle (days), and data cost and availability. Resolution of satellite image is determined by size and numbers of picture elements or pixel used to form an image. The smaller pixel size of an image is the greater the resolution of the data. For example, the pixel size of an image 30 m x 30 m is low resolution than 5 m x 5 m pixel size of an image. Spectral resolution also needs to be taken into consideration when selecting the type of data since different sensors are designed to cover different spectral regions. Spectral resolution refers to the number

of spectral bands and the bandwidth offered by the sensor. The temporal occurrences of natural events will also affect the utility of remotely sensed data. For instance, Landsat and IRS-1D sensors can detect a phenomenon; according to their repeat coverage are very 16 days and 5 days. Events, which are seasonal, predictable, or highly correlated with other events, are more likely to benefit from imagery than events that occur randomly such as earthquakes, tsunamis or landslides.

However, in order to assess landslide-prone ground as a precursory measure for effective disaster in mitigation, remote sensing can contribute with exclusive data and information. Remote sensing imagery should be regarded as data available to assist the study in the assessment of landslide hazard throughout the study area. The meaning and value of remote sensing data is enhanced through target-oriented data processing and skilled interpretation used in conjunction with conventionally mapped information (e.g. topographic map and geologic map) and ground-collected data.

A map derived from the interpretation of remote sensing data is influenced by subjective factors. For example, maps generated based on automatic classification techniques depend on the quality and appropriateness of the input data and analysis techniques used. Therefore, it is particularly important to spot-check interpretations of remote sensing data in the field. Field or ground checks may be necessary at the start and during a remote sensing project to establish a key for interpreting the data or to check intermediate interpretations.

This study outlines the scope of a typical remote sensing work, starting with definitions and goals of remote sensing, covering digital data rectification and enhancement techniques, and describing data interpretation and map production approaches, referring to the Wang Chin area.

2.5 Technical Aspects of Geographic Information Systems

Geographic information systems (GIS) are computer-based systems for data capture, input, manipulation, transformation, visualization, combination, query, analysis, modeling and output, with its excellent spatial data processing capacity. In addition, it has been used widely in landslide hazard assessment (Carrara *et al.*, 1999). GIS is very useful tool for spatially distributed data processing and analysis. Conceptually, GIS should be able to utilize spatial data in any form, whether raster, vector or tabular. GIS provides the following tasks of capabilities to handle geo-reference data.

2.5.1 Data Input

Data input components convert data from their existing form into the other one that can be used by GIS. The input data are usually derived from available data (paper maps, and tables of attribute, etc.) assessment during field visits, and possibly supported by satellite image interpretation. Geographic reference and attribute data must be entered into GIS. Geographic reference data are coordinates (either in terms of latitude and longitude or columns and rows), which give the locations of information being entered. Attribute data are associated with a numerical code to each cell or set of coordinates and for each variable, or to represent actual values (e.g., 1,200 m elevation, 20 degree slope gradient) or to geo-information (land use category, vegetation type, and rock type, etc.)

2.5.2 Data Structures

The input data from earlier step are needed to store in GIS as a spatial database. The spatial data (vectors and raster model) are structured and organized within the GIS according to their location, interrelationship, and attribute design as a

systematic database of analysis. These databases can be easily to update, deletion and retrieval in GIS. In this study, vector and raster model are used for landslide analysis.

Vector model: The vector model represents all information as points, lines or polygon, assigns as a unique set of x, y coordinates to each piece of information (Figures 2.3–2.5). Vector data can offer a large number of possible overlay inputs or layers of data. The vector model does represent the mapped areas more clearly than a raster model. However, each layer of vector-based model defined uniquely, analyzing information from different layers is considerable more difficult than raster model.

Raster model: The raster model uses grid cells to reference and store information. The spatial data map is divided into a grid or matrix of square cells identical in size, and information attribute of the database (Figure 2.6). A cell can display either the dominant feature found in that cell or percentage distribution of all attributes found in the same cell. Raster-based model define spatial relationship between variables more clearly than vector-based, but the coarser resolution caused by using a cell structure reduces spatial accuracy.

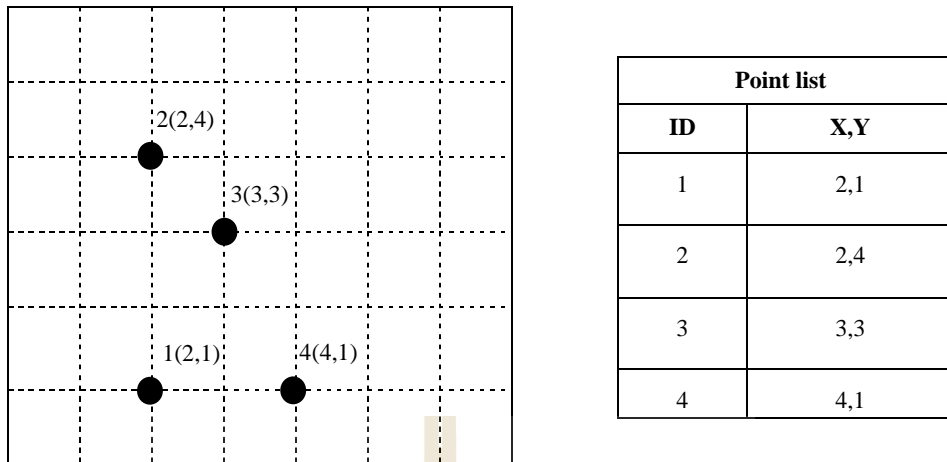


Figure 2.3 Vector data of points with x, y coordinates (modified from Rolf et al.; 2000).

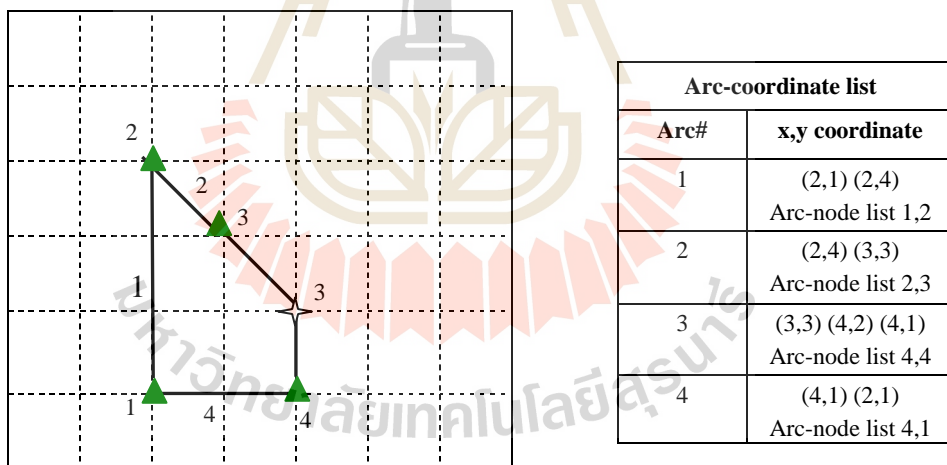


Figure 2.4 The data structure of line data model (modified from Rolf *et al.*, 2000).

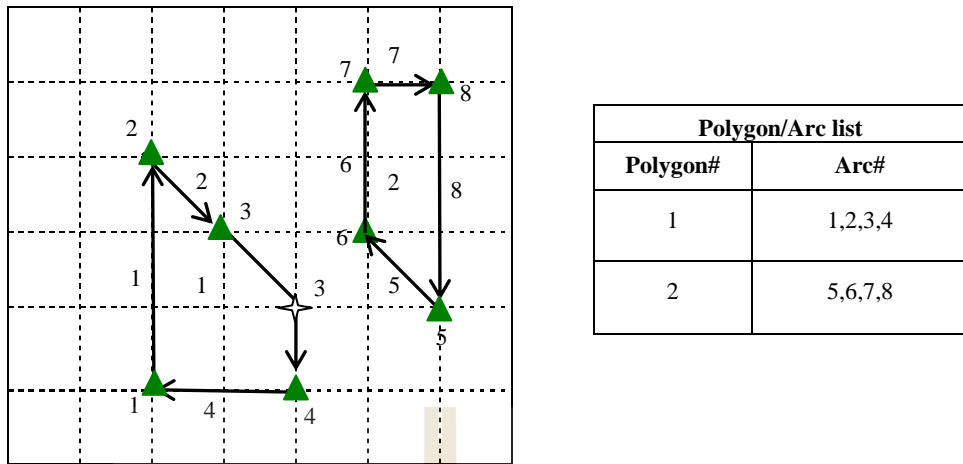


Figure 2.5 The data structure of an area data model (Polygon) (modified from Rolf *et al.*, 2000).

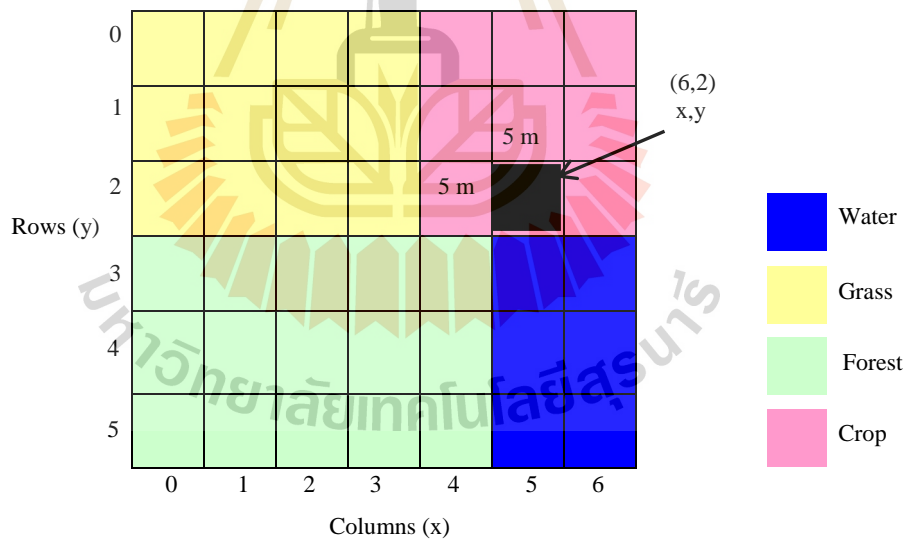


Figure 2.6 Typical file coordinate with resolution and information attribute of raster data model (modified from Rolf *et al.*, 2000).

2.5.3 Data Manipulation and Analysis

Data manipulation is performed to obtain useful information from a systematic spatial database in the GIS. These are the operations using analytical techniques to answer specific question formulated by the user. The manipulation process can range from the simple overlay of two or more maps to a complex extraction of output data and information from a wide variety of data sources.

2.5.4 Data Output

Data output refers to display or presentation of data and information employing commonly used output formats that include maps, graphs, reports, tables, charts, either as a hard copy, as an image on the screen, or as a text file that can be carried into other software for further analysis.

2.6 Integrating Remote Sensing and GIS for Geo-Spatial Analysis

Remote sensing data can be readily merged with other sources of geo-coded information in a GIS. This permits the overlaying of several layers of information with the remotely sensed data, and information derived from remote sensing data, and the application of virtual unlimited number of forms of data analysis. The integration of GIS with remote sensing data and thematic map data may facilitate greatly the assessment and estimation of regional landslide hazard (Musaoglu *et al.*, 2002).

GIS is suitable for the requirements of synthesizing the available information. The strength of a GIS lies in its capability of storing interpreted information, available information, and linked attributes. A GIS application as a landslide assessment tool is developed for landslide hazard analysis. The parameters considered for assessment of landslide hazard include a landslide map, major land use/cover categories and

topographic factors (Seker *et al.*, 2004). The results from landslide assessment tool will aid in the identification of the occurrence of landslides.

In Thailand, most of landslides are occurred in the mountainous areas, which cover generally large areas, and are very hardly accessible. Therefore, the availability of database and archival data are limited. However, the potential of satellite remote sensing in combination with GIS-based analysis can be utilized to remote efficiently investigate the mountainous area. The remote sensing can be applied for an inventory of landslide events and a spatial differentiated characterization of factors related to landslide occurrences. The landslide information derived from remote sensing data has to be stored and analyzed in combination with additional landslide-related data using GIS techniques. Then, the relationships between factors related to landslide and landslide event are calculated in terms of the likelihood of landslide occurrence on each factor. There are various integration methods, which can be utilized to combine spatial data from remotely sensed and other sources together, to describe and analyze interactions, to make predictions and to prepare landslide hazard zonation maps.

2.7 Methods of Approaches to Landslide Hazard Assessment

Landslide hazard assessment usually involves in predicting and expressing the probability of landslide occurring. The approaches vary from qualitative method to quantitative method. The following method modified from a classification proposed by Van Westen (1993), reviewed the main aspects of these methods in Table 2.3.

Table 2.3 Summary of Landslide susceptibility mapping methods in the landslide occurrence zone (from Resources Inventory Committee Government of British Columbia, 1996).

Type of analysis	Methods of analysis	Summary
Qualitative analysis	Landslide distribution	<ul style="list-style-type: none"> - objective and qualitative - useful data base of existing landslides - no prediction
	Landslide activity	<ul style="list-style-type: none"> - objective and qualitative - useful data base of existing landslides during different time period - no prediction
	Landslide density	<ul style="list-style-type: none"> - objective and qualitative - useful data base of landslides - no prediction
	Subjective geomorphic	<ul style="list-style-type: none"> - subjective and qualitative - flexible, unspecified terrain stability/landslides hazard class criteria - requires expert skills - Useful data base of landslides and some terrain attributes - difficult to review
Quantitative to semi-quantitative analysis	Subjective rating	<ul style="list-style-type: none"> - Subjective and qualitative to semi-quantitative - flexible, but specified terrain stability/landslide hazard class criteria - requires expert skills - useful data base of many relevant terrain attributes - work can be delegated and checked - danger of oversimplification
	Relative bivariate	<ul style="list-style-type: none"> - objective and qualitative to semi-quantitative - relative statistically based - shows effects of individual terrain attributes - data and analytically intensive -relies on quality data

Table 2.3 Summary of Landslide susceptibility mapping methods in the landslide occurrence zone (from Resources Inventory Committee Government of British Columbia, 1996), (continued).

Type of analysis	Methods of analysis	Summary
Quantitative analysis	Probabilistic bivariate	<ul style="list-style-type: none"> - objective and quantitative - probabilistic statistically based - simple to implement and test - danger of selection of wrong terrain attributes - data and analytically intensive - relies on quality data
	Probabilistic multivariate	<ul style="list-style-type: none"> - objective and qualitative, precise - probabilistic statistically based - danger of selection of wrong terrain attributes - removes experience and judgment of mapper - very data and analytically intensive - relies on highly quality data
	Slope stability	<ul style="list-style-type: none"> - objective and qualitative, precise - can be review - difficult to use for mapping a large area - shows influence of terrain attributes - requires precise estimates of slope geometry, material strength properties and ground water conditions - danger of oversimplification - conceals lack of knowledge

2.7.1 Qualitative Methodologies

In general, qualitative approaches are based on the judgment of the persons or persons carrying out the susceptibility or hazard assessment. The input data are usually derived from assessment during field visits, possibly supported by remote sensing interpretation. The following methods are the qualitative method

Landslide distribution analysis: Landslide distribution analysis requires the preparation of a process inventory map of individual landslides such as debris slides or debris flows, or for a group of landslides. It shows the distribution and magnitude of recent landslide events by the number and size of landslides. It can then be used for more elaborate landslide hazard analysis.

Landslide distribution analysis is particularly unreliable if a prediction of landslide hazards is required for changed conditions, such as following road construction, clear-cut logging or reservoir flooding. In such cases, it is necessary to use statistical or judgmental extrapolation from areas that have already undergone such change, described below as a probabilistic bivariate analysis.

Many publications are concerned with landslide distribution analyses. These range from maps of large rock avalanche sites by Abele (1974) and Cruden *et al.* (1988), through maps of debris slides by Rood (1984), and snow avalanches by Schleiss (1989).

Landslide activity analysis: Landslide activity analysis is a refinement of the landslide distribution analysis, by which information is included on a process inventory map from several different periods. Landslide activity analysis maps show changes in landslide sites with time. The objective of qualitative data is usually obtained from the interpretation of remotely sensed data from several different

years. Landslide activity analysis still may not recognize areas, which have not been active, but are potentially unstable.

The most useful landslide activity analysis is carried out in areas of slow movement where it is possible to distinguish sequential activity. For example, Bonnard and Noverraz (1984) applied this method of mapping to land use planning in Switzerland. A special application of landslide activity analysis is the comparison of landslide occurrence before and after a certain activity, such as timber harvesting by Swanson *et al.* (1982).

Landslide density analysis: The landslide density analysis is a second possible approach in the processing of landslide distribution or landslide activity, and is used to calculate landslide density in a given area. This calculation may be done in three ways: average the number of landslide per unit area in a map unit (Howes, 1987), calculate the percentage of unstable area in a map unit (O'Loughlin, 1972), or draw contours of equal landslide density (Wright *et al.*, 1974; DeGraff, 1984; Degraff and Canuti, 1988).

The first method of calculation is suitable for medium or small-scale mapping. The second is more appropriate for larger map scales, especially where the size of the unstable areas varies. The isopleth's method is more suited to areas of weak rocks or fine-grained soil, characterized by abundant and relatively deep-seated landslide. Landslide densities are sometimes subjectively grouped into susceptibility classes (Hicks and Smith, 1981).

The most important aims of all three methods (landslide distribution, landslide activity and landslide density) are to document past events and to provide calibration for predictive techniques using other terrain stability mapping method.

Geomorphologic analysis: Geomorphologic analysis involves the delineation of areas based on several terrain attributes from remotely sensed data interpretation and fieldwork. The map then subjectively assigns qualitative terrain stability/landslide hazard class to each terrain attributes, based on the remote sensing interpretation, field observations and experience of the interpreter. Geomorphic recognition of potentially unstable terrain is often strongly guided by observations of existing landslides.

Examples of studies using this method is very frequent in literature of the 70s and 80s (Bosi *et al.*, 1982; Carrara and Merenda, 1976; Fenti *et al.*, 1979; Guerricchio and Melidoro, 1979; Kienholz, 1978; Ives and Messerli, 1981; Rupke *et al.*, 1988). One of the most comprehensive projects reported in the literature is the French ZERMOS procedure (Antoine, 1977; Humbert, 1977; Meneroud and calvinoi, 1976) which involves two main phases: analysis and extrapolation. In the first phase, all factors which may influence the stability are examined, both permanent (topography, geology, hydrogeology, and hydrology, etc.) and temporary (climate, land use and other man-made factors). Active and/or inactive landslides may be analyzed. In the next phase all the factors are extrapolated by the author to areas with similar physical conditions, thus enabling zonation of the area into their sections with varying degrees of hazard. These are low hazard area, in which no stability should occur, uncertain hazard, area with potential instability of uncertain nature and extent, and ascertained hazard, areas with declared instability and certain threat of failure. The hazard calculated in this method is a relative nature and the author knowledge that the various hazard categories cannot be compared from one area to another area.

Rating analysis: The rating approach is based on the priority knowledge of the causes of landsliding in the area under investigation. In this approach, the expert selects and maps the factors, which affect slope stability and, based on personal experience, and assigns ranking and weighting according to their assumed or expected importance in causing landslide. The following operations were carried out (Soeters and Van Westen, 1996):

- 1) Subdivision of each parameter into a number of relevant classes.
- 2) Attribution of weighted values to each class.
- 3) Attribution of weighted values to each of the factors.
- 4) Overlay mapping of the weighted map.
- 5) Development of the final map showing hazard classes.

Relevant terrain attributes are usually assigned based on map polygons or raster map. The terrain attributes most often used include slope gradient, surficial materials, and geomorphic processes. Additional factors such as soil drainage, soil depth, and vegetation cover may also be used. Many subjective rating analyses include the presence of existing landslides as an important factor.

The algorithm of rating analysis can vary from simple qualitative combinations of terrain attributes to complicated quantitative tables of weighting factors. According to Gee (1992), an increasing of complexity algorithm does not often improve the reliability of the results. Defining a subjective rating algorithm requires a high degree of specific knowledge and experience of person.

An advantage of a rating analysis method is that a record of the procedure exists and the assignment of classes can be independently reviewed in GIS. Furthermore, it enables the standardization of data management techniques, from

acquisition through final analysis. This technique can be applied at any scale, and especially where large areas are involved. The problem of subjective in attributing weighted values to each factor also remains in rating analysis, as well as the difficulty of extrapolating a model developed in a particular area to other area (Carrara, 1983).

Its reliability is directly dependent on the knowledge of the surveyor in the geomorphologic processes acting upon the terrain. Landslide hazard maps obtained by this method cannot be evaluated in terms of reliability or certainty.

2.7.2 Quantitative Methodologies

The statistical or probabilistic approach is based on the observed relationship between each instability factor and the past and present landslide distribution. Statistical approaches have generally taken the form of bivariate or multivariate statistical analyses of terrain characteristics that have led to landslides in the past (Carrara *et al.*, 1991; Lorente *et al.*, 2002) or weighted hazard ratings based on environmental attributes related to landsliding (Donati and Turrini, 2002; Lin *et al.*, 2002; Lineback *et al.*, 2001). The reliability of this functional approach is directly dependent on the quality and quantity of the collected data.

Bivariate statistical analysis: In bivariate statistical analysis, each individual factor is compared to the landslide map. The weighted values of the classes are determined based on landslide density in each individual class. These are used to category the rank of importance of every factor. The following operations are required:

- 1) Selection and mapping of significant factors and their classification into a number of relevant classes.

- 2) Landslide mapping.

- 3) Overlay mapping of the landslide map which each factor map.
- 4) Determination of density of landslides in each factor class and definition of weighted values.
- 5) Assignment of weighting values to the various factor maps.
- 6) Final overlay mapping and calculation of the final hazard or susceptibility value of each identified unit.

The bivariate statistic approach is widely employed by the earth scientists, and numerous factors may be taken into consideration such as lithology, slope angle, slope length, land use, distance from major structures, drainage density, relief morphology, closeness of the facet to a river, and attitude of lithology (Aleotti *et al.*, 1999).

Multivariate statistical analysis: Multivariate statistical approach is to establish a correlation between probability of landslide occurrence and a group of factor attributes. The method can be applied on a site-specific basis (Pack, 1985), or on an overlay basis (Carrara, 1983).

The conceptually simplest technique is conditional analysis, which attempts to assess the probabilistic relationship between relevant environmental factors and the occurrence of landslides over a given area. The technique is based on Bayes theorem (Morgan, 1968) according to which data such as the area of landslides and number of landslides, can be used to calculate probabilities that depend on knowledge of previous landslide events. Conditional analysis can be applied with a classification of the study area into unique-condition units (Dowds, 1961; Harbaugh *et al.*, 1977; Bonham-Carter *et al.*, 1990). The resulting map from overlay of two or more factor maps is unique-condition units. The probability of landslide occurrence is

simply calculated as “the area of landslide in unique-condition unit’s area divided by unique-condition unit’s area”. Then the probabilities of landslide in each unique-condition unit’s area is compared to landslide occurring in the region under the investigation, with the average landslide probability over the entire region investigated (Average landslide probability over the entire region investigated = Total Landslide area/entire region area). The result is possible to rank the region into belts at different hazard levels as the latter grouped into appropriate classes.

The other simple version of probabilistic multivariate analysis is the matrix approach suggested by DeGraff and Romeburg (1984). Using overlays of map delineated by terrain attribute polygons, which is defined a separate class for each combination of independent terrain attributes. For example, using tree terrain attributes such as bedrock, slope and drainage, with four classes in each, the resulting matrix had $4 \times 4 \times 4 = 64$ possible cases.

More formal multiple regression and discriminant statistics analyses, have been conducted by Carrara (1983, 1991) with the help of a GIS. Van Westen (1993) tested similar procedures on a carefully study area and found that no significant correlation resulted due to insufficient quality of the input data. In addition, he found that both relative and probabilistic bivariate analysis produced satisfactory result with the same data.

The main disadvantage of probabilistic multivariate analysis is that excludes the experience and judgment of the researchers in producing correlations between factors and landslide. Thus, the results are very dependent on the quality of the factors data and landslide mapping.

2.8 Landslide Assessments

Landslide assessments are usually involved in landslide initiation zones and landslide-related factors mapping. In addition, landslide location and landslide-related factors were used to analyzing landslide susceptibility map. The two mainly used approaches are qualitative and quantitative methods that have been developed and tested by many researchers worldwide (Aleotti and Chowdhury, 1999). They often delineate areas of equal probability of landslide initiation, such as a probability of occurrence, or the probability of occurrence combined with magnitude and/or some other characteristics of the landslide. The qualitative approach is mainly based on the site-specific experience of experts with the hazard determination directly in the field or by combining different index maps. Quantitative techniques utilize statistical analysis (bivariate or multivariate) and deterministic methods that involve the analysis of specific sites or slope based on geo-engineering models.

A landslide hazard zonation map is commonly a result of landslide assessment. Landslide hazard zonation is generally known as the division of the slope stability into homogeneous areas according to different degree of hazard due to mass movement (Varnes *et al.*, 1984). Landslide hazard zonation may be defined as a technique of classifying an area into zones of relative degree of potential hazard by equal classification of landslide probability of various causative factors in a given area.

Before starting a landslide assessment project, thorough reviews of all relevant mapping and studies should be carried out. This should include the factors related to landslide and site-specific reported as follows:

2.8.1 Factors Related to Landslide

Landslide is a general term used to describe the mass movement of rock and soil down slope under gravitational influence. Common landslide triggering factors include intense rainfall, rapid snow melt, and water-level changes, volcanic eruptions, and strong ground shaking during earthquakes (Wang, 2001). In recent years, the man-made causes combined with the natural causes of the hazard have brought about severe losses and disaster to the potential hazard regions. The problem is getting particularly serious when economically developing in mountainous and nearby areas. The following literatures reviewed are concluded about the factors related to landslide by many authors.

Varnes and Iaeg (1984), Hutchinson (1995), Aleotti and Chowdhury, (1999), stated that landslides would occur in the same geological, hydrological, and climatic condition as in the past. The main conditions that cause landsliding are controlled by identifiable physical factors, and the degree of hazard can be evaluated.

Lin *et al.* (2002) studied in the assessing debris flow hazard in a watershed in Taiwan, stated that the initiation of debris flow requires three fundamental condition and at least one trigger condition. The three fundamental conditions are geology, topography, and hydrology. These can be divided into nine factors. The first three factors, rock formation, fault length and landslide areas are grouped under the category of geology. These factors influence the production of abundant debris. The next three factors, slope angle, slope aspect and stream slope are associated with the topographic condition. These factors have impact on the initiation and transportation of debris flows. The last three factors, watershed area, form factor of watershed and cultivation factor are influent the peak flow rate of

stream. These factors have impact on the initiation and transportation of debris flows, which are grouped under the category of hydrology.

The statistical analysis of landslide susceptibility at Yougin, Korea studied by Lee and Min (2001), instability factors include surface and bedrock lithology and structure, bedding, altitude, seismicity, slope steepness and morphology, stream evolution, groundwater condition, climate, vegetation cover, land use, and human activities.

2.8.2 Application of Remote Sensing and GIS on Landslide Assessment

In recent years, there are many studies involving landslide hazard evaluation and numerous methods have been proposed for landslide zonation of the landscape. The use GIS and Remote Sensing (RS) has increased because of the rapid development in the field of hardware and software, and the quick of access to data obtained through Global Positional System (GPS) and remote sensing (Gorsevski *et al.*, 2000).

Application of remote sensing: According to the remote sensing techniques for landslide studying and hazard zonation in Europe, the use of remote sensing data can be differentiated for the various phases within landslide study, such as, detection and classification of landslides, monitoring the activities of existing landslide, and analysis and prediction of slope failure in space and time, Mantovani, (1996).

Montovani *et al.* (1996) summarized the feasibility and usefulness of obtaining information needed for the approaches of hazard zonation using remote sensing techniques at three different scales (Table 2.4). According to this table, landslide hazard mapping based on landslide inventory maps benefits the most from

information collected using remotely sensed data, followed by heuristic approaches at regional and medium scales, statistical and landslide frequency analysis using at regional and medium scales, statistical and landslide frequency analysis using indirect methods (for medium and large scale studies).

Table 2.4 Summary of the feasibility of usefulness of applying remote sensing techniques for landslide hazard zonation in three working scales (Montavani *et al.*, 1996).

Type of landslide hazard analysis	Main characteristics	Regional scale	Medium scale	Large scale
Distribution analysis (landslide inventory approach)	Direct mapping of mass movement features resulting in a map that gives information only for those sites where landslide occurred in the past.	2-3	3-3	3-3
Qualitative analysis (heuristic approach)	Direct or semi-direct method in which the geomorphologic map is reclassified to a hazard map, or in which several maps are combined into one using subjective decision rules based on expert-knowledge.	3-3	3-2	3-1
Statistical approach (stochastic approach)	Indirect methods in which statistical analysis are used to obtain predictions of mass movement from a number of parameter maps.	1-1	3-3	3-2
Deterministic approach (process-based)	Indirect methods in which parameter are combined in slope stability calculation.	1-1	1-2	2-3
Landslide frequency analysis	Indirect methods in which earthquakes and/or rainfall records or hydrological models are used for correction with known landslide dates to obtain threshold values with a certain frequency.	2-2	3-3	3-2

The first number indicates the feasibility of obtaining the information using remote sensing (1 = low: it would take too much time and money to gather sufficient information in relation to the expected output; 2 = moderate: a considerable investment would be needed, which only moderate justifies the output; 3 = good: the necessary input data can be gathered with a reasonable investment related to expected output. The second number indicates the usefulness (1 = of no use: the method does not result in very useful maps at the particular scale; 2 = of limited use: other techniques would be better; 3 = useful).

However, the spatial resolution of the most widely used satellite data, Landsat TM and SPOT are generally too coarse for landslide characterization unless the landslide is very large in size, or the image data is resampled and merged with other higher resolution satellite images (Rengers *et al.*, 1992; Koopmans and Ferero, 1993; Singhroy, 1995). In recent years, the high spatial resolution satellite imagery from Ikonos, Quickbird, SPOT-5 and the Indian satellites of the IRS series are available for the production of landslide inventory maps. Some research has been conducted using the 5.8 m resolution IRS-1D (Gupta and Saha, 2001), or simulated Ikonos data (Hervas *et al.*, 2003).

Zomer *et al.* (2002) used Aster satellite remote sensing data for DEM extraction in complex mountainous terrain of the Makalu Burun National Park in Eastern Nepal. It is extremely useful for terrain analysis of topographic condition. Hydrologic model, automated stream and watershed delineation is easily facilitated by the extracted DEM. Three-dimension terrains perspective views are able to display from DEM.

Singhroy and Molch (2004) mentioned two different approaches that can be adopted for determining the characteristics of landslides from remotely sensed data. The initial approach determines more qualitative characteristics such as number, distribution, type and character of debris flows. This can be achieved with either satellite or air-born imagery collected in the visible and infrared region of the spectrum. The second approach is quantitative characterization by estimating dimension (e.g., length, width, thickness and local slope, motion, and debris distribution) along and across the mass movement using stereo SAR, interferometric SAR and topographic profiles.

Application of GIS: GIS has been recognized as a useful tool to process spatial data and display results. It offers map overlaying possibilities and calculation facilities of superior to conventional techniques. GIS is very important in analyzing the complex combination of factors leading to the slope instability. Numerous methods of analysis have been proposed for landslide assessment using GIS. GIS is a tool that can be combine, organize, manage and evaluate many different sets of data. It cannot be compared directly with field mapping, and cannot replace field mapping; GIS can also be used to efficiently deal with data collected in the field using traditional methods.

The use of multivariate statistics approach with GIS has been studied for a long time (Carrera *et al.*, 1983, 1991, and 1995). At the beginning stage of landslide hazard modeling large grid cells with a ground resolution of 200 by 200 m were used. Although the method based on spatial correlation has not undergone major changes, the basic modeling element (cell size) and the tools for modeling have improved significantly.

The statistical model developed by Carrera *et al.* (1991) is built up in a training area where the spatial distribution of the landslides is well known. After the model is extended to the entire study area. It is assumed that factors that cause slope failures in the study area are the same as these in the training area. The landslide hazard modeling is achieved by discriminant analysis and multiple regression.

Mark and Ellen (1995) applied logistic regression for predicting sites of rainfall induced shallow landslides that initiate debris flow. In there study, statistics were used to determine the based correlation between mapped debris flow sources and

physical attributes thought to influence shallow landsliding.

Lee (2000) evaluated the susceptibility of landslide at Yongin, Korea using a GIS-technique and remote sensing. Landslide locations were identified from interpretation of aerial photographs and field surveys. The relationship between landslide occurrence and cause factors were analyzed using probability, logistic regression, fuzzy logic, and neural network methods for landslide susceptibility assessment. The result of these studies is landslide susceptibility maps.

2.8.3 Landslide Assessment based on Slope Stability Model by Gunther

Gunther *et al.* (2004) presented the development of RSS-GIS (Rock Slope Stability GIS), an expert system based Arc View GISTM software of ERSI (Environmental Systems Research Institute inc.) Grid-based RSS-GIS is built of several extensions (modules) for Arc View GISTM that can be used for a rapid automated mapping of geometrical and kinematical slope properties, and spatially distributed, pixel-based stability calculations of rock slopes. Besides DEM data, this expert system includes regional continuous grid-based data on geological structures that might be act as potential sliding or cutoff planes for rockslides. Application is demonstrated for a study area in the Harz Mts., Germany. The results produced with RSS-GIS are only models of slope stability obtained at a regional scale. The quality of the database and the limitations of the methods are influenced to the result interpretation. Resolution and validity of the model produced with RSS-GIS mainly depend on the amount, density, quality and kind of input data.

According to the reviews of all relevant mapping and studies related to landsliding and site-specific reports in this chapter, it can be concluded that the method, and technique used are based on GIS tools and remote sensing. Factors

related to landslide are physical factors such as geologic, topographic, and hydrologic factors. Each of these three factors can be divided into the sub-factors. For example, slope angle, slope aspect is sub-factors of topography factors. Type and number of factors were used in each paper depending on experience of researchers, geographic condition, environment, type of landslide and triggering factor. Most of factors were derived from satellite image and aerial photography interpretation, and input to GIS as a database. The statistic methods used to landslide assessment comprise bivariate analysis, multivariate analysis, and direct and indirect geomorphic methods. The mathematical algorithms applied are probability, weighting and regression methods. The results of the analysis showed relative landslide hazard occurrence in terms of very low, low, moderate, high, and very high.

In this study, the methodology of landslide assessment is improved and modified from the method of Lee *et al.*, (2001) and Greenbaum *et al.*,(1995). The method approach of Greenbaum *et al.* (1995) is based on the correlation between probability of landslide occurrence and a group of terrain attributes. The method can be applied on a site-specific basis. The statistic approaches of this study and Lee *et al.*, (2001) are on the basis of the observed relationship between each terrain attribute and past landslide event.

However, all of these methods show the results of analysis in relative term of hazard level. The reliability of the landslide susceptibility maps is based on the quality of database. Table 2.5 shows the method of landslide susceptibility analysis of this study compared with Lee *et al.*, (2001) and Greenbaum *et al.*(1995) studies.

Table 2.5 The method of landslide susceptibility analysis of this study compared with Lee (2001) and Greenbaum (1995) studies.

Causative Factors	Method/techniques	Authors	Summary	Comments
<p>-Geological data, topographic data sets (slope, aspect), Forest data sets (type, diameter, age, density), Soil data sets (texture, topography, material, drainage, depth)</p> <p>(Scale1: 25,000-1:50,00)</p>	<p>Remote sensing interpretation integrated with topographic maps and field survey, On the basis of GIS tool and probability analysis</p>	<p>Lee (2001) Yongin area, Korea</p>	<ul style="list-style-type: none"> - Bivariate Statistical -probability ratio is as a weighted - Simple to implement and test - Data and analytically intensive - Relies on quality data - Result map based on 1 model. - Relative hazard level 	<p>Using the probability method, the spatial relationship between landslide occurrence location and each landslide related factors such as slope, aspect, curvature and so on, were calculated. The analysis method is bivariate and likelihood ratio method. The landslide susceptibility index (LSI) is calculated by summation of each factor's type and landslide susceptibility map was made as the LSI value index.</p>
<p>- Geological data, slope angle, lineaments, elevation and catchments.</p> <p>(Scale: 1:100,000 -1:50,000)</p>	<p>Air Photo and remote sensing interpretation integrated with topographic maps and field surveys using GIS techniques Probability and weighting analysis</p>	<p>Greenbaum et al.(1995) Papua New Guinea</p>	<ul style="list-style-type: none"> - Multivariate statistical - Statistical weighted - More complex to implement - Very data and analytically intensive - Relies on highly quality data - Result map based on 5 models. - Relative hazard level 	<p>Input to GIS database for multivariate modeling. Using the probability method, compile a map in combination of the bedrock, slope steepness, elevation and lineaments. The complied map will be composed of cartographic units delineating certain bedrock type and slope values, e.g. Bedrock Sandstone on slope between 25-50%. Weighting was used to identify the reliability probability and accountability probability of each factor. The landslide susceptibility map was produced from recalculated weightings within combination of reliability and accountability weights.</p>

Table 2.5 The method of landslide susceptibility analysis of this study compared with Lee (2001) and Greenbaum (1995) studies, (continued).

Causative Factors	Method/techniques	Authors	Summary	Comments
- Land use/cover, lithology unit, lineament, slope angle, slope aspect, elevation, flow direction, soil unit, NDVI (Scale: 1:100,000-1:50,000)	NDVI, Landsat TM, Landsat 7, Aster and IRS1-D image interpretation Probability and weighting analysis	Present study Teerarungsigul (2006) Wang Chin Area ,Northern Thailand	- Bivariate Statistical - Statistical weighted - More complex to implement - Very data and analytically intensive - Relies on quality data - Result map based on 3 models. - Relative hazard level	Nine factors are used for assessing debris flow hazard using GIS and Remote Sensing techniques. All data are inputted to GIS database. Using the probability method, the spatial relationship between landslide occurrence location and each landslide related factors such as slope, aspect, and curvature and so on, were calculated. The analysis method is bivariate and probability ratio method. Weighting and Ranking were used to identify the reliability, Probability and accountability probability of each factor. The landslide susceptibility maps were produced from reliability, accountability, and combinations of both weightings. Then compared these map with landslide slope stability map of Guenther (2004).

CHAPTER III

METHODOLOGY

A landslide hazard map was generated to identify areas with differing landslide hazard degree. This map is divided the entire study area into sub-areas based on the degree of a potential hazard from landslides. The landslide hazard map is produced by analysing the data represented by the maps of inventoried landslides and the factors found to influence the occurrence of landslides.

In this study, the factors related to landslide were chosen according to the triggering factor, human activities, geographic environment and types of landslide. The methodology is the combination between probability method of bivariate analysis, and ranking and weighting of factor's important on landslide occurrence. The result is landslide hazard map. Then, the result was validated with the past landslide event using probability method, and was compared with the slope stability map of the study area derived from Guenther's slope stability model.

Assessing relative landslide hazard is the objective of the method described in this chapter. The research will be carried out according to the six categories of the methodology. The flow chart of thesis methodology is shown in figure 3.1.

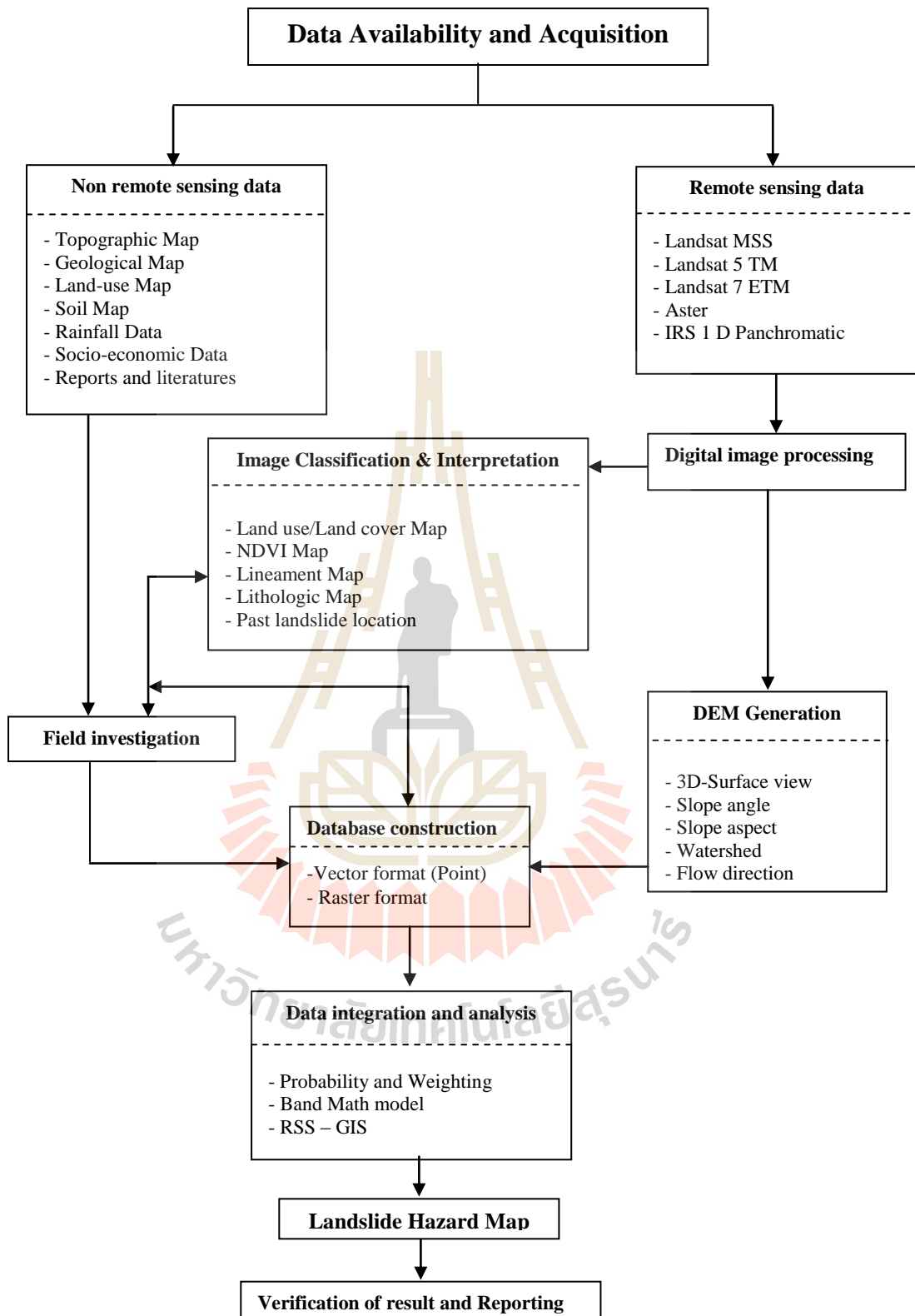


Figure 3.1 Flow chart of thesis methodology.

3.1 Data Acquired and used

The first task of this study includes collecting, storage and selecting all data and information that is available, derived from remote sensing as well as field investigation and of necessity for this study. All kind of data and information will be collected, mapped and reformatted if required and stored in GIS as a database.

According to the data sources, data acquired and used for landslide hazard assessment can be divided into two groups, remote sensing data and non-remote sensing data.

3.1.1 Remote Sensing Data

Remote sensing is one of the most important data for landslide assessment. It is very useful in detecting and mapping landslide scars/landslide location, land use/land cover, forest, topographical, and geological conditions.

There are several types of remote sensing data, which are used to integrated landslide hazard assessment. Data of the Landsat TM, Landsat 7, ASTER, and IRS-1D (PAN) could be acquired for this study. Table 3.1 shows an overview of the satellite data used for this study, and Table 3.2 summarizes the major technical parameters of the satellites and the data recording sensors.

3.1.2 Non-Remote Sensing Data

Non-remote sensing data comprise all maps from available data sources and fieldwork, which are related to the study area such as topographic map, land use/land cover map, geological map, lineament map, etc. as well as other relevant reports and documents collected from concerning organizations (Table 3.3).

Table 3.1 Overview of satellites data of the study area.

No.	RS-system	Path/Row	Acquisition date	Image quality Cloud coverage
1	Landsat MSS	140/48	26 January 1973	Quality is very good; no clouds
2	Landsat 5 TM	130/48	10 April 2001	Quality is very good; no clouds
3	Landsat 7 ETM	130/48	14 March 2001	Quality is very good; no clouds
4	Landsat 7 ETM	130/48	28 November 2001	Quality is very good; no clouds
5	Aster	-	28 November 2001	Quality is very good; no clouds
6	IRS-1D	126/026	27 December 2001	Quality is very good; no clouds



Table 3.2 Technical parameters of the satellite remote sensing systems used.

List	Landsat TM	Landsat 7	Aster	IRS-1D (PAN)
Operating Country	USA	USA	USA and Japan	India
Year of Launch	1984	1999 (failure in 2005)	1999	1997
Orbit (km)	720	720	705	780
Repetition Cycle (days)	16	16	16	24
Sensor	Scanner (7 bands multispectral)	Scanner (7 bands multispectral, 1 Panchromatic)	Scanner(3 bands VNIR, 6 bands SWIR, 5 bands TIR)	Scanner (Panchromatic)
Spectral Bands (micrometer)	0.45-0.52 0.52-0.60 0.63-0.69 0.76-0.9 1.55-1.75 10.40-12.50 (TIR) 2.08-2.35	0.45-0.52 0.52-0.61 0.63-0.69 0.78-0.90 1.55-1.75 10.40-12.50 (TIR) 2.09-2.35 0.52-0.90 (Pan)	(VNIR 0.52-0.60, 0.63-0.69,0.76-0.86 (Nadir and Backward looking)), (SWIR 1.60-1.70, 2.145- 2.185, 2.185-2.225, 2.235-2.285, 2.295- 2.365, 2.360-2.430), (TIR 8.125-8.475, 8.475-8.825, 8.925- 9.275, 10.25- 10.95, 10.95-11.65)	0.50-0.75
Ground Resolution (m)	30x30 120x120 (TIR)	30x30 60x60 (TIR) 15x15 (PAN)	15x15 (VNIR) 30x30 (SWIR) 90x90 (TIR)	5.8x5.8
Field of View (Km)	185x170	185x170	60x60	70x70

Table 3.3 Overview of non-remote sensing data types and sources for the study.

Data types	Scale	Original of data format	Sources
Geologic map	1:50,000	Shape file of Arc View	Department of Mineral Resources
Soil map	1:50,000	Shape file of Arc View	Land Development Department
Land use map	1:50,000	Shape file of Arc View	Land Development Department
Topographic map	1:50,000	Hard copy	Royal Thai Survey Department

3.2 Methods of Remote Sensing Data Processing and Interpretation

The remote sensing laboratory that has been setup by Thai-German Technical Cooperation Project since January 2000 consists of the personal computer, ENVI 4.1 image processing software and a HP 2500 plotter (A0, photographic quality), which is used to process and classify satellite images in this study.

All of the remote sensing data for the Wang Chin area are provided in digital format. This original data was already corrected for systematic and radiometric errors and stored on CD in standard remote sensing formats. Further digital data processing was carried out in the framework of the research. Purpose of image processing is to derive enhanced imagery for data interpretation and mapping. The functional categories of image processing are shown in Figure 3.2 and described as follows.

3.2.1 Image Processing

In this study, digital image processing can be carried out for image registration, image enhancement and image classification. During the digital processing, new or altered digital images are created, which show information of interest in enhanced conditions. The processed image is interpreted, visually and/or

digitally, to extract information about the target object, which was illuminated. It was aimed on the extraction of geological information, land use/cover, NDVI and digital elevation model (DEM).

The categories of digital image processing are herein demonstrated with reference to IRS-1D Pan and Landsat 7 satellite image data but the techniques are equally applicable to other sets of digital image data.

Image registration: Generally, image registration is the process of superimposing an image over a map or another already registered data. The geometric registration process involves identifying the image coordinates (i.e. row, column) of several clearly discernible points, called ground control points (GCPs), in the distorted image, and matching them to their true positions in ground coordinates (e.g. latitude, longitude). The true ground coordinates are measured from a map in hard copy or digital format or collected with GPS in the field. This is called image to map registration, which is used for registration all satellite image in this study.

All satellite images are registered using the image to map geocoding-techniques with reference to the Thai-Vietnam Map Datum, UTM Map Grid Zone 47 (Figure 3.3a-3.3b).

Image enhancement: The purpose of image enhancement is to make the images more interpretable for specific applications. Image enhancement is the modification of an image in order to alter its impact on the viewer. Generally, image enhancements change the original digital data values, and it should be carried out after geo-coding. Image enhancement is able to highlight features of thematic interest (lithology, lineaments, land use/cover, etc.) and to suppress redundant information.

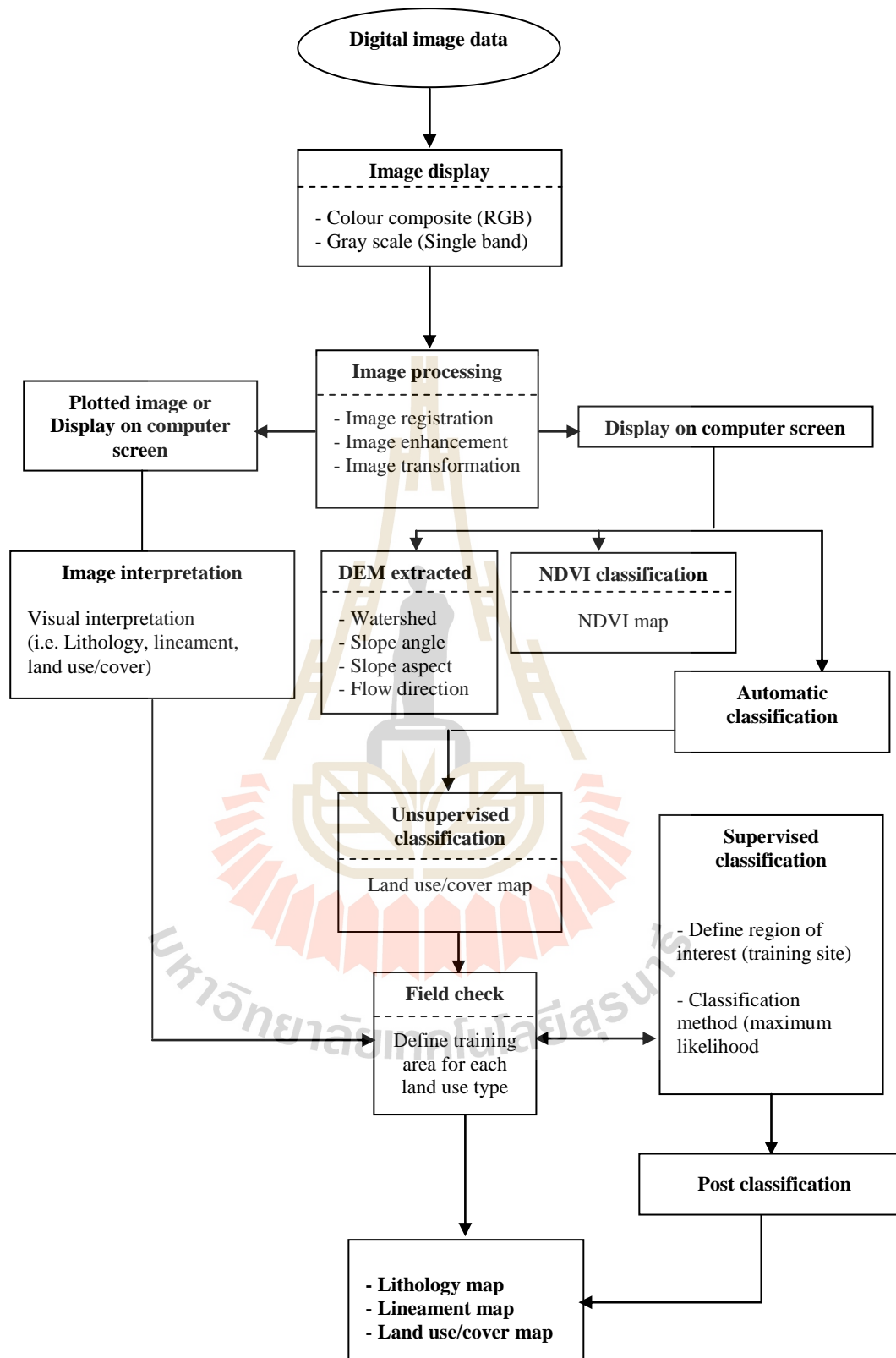


Figure 3.2 Flow chart shows the method applied of remote sensing.

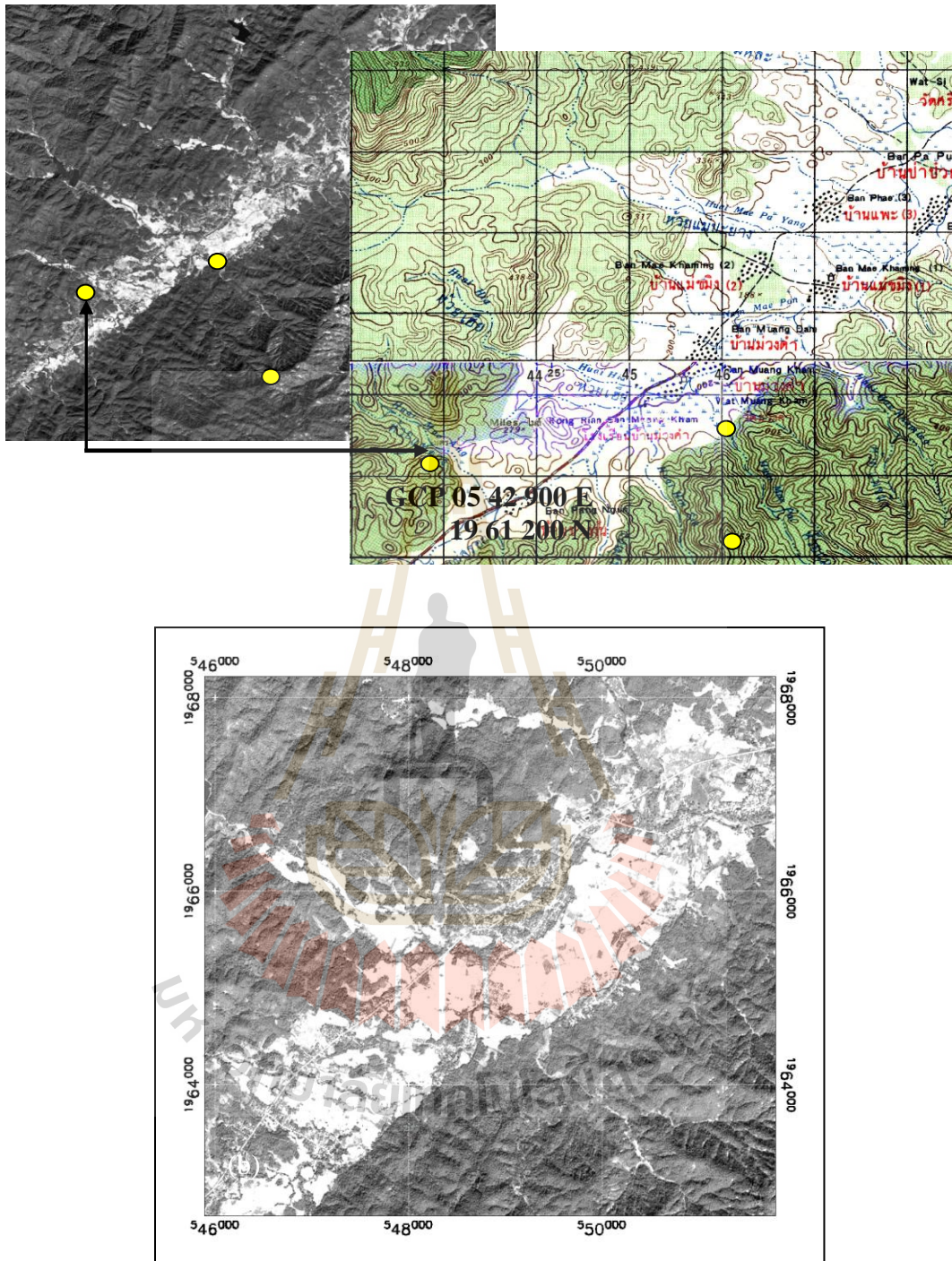


Figure 3.3 (a), concept of the image-to-map registration using ground control points, which are uniquely located on the image and on the 1:50,000 scale topographic map. (b), Geocoded IRS-1D satellite image.

Contrast, RGB-colour composite and spatial filtering enhancements are major tools applied on image enhancement in this study.

1) Contrast enhancement involves changing in the original brightness values, which is increased the contrast between target objects and their backgrounds. Nominally, an 8-bit image corresponds to a dynamic range of 256 grey tones. Original images usually occupy only small portions of the possible brightness range. Therefore, they appear dark and low contrast. Contrast enhancement is an image processing techniques that improves the contrast ratio of the image. The original narrow range of the digital values is expanded to utilize the full 8-bit dynamic range of available digital values. It is also called contrast stretching (Sabins 1997). In the case of 3-band Landsat TM False Colour Composites, it is often necessary to stretch each of the single bands independently. This leads to balanced colour tones allowing the maximum discrimination between certain targets at the ground surface (Figure 3.4a-3.4b).

The most frequently used contrast stretching types in this study is the linear expansion of the digital value range. Depending on the distribution of the digital values in the input image, and depending on the interpretation targets, selected portions or of parts of an image (region of interest) of the data can be expanded. Apart from the standard linear stretching, Gaussian, equalization, special user defined approaches are used to test. The distribution of the digital values of the image before and after linear stretching is defined by the histogram (Figure 3.5a-3.5b).

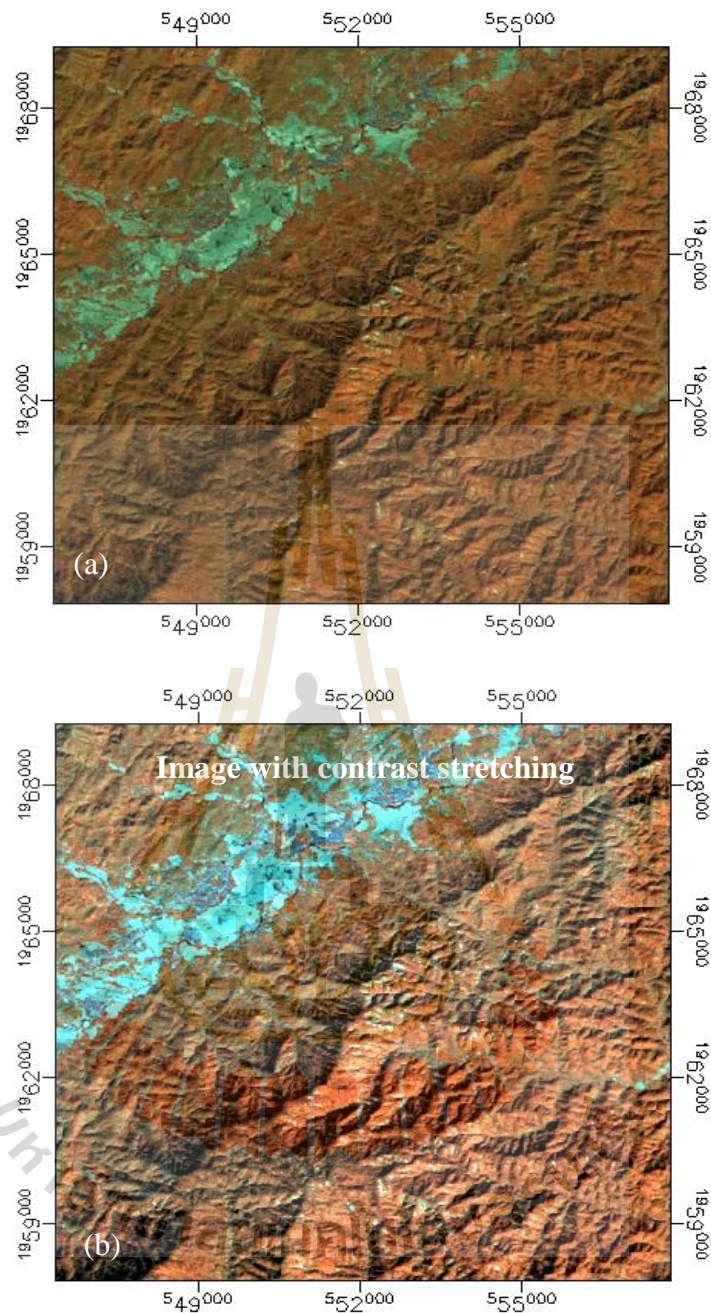


Figure 3.4 (a) Image without stretching; (b) linear contrast stretching enhancement applied to each of the three Landsat 7 bands 4, 5, 7 and coding with the colors Red/Green/Blue: land cover units can be distinguished more clearly in the stretched image.

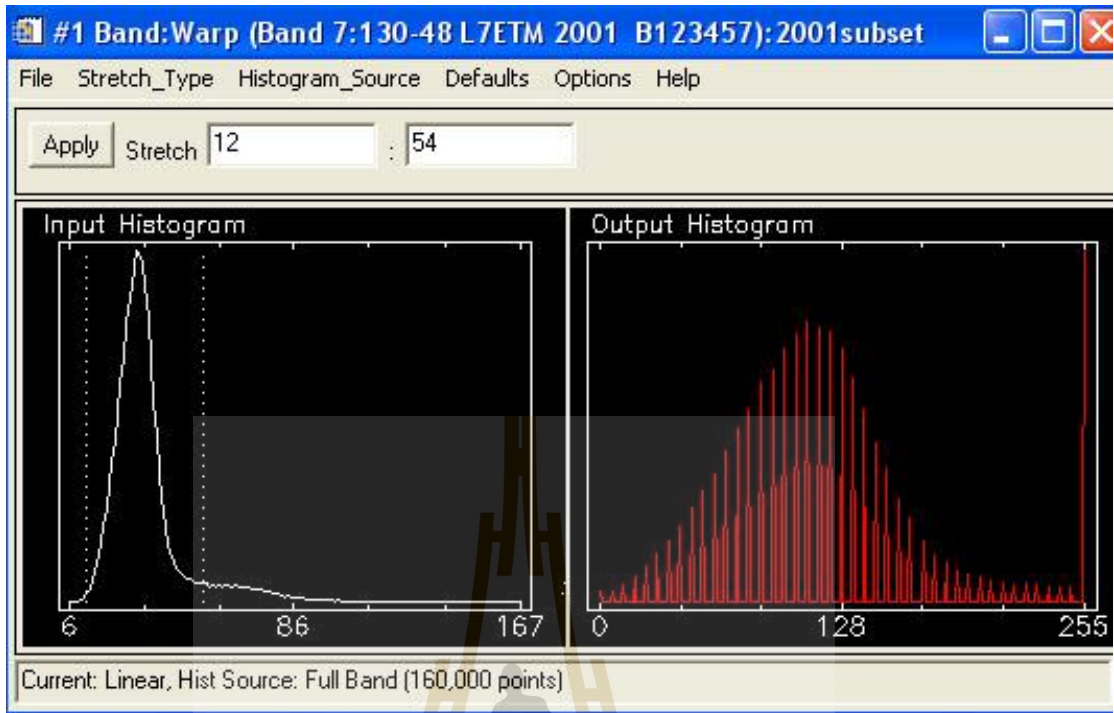


Figure 3.5 (left) Histogram showing the limited dynamic range as it is typical for original image data, (right) the dynamic range of the same image after application of linear stretching.

Contrast enhancement is a quantitative operation. Therefore, it relies on the subjective judgment and experience of the operator who decides when an image has the right contrast and colour balance for the final visualize and hard copy out put. For the Wang Chin area, it was important to apply in a way that allowed the optimum discrimination of land use/cover units, rock types, lineament and other targets of interests.

2) The RGB-colour composite image is image, which was prepared by combining three individual images in blue, green and red. It is one of the simplest ways to enhance features of interest by digital image processing in the following steps:

- Selection of the 3 single spectral bands, which show the highest differences in the locations of the clusters characterizing the investigation targets (cf. Gupta, 1991).

- Mixing of any of the three primary additive colours red, green and blue in various proportions is defined by the grayscale values of the pixels of three selected single bands of an n-dimensions multispectral data set.

The resulting colours of the colours composite image are defined by the RGB Colour Diagrams (cf. Gupta, 2002). BGR-Transformation is the most frequently used techniques in image processing. It is mostly combined with contrast stretching applied to any of the three selected bands. For Landsat TM and Landsat 7, most common band combinations are Band3/Red, Band2/Green, and Band1/Blue for colour composite images showing the terrain in natural-like colour (Figure 3.6), and Band4/Red, Band3/Green, Band2/Blue for false colour composite (FCC) image displaying vital vegetation in deep red colours (Figure 3.7). Depending

on the particular spectral response of targeted objects at the ground surface and the number and dimension of the spectral bands of the sensor controlled FCC images can be processed in order to highlight certain features at the ground surface.

3) Edge enhancement is an image processing technique that emphasizes the appearance of edges and lines in the image. Edge enhancement is achieved by spatial filtering or convolution using a box filter (kernel). General goal of edge enhancement is to increase the brightness difference between each pixel and its immediate neighbours. The filter kernel can be defined in different ways, so that high and low frequencies, as well as given directions can be emphasized or suppressed. A filter kernel procedure involves moving a window of a few pixels in dimension (e.g. 3x3, 5x5, etc.) over each pixel in the image, applying a mathematical calculation using pixel values under that window, and replacing the central pixel with the new value (Figure 3.8). The window is moved along in both the row and column dimensions one pixel at a time. The calculation is repeated until the entire image has been filtered and a new image has been generated. In this way, “edge”, i.e. abrupt changes in brightness within the image, such as lines or boundaries, appear emphasized and the overall image appear shaper (Figure 3.9). In this study, edge enhancement is a very useful tool for geological mapping, e.g. lineaments detection, and geological boundaries interpretation.

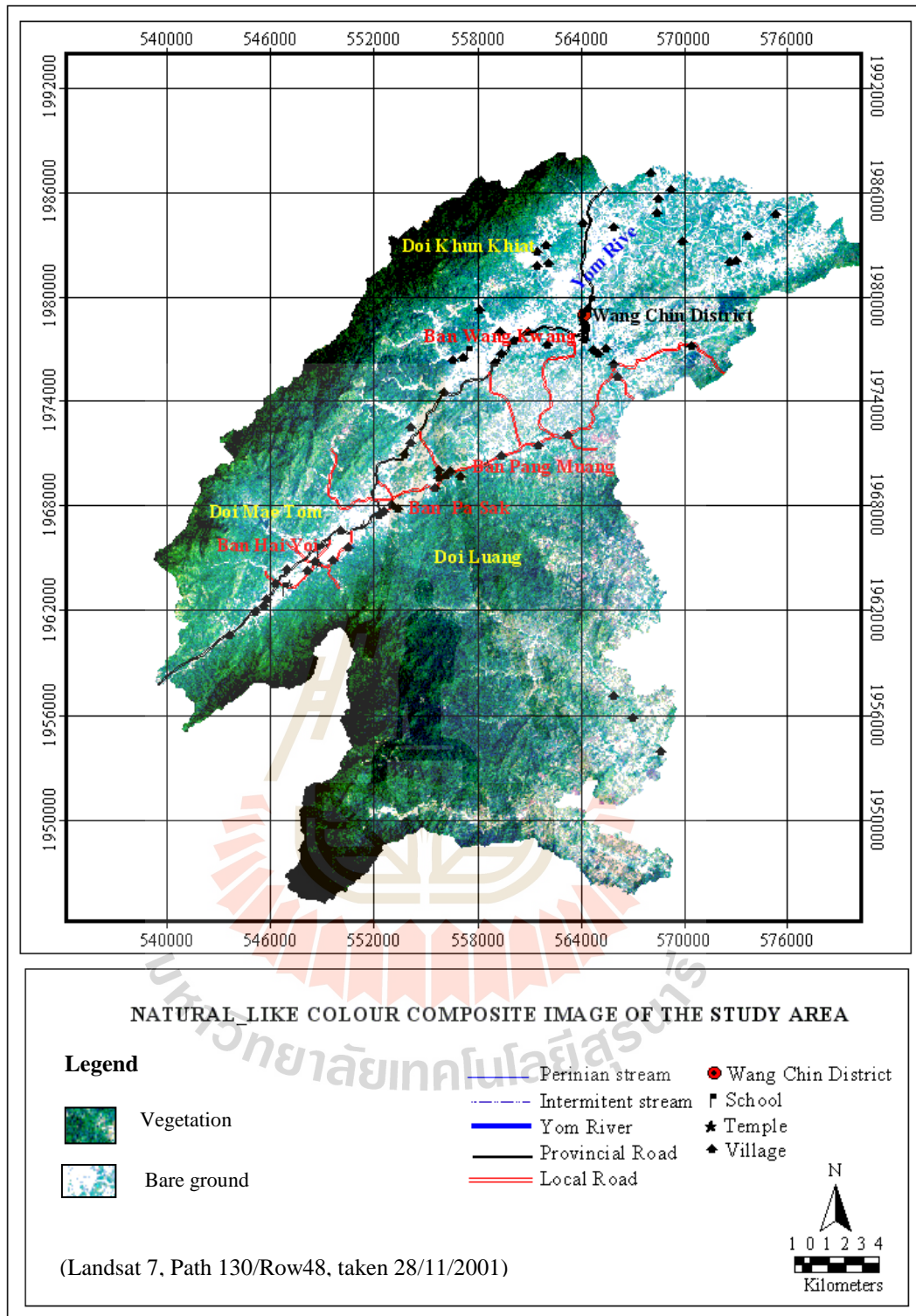


Figure 3.6 RGB composite images showing the terrain in natural- like colour based on band 3/Red, band 2/Green and band 1/blue of Landsat 7.

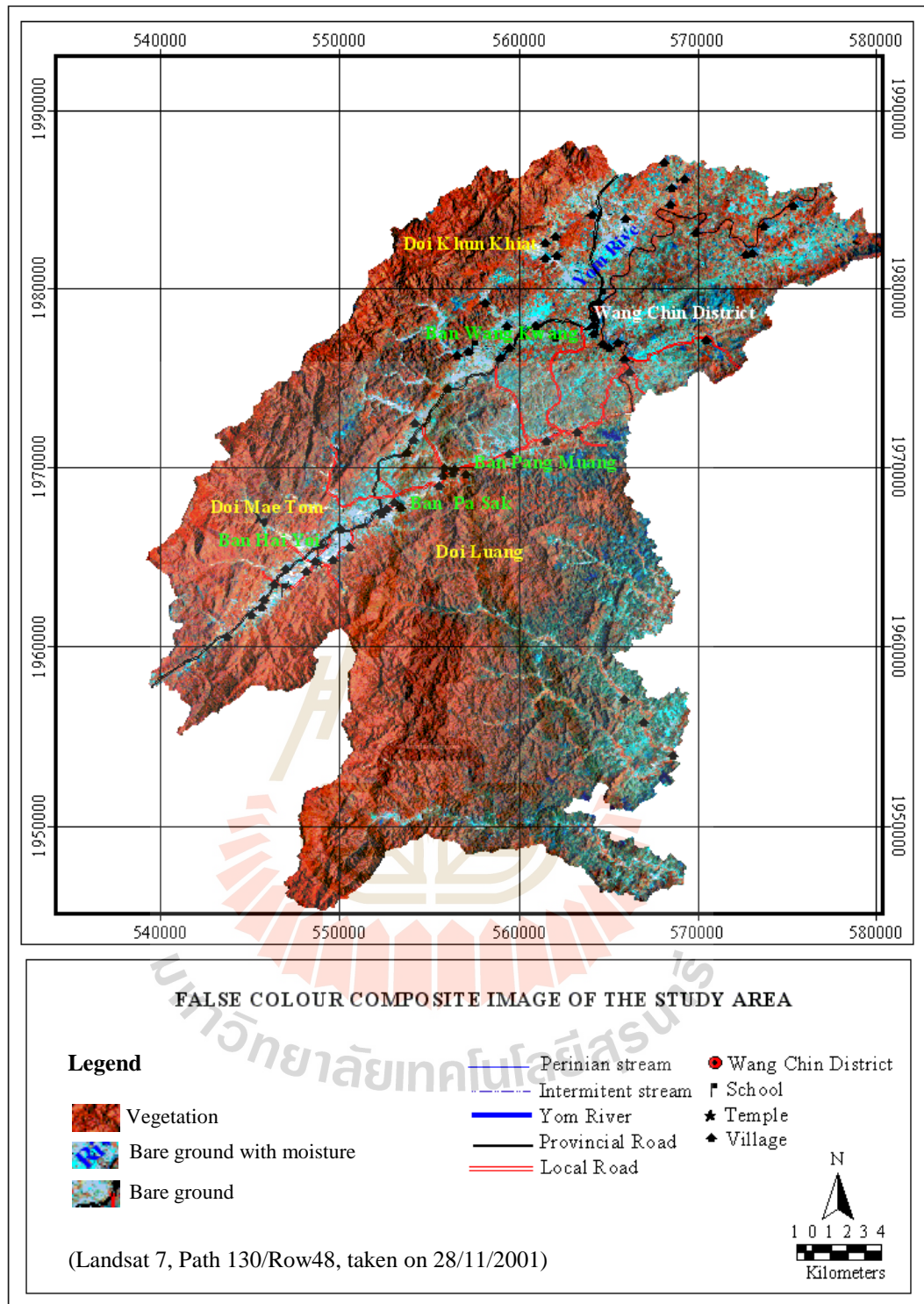
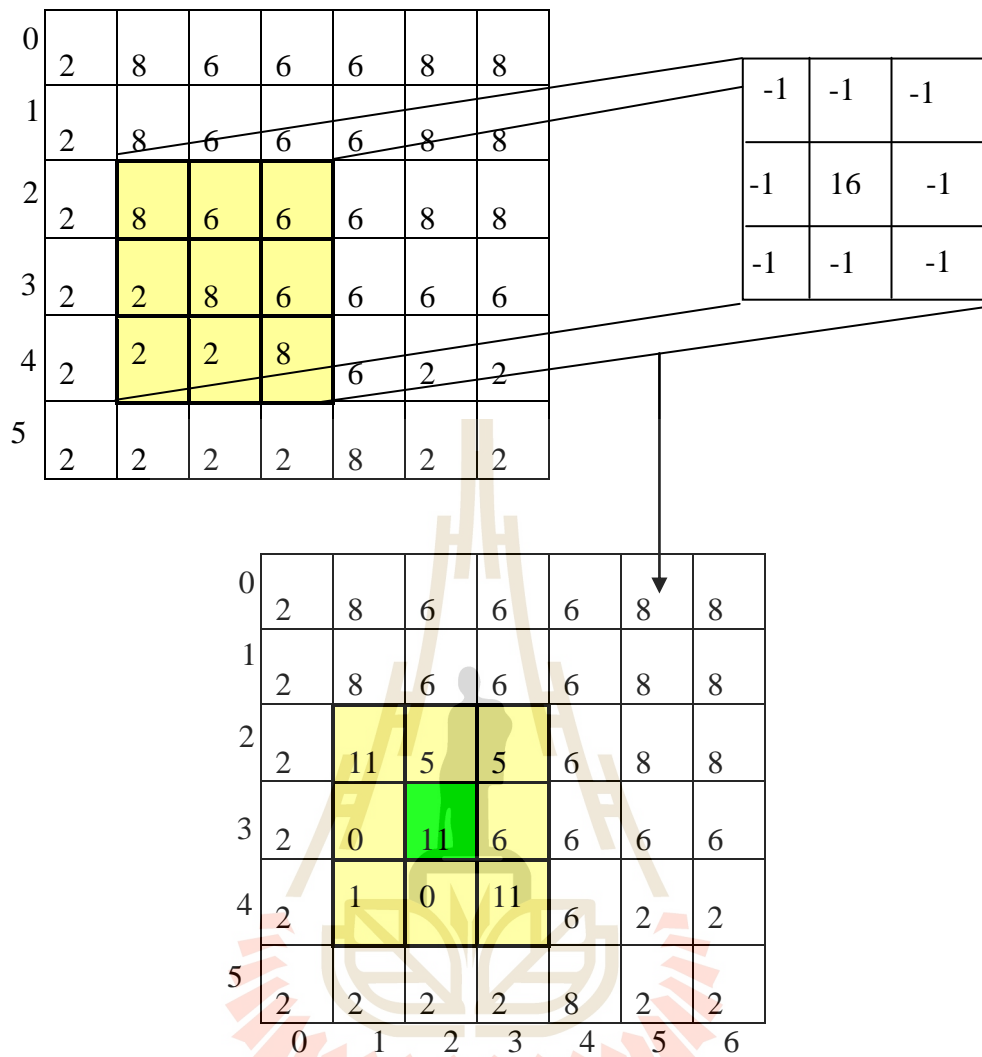


Figure 3.7 RGB in false colour composite image showing the terrain based on band4/Red, band 5/Green and band 7/Blue of Landsat 7.



$$\begin{aligned}
 11 &= \text{integer}\{(-1 \times 8) + (-1 \times 6) + (-1 \times 6)\} + \{(-1 \times 2) + (16 \times 8) + (-1 \times 6)\} + \\
 &\quad \{(-1 \times 2) + (-1 \times 2) + (-1 \times 8)\} / (-1 + -1 + -1 + -1 + 16 + -1 + -1 + -1 + -1) \\
 &= \text{int}\{(128 - 40) / (16 - 8)\} = \text{int}(88 / 8) = \text{int}(11) = 11
 \end{aligned}$$

Figure 3.8 A 3x3 convolution kernel being applied to a pixel in the third column, third row of sample data (the pixel that corresponds to the center of the kernel) (modified from Yamakawa *et. al.*, 1998).

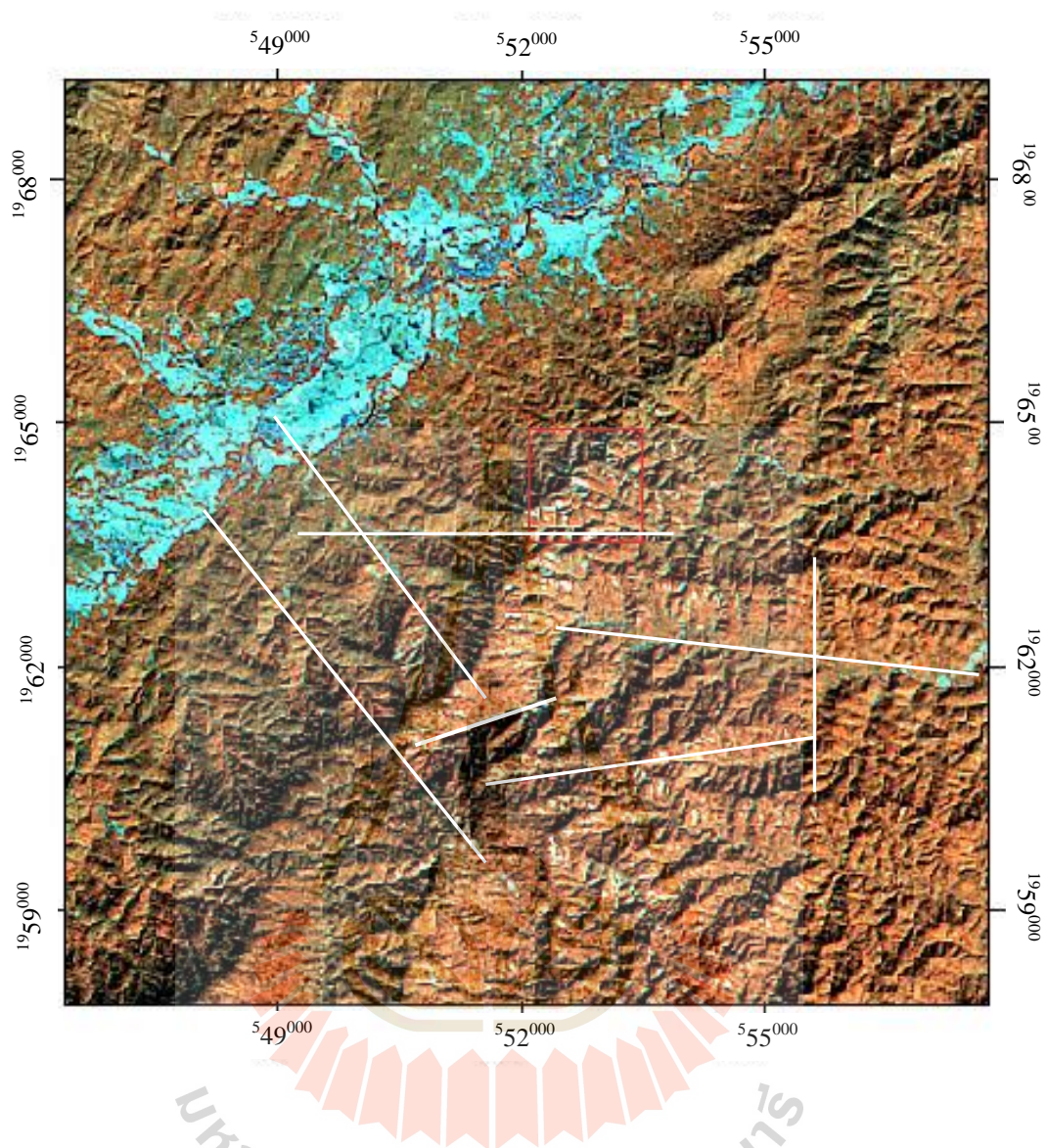


Figure 3.9 The edge-enhanced image is the result of 3 x 3 kernel high pass filtering and highlights linear arrangements of small topographic features that can be interpreted as lineaments (white color lines) (Landsat 7, Path 130/Row 48, taken on 28/11/2001).

Image transformation: Image transformations typically involve the manipulation of multiple bands of data, whether from a single multispectral image or from two or more images of the same area acquired at different times (i.e. multi-temporal image data). Image transformations generate new images from two or more sources, which highlight particular features or properties of interest, better than the original input images. Image division or band ratio and principal component analyses were used in this research.

1) Image division or band ratio serves to highlight subtle variations in the spectral responses of various surface covers. In this study, band ratioing has been used in the version of the NDVI in order to characterize the land cover by assessing the degree of vegetation coverage. For example, the healthy vegetation reflects strongly in visible red. Other surface types, such as soil and water, show near equal reflectance in both near infrared and red portions. Thus, a ratio image of landsat 7 Band 4 (Near Infrared) is divided by Band 3 (Red) would result in ratios much greater than 1.0 for vegetation, and ratio around 1.0 for soil and water. This is also used for land use/land cover interpretation. The normalized difference vegetation index ($NDVI = \frac{Band4 - Band3}{Band4 + Band3}$) is used to detect vegetation conditions in the study area. The ranges of NDVI are from zero (0) to one (1). When the land is free of vegetation, the NDVI value is assigned to zero, and when the land is covered with full vegetation, the NDVI approaches one.

2) The principal component (PC) transformation is used to compress the number of multispectral data sets by calculating a new image coordinate system. Gupta (1991) describes the theoretical background and the advantage of the principal component transformation as follows:

- Most of the variance of multispectral data set is compressed into the first three PC images.
- Noise is generally relegated to the less-correlated PC images.
- Spectral differences between materials may be more apparent in PC images than individual bands.

The use of principle component analysis in this study, six bands of Landsat 7 data set may be transformed such that the first three principal components contain over 90 % of the information in the original six bands (Figure 3.10). These three bands can be used to improve visual interpretation of land use/land cover and landslide detection. The image in Figure 3.11 shows how this technique can be used to map area affected by landslide (pink colour). Using the same procedure, certain features of land use/cover can be addressed more reliably, too.

3.2.2 Data Interpretation

Satellite imagery can provide information on previous and recent land use/cover, geo-hazards, geological structures (faults, fractures or lineaments), erosion and depositional processes in time and space and on other issues. Furthermore, items of infrastructures including the road net works and settlements can be mapped. In the present study, different types of satellite images were used in order to contribute to identifying the land use/cover characterize, to mapping lineaments, to assessing the scope of landslide-hazard, to extract digital elevation model, to updating topographic maps and to acquiring other useful information relating to various developments and planning activities.

The method of data interpretation for gathering this information can be divided into visual interpretation and automatic interpretation. The two methods will

be described below (cf. Figure 3.2).

Visual interpretation: The visual interpretation uses hard copy plots of the digitally enhanced remote sensing data. Either the visually derived information such as traces of lineaments, features representing boundaries between rock and soil units, and land use categories, which can be annotated onto a transparency sheet overlaying the plotted-image or it can be directly digitized on the computer screen using geographic information systems.

In this study, the visual interpretation was used for the Landsat TM, Landsat 7, Aster, IRS-1D and IRS-1D merged with Aster satellite images. FCC images TM4/Red, TM5/Green, TM7/Blue, and TM4/Red, TM3/Green, TM2/Blue as well as natural-like coloured composites TM3/Red, TM2/Green, TM1/Blue of Landsat7 were processed and visualized on the computer screen and as photographic hard copies in given scales. These techniques are equally applicable to other sets of digital image data such as Aster and IRS-1D merged with Aster images.

Categories of land use/cover like the forest, deforestation and teak plantations were identified and mapped by discrimination on the image processing display screen using Arc View 3.2-GIS or traced onto transparencies overlaying the geometrically rectified and geo-coded hard copy.

Automatic interpretation: The automatic interpretation is a technique of digital processing of remote sensing data. The concept of automatic interpretation is the classification of pixels of the multispectral data set into various thematic groups, based on the multispectral responses. In this case, the spectral response of certain surface materials is used to automatically identify and extract specific pieces of information. Precondition is that the operator instructs the computer which kind of

information is required, and which information has to be suppressed. For the Wang Chin study, automatic image classification techniques were employed to classify land use/land cover information.

In order to classify selected land use/land cover categories in the Wang Chin area, a combined approach of unsupervised classification and supervised classification was applied as follows:

- 1) Unsupervised classification process was conducted using the ENVI 4.1 ISO-data cluster analysis tool. The unsupervised classification divides the pixel into statistically defined classes (Figure 3.12). The programme creates a new image in which the pixels are arranged in clusters, groups or classes depending on their spectral properties and the number of classes set. Then the interpreter assigns each class with a name. Primarily the programme has defined the number of classes by unsupervised classification image, which was produced with ENVI 4.1. The resulting of number of classes from this processes were reviewed and then combined together, or broken down further. In addition, the classification results were verified by field checking. Each of the classes was then assigned with a certain land cover types. In this case study, the unsupervised classification provided the input information for the supervised classification.

- 2) Supervised classification identifies the homogeneous representative samples of the different surface cover types (information classes) of interest in the imagery. These sampling areas are referred to as training areas. The selection of appropriate training areas is based on their knowledge of the actual surface cover types present in the image, and on the field check results of the unsupervised classification. Each of the training areas should be representative for the

land use/land cover categories of interest (Figure 3.13). They should consist of one percent of the measurement space, and be mutually exclusive, homogeneous and comprehensive. Furthermore, sufficiently large number of pixels should be available for the training of the computer, usually 10 to 100K, where K is the number of spectral bands. Statistically, each class should exhibit a normal distribution. The aim of the training is to enable the computer to identify patterns based on a-priori ground truth.

Next step is the attempt to check how far the classes can be distinguished from each other using multispectral data. This leads to decision rules, which then are used to classify the rest of the scene automatically (Gupta, 1991).

Figure 3.14 shows some of the training sets located in the study area. Their locations and sizes are indicated by colour rectangles. Most of the land use categories are represented by more than one training site in order to cover the full range of reflectance characteristics. The resulting supervised classification image is shown in Figure 3.15. Colours represent the major terrain classes, and black indicates unclassified pixels. The estimated classification error is 15 percents.

3.2.3 Digital Elevation Model Data Generation

In this study, Digital Elevation Model (DEM) data are provided by automatically generated from ASTER satellite data. DEM data are generated from Aster stereo pair (level 1B) of 1,980 pixels x 4,200 lines (75 x 63 km, band 3N and 3B) as shown in Figure 3.16.

DEM data are essential for landslide hazards investigation since they are base data to derive relevant topographic information such as slope angle, slope aspect, watershed boundary, and stream network.

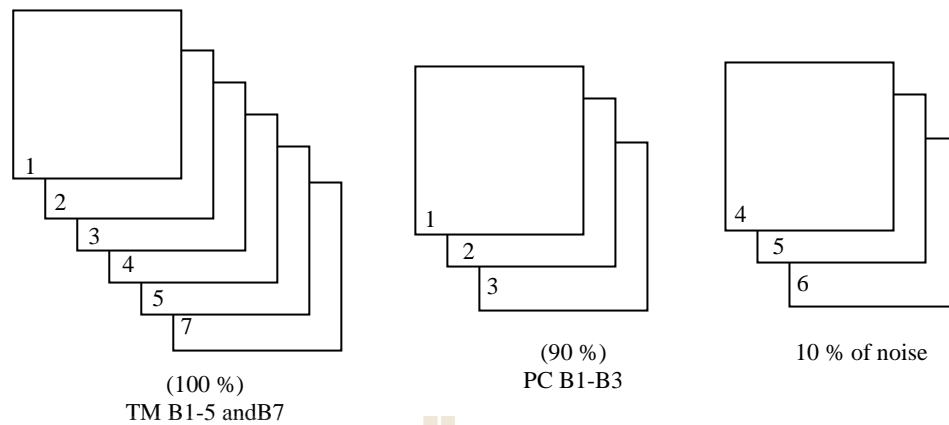


Figure 3.10 Example of the use of principal components analysis, a six-band Thematic Mapper (TM) data set may be transformed such that the first three principal components contain over 90 percent of the information in the original six bands.

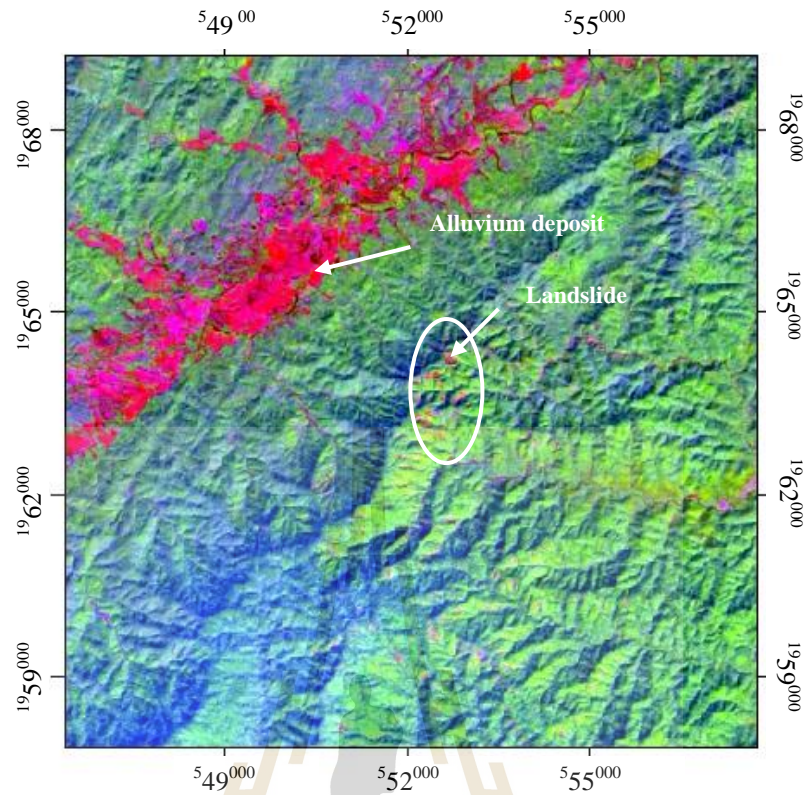


Figure 3.11 RGB color composite based on PC1/Red, PC2/Green and PC3/Blue, area of landslide and alluvium deposit (pink color) can be separated from the other area.

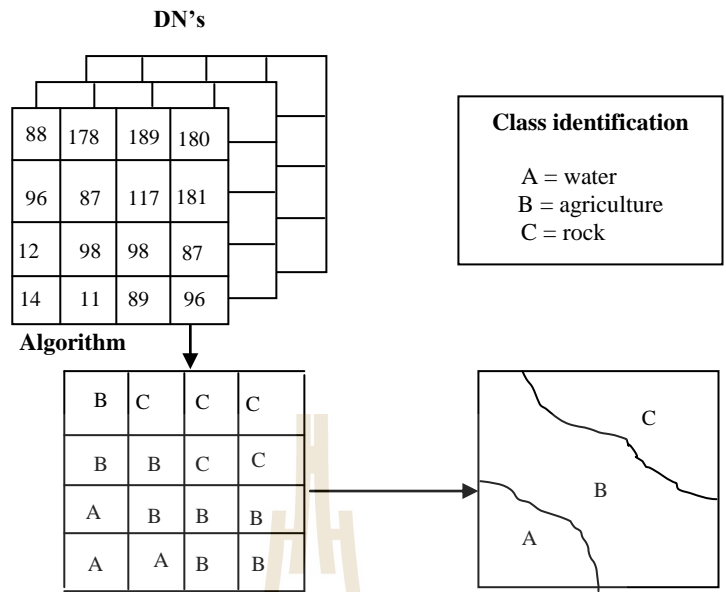


Figure 3.12 A Clustering algorithm of unsupervised classification dividing the pixel into statistically defined classes (modified from Alfoldi, 2000).

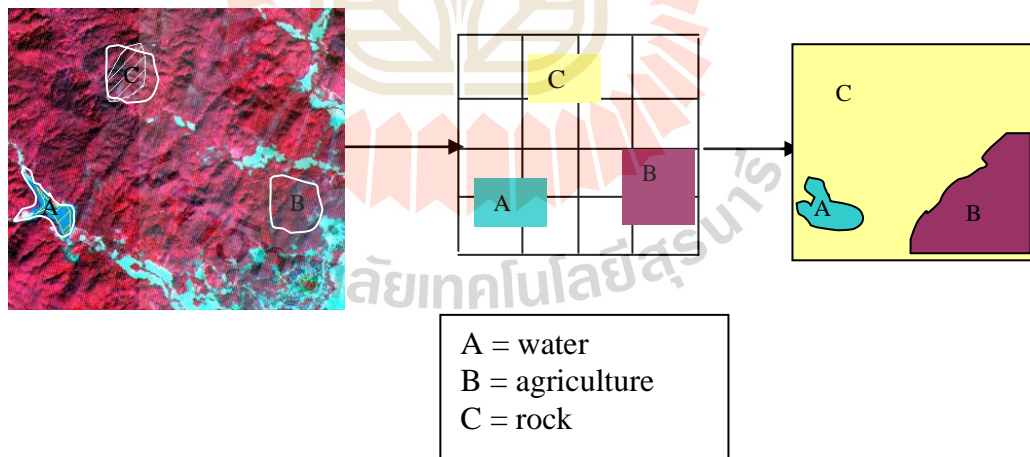


Figure 3.13 Supervised classification; the analyst identifies in imagery homogeneous representative samples (training areas) of the different surface cover types (information classes) of interest (modified from Alfoldi, 2000).

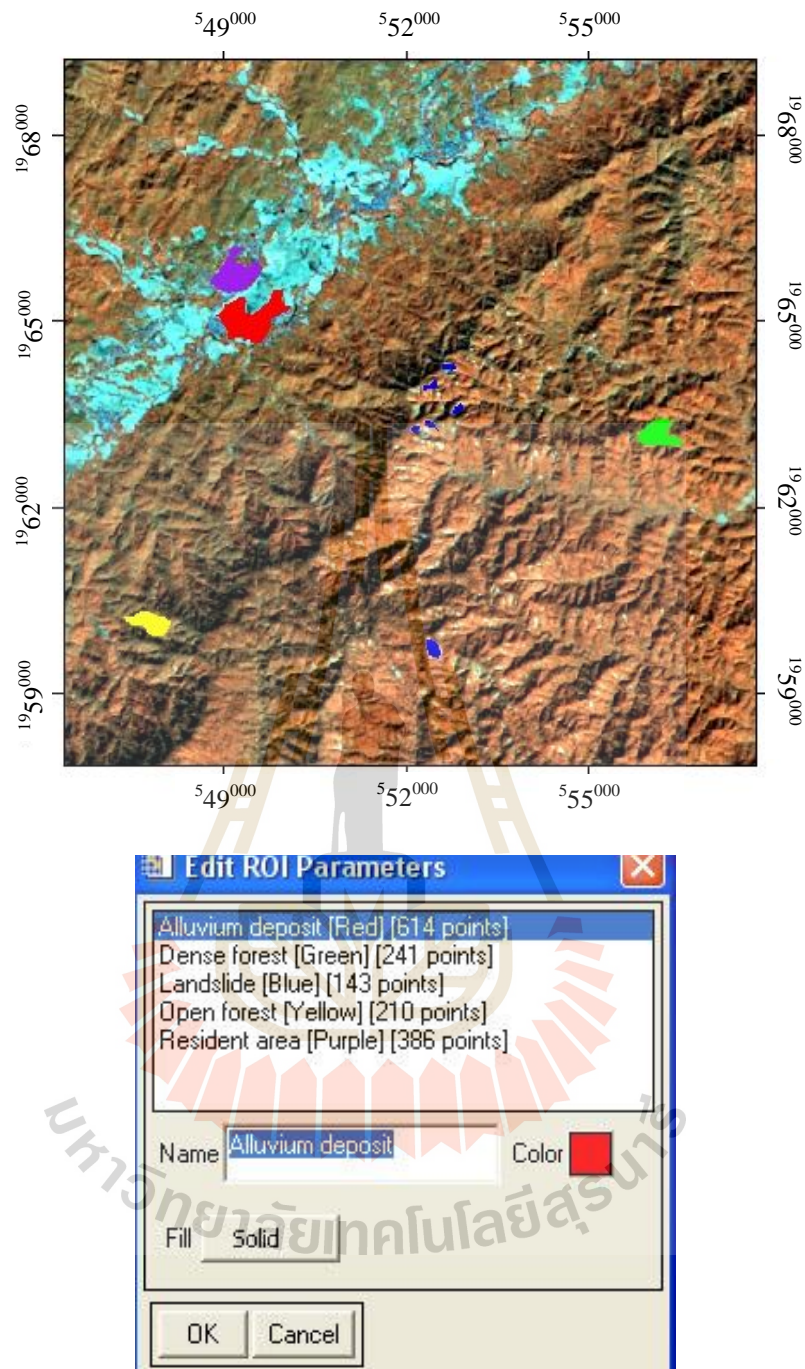


Figure 3.14 Training sites selected for supervised classification on Landsat 7, Path 130/Row 48, taken on 28/11/2001 (colored rectangles).

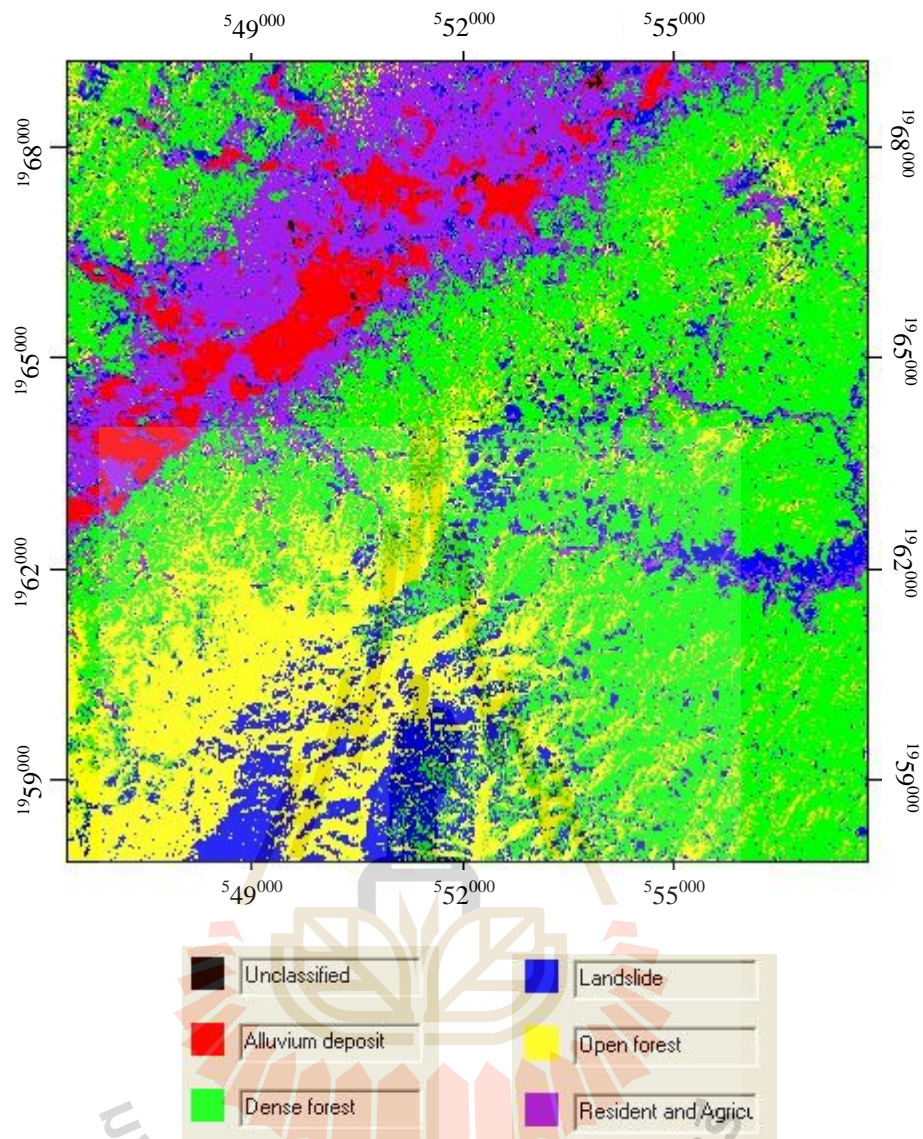


Figure 3.15 Result of the supervised classification for some part of the Wang Chin area (Landsat 7, part 130/Row 48, taken on 28/11/2001).

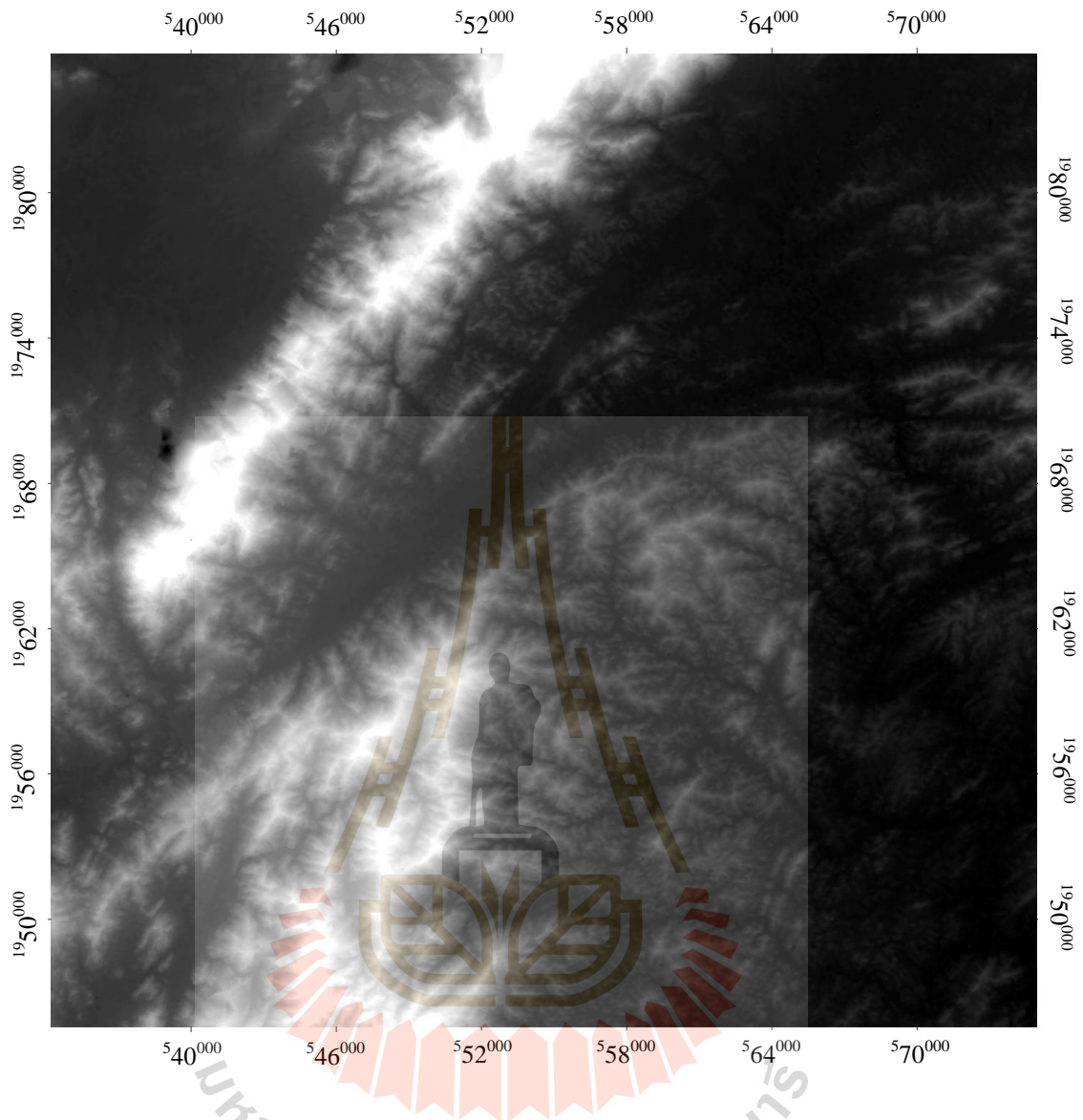


Figure 3.16 Digital elevation model (DEM) data generated from Aster satellite data (band 3N and 3B) taken on 28/11/2001 (white colour is high elevation, black colour is low elevation)

3.3 Fieldwork

In this study, fieldwork is an important part of the remote sensing data interpretation. It is crucial precondition for the provision of accurate and reliable interpretation results. Field checking was carried out as follows:

- 1) Record and documentation of the GCPs with hand-held GPS.
- 2) Spot-check and to verification of image interpretation result.
- 3) Data and information collection for the automatic image classification.
- 4) Collected ground truth information for the comparison with the processed satellite images and preliminary products.
- 5) Collected background information by interviewing locals (on reasons of land use changes, past landslide events, etc.).

During the investigations, landslide locations recognized on remote sensing data will be verified. All types of slope failure will be identified and classified. Other factors related to landslide (e.g., geological map, soil map and land use map) were updated by spot-check depending on accessibility.

3.4 GIS Grids Preparation

This step will describe the technique of GIS and database construction conducted in this study (Figure 3.17).

3.4.1 GIS Technique

In this study, map overlay functions and other functions of the Arc View are used to perform the database for the spatial analysis of landslide assessment. The functions that will be used to construct the database map and to analyse the relationship between landslide occurrence and related factors, are shown as follows:

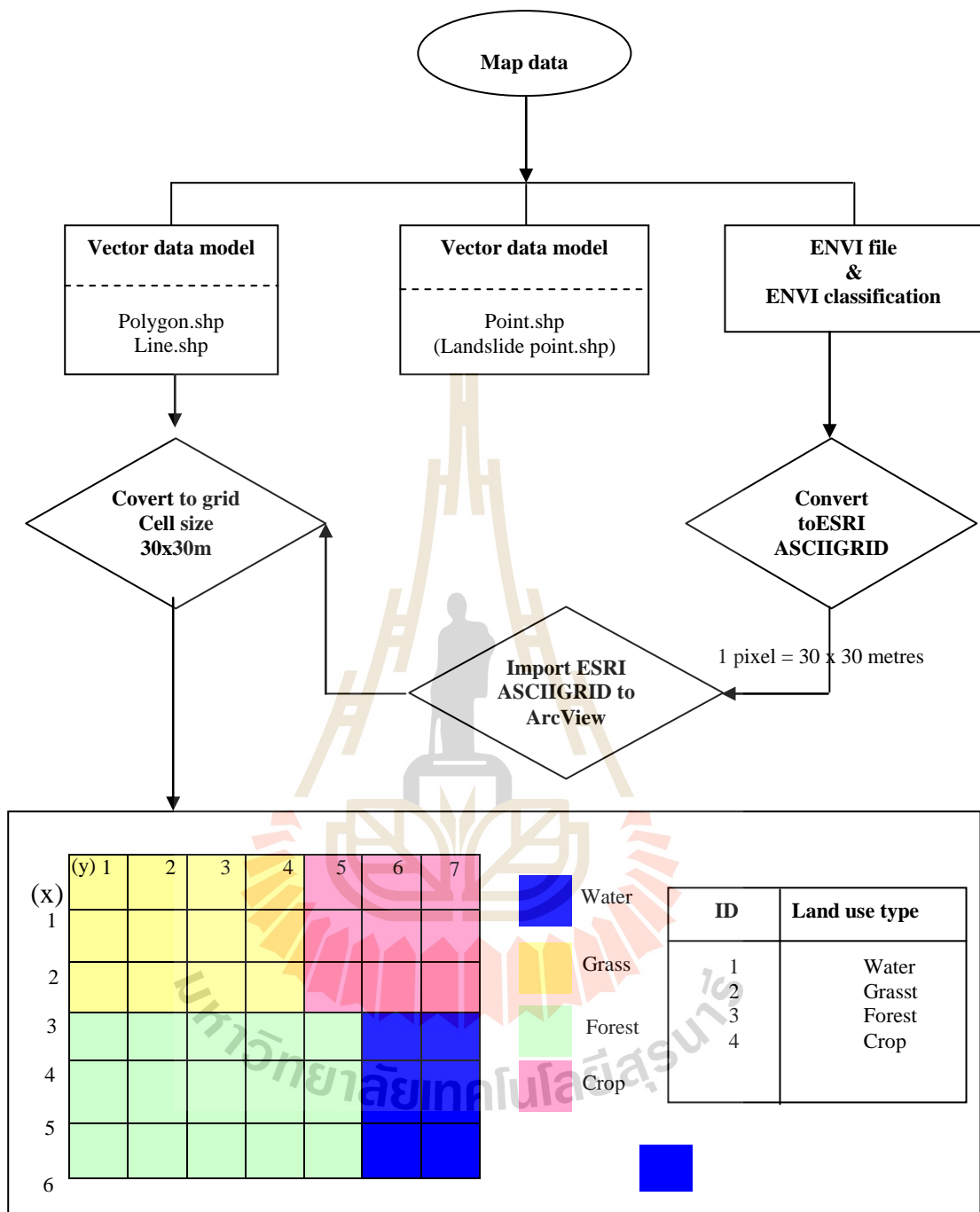


Figure 3.17 Flow chart of the database construction into GIS.

Buffer zone: Buffer command of Arc View is used to prepare the lineament buffer map, which has a distance of 100 metres, 200 metres, and 300

metres, 400 metres, 500 metres, 600 metres, 700 metres, 800 metres, 900 metres and 1000 metres from the lineament location, respectively. This map will be used to analyse the relationship between landslide occurrence and lineament factor.

Cross-tabulated area: A Cross-tabulated area of ArcView is used to sort out the relationship between different thematic data maps. It is the technique, which combines two spatial data layers, between landslide location map and individual factor map to produce the landslide occurrences on each factor map. The principle concept of spatial cross-tabulated technique is to compare the characteristics of the same location on both data layers, and to produce a new characteristic for each location in the output data layer, for example, the display of landslide locations on the land use/land cover type (Figure 3.18).

Data classification: The data classification tool of Arc View was used for creating new attribute data and new maps as well as for data visualization. Raster data reclassification is an important function in data exploration and data analysis. Creating a new raster model by classification is often referred to as reclassification, recording, or transforming through look-up table. Two methods of data classification are used in this study. The first method is “one-to-one change”, meaning a cell value in the input grid is assigned a new value in the output grid. For instance, landslide occurrence in deforestation attribute of land use/land cover grid is assigned a value of 1 in the output grid map. The second method assigns a new value to a range of cell values in the input grid that is called “value to range of cell values change”. For example, grid cells with landslide hazard probability index between 0-25 in land use/land cover grid are assigned a value of 1 in the output grid. The following applications of data classification were used in this study.

1) Data isolation: Data isolation classification is used to create a new grid that contains a unique category or value such as deforestation or a range of value such as slope of 9-13 degree (Figure 3.19).

2) Data simplification: Data simplification classification is used to group continuous slope values, for example, into a set of classes, for instance, 1 for slope of 0-4 degree, 2 for slope 5-9 degree, and so forth.

3) Data ranking: Data ranking classification is used to create a new grid that shows the result of the ranking of cell values in the input grid. For example, a reclassified grid can show the rank of 1 to 5 with 1 for the least suitable and 5 the most suitable.

3.4.2 Data Base Construction

The data sets related to landslide occurrences in the study area were transformed to digital formats and stored as database of GIS. All data sets were built on a raster base (cell base) and assigned with an attributes database. Each pixel corresponds to a ground resolution cell of 30 metres by 30 metres, and contained the value (class number), symbol and class of data maps. The data maps and its attributes are constructed as a database into the GIS using ArcView 3.2 software.

The factors affected on landsliding are primarily lithology, lineament, elevation, slope steepness, slope aspect, land use/land cover, normalized vegetation index, flow direction of a watershed, soil type and past landslide location (Table 3.4). These can be divided into five groups of a factors map for this analysis as followings:

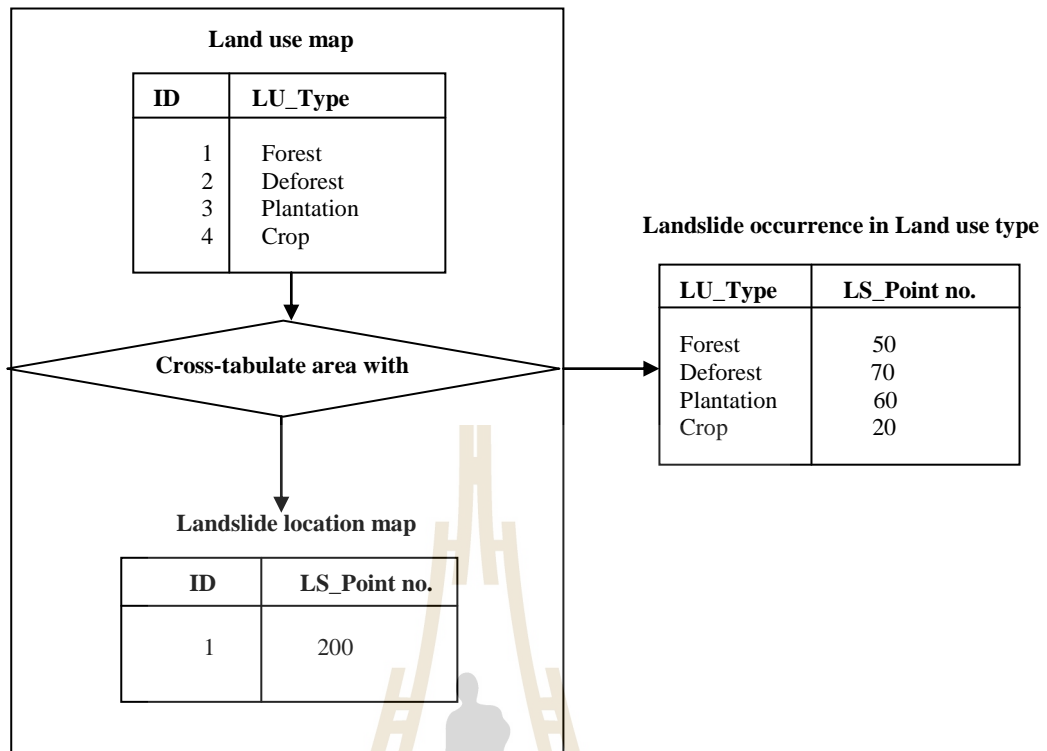


Figure 3.18 Concept of cross-tabulate area aggregation (modified from Alfoldi, 2000).

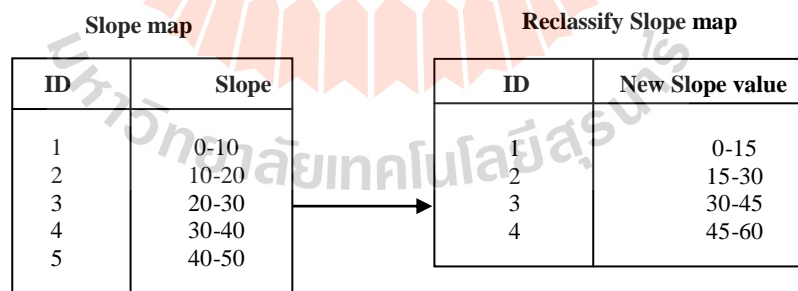


Figure 3.19 Concept of reclassification function (modified from Alfoldi, 2000).

Table 3.4 Factors map for landslide assessment of Wang Chin area.

Layer	Factor	*Value	Symbol	Class
1	Lithology	1 2 3 4 5 6 7 8 9 10 11 12 13	Qt Tr3 Qa Pm2 SD CP Pm3 Rht2 Tr3-2 Tr3-1 Rht1 Tr3-3 Pm1	Terrace: Sand, Silt, Gravel and Clay Shale, Sandstone and Conglomerate Alluvium: Sand, Silt, Gravel and Clay Limestone Phylite, Quartzite and Quartz-Schirst Undifferentiated Sandstone, Shale, Chert and Pebbly Shale Sandstone, Siltstone, Phylite and Quartz-mica Schirst Andesitic tuff Sandstone, Siltstone and Shale Shale, Sandstone, Siltstone and Agilaceous limestone Rhyolite, Andesitic tuff and Agglomerate Sandstone and Siltstone Conglomerate, Sandstone, Shale and Chert
2	Lineament	1 2 3 4 5 6 7 8 9	- - - - - - - - -	0 m – 100 m 100 m – 200 m 200 m -300 m 300 m – 400 m 400 m – 500 m 500 m – 600 m 700 m – 800 m 800 m – 900 m 900 m – 1,000 m
3	Land use/Land cover	1 2 3 4 5 6 7 8 9 10 11 12 13 14 15	- - - - - - - - - - - - - - -	Disturbed open forest Teak plantation Crop_Orchard Deforestation Crop Village Rain paddy field Teak_Crop Water body Orchard Waste land Teak Orchard Open forest Reservoir Deforestation_Orchard
4	NDVI	1 2 3 4 5 6 7 8	- - - - - - - -	-1.00 to -0.75 -0.75 to -0.50 -0.75 to -0.25 -0.25 to 0.00 0.00 to 0.25 0.25 to 0.50 0.50 to 0.75 0.75 to 1.00
5	Slope angle	1 2 3 4 5 6 7 8 9 10 11 12	- - - - - - - - - - - -	0°-5° 5°-9° 9°-14° 14°-19° 19°-23° 23°-28° 28°-32° 32°-37° 37°-42° 42°-46° 46°-51° 51°-56°

Table 3.4 Factors map for landslide assessment of Wang Chin area, (continued).

Layer	Factor	Value	Symbol	Class
5	Slope angle	13	-	56°-63°
6	Slope aspect	1	-	North
		2	-	Northeast
		3	-	East
		4	-	Southeast
		5	-	South
		6	-	Southwest
		7	-	West
		8	-	Northwest
7	Flow direction	1	-	North
		2	-	Northeast
		3	-	East
		4	-	Southeast
		5	-	South
		6	-	Southwest
		7	-	West
		8	-	Northwest
8	Soil unit	1	62	-
		2	47E	-
		3	47D/55C	-
		4	47C	-
		5	47B/29B	-
		6	47B/55B	-
		7	33	-
		8	18/5	-
		9	48C/55C	-
		10	29B/46B	-
		11	47D	-
		12	35B/61B	-
		13	48B	-
		14	18	-
		15	47B	-
		16	18/18B	-
		17	46B	-
		18	59B(59)	-
		19	15	-
		20	55B/61B	-
		21	59	-
		22	47C/49C	-
		23	47B/31B	-
		24	7/15	-
		25	47D/47E	-
		26	47B/447C	-
		27	7	-
		28	47C/47D	-
		29	47E/47D	-
		30	33B	-
		32	15/61B	-
		33	15/59	-
		34	59/61B	-
		35	61B	-
		36	15/33B	-
		37	47C/55C	-
		38	47B/56B	-
		39	47D/56D	-

Table 3.4 Factors map for landslide assessment of Wang Chin area, (continued).

Layer	Factor	Value	Symbol	Class
9	Elevation	1	-	17-122
		2	-	122-173
		3	-	173-224
		4	-	224-275
		5	-	275-326
		6	-	326-377
		7	-	377-428
		8	-	428-479
		16	-	836-887
		17	-	887-938
		18	-	938-989
		19	-	989-1040
		20	-	1,040-1,091
		21	-	1,091-1,142
		22	-	1,142-1,193
		23	-	1,193-1,244
		24	-	1,244-1,295
		25	-	1,295-1,346
		26	-	1,346-1,397
		27	-	1,397-1,448
		28	-	1,448-1,499
		29	-	1,499-1,550
		30	-	1,550-1,602

*Value of class ID

Geological factors: Lithological map and lineament map are grouped as a geological factor. These maps are modified from the geological map at the scale 1:50,000 and 1: 250,000, published by the Department of Mineral Resources. Then the remote sensing interpretation and field checking are conducted to verify these maps. In this study, lithological map delineate bedrock and/surficial units, based on rock type. Lineament map is represented by the bedrock structures, such as, fractures and faults.

Topographical and surficial material factors: The topographical factors represent surface units based on a number of terrain attributes, including surficial material genesis, surface expression and geomorphic process. These factors show the distribution of soil type, slope gradient, slope aspect, and elevation. Consequently, topographical factors database comprise soil map, slope angle map, slope aspect map, and elevation map.

Vegetation and Land use/Land cover factors: The vegetation factors represent the density of vegetation on the surface and type of vegetation. The land use map describes how a given area is being used for agriculture, settling, industry, national park and others. The land cover map describes the materials, which are present at the land surface. The land use map characterized their usage based on the human activities on the land. For example, the land cover of an area may be evergreen forest, but the forest may be used for recreation or various combinations of activities. These factors are derived from satellite image interpretation, and from the Land Development Department. These factor databases comprise land use/land cover map and normalized vegetation index map.

Hydrological factors: This study uses the watershed boundary and flow direction as a hydrological factor. It affects the peak flow rate of a stream and transportation of debris flow. Flow direction is generated from DEM.

Landslide location map: A map of existing landslides serves as the basic data source for understanding conditions contributing to landslide occurrence. This map was prepared by visual interpretation of satellite remote sensing imagery and field examination of selected locations. The accurate detection of landslides location is very important for landslide susceptibility analysis.

3.5 Spatial Data Analysis and Data Integration

The spatial data analysis and integration or factor analysis is a step-by-step approach used to prepare a landslide hazard zonation map of the study area (Figure 3.20). There are three steps to complete the factor analysis and produce a hazard map as follows:

3.5.1 Overlaying the Landslide Inventory Map on each Factor Map

The first step is to overlay the landslide distribution map with the factor map. This will identify which of the factor's attributes are associated with past landslides and which are not. Database of all factors from section 3.4 are used to prepare the maps that show the relationship between landslide occurrence and factors. The method applied is to cross-tabulate the past landslide location map with each factor map. Then, a landslide distribution table is developed and it indicates the total location of landslides occurring on each specific area of attribute of each factor.

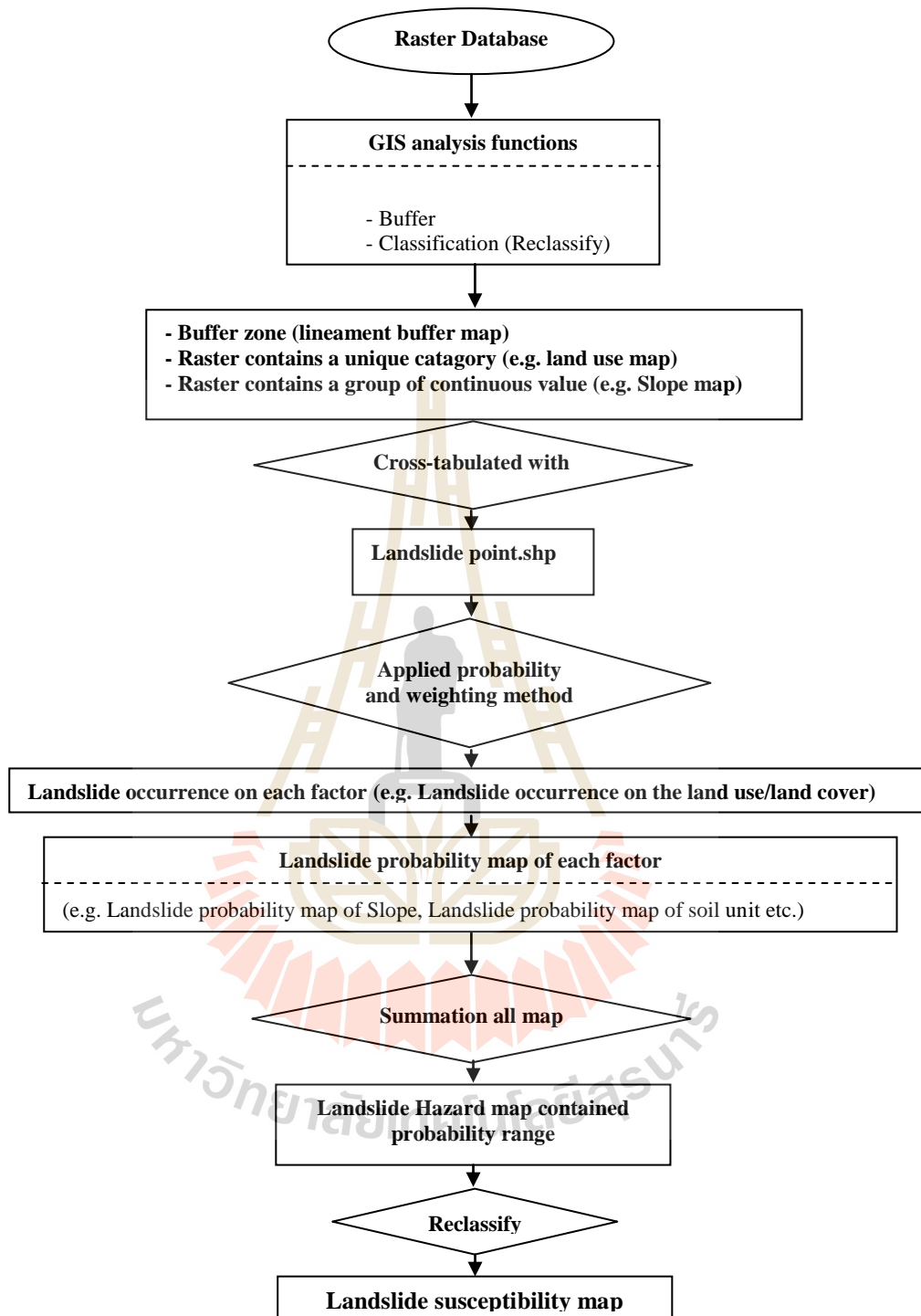


Figure 3.20 Flow chart shows the procedure of spatial data analysis and integration for landslide hazard assessment.

3.5.2 Landslide Assessment Analysis

This step is to group combinations of factors in order to classify and define the landslide hazard to five levels. This grouping is achieved by performing probability analysis, and ranking and weighting for assessing the factor's importance as follows:

Performing probability analysis: Probability of landslide occurrence is the chance of landslide probability hazard to occur. It can be represented as a real number between zero (0) and one (1). An impossible event has a probability of exactly 0, and a certain event has probability of 1, but the converses are not always true. Most probabilities that occur in practice are numbered between 0 and 1, indicating the event's position on the continuum between impossibility and certainty. The event's probability closer to 1 is the more likely to landslide occurrence.

The methodology used for landslide hazard assessment in this study is the "probability bivariate analysis". The probability of landslide occurrence is usually a spatial distribution. In this method, a statistical correlation between the probability of landslide occurrence and several factors' classes was carried out as follows:

1) The first step is to measure the percentage of the total number of landslide location, and the total area for every classes of every factor in the study area Then the total percentage of landslide location associated with each class of each factor is divided by the total percentage area of the same classes of factors found in the study area (3.1). This result represents the probability of landslide occurrence in each class of each factor.

$$\text{Probability of Landslide on each factor's class} = \frac{\% \text{ total landslide number in factor's class}}{\% \text{ total area comprising in the same class}} \dots (3.1)$$

For example, in the case of landslide occurrence on slope angle 19°-23° (class 5) of slope angle factor. The landslide occurrence probability on this class can be calculated as below:

$$\frac{\% \text{ total landslide number in slope class 5}}{\% \text{ total area of class 5}} = 16.00/9.58=1.67$$

This means that 16.7% (1.67x100) of landslides occur on the area with slope angle 19°-23° (class 5) and it is divided by percent of the total area of the same class (9.58%).

2) The second step, the probability of landslide occurrence for the whole area was calculated from percent total landslide number in the whole area divided by percent total of the whole area (equation 3.2).

$$\text{Probability of landslide for the whole area} = \frac{\% \text{ Total landslide points}}{\% \text{ Total area of study area}} = \frac{100}{100} = 1 \dots \dots \dots (3.2)$$

Then, the probability of landslide occurrence on each factor's class was compared with the probability of landslide occurrence for the whole area (equation 3.3). This result represents the probability ratio of landslide occurrence in each class of each factor compared with the probability of landslide for the whole area.

$$\text{Probability ratio of landslide on each factor's class} = \frac{\text{Probability of Landslide on each factor's class}}{\text{Probability of landslide for the whole area}} \dots \dots (3.3)$$

For example, the landslide occurrence probability on slope angle 19-23 degree from is 1.67 and it is compared with the probability of landslide occurrence for the whole area.

$$\begin{aligned} \text{Probability ratio of landslide on slope angle 19°-23°} &= \frac{\text{Probability of Landslide on slope angle 19°-23°}}{\text{Probability of landslide for the whole area}} \\ &= 1.67/1 = 1.67 \end{aligned}$$

This means that the incidence of landsliding on slope angle 19 - 23 degrees is 1.67 times greater than the probability of landsliding for the whole area. Considering as a measure of prediction, this slope category is 1.67 times more likely to occur than the whole area. Thus, the probability of landslide occurrence for the whole area is the mean value of landslide incidence for the study area and it is called the regional average incidence of landslides. This can be explained that if the probability ratio of landslide occurring in each class of each factor is greater than 1, it means a higher likelihood and if it's lower than 1 it means a lower likelihood of landslide hazard occurrence.

Ranking and weighting for assessing the importance of factor: The identification of potential landslide areas requires that the factors are considered to be combined in accordance with their relative importance to landslide occurrence. The importance of factors as a predictor of landsliding can be considered in different ways. Two possible approaches were used in this study. These approaches are the reliability probability method and the accountability probability method.

The reliability probability (RP) was calculated by the percentage area of factors corresponding to landslides. It was computed for each factor as equation 3.4.

$$RP = \frac{\sum \% \text{Landslide point in classes having a probability ratio} \geq 1}{\sum \% \text{Landslide \& non-landslide area in the same classes}} \dots (3.4)$$

The accountability probability (AP) was calculated by the total landslide population accounted for each factor. It was computed for each factor as equation 3.5.

$$AP = \frac{\sum \% \text{Landslide point in classes having a probability ratio} \geq 1}{\sum \% \text{Landslide point over the entire study area}} \dots (3.5)$$

According to the step of performing probability analysis, probability ratio of factor's classes less than 1 indicates a lower likelihood of landslides incidence and probability ratio of factor's classes higher than 1 indicates a higher likelihood of landslides incidence. Therefore, in both performance measures, only probability values of attributes ≥ 1 (i.e. mean and above mean value of landslide incidence) are considered. The mean landslide incidence value means the probability of landslide occurrence for the whole area (cf. equation 2.2). The results of RP and AP of each factor were used to ranking and weighting the relative importance of each factor on landslide occurrence.

The relative importance of factors to landslide occurrence can be achieved by developing a ranking scheme to factors. The straight ranking (the most important=1, second important=2, etc.) is used in this study. Once the ranking is established for a set of factor, the numerical weights from ranking values are generated. In this study, the weights were calculated according to the formula 3.6.

$$w_i = (n_j - r_i) + 1 \dots \dots \dots (3.6)$$

n_j is the number of factor under consideration whereas $j = 1,2,3,\dots,m$, with $m = 9$, in this study.

r_i is the rank position of each single factor considered ($1 \leq i \leq n$, with $n = 9$, in this study).

w_i is the weight of each single factor considered ($1 \leq i \leq n$, with $n = 9$, in this study).

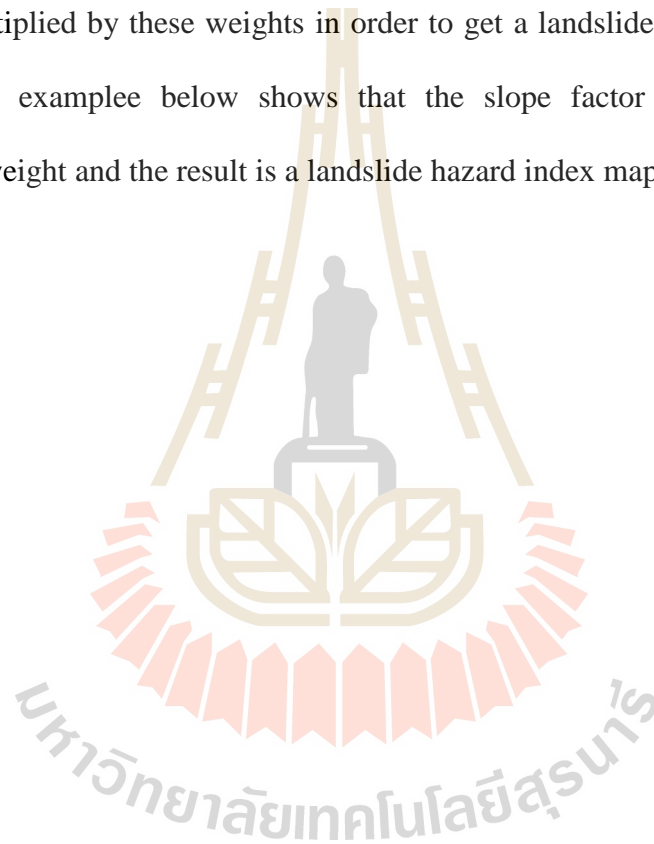
Before the weights can be combined, they need to be normalized. Each factor is weighted as $(n_j - r_i) + 1$ and then normalized by the sum of all weights, that is, $\sum (n_j - r_i) + 1$ as follow.

$$w(n_j) = \frac{(n_j - r_j) + 1}{\sum(n_j - r_j) + 1} = \frac{w_i}{\sum w_i} \dots \dots \dots (3.7)$$

$w(n_j)$ is the normalized weight of each single factor.

$\sum w_i$ is the sum of all factor's weights.

The normalized weights of each factors are represent to the relative importance of each factor. The probability ratio of landslide occurrence of each factor is multiplied by these weights in order to get a landslide hazard index of each factor. The examplee below shows that the slope factor is multiplied by its importance weight and the result is a landslide hazard index map (Figure 3.21).



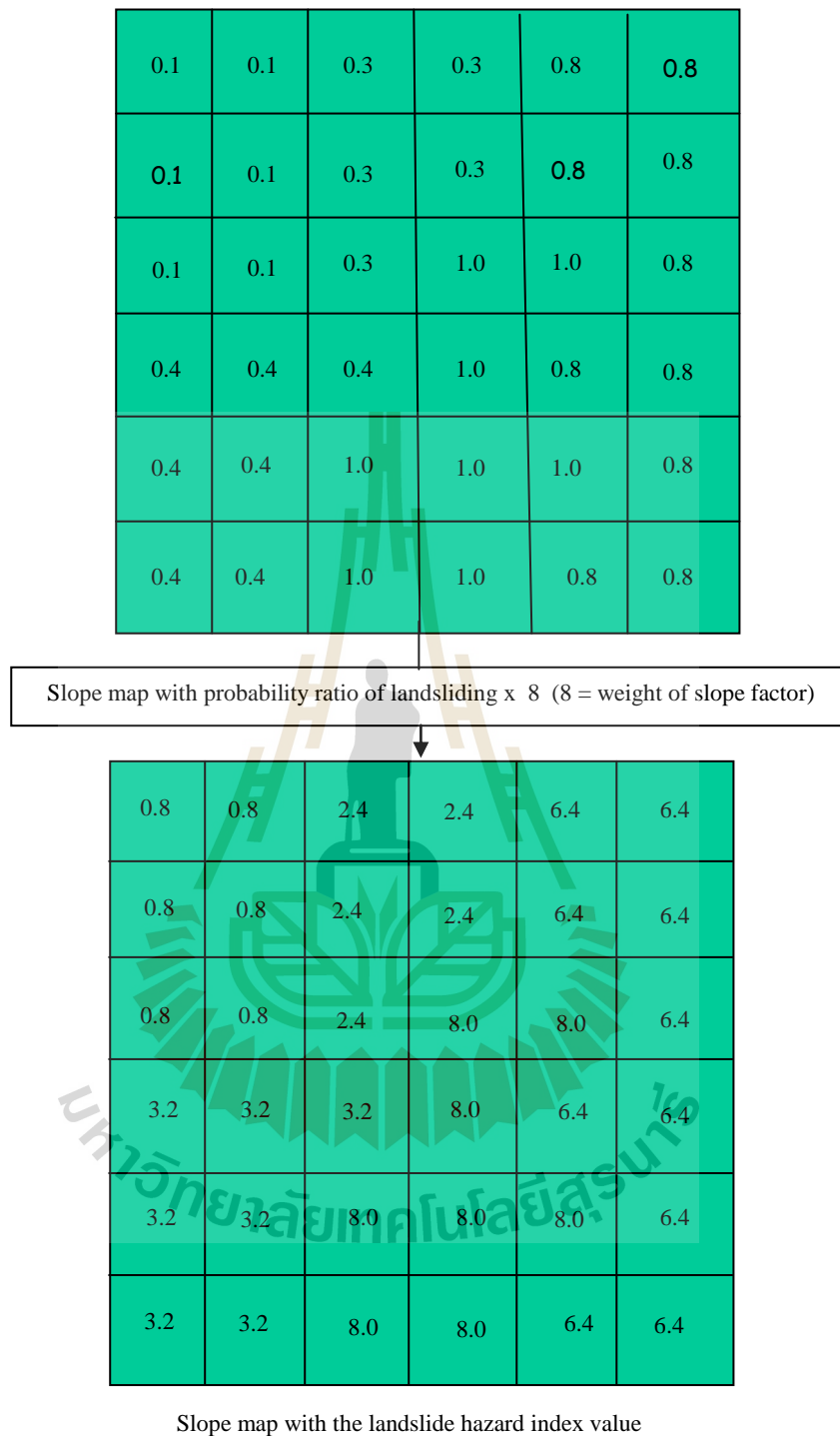


Figure 3.21 This example shows that the slope factor contained probability ratio of landslide occurrence is multiplied by its importance weight in order to get the landslide hazard index of slope map.

3.5.3 Producing Landslide Hazard Map

The third step uses the group combination to produce landslide hazard zone. The numerical data layers representing weight values of the factor attributes as the information of attribute were generated from the thematic data layers for data integration and spatial analysis in the GIS. The input data layers were multiplied by their corresponding weight and were added up to obtain the Landslide Probability Index (LPI) for each 30 by 30 m cell as the equation 3.8.

$$LPI = \sum_{j=1}^n (F_j W_j) = F_1 W_1 + F_2 W_2 + \dots + F_j W_j \dots \dots \dots (3.8)$$

F_j is the factor map, which is contained probability ratio of landslide occurrence.

W_j is the weight for factor j .

The landslide potential index map is used to produce landslide hazard zonation map. A judicious way for the landslide hazard zonation is to use the relative interval to separate the landslide potential index into landslide susceptibility class level. The level of landslide hazard is measured on the ordinal scale based on the equal interval values. Landslide potential index can be divided into very high, high, moderate, low, and very low of hazard levels in one single map as prediction image. The group of proportions with the larger value toward the end of the range represents combinations defining very high landslide hazard. The group of proportion with the smallest values represents very low landslide hazard. Landslide hazard map is useful for the development project planning or the areas, which should be avoided.

3.6 Band Math Approach for Landslide Prediction Model

3.6.1 Introduction

There are two ENVI's function tools, which can be applied for landslide prediction model development. The first one is a decision tree classifier. The second is a band math function tool. Both of them can be applied to a single image or to any other set of rasterized data, see ENVI Users Manual. The expression uses in ENVI's decision tree classifier are similar to a band math.

The decision tree classifier performs multistage classifications by using image or to any other set of rasterized data, see ENVI Users Manual. The expression uses in ENVI's decision tree classifier are similar to a band math.

The decision tree classifier performs multistage classifications by using a series of binary decision to place pixels into classes. They must produce single band output and have a binary result of 0 or 1. The 0 result is sent to the "No" branch and the 1 result is sent to "Yes" branch of the decision tree. The decision tree expression can be "pruned" and edited interactively. The tree can be saved and applied to other data sets of another area. Nevertheless, there is no single decision in the decision tree performs the complete classify of the image into classes. Instead, each decision divides the data into one of two possible classes or groups of classes.

Band math provides one of the simplest programming interfaces for adding processing functionally. Creating a single function for processing spatial data allows extensions of ENVI through these interfaces. This function can be used to call a customized processing function that have to be written and applied to other data set. The band math interfaces is used to define the bands or files used as input, call the function, and write the result to file or memory. Band math tool allows defining

their own processing algorithm and applying them to bands of all files opened in ENVI. The customized processing may be as a simple or complex.

In this study, the landslide prediction model was developed based on the band math tool. The base idea of band math is to link different sets of data according to a defined mathematic expression or formula. Precondition is that all data sets have the same size in terms of sample and line number, and are oriented over the same coordinate system. The band math input bands are the raster data selected for this operation. Input bands usually are single spectral bands or multispectral data sets, single bands of derived products, or rasterized point and vector data. Vector and point data have to be transformed to raster formats before using them as band math input data.

The mathematic formulas used in band math are simpler than the decision tree. A decision tree is made up of a series of binary decision that are used to determine the correct category for each pixel. Each decision divides the pixels in a set of images into two classes based on an expression. The result image produces single band out put and have a binary result of 0 (No) or 1 (Yes). The single decision tree classifier cannot complete the classification of an image into classes of interested. Therefore, the custom processing algorithms are more complicated than a band math.

The landslide prediction model was developed from data obtained from the result of probability analysis and weighting of factors of the study area. The purpose of landslide prediction model construction is to predict future landslide prone ground in the area that has similar condition factors i.e. lithology, elevation, and aspect, etc.

3.6.2 Basic Concept of the Band Math

Band Math provides one of the simplest programming interfaces for adding processing functionality. Creating a single function for processing spatial (Band Math) data allows extensions of ENVI through these functions. This Band Math function can be used to call a custom processing function that has written. The Band Math Tool is used to define the bands or files used as input, call the function, and write the result to file or memory. Band Math accesses data spatially by mapping the factors to bands of files.

A Band Math function is written using factors named b1 (or B1), b2, etc. The function is called by entering its names and factors in the Band Math expression text box. The factors are assigned to bands or files using the Band math dialog. For example, Figure 3.22 depicts the band math processing for the addition of three bands. Each band of an input image band was calculated by summing up together in the band math formula, and output as the resulting image data. Constructing Band Math, expressions are used the Band Math's array operators. Table 3.5 shows the array operators of the basic arithmetic and the relational operators that were used in this study, and Table 3.6 describes the order of precedence of each operator.

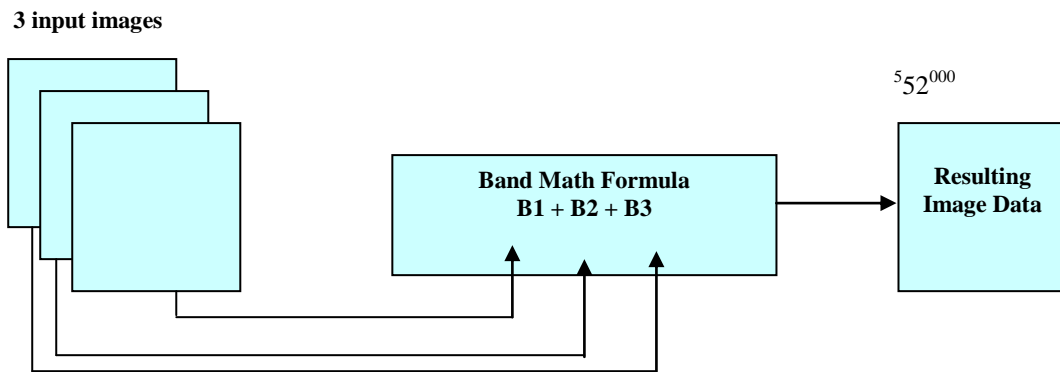


Figure 3.22 Band Math processes – Additional of three bands.

Table 3.5 The Band Math’s basic arithmetic and relational operators (from ENVI user’s manual online, 2006).

Category	Available function
Basic Arithmetic	Addition (+) Subtraction (-) Multiplication (*) Division (/)
Relational	Less than (LE) Less than or equal (LE) Equal (EQ) Not equal (NE) Greater than or equal (GE) Greater than (GT)

Table 3.6 The operator precedence (from ENVI user's manual online, 2006).

Order of precedence	Operator	Description
First	()	Parentheses to group expressions
Second	^	Exponents
Third	*	Multiplication
	# and ##	Matrix multiplication
	MOD	Modulus
Fourth	+	Addition
	-	Subtraction and negation
	<	Minimum
	>	Maximum
	NOT	Boolean negation
Fifth	EQ	Equal
	NE	Not equal
	LE	Less than or equal
	LT	Less than
	GE	Greater than or equal
	GT	Greater than
	Sixth	AND
OR		Boolean OR
XOR		Boolean exclusive OR

3.6.3 Landslide Prediction Model Construction

The landslide prediction model construction was carried out step-by-step as follow:

Factor database preparation: Band Math input data are the maps of nine independent factors, which have been derived already for the landslide susceptibility map. Before using these factor maps, each of them had to be transformed from Arc View raster format to an ENVI-readable format using the ENVI dialogs “Export File” and “Export Grids”. The resulting ENVI-readable files for the 9 factor layers are then in ASCII-format. Figure 3.23 shows a simplified scheme of this transformation. The files stored in ASCII-format are interim data and had been further transformed into ENVI raster format using the “ENVI Rasterize Point Data” dialog. Results are the nine factor maps stored in ENVI standard raster format and can now be used to run the Band Math procedure.

These processes were repeated for every factor. The output file of each factor represents only the number of attribute classes of the factor and used to analysis in the next step of band math tools.

Using the Band Math Tool in ENVI for landslide prediction model construction: The relation and basic arithmetic operators were used to customize the band math formula systematically as follow:

- 1) The ENVI-readable files format of nine factors were used to produce the landslide prediction model as a landslide probability index map of each factor. The procedure was replaced the number of classes by the data value (probability ratio of each class of each factor, which is already multiplied by the combination weighted of reliability and accountability). The results from this

step characterized probability index of landslide hazard occurrence of each factor image.

Factor names for band math formula must begin with the character “b” or “B” followed up to 5 numeric characters. Therefore, nine factors of this study are assigned with band names as shown in table 3.7.

These factor’s band names are used to derive the landslide probability index map of each factor as follow:

On ENVI menu bar select Basic → Tools Band Math. The band math dialog appears (Figure 3.24), and then enters the band math expressions that used to analyses data in an expression text box and add to list.

The equation 3.9 represented an example of band math formulas, and used to evaluate the landslide probability index of lineament factor.

$$\text{Band Math equation of Lineament} = (b1 \text{ eq } 1) * 48 + (b1 \text{ eq } 2) * 24 + (b1 \text{ eq } 3) * 8 + (b1 \text{ eq } 4) * 5 + (b1 \text{ eq } 5) * 3 + (b1 \text{ eq } 6) * 5 + (b1 \text{ eq } 7) * 2 + (b1 \text{ eq } 8) * 1 + (b1 \text{ eq } 9) * 1 + (b1 \text{ eq } 10) * 1 \dots\dots\dots(3.9)$$

(b1 = band number of lineament, eq = equal, * = multiply, (b1 eq 1) * 48 means the lineament class 1(the distance 100 m from lineament line) will be replace by 48 (probability ratio of each class of lineaments multiply by the combination weight of reliability and accountability weight.)

After an expression is entered in the space of an enter expression space of band math dialog, click OK. The factor to band pairings dialog appears. In the variable to bands pairings dialog, click on the factor B1 (lineament) in the available band list, and it appears in variable used in expression text box (Figure 3.25).

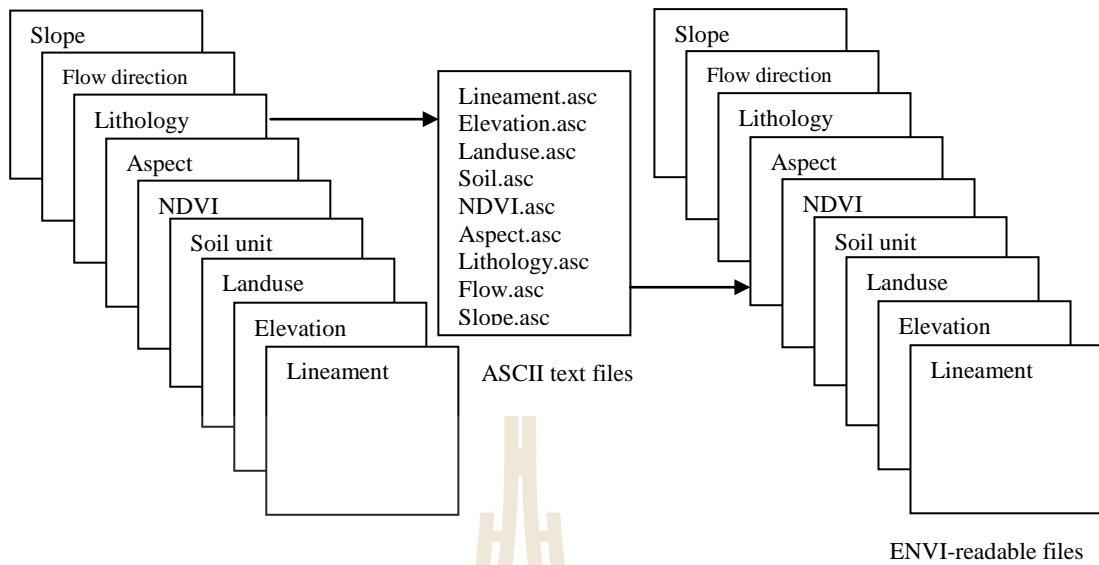


Figure 3.23 Exported data of nine factors to text file format and ENVI-readable files.

Table 3.7 Band names of the nine factors used in landslide prediction model construction.

Factor layers	Band names	Band names used in equation
Lineament	Band 1	b1
Elevation	Band 2	b2
Land use	Band 3	b3
Soil unit	Band 4	b4
NDVI	Band 5	b5
Aspect	Band 6	b6
Lithology	Band 7	b7
Flow direction	Band 8	b8
Slope	Band 9	b9

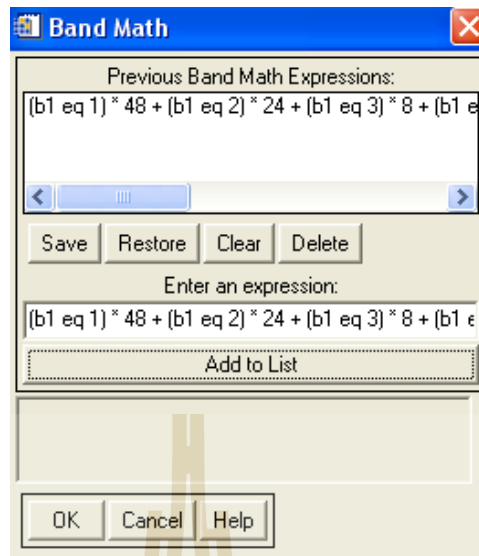


Figure 3.24 Band math dialog.

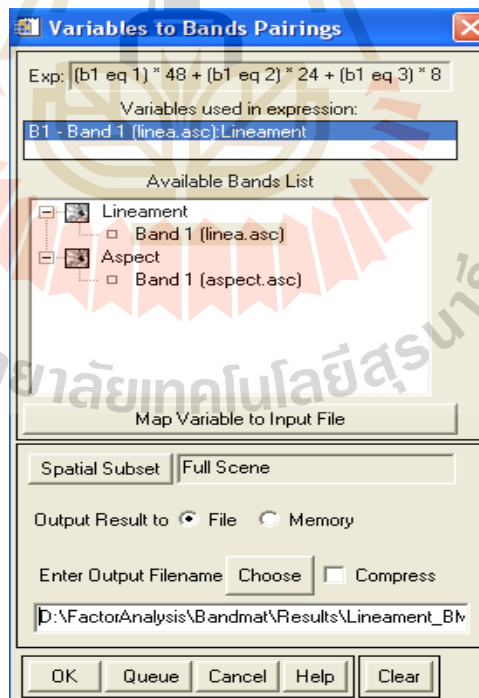


Figure 3.25 Variables to bands pairings dialog.

This process was repeated for every factor. The out put file of each factor represented landslide probability index of each classes of each factor and used to produce landslide hazard zonation map in the next step of band math tools.

2) The landslide hazard zonation map was produced by summing the landslide probability index map of each factor. The band math expression was custom to construction the landslide hazard zonation map using addition operator. It was represented by the equation 3.10.

$$\text{Landslide Hazard Map} = B1 + B2 + B3 + B4 + B5 + B6 + B7 + B8 + B9 \dots (3.10)$$

Enter the band math formula that used to produce landslide hazard zonation map in the enter an expression text box and add to list. The process was the same as the step of producing landslide probability index map of each factor. The result is the landslide hazard map. This map was classified in to five levels of landslide hazard zonation using the density slice in overlay function of ENVI. Then, five levels of relative hazard were defined on a landslide susceptibility map: (1) very low; (2) low; (3) moderate; (4) high; and (5) very high hazard.

3.7 Comparison with Slope Stability Model

The Rock Slope Stability GIS (RSS-GIS) is a modular system built of several extensions for Arc View GIS 3.x for ESRI. RSS-GIS is developed by Guenther (2003), Federal Institute for Geosciences and Natural Resources, Germany. The programme suite is mainly designed for scalable, spatially distributed stability calculations of rock slopes with topographic (DEM), structural, geotechnical and hydrological data. However, other applications of RSS-GIS in structural or environmental geology, hydrogeology, geomorphology or remote sensing would also

be possible. The system is designed for raster-based calculations on a pixel-by-pixel base. This system can be used for rapid automated mapping of slope properties, and spatially distributed, pixel-based stability calculations of rock slopes.

In this study, the expert system of the RSS-GISTM (Rock Slope Stability GIS) was used to produce the landslide hazard map for Wang Chin area. DEM and engineering properties of rock were used as a database for the analysis. In this case, the engineering properties of rock material are derived from standard engineering properties material (Table 3.8). The result of this analysis has referred the slope stabilities of the Wang Chin area, and it will be compared to the landslide susceptibility map using probability and weighting analysis, and Band Math approach.

3.8 Verification of the Result and Reporting

The verification method is performed by cross checking between existing landslide location and the result of landslide susceptibility map using probability method. Then thesis writing has been done.

Table 3.8 Engineering properties of geological material (After Guenther, 2005).

Geology_ID	Symbol	Description	Friction[°]	Conductivity [m/hr]	Density[gr/cm ³]
1	Rht2	Tuff	25-30	0,072-3,6	1,6-2
2	Pm1	Congl.	35-40	0,36-3,6	1,6-2
3	Pm2	Limestone	30-35	0,36-3,6	1,3-1,8
4	Rht1	Rhyolite	30-35	0,36-3,6	1,6-2
5	Qt	River Gravel	35-45	3,6-360	2-2,2
6	Tr3-3	Siltst.-Sandst.	30-35	0,36-3,6	1,6-2
7	Tr3-2	Sdst-Shale	30-35	0,072-3,6	1,6-2
8	Pm3	Sdst.-Siltst.	30-35	0,36-3,6	1,6-2
9	Tr3	Shale	25-30	0,072-3,6	1,6-2
10	Tr3-1	Shale-Sdst.	25-35	0,072-3,6	1,6-2
11	Qa	Terrace Gravel	35-45	3,6-360	2-2,2
12	CP	Undif. Sdst.	30-35	0,36-3,6	1,6-2
Thickness 2 m Precip.Max 0,02 m/hr Precip.Min 0,00416 m/hr Global Conductivity: 2,3 m/hr Global Friction: 33° Global Density: 1,7 gr/cm ³					

CHAPTER IV

RESULTS

In this study, the GIS techniques of Arc View software are used to performed the spatial database for the spatial analysis of landslide assessment. The data sets related to landsliding in this study were derived from remote sensing data, available maps, and field investigation. Landslide susceptibility map is the result of landslide assessment analysis. It was analyzed using the factors related to landslide occurrence by bivariate probability and weighting methods. The method approach is based on the observed relationship between each landslide occurrence factor's class and past landslide event. The relationship between landslide distribution location and each landslide occurrence factor's class was analyzed in term of probability ratio of landslide occurrence. In addition, the weighted of importance of each factor was determined based on probability ratio of landslide occurrence on each factor. The reliability of this method approach is directly dependent on the quality of factors data and landslide mapping.

There are three steps to complete the factor analysis and produce a landslide susceptibility map as the following: (1) landslide information construction (LSIC); (2) landslide assessment analysis; (3) produce a landslide hazard zonation map.

4.1 Landslide Information Construction (LSIC)

All data are input into GIS as a spatial database of vector model (point) and raster format. These spatial database comprise the landslide location map, the factors map related to landslide as described below:

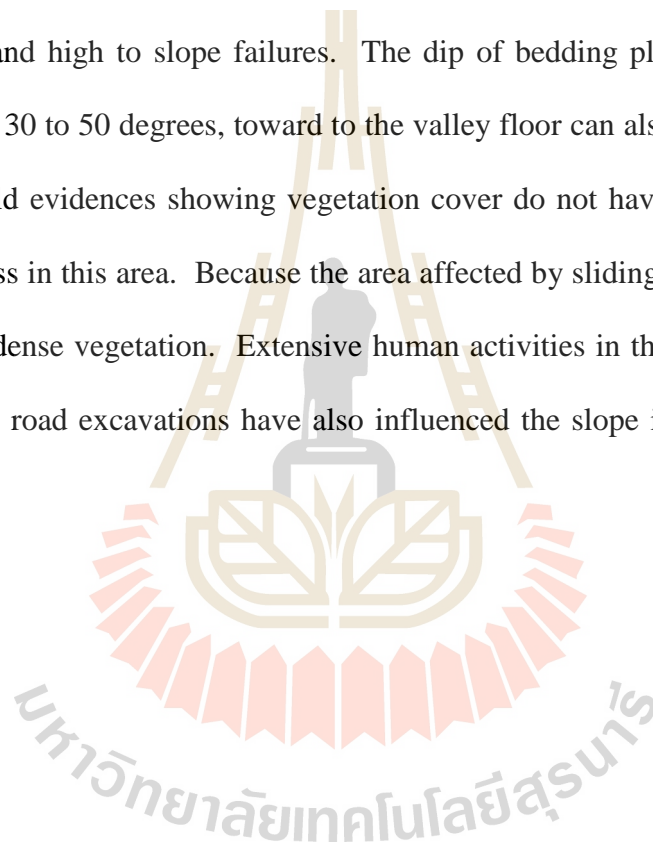
4.1.1 Landslides in Wang Chin Area

Landslides occurred on May 4, 2001 were triggered by continuous and heavy rainfall, which cause water percolated through the weathered profile of bedrock and reduce its stability. These landslides are relatively shallow and mobilizing only the weathered profile of bedrock mixed with wood fragments, logs and water (Figure 4.1). Landslides size are vary from small slumps of a few square metres area to some of large landslides with surface areas in excess of about one thousand square metres. Landslide occurrences location are closed to the first order stream or on the convex slope of mountain (Figure 4.2).

The masses of weathered surface rocks, wood fragments, logs and water moved down from the mountain slopes to the low land areas. Some materials partly blocked the water, which flow from upper streams and then became saturated and liquefied by the water from the stream supplemented by the heavy rainfall, and were transformed into debris flow. This debris flow moved quickly downward along the channel or stream and pour out at the valley floor as a special flood, which was a mixture of water, mud, sand, rock, and wood fragments (Figures 4.3-4.4). Landslide event at Wang Chin area was classified as a complex landslide (debris slide-debris flow). Because of the materials started to move as a debris slide, then they take on the character of another type of movement as a debris flow. This event damaged houses and properties, transportation lines and farmlands at Hong Village, Kham Muak

Village and Pa Sak Village very seriously (Figures 4.5-4.6), resulted in 40 peoples died, 3 peoples still missing, and 60 houses completely destroyed.

The highest frequency of landslides is occurring in the area consisting of shale intercalated with sandstone. Bedding planes between shale and sandstone horizons, fractures and fissility in rocks mass act as weak zones which allow high infiltration of rain water. These weak zones cause the rocks to be subjected to high weathering, and high to slope failures. The dip of bedding plane of the study area varying from 30 to 50 degrees, toward to the valley floor can also accelerate the slope failures. Field evidences showing vegetation cover do not have much resistance for sliding process in this area. Because the area affected by sliding is mostly covered by moderate to dense vegetation. Extensive human activities in the form of agricultural activities and road excavations have also influenced the slope instability phenomena (Figure 4.7).



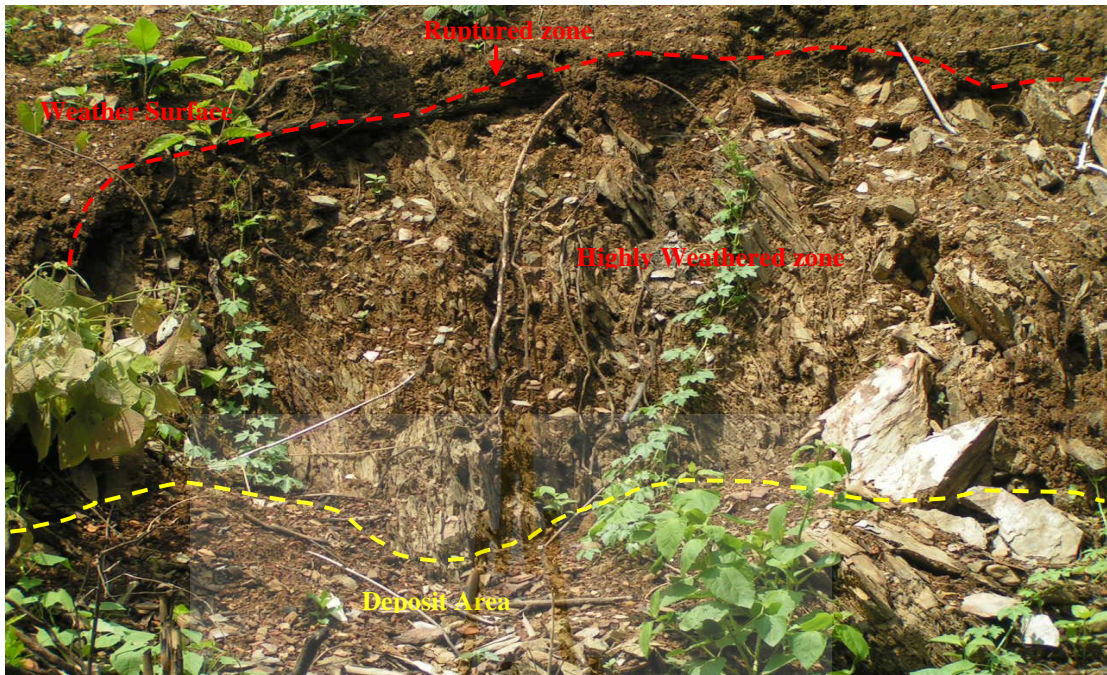


Figure 4.1 Shallow landslide of weathered surface in the study area.





Figure 4.2 The initiation zone of landslide occurrence is close to the mountainous ridge and the first order stream in the study area.



Figure 4.3 The masses of weathered surface rocks and wood fragments moved down from the mountain slopes and stream to the low land area.



Figure 4.4 The debris flow moved quickly downward along the channel and pour out at the valley floor at Hong Village as a special flood, which is a mixture of water, mud, sand, rock, and wood fragments.



Figure 4.5 Debris flow sediments at Muang Kham Village, Wang Chin District.

มหาวิทยาลัยเทคโนโลยีสุรนารี



Figure 4.6 Landslide damaged the house at Pa Sak Village.



Figure 4.7 The human activities in form of deforestation and agricultural has also influenced landslide occurrences (in white circles).

4.1.2 Factors Map Related to Landslide and Database Construction

This task is to prepare a map of the existing landslide inventory and factor maps related to landslide occurrences. Various parameters that affect directly or indirectly to slope failure processes need to be assessed for landslide hazard zonation analysis. These include geological factors, topographical factors, vegetation and land use/land cover factors, hydrological factors and landslide location map. Therefore, it is necessary to develop a digital spatial database, which comprises all variables affecting the occurrence of landslide, in the GIS. All factors or maps are input to the GIS using ArcView GIS software as a spatial database. The structures of database can be described as entering the spatial data, entering the attributes, and linking the spatial to the attributes data, which can be manipulated, reviewed in combination, and also analysed.

The landslide distribution map is inputted and processed in GIS as a vector model (point). The factor maps related to landsliding (lithological, lineament, slope angle, slope aspect, flow direction, elevation, land use/land cover, NDVI and soil unit map) are inputted and processed in GIS as a raster format with 30 x 30 metres grid. The study area comprises 1,007,197 grid cell number and 1,630 points of landslides location. The spatial database of each factor is described as follows:

Landslide distribution map: Direct landslide mapping has been worked out using the Landsat 7, Aster and IRS-1D satellite images. These data are acquired after the past landslide event and during the season of green vegetation. These types of imagery provide information of the ground surface, which is associated with landslide occurrence such as landslide location, and land use/cover. Features such as scarps, disrupted vegetation cover and deviation in soil moisture are generally

conspicuous on the satellite image. These features are assumed as landslide scars.

Landslide distributions were classified from the band combination of Landsat 7 imagery for a small size landslide. It could be shown that false color composites (FCC) based on combinations of the Landsat 7, bands 4 (near infrared - NIR), 5 and 7 (both shortwave infrared - SWIR) are suitable for clarifying features, which were created by mass movements and can separate a bare soil from vegetated conditions and water (Figure 4.8). A 3 x 3-edge enhancement filter kernel is applied to increase the contrast. Bare soil in this filtering image varies from light to dark blue depending on light incidence and moisture content, and the areas of forest (deep red) and cultivation (bright pink/orange) can be separate. A small difference in colour is noted between landslides and other areas of bare soil. However, morphological evidences of a clear vegetated back scarp, a run out track and an accumulation zone could be used to support the classification. Bare soils associated to morphology of the mass movements are assumed as landslide scars.

Good results were achieved through the use of Landsat 7, RGB 542 FCC, enhanced with 3x3 pixels edge filter kernel and contrast stretching in each band (Figure 4.9). This composite highlighted wet, bare soil of blue tones, will become darkening blue colour with increase of moisture content. Vegetation is appeared as bright green and dry bare soil as brown tones. Thin vegetation representing areas of well managed paddy cultivation are highlighted as purple colour. Areas of gravel alluvium are represented by a light pink and water is appeared as dark blue color. The ability to ascertain the soil moisture level of bare soil greatly assists the interpretation. The best results are achieved where the RGB 542 and RGB 457 FCCs are examined together using a visual interpretation and GIS technique.

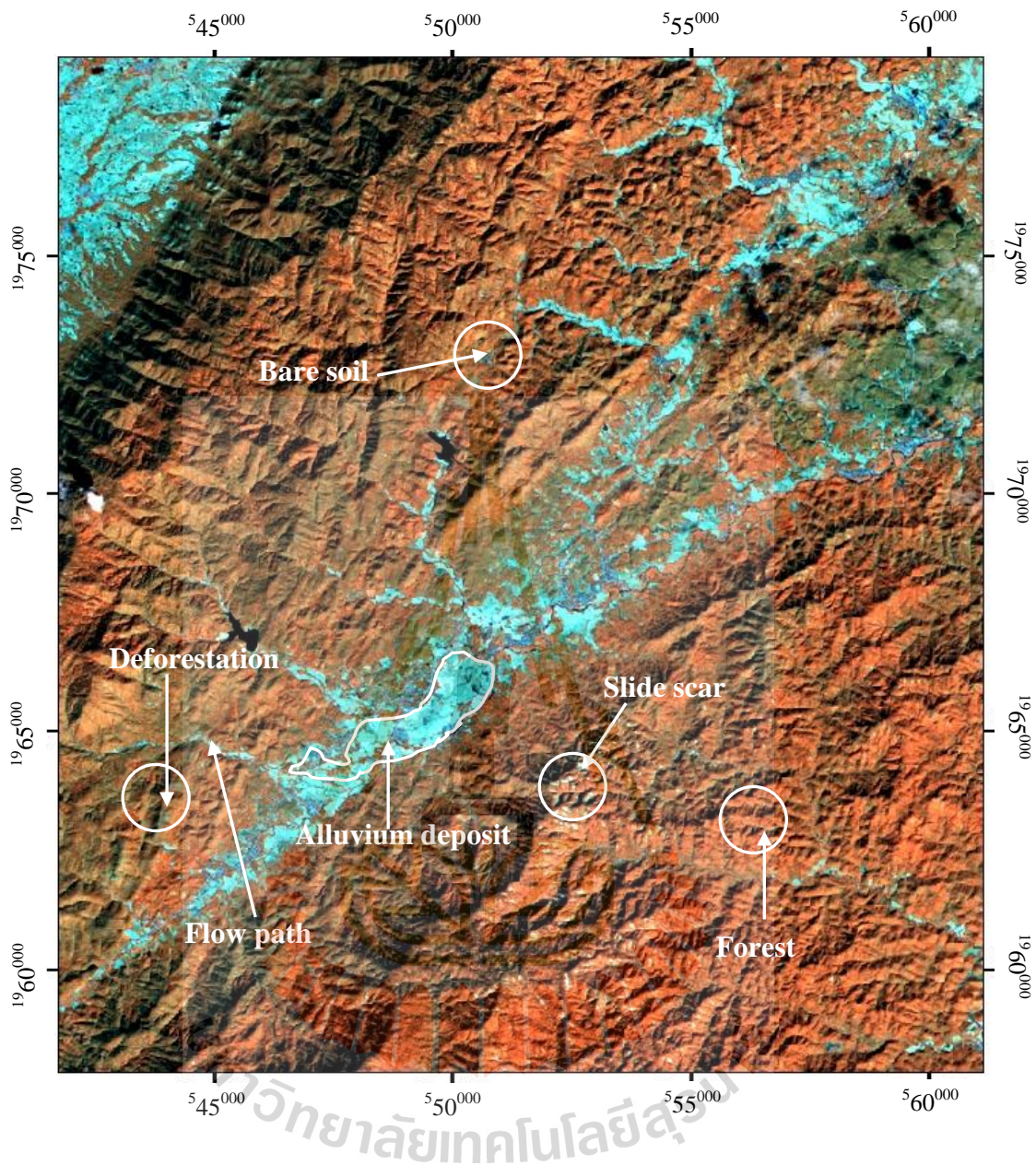


Figure 4.8 False color combinations of Landsat 7, B4, B5 and B 7 shows characteristic of the study area such as alluvium deposit, flow path, slide scar, forest, deforestation and bare soil (Landsat 7, path 148 / row 48, taken on 28/11/2001).

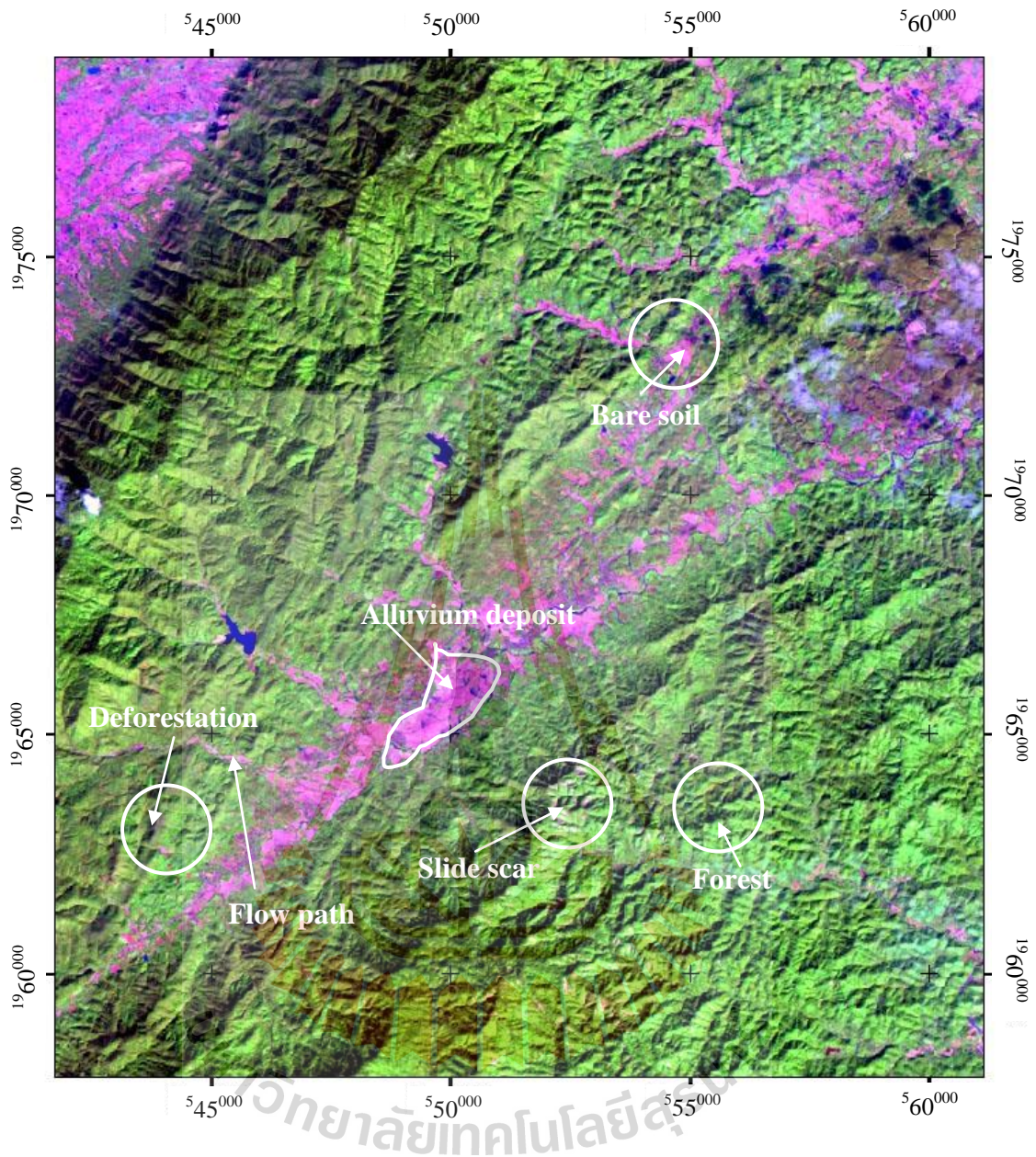


Figure 4.9 False color combinations of Landsat 7, B5, B4 and B 2 shows characteristic of the study area such as alluvium deposit, flow path, slide scar, forest, deforestation and bare soil (Landsat 7, path 148 / row 48, taken on 28/11/2001).

The usefulness of a Principle Components Analysis (PCA) approach using an RGB 123 FCC was also tested (Figure 4.10). The resulting image exhibits a very diverse range of colours. Areas of bare soils and landslides are particularly distinct and appeared almost pink. In contrast to this, all other colours are relatively green. This is particularly useful for relatively detecting small landslides.

Landsat 7 image has fair spectral resolution, its 30 x 30 metres spatial resolution is low and generally not suitable for detailed landslides mapping. So merging of Aster data and IRS-1D images have been used for visual interpretation to improve landslides detection from visual interpretation of Landsat 7 image (Figures 4.11a,b-4.13). Because it creates the relatively high spatial resolution 5 x 5 metres of IRS-1D image and has the colour composite of band 1, 2 and 3 from Aster image. This is suitable for small landslide scars mapping and morphology analysis related to landslide such as run out track and accumulated zones. Once landslide locations from Landsat 7 image interpretation are verified using merging Aster image and IRS-1D image. Some landslides can be considered as relict features that have been inactive for many years. They occupy areas of different vegetation type and density from surrounding areas. But the most important part of providing data for the landslides distribution maps is a ground truth investigation. In this stage, all of marked landslide locations on the satellite images were checked with field observations. The marked locations that probably were not the landslides, were removed. Total numbers of 1,625 landslide locations were identified from RGB 457 and RGB 542 FCCs, the RGB 123 PCA, and the merging Aster and IRS-1D Images. The ground truth checking can be detected 29 landslide locations, which cannot be seen on the satellite images such as landslides on the shadowed slope, and 24 landslide locations from

satellite imagery interpretation, which are actually unvegetated slope were removed. These anomalies are depending on the following reasons: (1) landslides on the shadowed slopes in the imagery are consistently under represented, (2) the areas which are affected by shadows the unvegetated slopes have a similar appearance to those that has vegetation due to their low reflectance in many bands, and (3) the spectral resolution of all images used is still not really good enough to be able to produce finely-tuned, high quality FCC images. Finally, the landslide distribution map with 1,630 landslide locations was produced and input to GIS as a point format using Arc View software (Figure 4.14).

Lithological map: The geological boundaries are digitized from the published 1:50,000 scale geological maps contributed by the Department of Mineral Resources, Thailand. These geological maps are very good quality systematic and contain the require information. Rock units show a series of sedimentary, igneous, and metamorphic rock types. These geological maps were modified into lithological maps using visual interpretation of Landsat 7, and Aster image, and field checking. The Landsat 7 image, RGB 457 FCC, pan sharpened using panchromatic IRS-1D and contrast stretched with 99 percent transform in all bands are the most appropriate for lithological interpretation. These combination and enhanced imageries are converted into the image format of ArcView for visual interpretation on the computer screen. The interpretation considers the following seven basic characteristics, or variation parameters such as: shape, size, pattern, shadow, tone, texture, site and association. For example, areas of terrace and fluvialtile deposits are represented by a light to light grey tone, very low drainage density and located on the foot slope of the mountain. The bedrocks with high density drainage indicate shale. The straight lines of

vegetation in the image indicate lineament or bedding plane of hardrocks. The geological information including bedding traces, rock types and lineaments (faults and joints) is delineated. Lithological map of Wang Chin area comprises twelve units and was entered to GIS as a raster format using ArcView software (Figure 4.15).

Lineament map: The term lineament as used by geologists is represent straight or slightly curved feature, or alignment of discontinuous features, apparent on photograph, image or map. The size of lineaments is related to the scale of the photograph or imagery used.

In the present study, lineaments were identified from landsat 7 image, 457 RGB FCC, pan sharpened using the panchromatic IRS-1D, contrast stretched with a 99 percent and 3x3 edge filter kernel enhancement (Figure 4.16), which increases the contrast and the clearness of lineament line on the image. Then lineaments were interpreted by visual interpretation on the computer screen. The straight or slightly curved feature or alignments of discontinuous features, apparent on the image were mapped as a lineament. They correspond to various types of geological features including fractures (faults and joints), bedding, dykes/veins and lithological boundaries, as well as to spurious man-made feature (road, power line, and etc.). In relation to landslides, fracture-related lineaments may be significant in controlling the location or form of landslides. The lineament map is entered to GIS as a raster format using ArcView software. The buffer command is used to prepare ten separated lineament buffer maps having distance 100 m, 200 m, 300 m, 400 m, 500 m, 600 m, 700 m, 800 m, 900 m, and 1,000 m, and having the ten different distance zones (Figure 4.17).

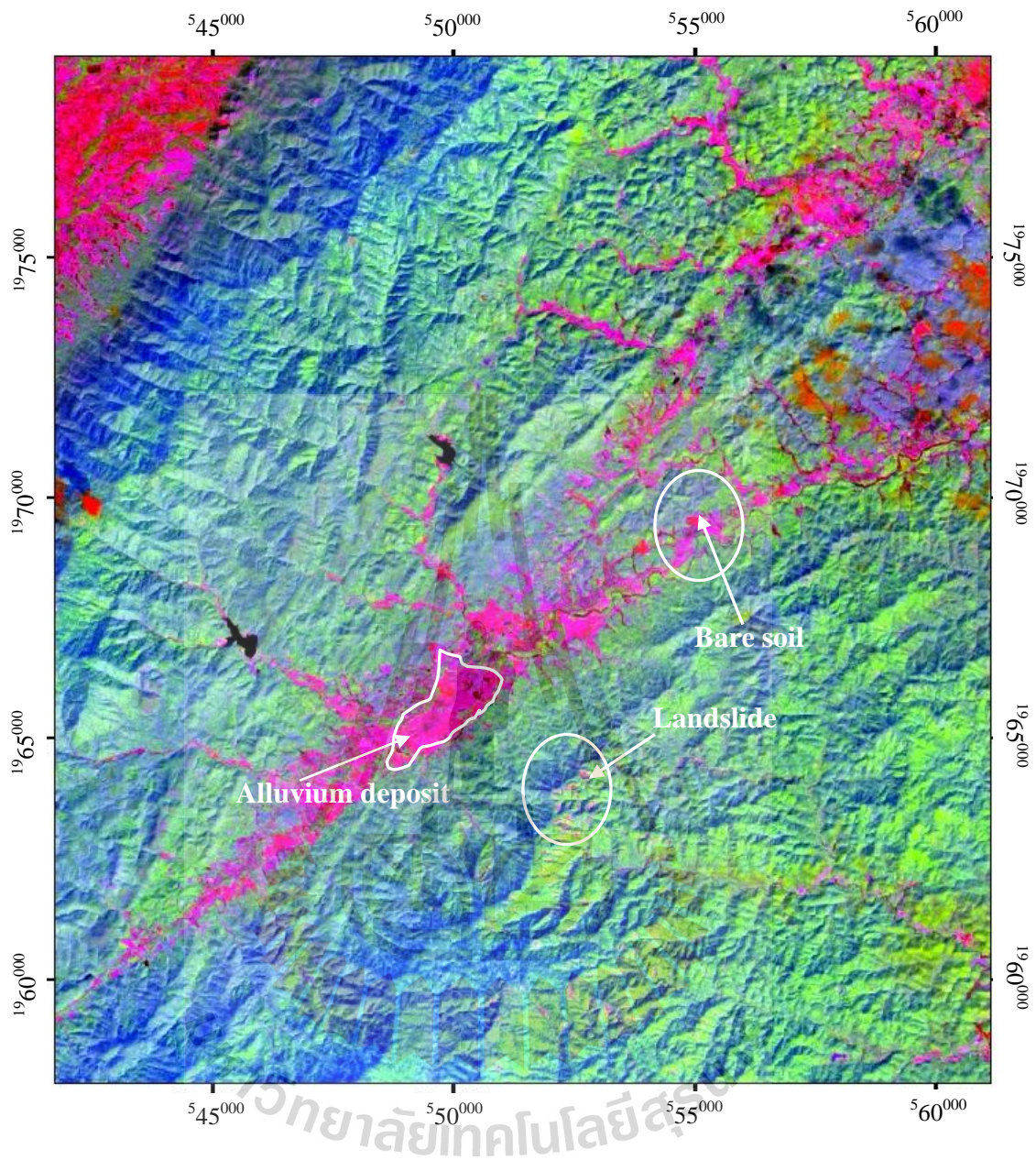


Figure 4.10 RGB color composite based on PC1/Red, PC2/Green and PC3/Blue, areas of landslide and alluvium deposit and bare soil are appeared almost pink (Landsat 7, path 130 / row 48, taken on 28/11/2001).

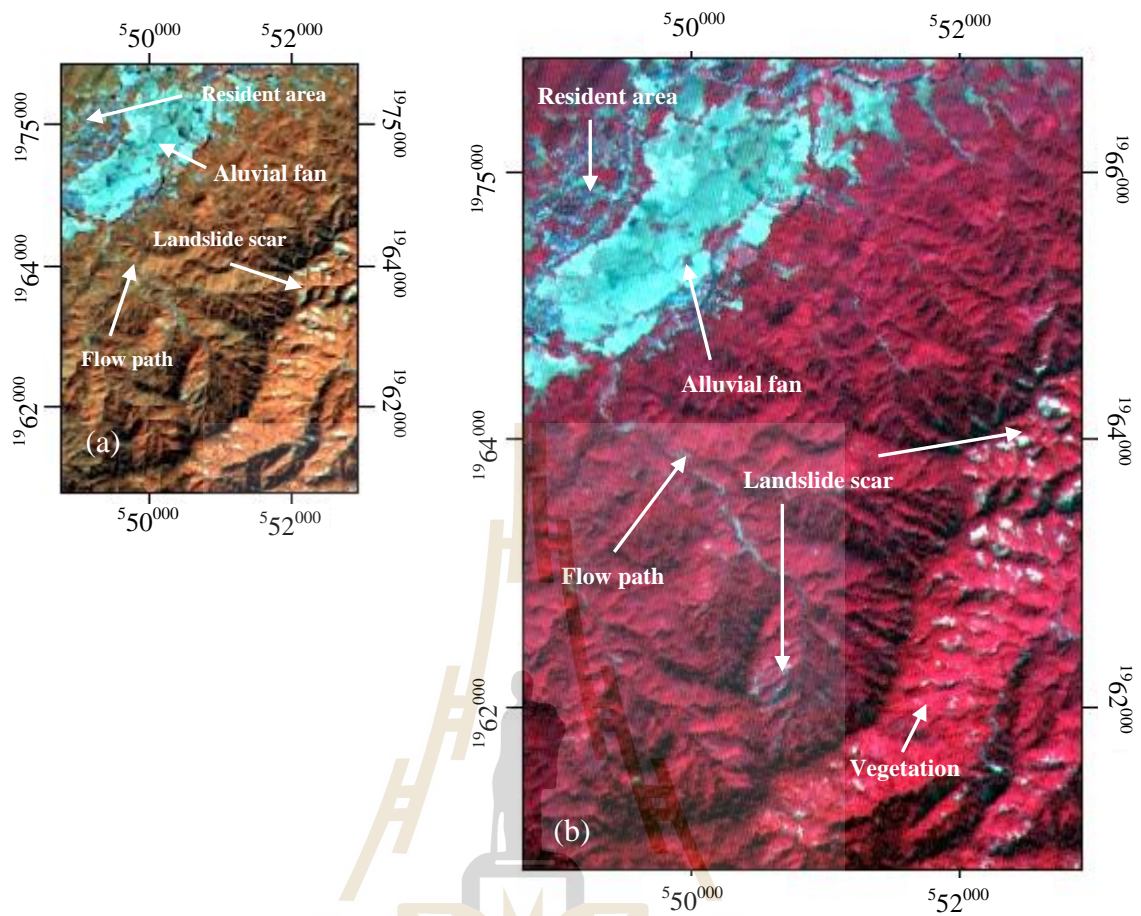


Figure 4.11 Comparative images of the same area for landslide detection between; (a) Landsat ETM, B4, B5 and B7 false color composites with 30 x 30 metres resolutions for clarifying the characteristics of the study (light blue color = alluvial fan deposit, blue color = resident area, white color = bare soil or slide scar, orange color = vegetation); (b) Aster data B1, B2 and B3 false color composites with 15m x 15 m resolutions, showing more clearly landslide location than Landsat image (landsat 7, path 130 / row 48, taken on 28/11/2001, and Aster, taken on 28/11/2001).

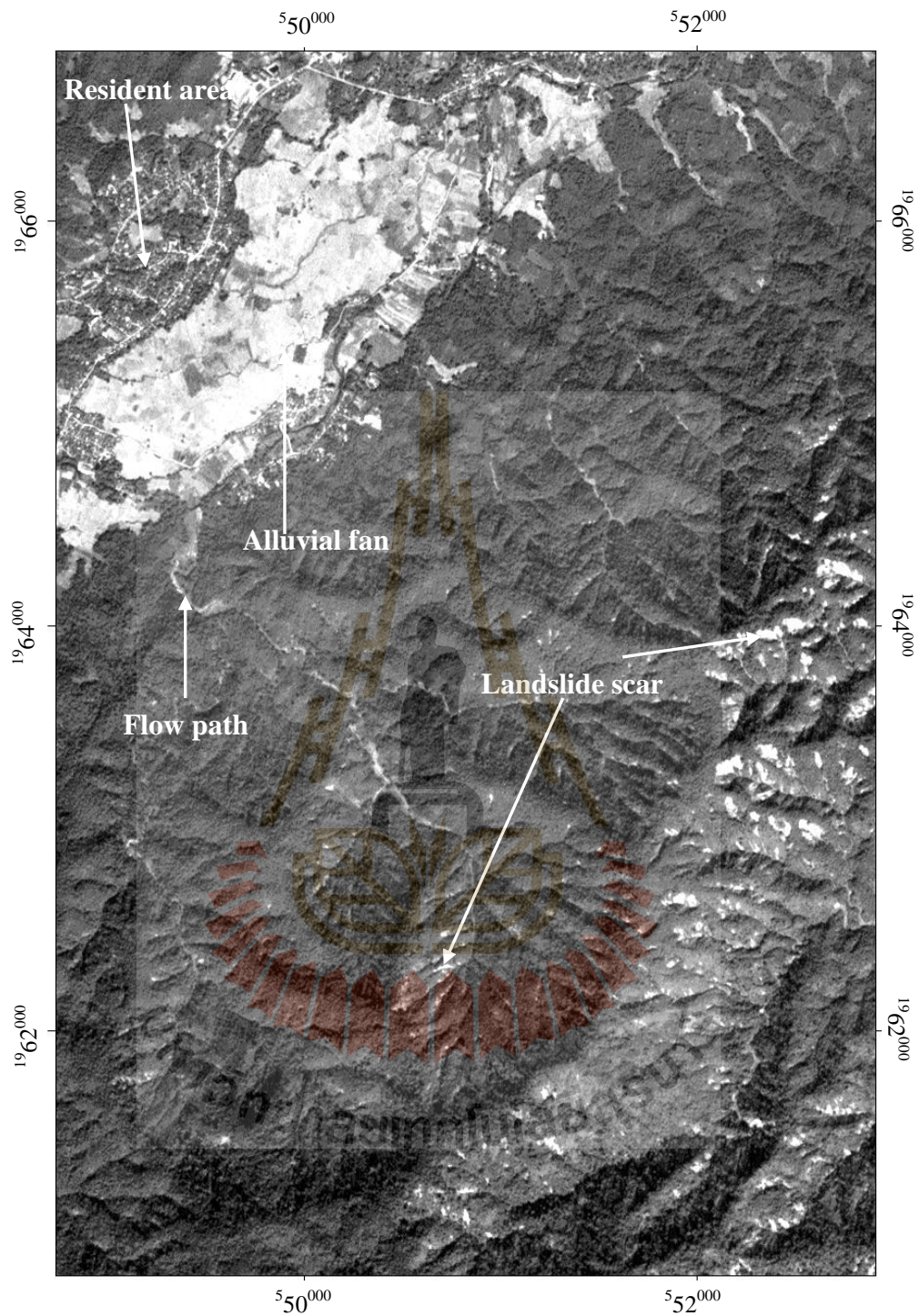


Figure 4.12 IRS-1 D panchromatic band with resolution 5 m x 5 m shows very clear landslide scars in white color on the mountainous area (IRS-1D, path 126 / row 026, taken on 27/12/200).

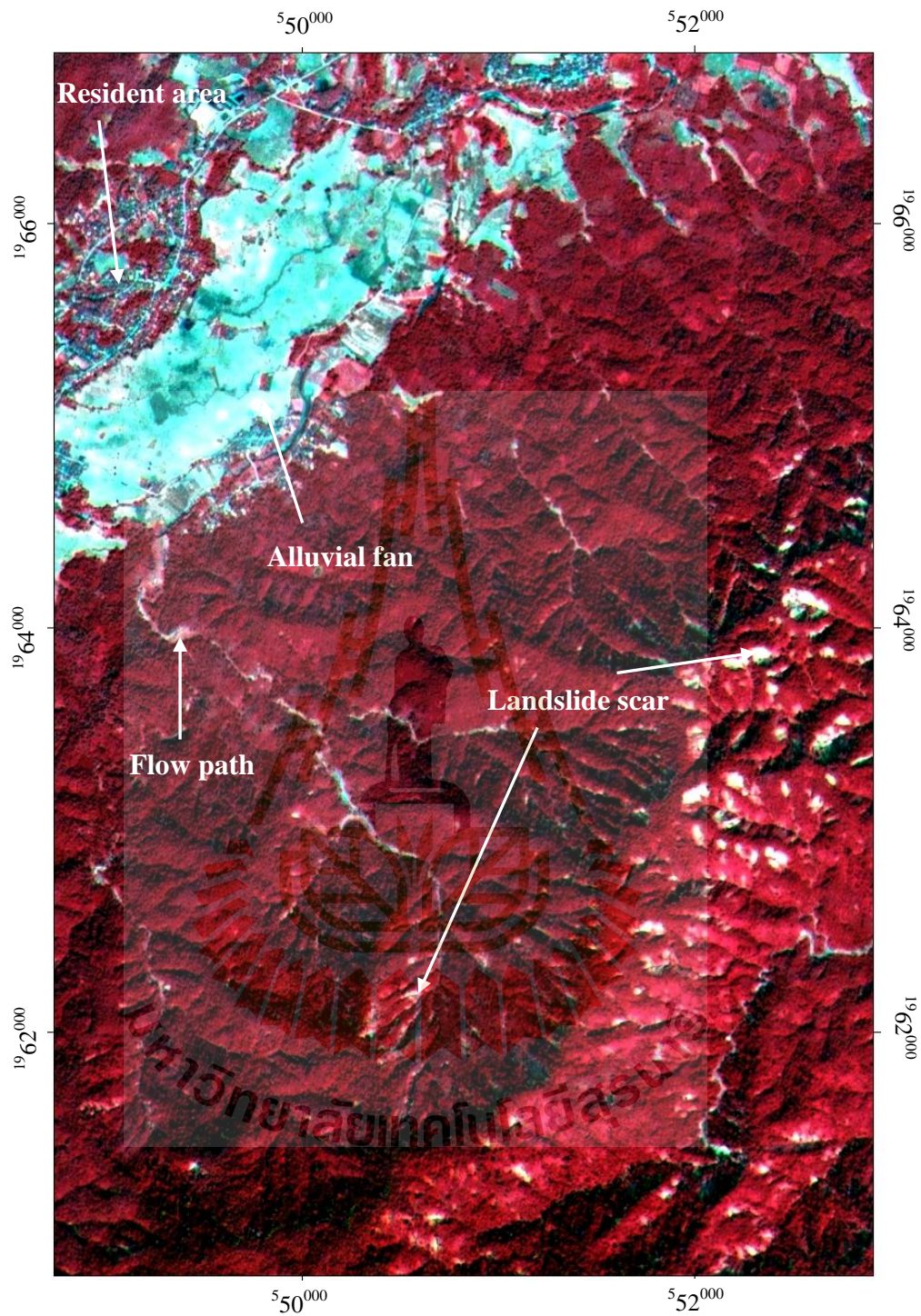
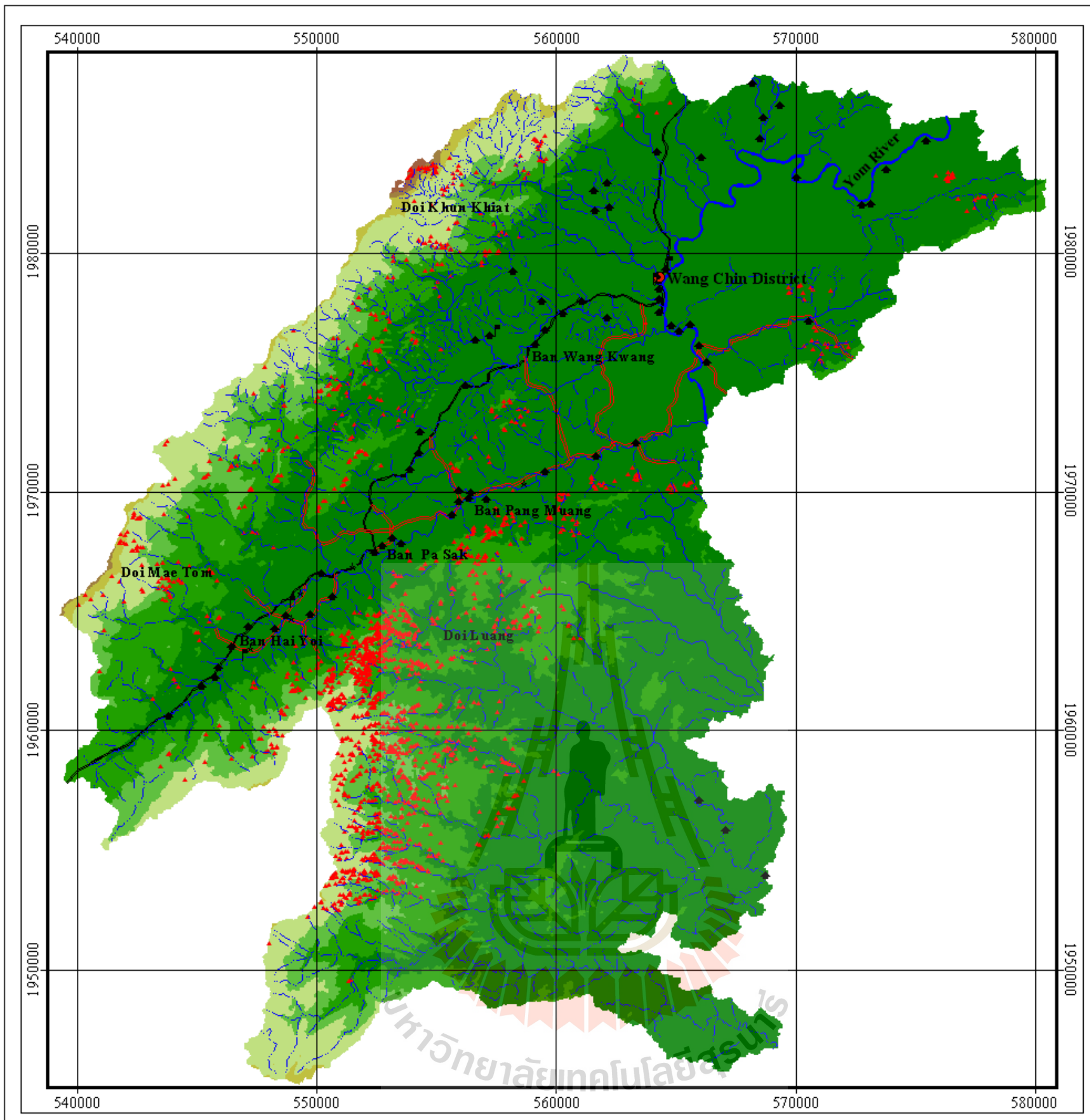


Figure 4.13 Merging IRS-1D PAN (5 m x 5 m) and Aster (15 m x 15 m) B1, B2, and B3 shows very clear landslide scars in white color on the mountainous area (IRS-1D, taken on 27/12/200, and Aster, taken on 28/11/2001)



LANDSLIDE DISTRIBUTION MAP

Legend

- ▲ Landslide Point

Elevation in metres

71 - 241	922 - 1091
242 - 411	1092 - 1261
412 - 581	1262 - 1431
582 - 751	1432 - 1602
752 - 921	

- Perennial stream
- - - Intermittent stream
- Yom River
- Provincial Road
- Local Road
- Wang Chin District
- ▣ School
- ★ Temple
- ▲ Village

N
 1 0 1 2
 Kilometers

Figure 4.14 Landslide distribution map based on satellite imagery interpretation (Landsat 7, path 130/row 48, taken on 28/11/2001; Aster, taken on 28/11/2001, and IRS-1D Pan, path 126/row 026, taken on 27/12/2001).

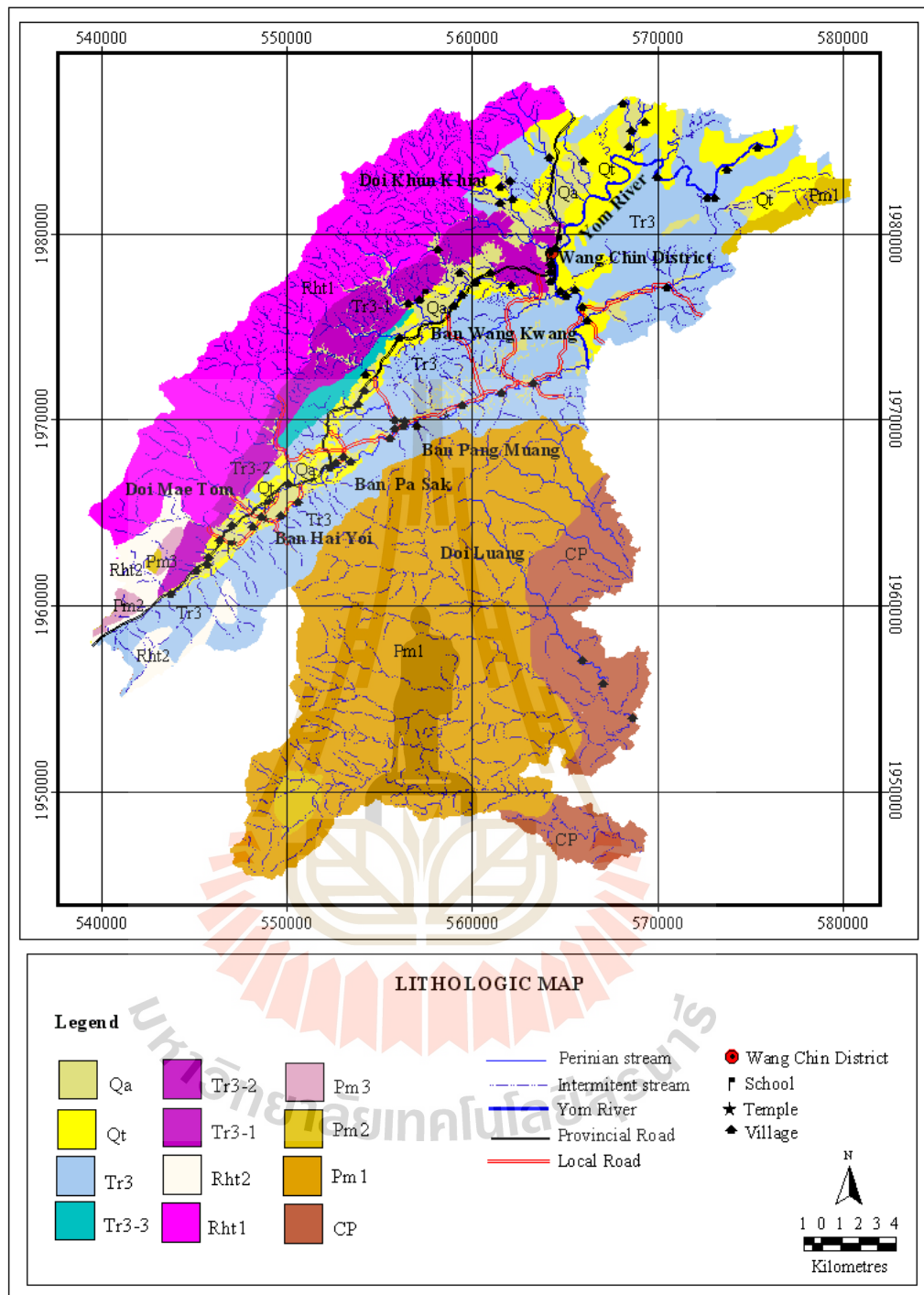


Figure 4.15 Lithologic map based on DMR, 1981-1991, and modified using satellite image data interpretation and fieldwork (Aster, path 126/row 026 taken on 27/12/2001 and Landsat 7, path 130/ row 48 taken on 28/11/2001).

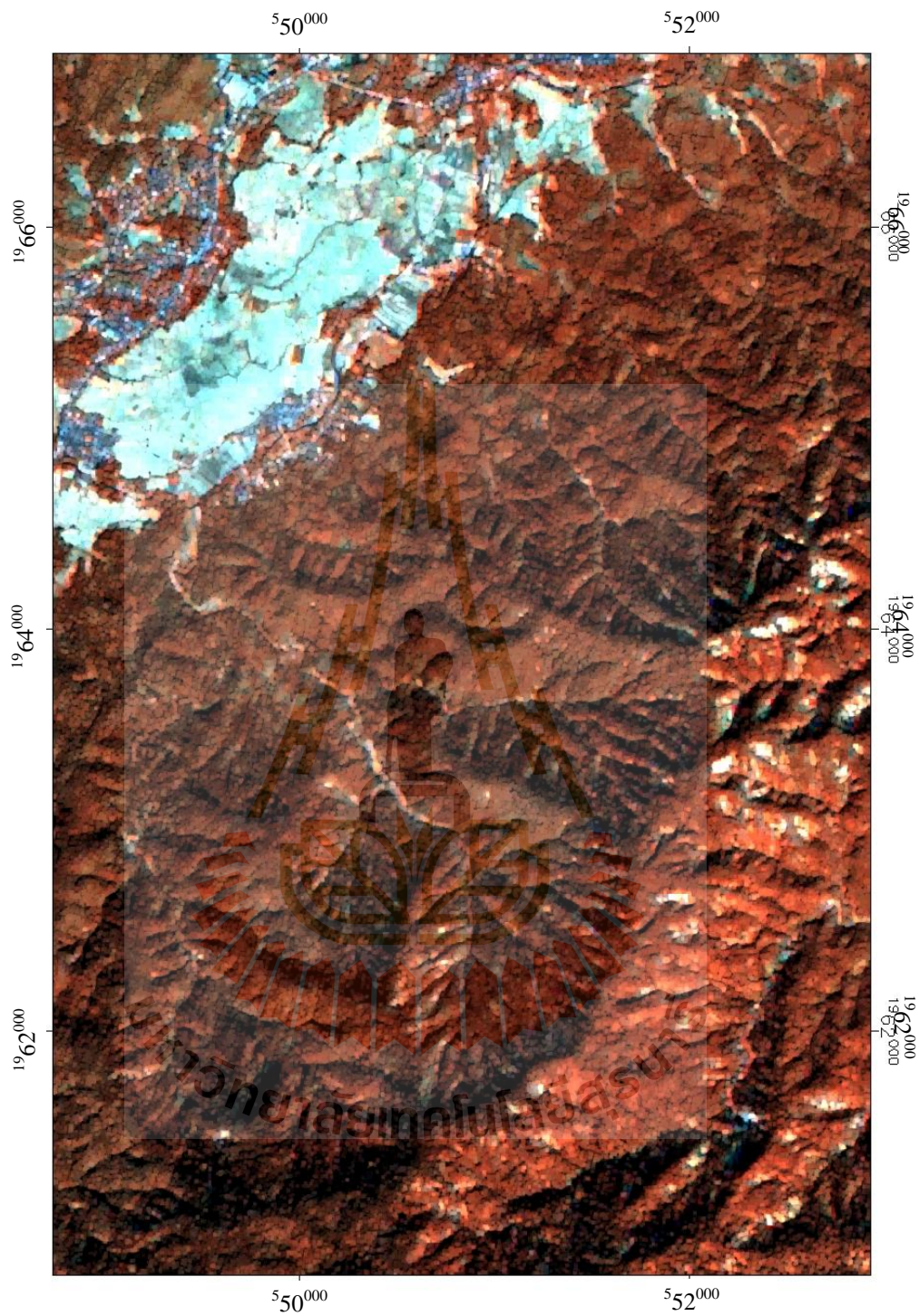


Figure 4.16 Merging IRS-1D PAN (5 m x 5 m, taken on 27/12/2001) and Landsat 7 (30 m x 30 m, , path130/row 48, taken on 28/11/2001) B4, B5, and B7 with filter enhancement shows clear lineament structure.

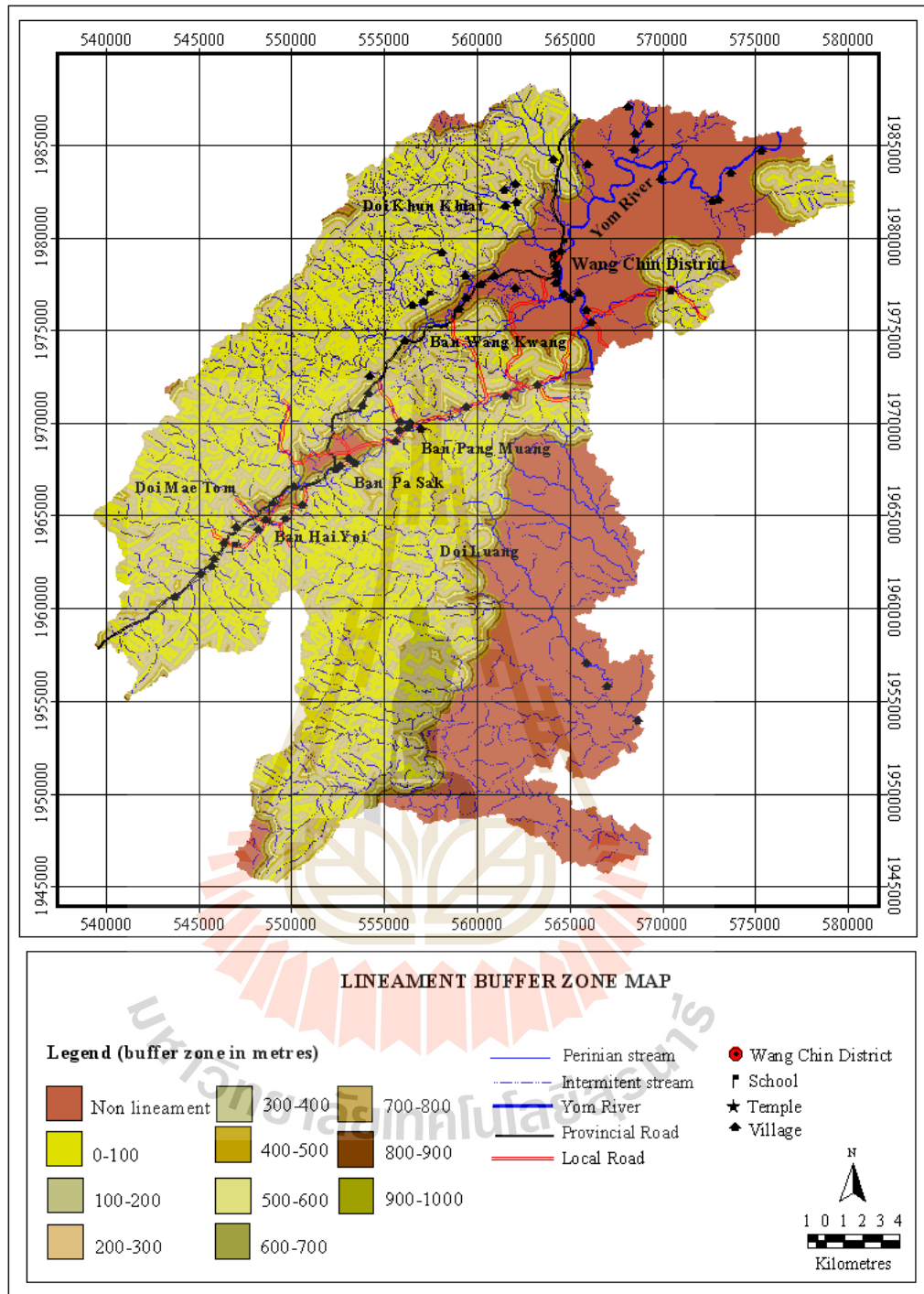


Figure 4.17 Lineament buffer zones map having distance 100 to 100 metres from the lineaments.

Land use/Land cover map: Landsat 7 images acquired in 2001 were processed and interpreted in order to extract land use and land cover information. Supervised classification for land use and land cover was carried out by using three bands of Landsat 7 image (3, 4 and 5) with a maximum likelihood algorithm. Main targets for the remote-sensing-based land use and land cover detection are the distribution and density of forests, the extension of plantations, and other land use types. The major present land use and cover units in the Wang Chin area extracted from Landsat satellite imagery and field observation composed of 15 classes. The resulting map of land use/land cover is given in Figure 4.18.

Normalized vegetation index: The vegetation index represents the plant-cover condition and ranges from one to minus one. When the land is naked, the NDVI value trends to minus one, and when the land is covered with full vegetation, the NDVI approaches one. The NDVI varies with the vegetation type, the seasonal change, and the percentage of the vegetation cover surface. NDVI map was obtained from Landsat 7 satellite image and computes in ENVI 4.1 software as below:

$$NDVI = (IR - R) / (IR + R) \dots \dots \dots (4.1)$$

Where IR is the infrared radiation value and R is the red light radiation value. NDVI is calculating on a pixel base. The result of NDVI calculation can be divided in to 8 classes as show in Figure 4.19.

Digital elevation model (DEM): Digital elevation model data was generated from Aster stereo pair of VNIR 3N and VNIR 3B (level 1B). ENVI 4.1 Aster DTM function is used to process Aster image, whilst minimum and maximum elevations are given from topographic map. DEM data can be used to generating contours as an elevation map, stream network, catchments boundaries, flow direction,

slope aspect, slope angle and shaded relief. Therefore, DEM data is an essential role for landslide assessment. The result of elevation has values ranging from 71 metres to 1,602 metres and was divided into 30 classes of elevation as show in Figure 4.20.

Slope angle map: Slope measures the rate of change of elevation in the direction of steepest descent. Slope has a great influence on the susceptibility of a slope to landsliding. Slope instability would normally be expected to increase with increase in steepness and slope length. For example, on a flat surface rain drops splash soil particles randomly in all directions and on sloping ground more soils are splashed down slope than up slope. Therefore, terrain could be divided into small facets of varying slope angles. In this study, slope map with slope angle values ranging from 0 to 63 degree was derived from DEM data. This map was divided into 13 classes of slope angle as shown in Figure 4.21.

Slope aspect map: Slope orientation or aspect is described in terms of the eight cardinals directions, e.g., north, northeast, and east. Slope aspects are measured in degrees of azimuth from 0 to 360 degrees. Each cardinal direction is defined by a set of azimuth values. For example, slope facing the northeast can have an azimuth reading ranging from 22.5 to 67.5 degrees.

The slope aspect plays a significant role in slope stability processes. The direction of a slope faces can be used as an indirect indicator of the hydrologic factor. The direction in which a slope face exposed to sunlight has more influence to landslide than other direction of slope. Due to the sunlight, the moisture present in the slope gets dry, and then there is less chance for growing vegetation. So the low vegetation areas on the mountainous slope may have a chance of landslides. In addition, the orientation of a slope face to the prevailing wind is an important in the

triggering of landslide. Most of the landslide incidents occur on slope facing to the wind direction. In the study area, the slope aspect map was derived from the DEM data and classified into 8 classes as shown Figure 4.22. The average value, which is taken to divide the aspect, is 22.5 degrees.

Flow direction map of a watershed: A watershed can be described with respect to the surface runoff. The surface runoff was produced inside the watershed and moves to a single watershed outlet. Information about the flow direction is recorded as an attribute of each spatial unit within the watershed to represent the flow direction. In this study, a 3x3 moving window is used over the flow direction of each cell. The steepest descent direction from the center cell of the window to one of its eighth neighbors was chosen as the flow path or flow direction. The flow direction factor has an influence on a transportation of landslide. Figure 4.23 provides 8 classes of the flow directions in raster format of ArcView.

Soil unit map: Soil map is based on factors concentrated in the upper meter or less of superfcerial material affected by agricultural activities. It delineates the distribution of 39 surficial unit attributes of soil types (Figure 4.24). This map was prepared based on lithology and land use pattern. Soils on the mountain slopes are about 10 to 50 centimetres depth, with medium-grained to fine grained texture.

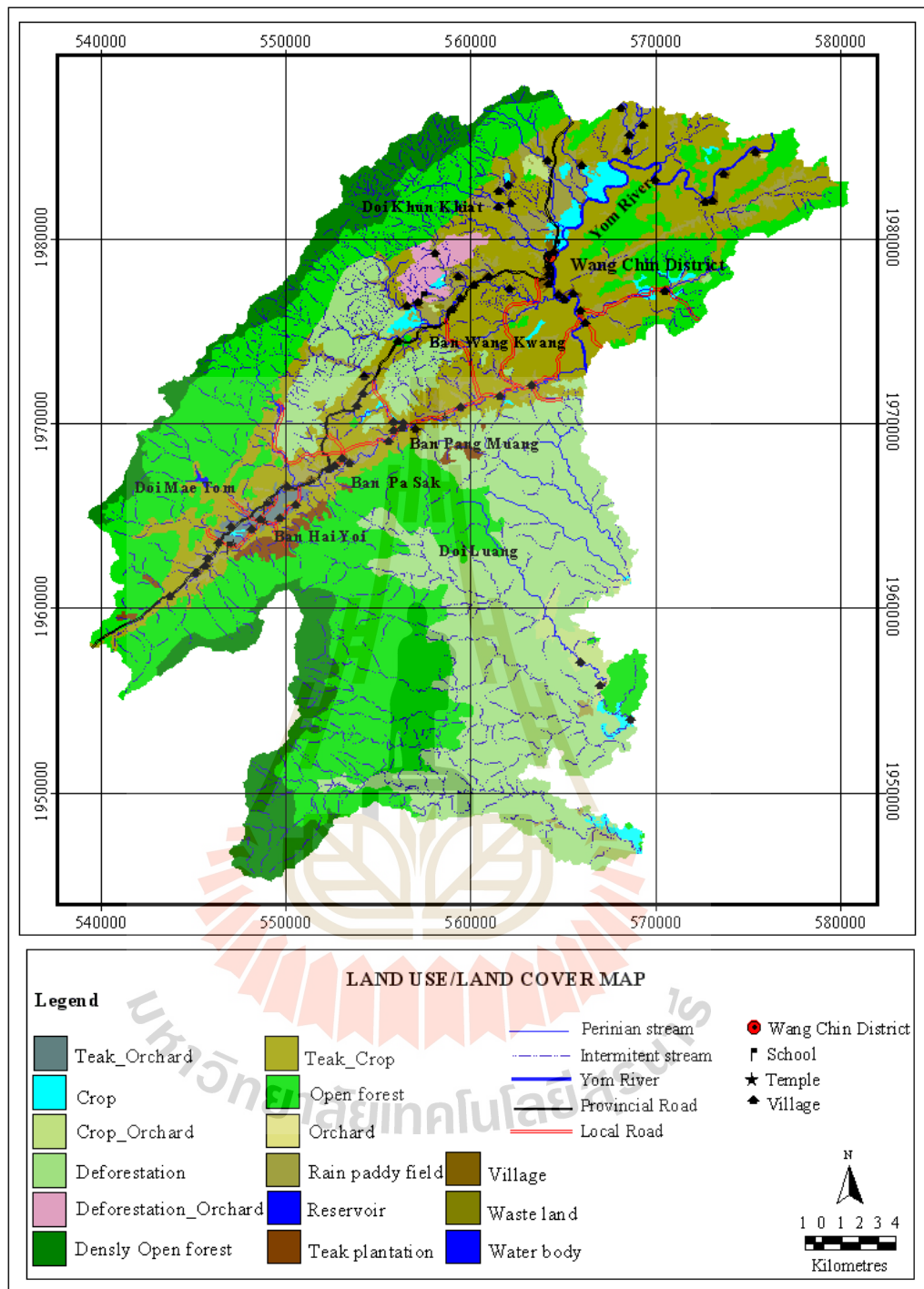


Figure 4.18 Land use map modified from LDD, 1996, and based on supervised classification using Landsat 7 (path 130/row 48, taken on 28/11/2001) and fieldwork.

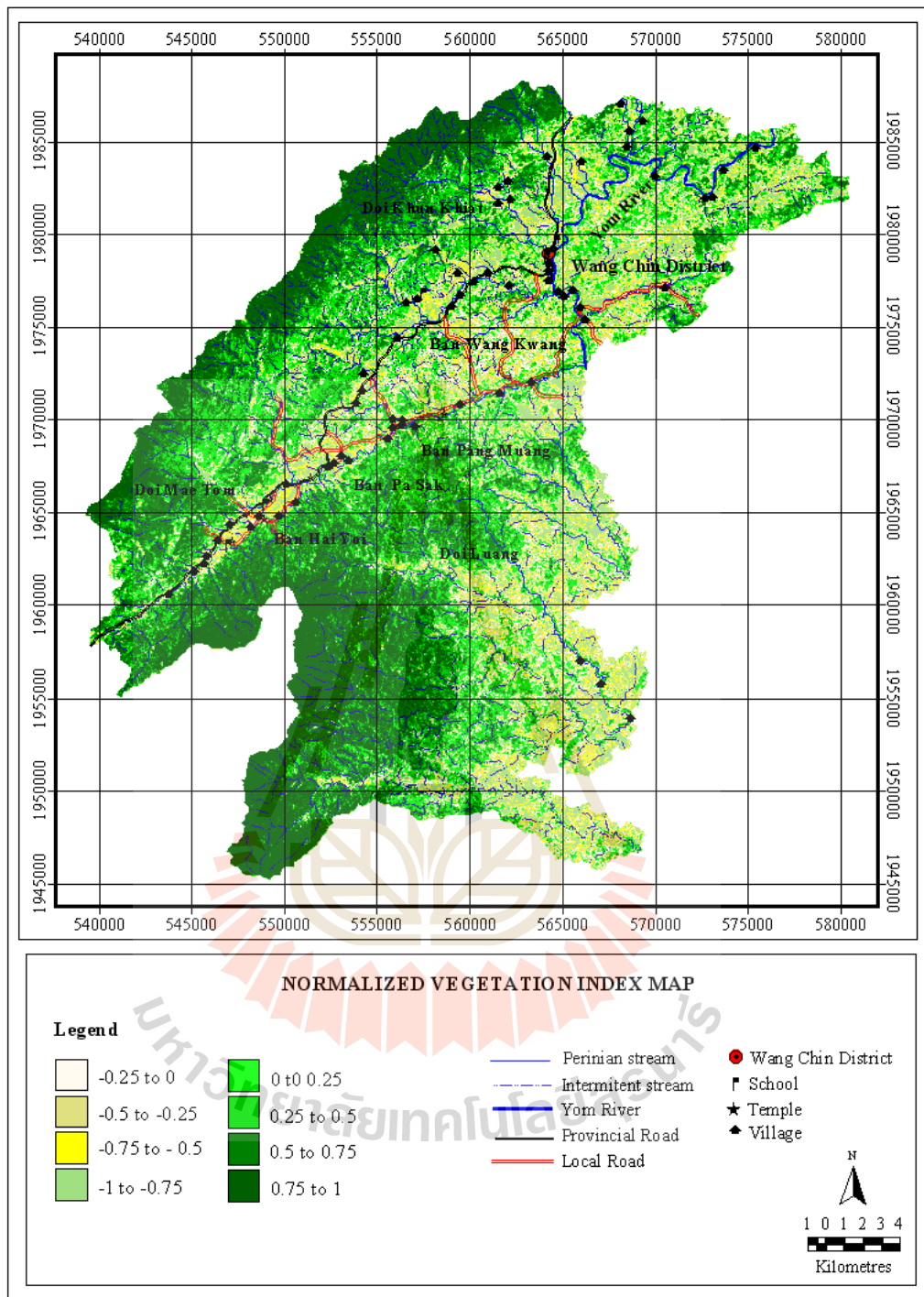


Figure 4.19 Normalized vegetation index (NDVI) map based on Landsat 7 image (path 130/row 48, taken on 28/11/2001) using NDVI function of ENVI.

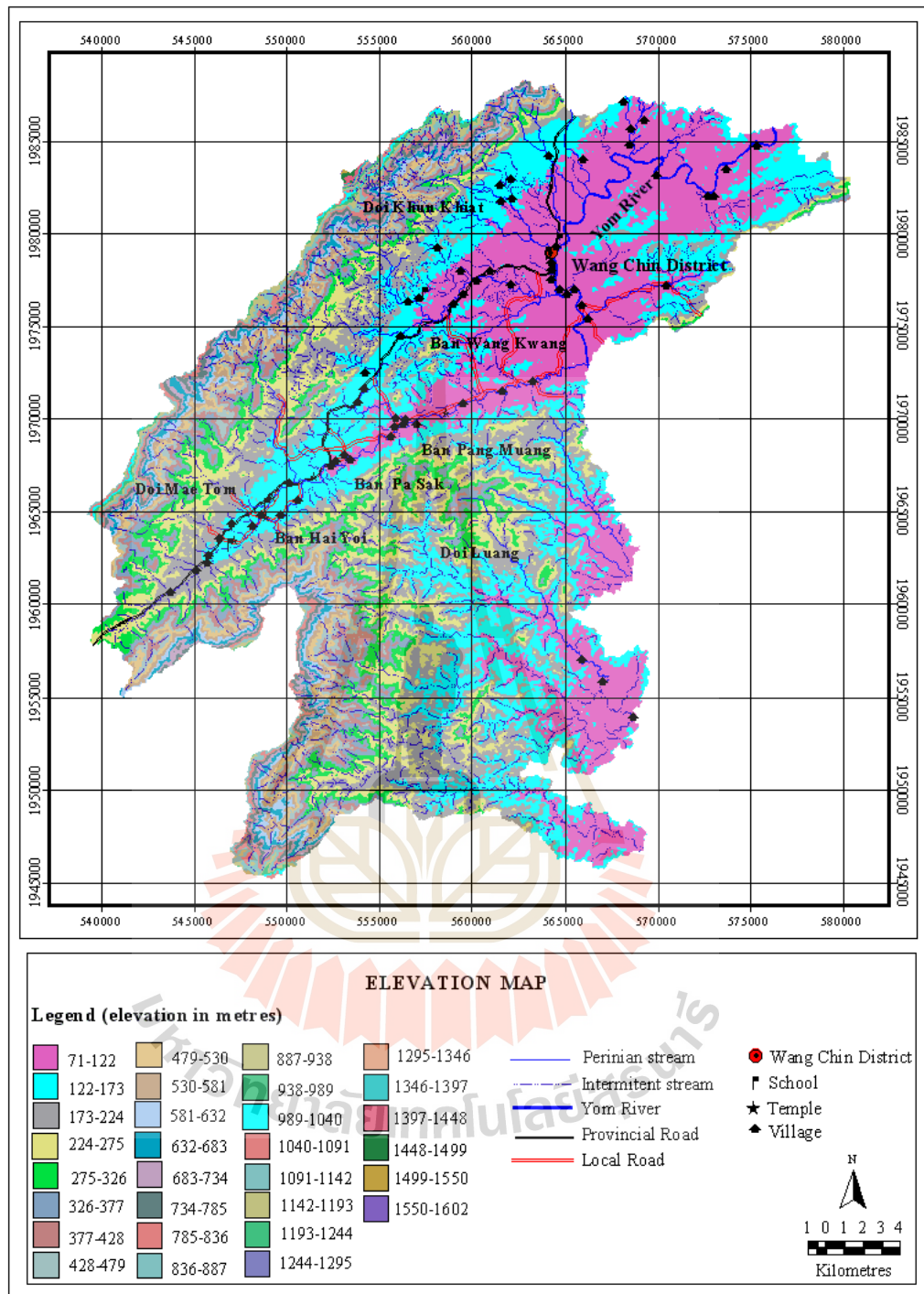


Figure 4.20 Elevation map based on DEM, which is derived from Aster data (taken on 28/11/2001).

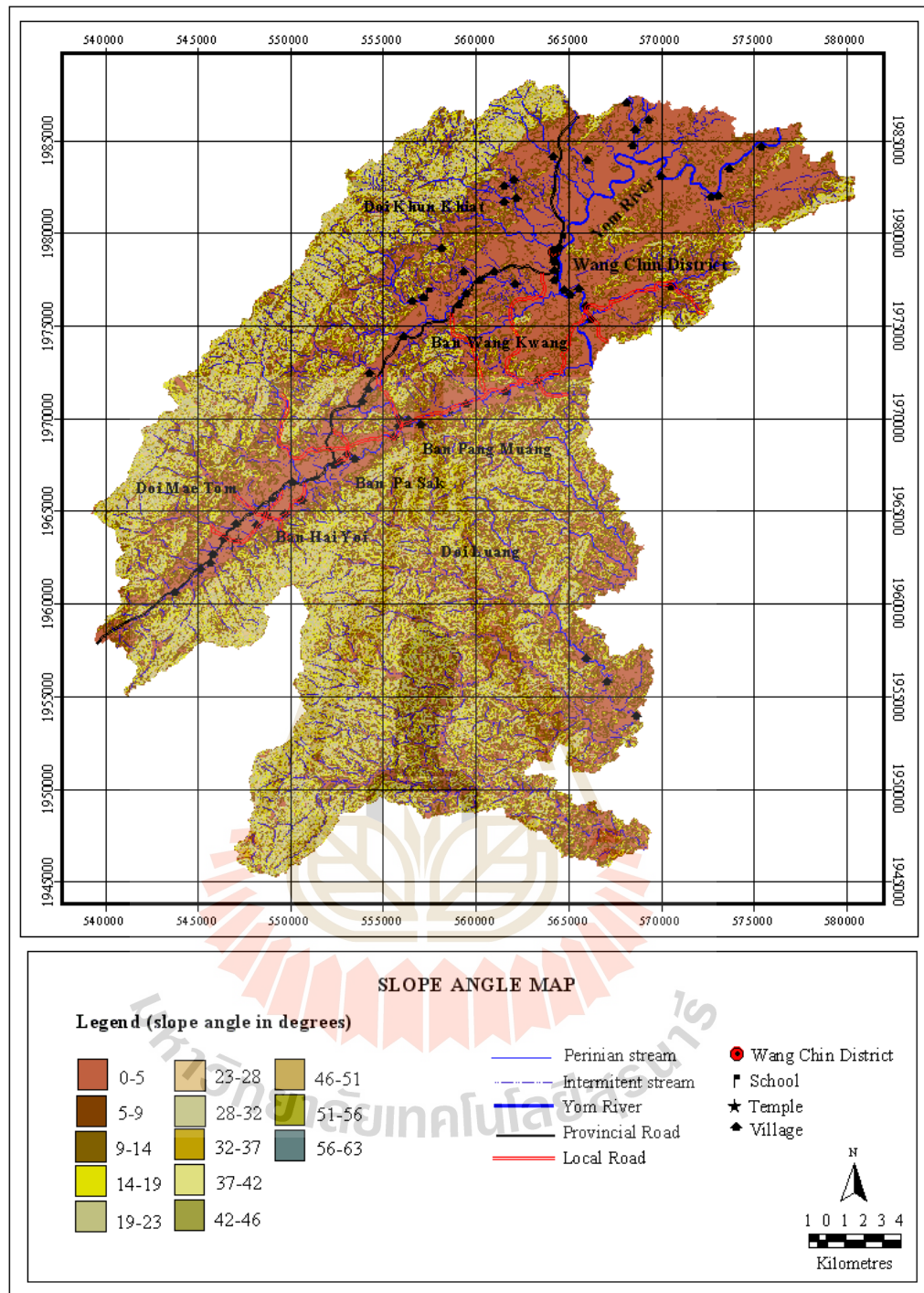


Figure 4.21 Slope angle map derived from DEM, which is derived from Aster data (taken on 28/11/2001).

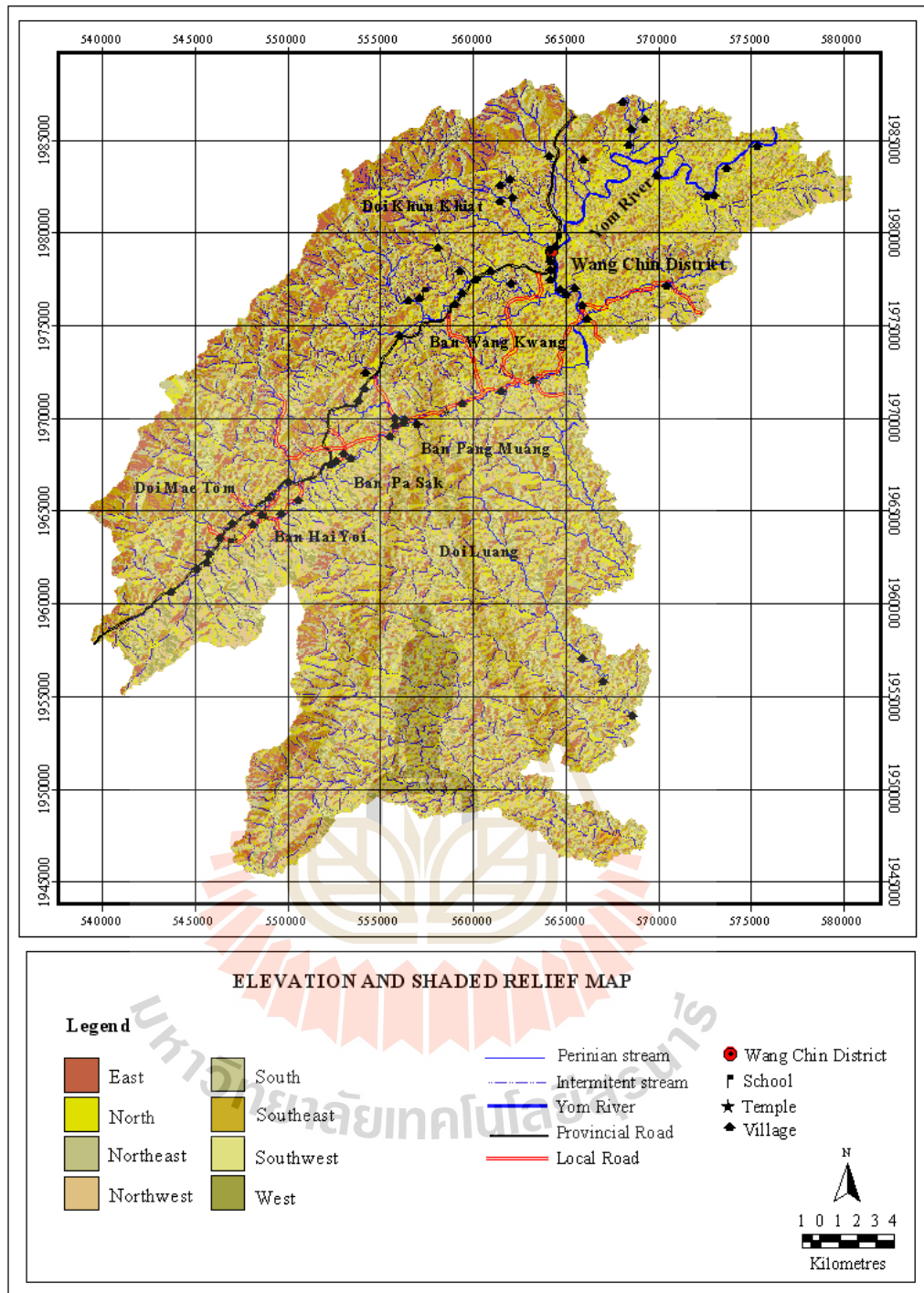


Figure 4.22 Slope aspect map based on DEM, which is derived from Aster data (taken on 28/11/2001).

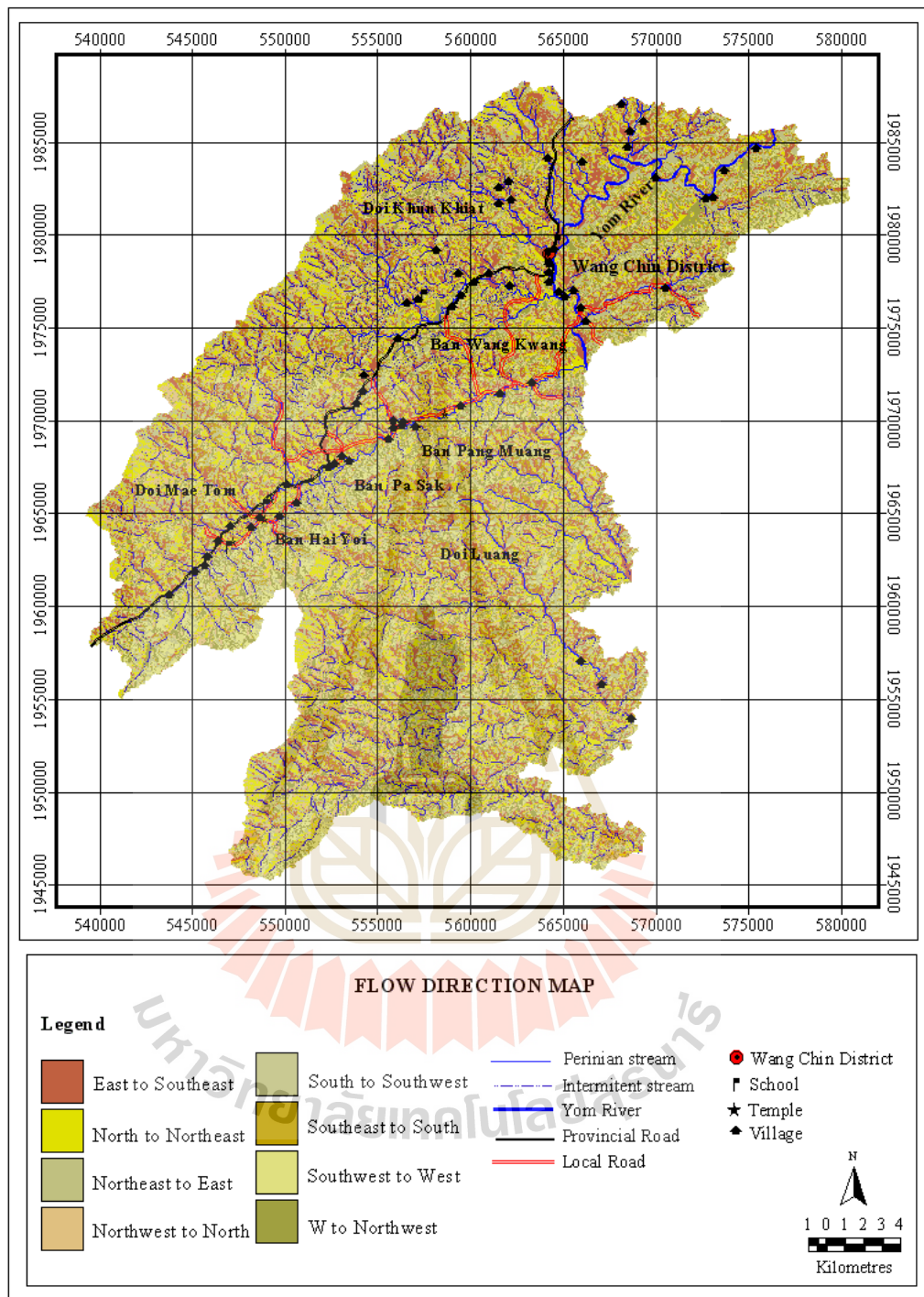


Figure 4.23 Flow direction map based on DEM, which is derived from Aster data (taken on 28/11/2001).

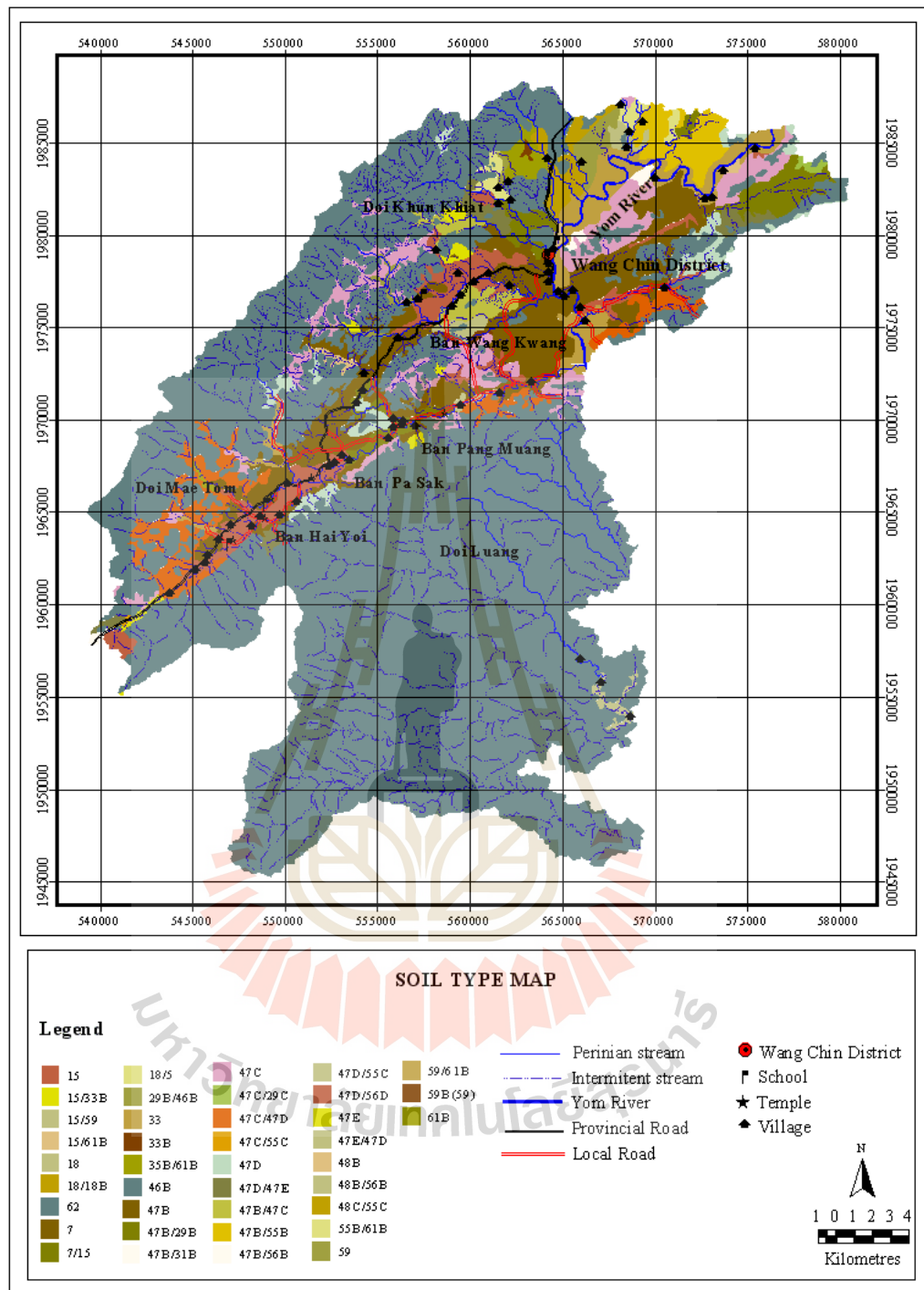


Figure 4.24 Soil type map based on Land Development Department, 1996.

4.2 Landslide Assessment Analysis

The probability analysis and weighting for landslide occurrence on the factor maps were calculated from a step of landslide assessment analysis. The probability analysis comprised the analysis of the relationship between landslide occurrence and factor maps, and the calculation of probability ratio, which is explained as follows:

4.2.1 Relationship between Landslide Occurrence and the Factors

The relationship between landslide occurrence and the factors relies on an examine the spatial relationships between interpreted landslide locations and individual factors. The method applied is to cross-tabulate the past landslide location map with each factor map. Then, a landslide distribution table is developed and it indicates the number of landslide location occurring on each specific area of attribute of each factor (e.g. each lithology attribute of the lithologic layer). The results of the relationship between landslide occurrence and the factors calculating are presented in the Appendix A (Tables 1A to 9A). They allow important deduction to be made regarding the role and possible significance of factors, as discussed belows:

Landslide occurrence on lithology factor: The relationship between landslide and lithology (Table 1A), the landslide occurrence value is very high in shale interbedded with sandstone and siltstone (Pm1), and is high in sandstone and andesitic tuff, rhyoritic tuff, and crystal tuff (Tr3 and Rht1). It is very low to low for landslide occurrence on the metamorphic rocks, metasedimentary rocks, sedimentary rocks, alluvium and terrace deposits (Pm2, Rht2, Tr3-1, tr3-2, Tr3-3, Qa and Qt). The presence of fissility, high fracture and weathered shale might be the cause of landslide occurrence on this lithology. The failure also occurs along the bedding plane. of interbedded rocks. Landslide has not been observed in the rock units of CP and PM3.

It might be due to the presence of the limestones in these units, which are relatively high resistance and the source of secondary cementing agent.

Landslide occurrence on the buffered lineament factor: Landslide occurrence on the buffered lineament has been shown in Table 2A. Most of landslide occurrences was occurred in the first and second order of buffered lineaments zone, which shows an increasing of the landslide affected area in the nearly distance to lineaments. The landslide occurrence is gradually decreased with increasing distance from lineaments. Because lineaments are acting as a weak zone of bedrocks. The degree of landslide occurrence on 0-100 metres buffer of lineaments is very high. The high landslide hazard occurrence is on 100–200 metres away from lineaments. Very low to low landslide occurrences are on the distance of 200–1,000 metres from lineaments.

Landslide occurrence on land use/land cover factor: The trend of landslide occurrence on the land use/land cover based on the observed data is shown in Table 3A. From the analysis, the landslide occurrence is higher on the natural forest and teak plantation area than other land use area. The landslide occurrence is very high on the open forest land cover, and high on densely open forest and deforestation areas. The observed landslide occurrence on the other land use type is low to very low. The reason is simply because the landslides occurred mainly on inclined and mountainous areas

Landslide occurrence on vegetation index factor: The relationship between landslide and vegetation index (Table 4A), the landslide occurrence is very high on the vegetation index value 0.75-1.0 (dense vegetation areas) and high on the vegetation index value 0.25-0.75 (slightly to moderately vegetation areas).

The observed landslide occurrences on the other NDVI values are very low to low. The landslide occurrence on vegetation index is conformed to the landslide occurrence on land use/land cover.

Landslide occurrence on slope angle factor: From Table 5A, the landslide occurrences within the slope ranging from 5–28 degrees are relatively high. The trend of landslide occurrence in Table 4.5 shows that the landslide occurrence is gradually increasing with the steeper slope, and is decreased when the slope higher than 32 degrees. It might be explained that the steep slope of higher than 35 degrees is relative stable due to the exposure of the hard bedrock.

Landslide occurrence on slope aspect factor: The trend of landslide occurrence given in the Table 6A shows that the southeast aspect and east aspect areas have been relatively highly affected by the 27.30 and 26.20 percent of landslide location number. From the analysis has been found that the north, west and southwest aspects are less affected by landslide occurrence. The reason is depending on the wind direction of the rain-storm. It has been observed that the loss of lives and houses by May 2001 disaster was found significantly on the east and southeast slopes.

Landslide occurrence on soil unit factor: The relationship between landslide and soil unit factors is shown in Table 7A. In the case of material, the landslide occurrence value is higher in the mountainous soil unit (soil unit 62) and lowers in valley consisting of alluviums and colluviums. Landslide occurrence on soil unit factor is related the topography and the geological condition.

Landslide occurrence on flow direction factor of a watershed: The landslide occurrence on flow direction is higher in northeast to east and east to southeast direction (Table 8A). It affects the peak flow rate of a stream and thus the

initiation of debris flow. The flow direction is depending on the direction of the steepest slope. Therefore, the surface runoff moved from the highest point to the lowest point. The lowest point is called the watershed outlet, which is indicated the risk area.

Landslide occurrence on elevation factor: There is a general increase in landslide incidence from low altitude to higher altitude (Table 9A). In the study area, landslides are highly occurred at altitudes from 326 to 428 metres.

4.2.2 Probability Analysis

The probability analysis is performed in term of the probability ratio. The probability ratio of landslide occurrence in each factor's classes can be calculated from percentage of landslide occurrence divided by percentage of total area of the same attribute of the factor from the result on Tables 1A to 9A (cf. equation 3.1). The probability ratio is used as a guide to where further landslides are likely occurring. The results of probability ratio of each factor's classes are shown in Appendix B (Tables 1B to 9B) and discussed belows:

Probability ratio of landslide occurrence on lithology: As already discussed that the percentage of landslide location and percentage of landslide affected area for the PM1 is the highest as compared to other classes. The landslide probability ratio of the Pm1 unit is the highest as can be observed from the Table 1B. The percentages of landslide location of the Tr3 and Tr3-3 units are 17.55 and 1.35, but the probability ratio of the Tr3-3 unit is higher than in Tr3 unit. The percentage of landslide affected area of Tr3 unit is very large (21.71 percent of the whole area) and the area of Tr3-3 unit is very low (0.83 percent of the total area). In this case, the landslide probability ratio is the value of likelihood landslide occurrence in the class

compared with its area. The results show that the probability of landslide occurrence on Ttr3-3 unit is higher than Tr3 unit.

Probability ratio of landslide occurrence on buffered lineament: In this case, the distance from lineament 0-100 metres has the highest probability ratio of landslide occurrence which indicates that this range of lineament has a very high hazard for the occurrence of landslides. The high hazard is represented the range of distance 100 – 200 metres from lineaments. (Table 2B).

Probability ratio of landslide occurrence on land use/land cover: Table 3B the landslide probability ratio in open forest area is very high. The teak plantation and densely open forest land use/cover types are high landslide probability ratio. This shows the high accuracy of the calculation as the result is conformed with very high occurrence of landslides in these areas based on the field survey.

Probability ratio of landslide occurrence on NDVI: The probability ratio of landslide occurrence on NDVI index values 0.5 to 1.0 is higher than in the other NDVI index values. It conforms with the probability of landslide occurrence on land use/land cover factor (Table 4B).

Probability ratio of landslide occurrence on slope steepness: The slope is one of the important factors affected the landslides occurrence in the portion of the study area that is located in the high mountainous area (Table 5B). The probability value for slope in the range 23–37 degrees is considered to be high for landslide occurrence. So the areas covered by these slope classes are quite unstable.

Probability ratio of landslide occurrence on slope aspect: From Table 6B, the probability ratio of landslide occurrence for the slope aspect to the east is the highest in term of landslide hazard, whereas the southeast and the south are

considered to be quite high.

Probability ratio of landslide occurrence on flow direction: The probability ratio of flow direction factor is the highest on northeast to east direction and high on southeast direction. This conforms with the direction of the slope aspect as shown in Table 7B.

Probability ratio of landslide occurrence on soil unit: The soil unit 62 shows the highest probability ratio of landslide as compared to the probability ratio of landslide on other attributes of soil unit factor (Table 8B). This unit contains 92.15 percent of landslide location and its area covers 66.64 percent of the whole area.

Probability ratio of landslide occurrence on elevation: From the elevation Table 9B, it shows that there are three classes of elevation ranging from 377 to 428 metres, which are very high probability ratio of landslide occurrence. The probability of landslide occurrence for elevation in the range 224 - 377 metres are considered to be relatively moderate to high landslide hazard zone.

4.2.3 Weighting for the Importance of Factors on Landsliding

The identification of potential landslide areas requires that the factors are considered to be combined in accordance with their relative importance to landslide occurrence. This can be achieved by developing a ranking and weighting scheme in which factors and their classes are assigned with numerical values. The importance of a factor as a predictor of landsliding can be considered in different ways. Two possible approaches were used in this study. These approaches are based on the reliability probability method, and the accountability probability method.

In both performance measures, only probability values of attributes ≥ 1 (i.e. mean and above mean landslide incidence) are considered. The mean landslide

incidence value means the probability ratio of landslide occurrence for the whole area (cf. equation 3.2). Then, each single factor is first assigned with a numerical ranking based on the probability ratio of landslide occurrences. The highest probability ratio was assigned with the first rank of importance. The rank value r_i is between 1 and n , whereas $r_i = 1$ is the rank of highest importance, and n is the number of all factors analyzed. In this study, 9 factors were ranked ($n = 9$). Weights are also assigned to each factor's rank of both methods (cf. equation 3.6). The larger the weight is the the greater chance the landslide occurs. Before the weights can be combined, they need to be normalized (cf. equation 3.7).

Weighting for the importance of factors on landsliding were calculated based on reliability probability ratio and accountability probability ratio of each factor as discussed below:

Weighting for the importance of factors on landsliding based on reliability probability ratio: Reliability means the value of factor corresponding to landslide. The reliability probability is calculated as the percentage area of factors corresponding to landslides. It is computed for each factor (cf. equation 3.4). The results are the reliability probability ratio of each factor, as a predictor of landsliding as shown in the Appendix C (Tables 1C to 9C).

Reliability probability ratio of each factor is meant the likelihood of landslide occurrence when compared to the probability of landslide occurrence for the whole area. For example, the reliability of lineament is 2.06 that means the chance of landslide occurrence in the area according to lineament factors is 2.06 times of the mean landslide incidence value. Then the results from Tables 1C to 9C were used for ranking and weighting of importance of factors as shown in Table 4.1.

Table 4.1 Rank order and weighting of importance of factors based on reliability probability ratio.

Type of Factors	Reliability	Rank	w	w _i	w _i x100
Elevation	2.21	1	9	0.20	20
Lineament	2.17	2	8	0.18	18
NDVI	1.98	3	7	0.16	16
Land use	1.96	4	6	0.13	13
Slope	1.86	5	5	0.11	11
Geology	1.65	6	4	0.09	9
Aspect	1.52	7	3	0.07	7
Flow direction	1.45	8	2	0.04	4
Soil unit	1.36	9	1	0.02	2
	Total	n=9	45	1	100

Weighting for the importance of factors on landsliding based on accountability probability ratio: Accountability means the value of landslides accounted for by factor. The accountability probability of factor is calculated from the total landslide population accounted for each factor compared to the total landslide point over the entire area. It is computed for each factor (cf. equation 3.5). The results of the accountability probability ratio of each factors as a predictor of landsliding are shown in Appendix C (Tables 10C to 18C).

The results of accountability probability were used to ranking and weighting the importance of factors on landsliding. Accountability importance of each factor means the likelihood of landslide occurrence according to that factor compared to the total number of landslide occurrence for the whole area. For example, the accountability of lineament is 0.95 that means the chance of landslide occurrence in the area according to lineament factor, which is 95 percent of all landslides location. The rank order and weighting of accountability probability ratio of each factor are shown in Table 4.2.

It can be seen that the two performances (reliability and accountability probability ratio) as mentioned earlier do not provide the same information, but it is impossible to say which is the better indicator. For example, three classes of lithology representing the high probability of landslide are called Rock A (Rht1, TR3-3, and PM1) in table 1C, which is representative to the lithology factor. Rock A accounts for 77.18 percent of all past landslides location and covers 46.71 percent of the total study area. The reliability probability ratio of lithology corresponds to landslide occurrence is 1.65 ($77.18/46.71$). Slope B (slope classes of angle ranging from 14-46 degrees and representative to the slope factor) accounts for 66.39 percent of total landslides

locations, and covers an area of 35.88 percent of the study area. Thus the reliability ratio of slope factor on landsliding corresponds to landslide occurrence is 1.86 (66.39/35.88). It can be concluded that the lithology factor has more accounts of landslide population than slope factor. But lithology factor is less reliable and indicates the less likelihood of landsliding than slope factor when both of them are compared to their own area. Nevertheless, each of these measures can provides useful information for landslide hazard mapping.

As mentioned above, it can be considered that the landslides are depended on both the distribution of landslides in each class and the area of each factor's classes corresponding to landslides. Then these two methods of quantifying the significance of factors as a predictor of landsliding were combined by summing the weights and applied the rank order of importance for each factor again (Tables 4.3-4.4). This is the final weight calculation, which used to produced the landslide hazard map, and it should provide a better result.

Table 4.2 Rank order and weighting of importance of factors based on accountability probability ratio.

Type of factors	Accountability	Rank	w	w _i	w _i x100
Soil type	0.96 = 96%	1	9	0.20	20
Lineament	0.94 = 94%	2	8	0.18	18
Land use	0.85 = 85 %	3	7	0.16	16
Aspect	0.81 = 81%	4	6	0.13	13
Flow direction	0.80 = 80%	5	5	0.11	11
Elevation	0.79 = 79%	6	4	0.09	9
Geology	0.77 = 77%	7	3	0.07	7
NDVI	0.69 = 69%	8	2	0.04	4
Slope	0.68 = 68%	9	1	0.02	2
	Total	n=9	45	1	100

Table 4.3 Combination weights and rank of reliability and accountability probability.

Type of factors	Reliability Probability (RP)	Accountability Probability (AP)	(RP) + (AP)
	$w_i \times 100 = W(R)$	$w_i \times 100 = W(A)$	$\{W(RP) + W(AP)\}/2$
Soil type	2	20	11
Lineament	18	18	18
Land use	13	16	14
Elevation	20	13	17
Aspect	7	11	9
Flow direction	4	9	7
Geology	9	7	8
NDVI	16	4	10
Slope	11	2	6
Total	100	100	100



Table 4.4 The importance of factors on landslide occurrence.

Type of factors	The importance on landslide occurrence	
	Rank	Weight
Lineament	1	18
Elevation	2	17
Land use	3	14
Soil unit	4	11
NDVI	5	10
Slope aspect	6	9
Lithology	7	8
Flow direction	8	7
Slope	9	6

4.3 Landslide Hazard Zonation Map

The probability ratio map of each factor and their weights are used to produce landslide hazard zonation map. The degree of landslide hazard present is considered relative, and represents the expectation of future landslide occurrence based on the conditions of that particular area. For another area it may appear similar but, in fact, have a differing landslide hazard due to slightly different landslide conditions. Thus, landslide susceptibility is relative to the condition of each specific area, and cannot be assumed to be identical for a different condition area.

In this study, landslide hazard map or landslide susceptibility map can be produced in different four models. These are landslide hazard map based on reliability probability weighted, landslide hazard map based on accountability probability weighted, landslide hazard map based on combination of reliability and accountability weighted, and landslide hazard map based on slope stability model.

For the model 1, 2 and 3 the analysis is based on the following formula:

$$LPI = \sum_{j=1}^J \{(F_j \cdot W_j)/100\} \dots \dots \dots (4.2)$$

LPI is landslide probability index.

J
 F_j is the data layers of each factor (1,2,3,...,j, with j = 9, in this study), which is represented the probability index values (cf table 1B-9B). For example, F_1 = Slope factor map contained the probability ratio of landslide occurrence of each slope class.

i
 W_i is the weight of each factor considered (1,2,3,...,i, with i = 9, in this study)

Landslide hazard map based on reliability probability weighted: The spatial data layers representing probability ratio values of the factor's classes were used as input data for spatial analysis in the GIS. The input data layers were multiplied by their corresponding reliability weighted, and were summed up together to obtain the Landslide Probability Index (LPI) for each 30 by 30 metres cell as shown in Figure 4.25.

The landslide probability index obtained ranges from 0.08 to 2.81. These could be classified into five landslide susceptible classes. A judicious way for this classification is to use the relative equal interval to separate the landslide potential index into landslide hazard classes level.

The level of landslide hazard is measured on the ordinal scale based on the equal interval values. Then, five levels of relative hazard are defined on a landslide susceptibility map: (1) very low; (2) low; (3) moderate; (4) high; and (5) very high hazard. The landslide probability index value and landslide hazard map I based on reliability probability weighting are shown in the Table 4.5 and Figure 4.26.

The landslide hazard map I shows that 2.49 percent of the whole area lies in the highest landslide prone area. The percentage of very low hazard area is the highest at 35.19 percent of the total area. Similarly, 28.01 percent, 19.44 percent and 14.87 percent of areas lie in the low, moderate and high landslide hazard levels, respectively. It is obvious from the result map that the areas under high and very high hazard level are located near the first and second stream orders of the study area.

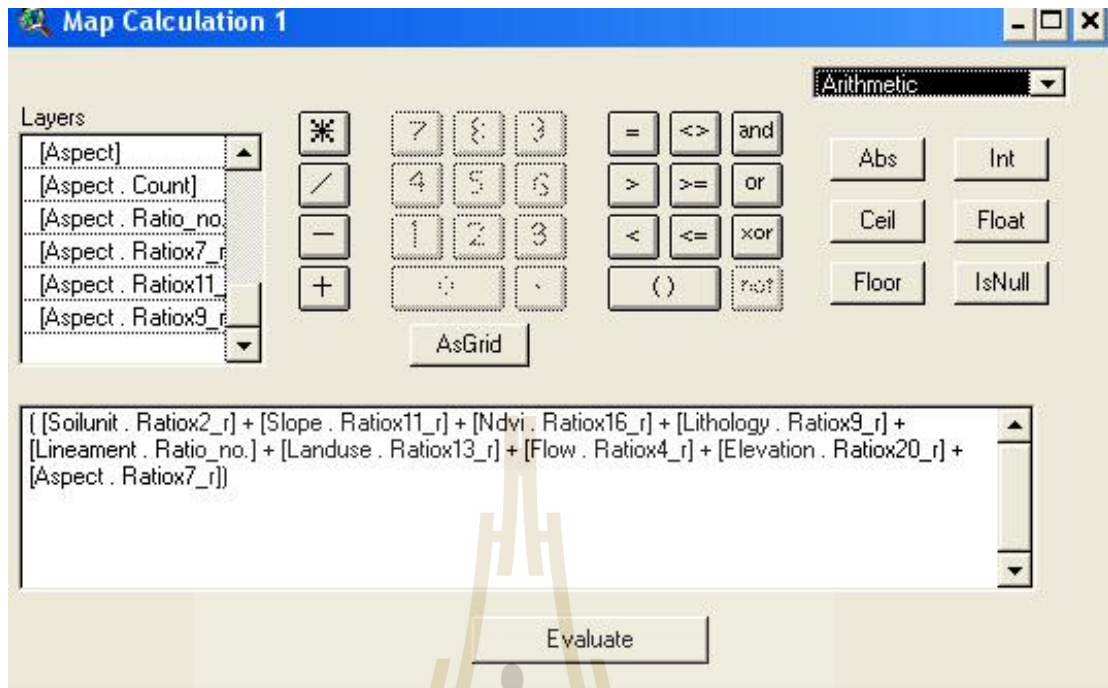


Figure 4.25 The input data layers were multiplied by their corresponding reliability weighted, and were summed up together to obtain the Landslide Potential Index (LPI) for each 30m by 30 m (Soilunit.Ratiox2_r = Soil unit map layer with probability index of landslide occurrence x reliability weighted of its layer (2)).

Table 4.5 Landslide probability index value and hazard level of the Wang Chin area based on reliability probability weighting.

Hazard level classes	Landslide Probability Index	Landslide Hazard Level	% of Area
1	0.08-0.62	Very Low	35.19
2	0.63-1.17	Low	28.01
3	1.18-1.71	Moderate	19.44
4	1.72-2.26	High	14.87
5	2.27-2.81	Very High	2.49

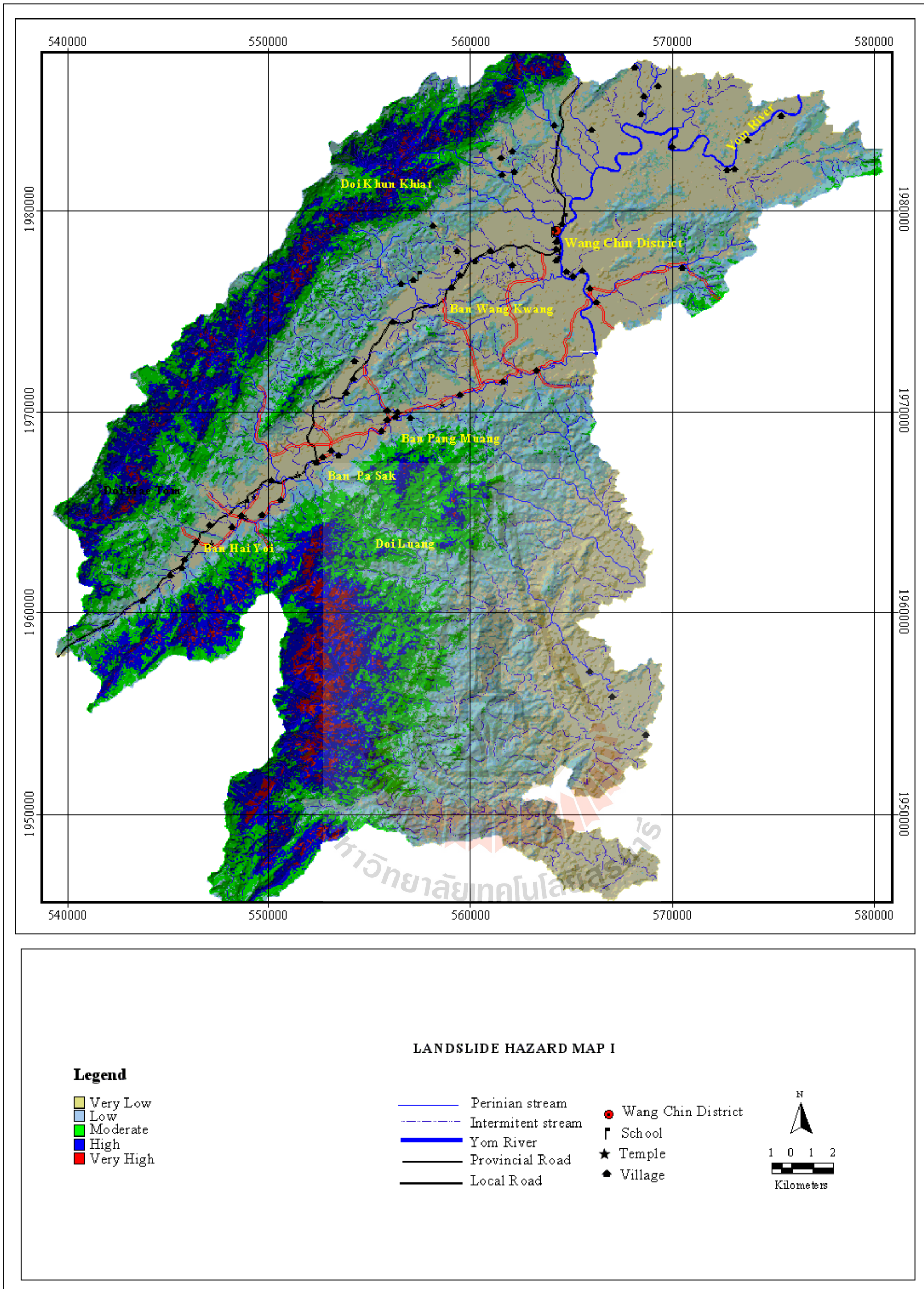


Figure 4.26 Landslide hazard map based on reliability probability.

Landslide hazard map based on accountability probability weighted: The spatial data layers representing probability ratio values of the factor's classes were used as input data for spatial analysis in the GIS. The input data layers were multiplied by their corresponding accountability weighted, and were summed up together to obtain the Landslide Probability Index (LPI) for each 30m by 30 m cell as shown in Figure 4.27.

The landslide probability index obtained ranges from 0.08 to 7.66. These could be classified into five landslide hazard classes. A judicious way for this classification is to use the relative equal interval to separate the landslide potential index into landslide hazard classes level.

The level of landslide hazard is measured on the ordinal scale based on the equal interval values. Then, five levels of relative hazard are defined on a landslide susceptibility map: (1) very low, (2) low, (3) moderate, (4) high, and (5) very high hazard. The landslide probability index value and the landslide hazard map II based on accountability weighted are shown in the Table 4.6 and Figure 4.28.

The landslide hazard map shows that 7.66 percent of the whole area lies in the highest landslide prone area. The percentage of low hazard area is the highest at 30.16 percent of the total area. Similarly, 19.69 percent 22.61 percent and 19.88 percent of the areas lie in the high, moderate and very low landslide hazard, respectively. It is obvious from the result map that the areas under high and very high hazard level are located near the first and second stream orders of the study area.

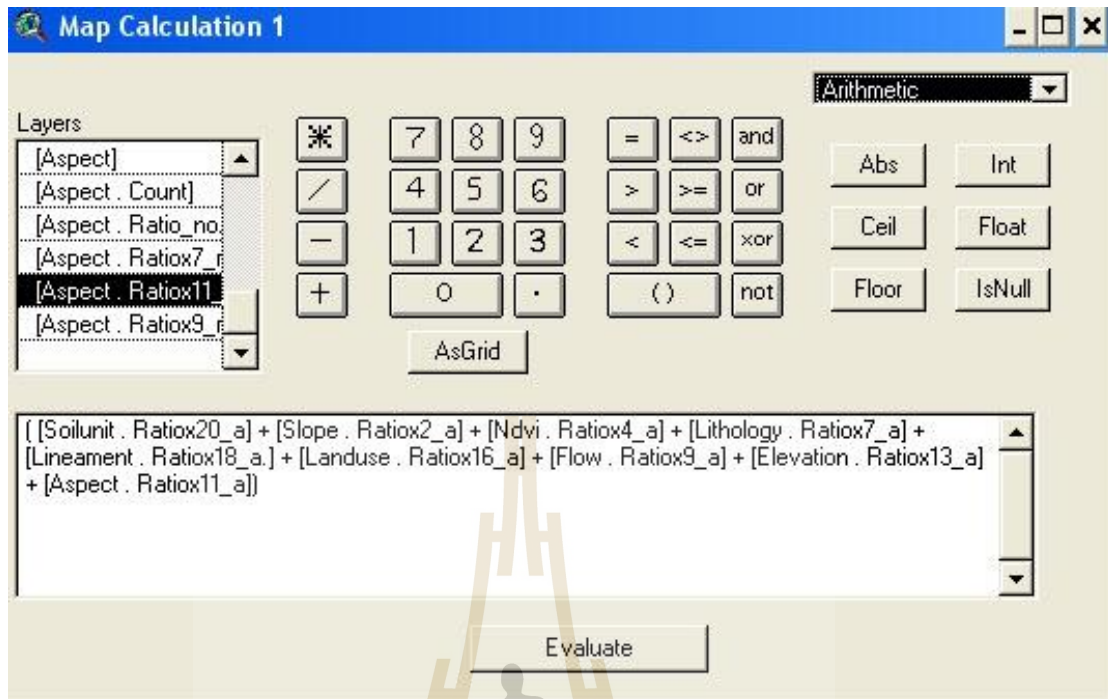


Figure 4.27 The input data layers were multiplied by their corresponding accountability weighted, and were summed up together to obtain the Landslide Potential Index (LPI) for each 30 by 30 metres (eg. Soilunit.Ratiox20_a = Soil unit map layer contained probability ratio of landslide occurrence x accountability weighted of its layer (20)).

Table 4.6 Landslide probability index value and hazard level of the Wang Chin area based on accountability probability.

Hazard level classes	Landslide Probability Index	Landslide Hazard Level	% of Area
1	0.08-0.52	Very Low	19.88
2	0.53-0.96	Low	30.16
3	0.97-1.41	Moderate	22.61
4	1.42-1.85	High	19.69
5	1.86-2.30	Very high	7.66

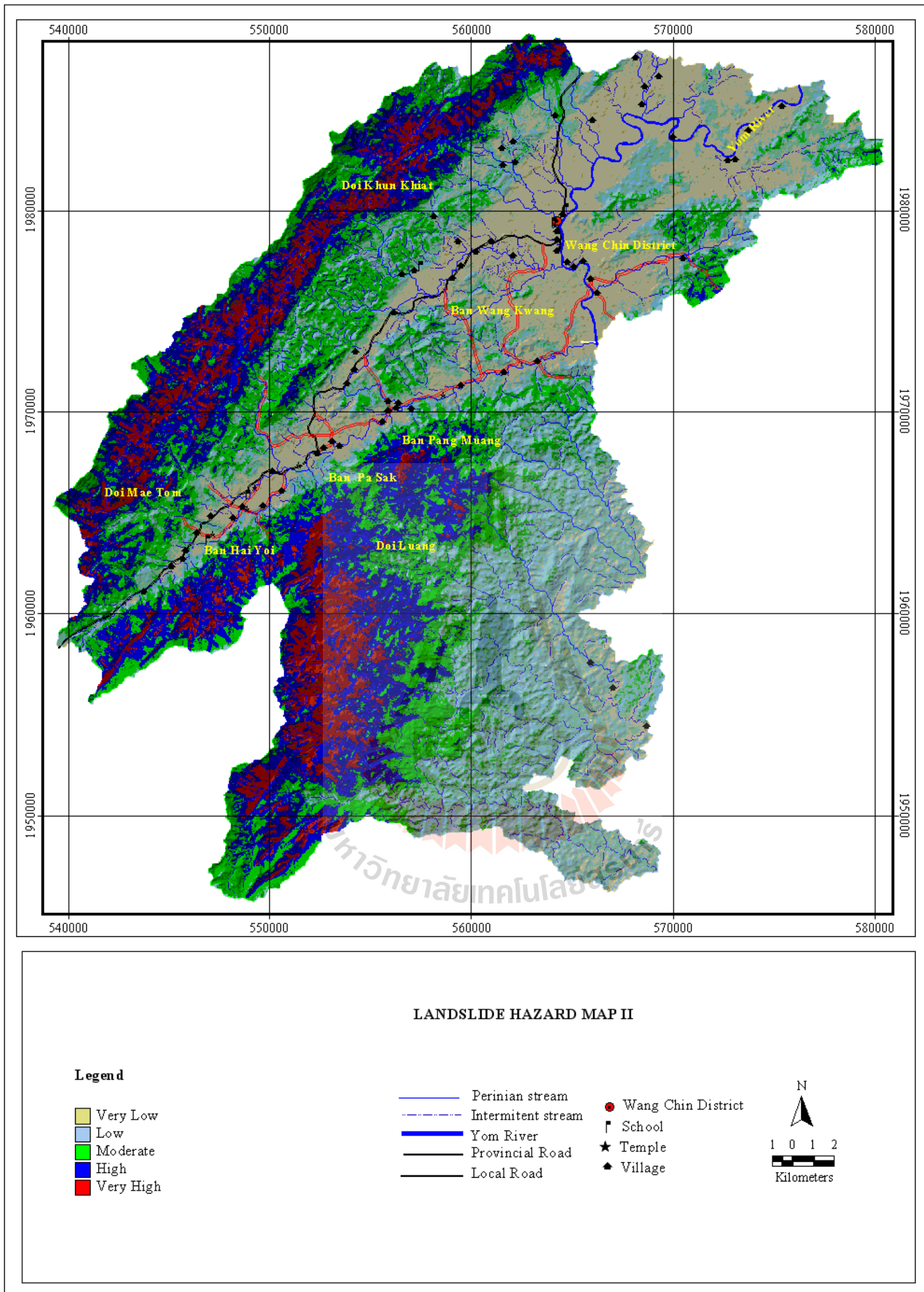


Figure 4.28 Landslide hazard map based on accountability probability.

Landslide hazard map based on combination of reliability and accountability probability weighted: The spatial data layers representing probability ratio values of the factor's classes were used as input data for spatial analysis in the GIS. The input data layers were multiplied by their corresponding combination of reliability and accountability weighted, and were summed up together to obtain the Landslide Probability Index (LPI) for each 30 m by 30 m (Figure 4.29).

The landslide probability index obtained ranges from 0.9 to 2.55. These could be classified into five landslide susceptible classes. A judicious way for this classification is to use the relative interval to separate the landslide potential index into landslide susceptibility classes level.

The level of landslide hazard is measured on the ordinal scale based on the equal interval values. Then, five levels of relative hazard are defined on the landslide hazard map: (1) very low, (2) low, (3) moderate, (4) high, and (5) very high hazard. The landslide probability index value and the landslide hazard map based on combination of reliability and accountability weighted are shown in the Table 4.7 and Figure 4.30.

The landslide hazard map shows that 3.88 percent of the whole area lies in the highest landslide prone area. The percentage of low hazard area is highest at 30.24 percent of the total area. Similarly, 17.44 percent, 20.40 percent and 28.03 percent of area lies in the high, moderate and very low landslide hazard, respectively. It is obvious from the result map that the areas under high and very high hazard level are near the first and second stream orders of the study area. The result from this study represents differing hazard levels that show only the order of relative hazard at a particular site and not the absolute hazard.

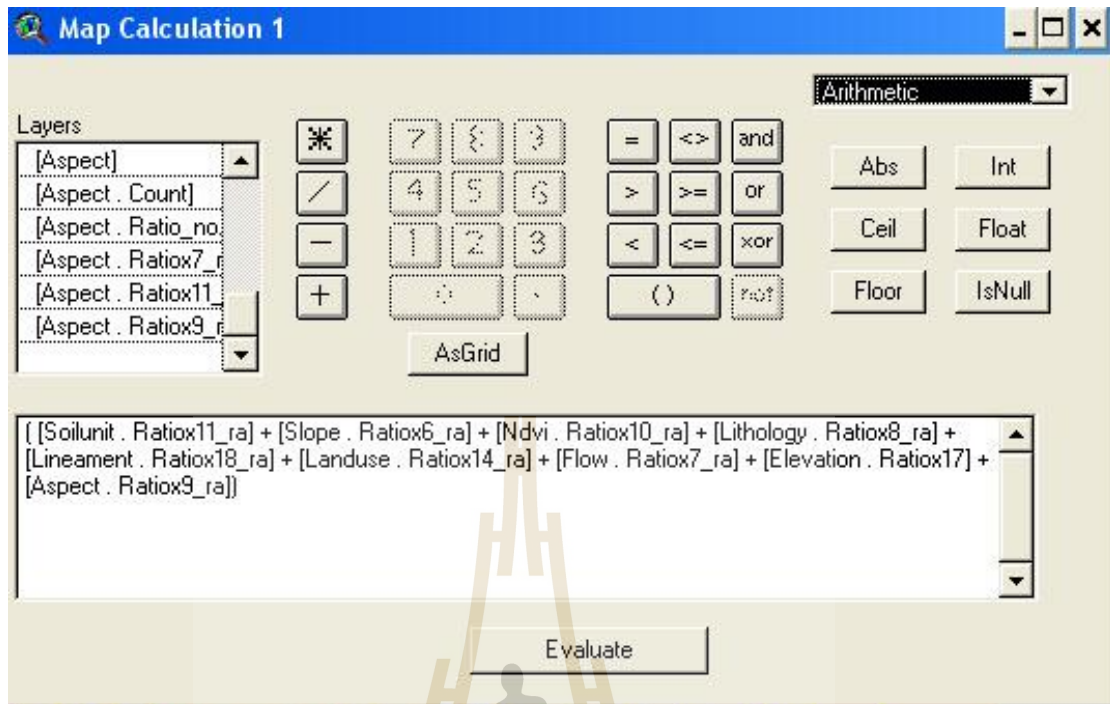


Figure 4.29 The input data layers were multiplied by their corresponding combination of reliability and accountability weighted, and were summed up together to obtain the Landslide Potential Index (LPI) for each 30 by 30 metres (eg. Soilunit.Ratiox11_a = Soil unit map layer contained probability ratio of landslide occurrence x combination weighted of its layer (11)).

Table 4.7 Landslide probability index value and hazard level of the Wang Chin area based on combination of reliability and accountability probability.

Hazard level classes	Landslide Probability Index	Landslide Hazard Level	% of Area
1	0.09-0.58	Very Low	28.03
2	0.59-1.07	Low	30.24
3	1.08-1.56	Moderate	20.40
4	1.57-2.05	High	17.14
5	2.06-2.55	Very High	3.88

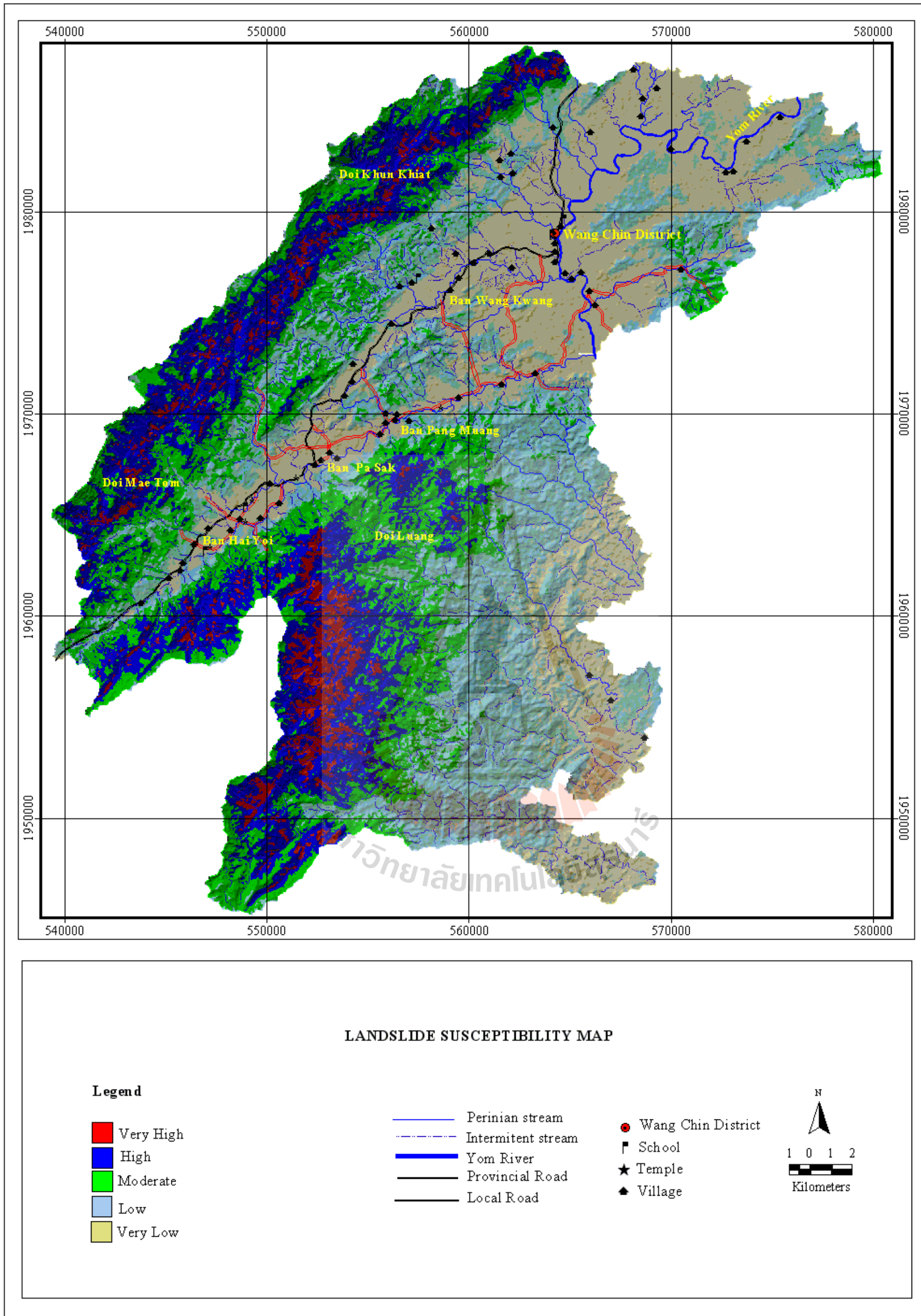


Figure 4.30 Landslide susceptibility map based on reliability and accountability probability.

The landslide hazard maps from these three models represent the differing hazard levels that show only the order of relative hazard at a particular site and not the absolute hazard. These maps are useful for hazard prediction, land use planning, and construction. In Figure 4.31, the villages, road and farm land situated at the flow path out let are under high risk area. By using the landslide hazard zonation map, the high risk areas are consisted of Ban Muang Kham, Ban Mae Kham Muak, Ban Hong, and Ban Pasak. These villages are located at the flow path out let and were directly damaged by the debris flow deposit and flood. The flat slopes of the valley floor (light blue colour on the map) are the risk area from inundation.

Landslide hazard map based on slope stability model: The Rock Slope Stability GIS (RSS-GIS) is used to derive the slope stability map in the Wang Chin area. The slope map is developed from SLOPEMAP extension of RSS-GIS. Required input data for SLOPEMAP extension is raster DEM and raster data defining rock mass discontinuity strength and slope saturation. The result is the slope stability map according to safety factors of slope in the study area, and then this map is compared with the landslide location of the study area, which is interpreted from remote sensing data (Figure 4.32). The validation results show satisfactory agreement between the slope stability map and the existing landslide location data. Some of landslides are located on the stable areas, and these probably depend on the accuracy of DEM data. In addition, the factors related to landslide occurrence are not depending on the slope safety factor only, but also other factors, such as topographical, human activity, and vegetation cover.

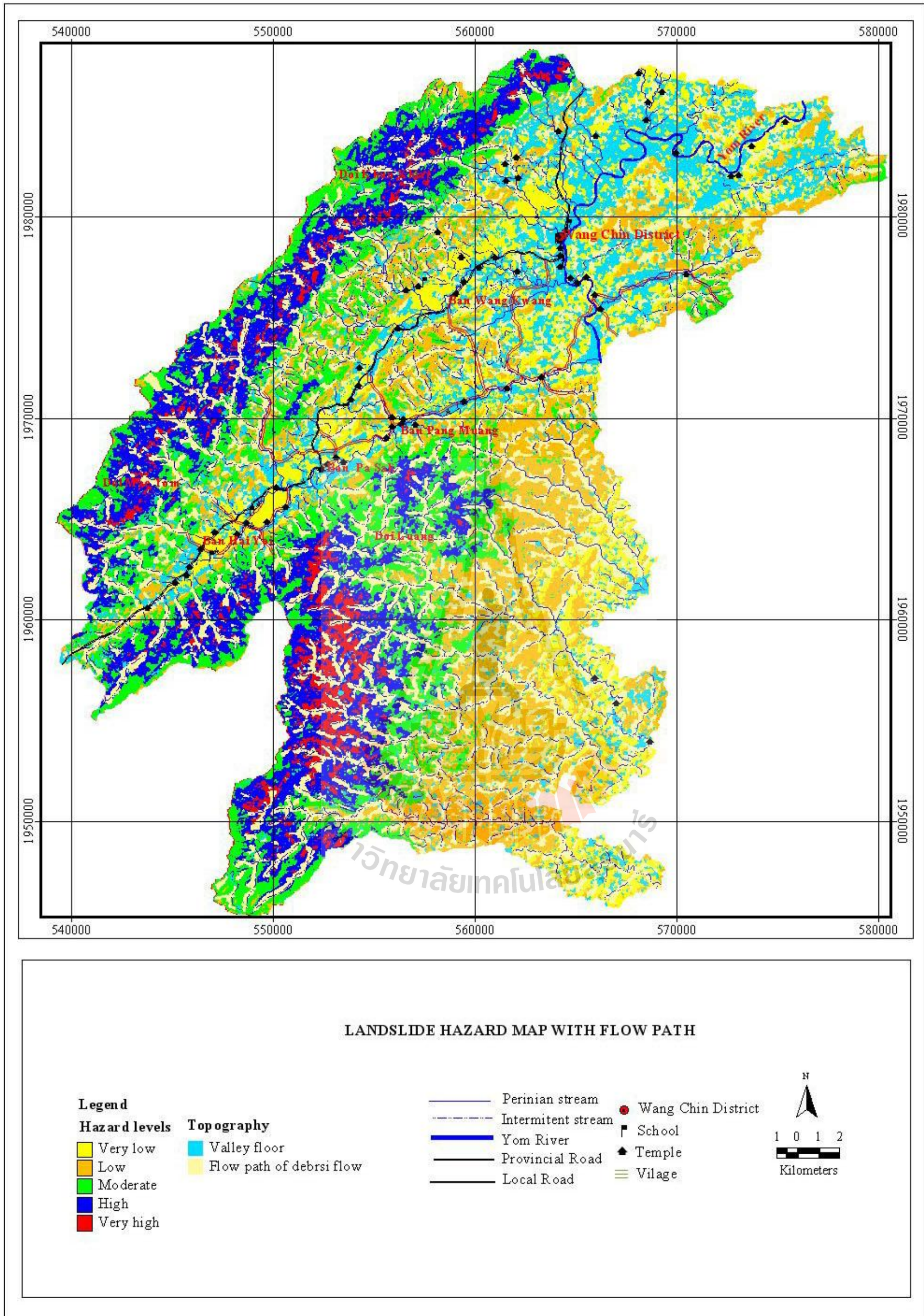


Figure 4.31 Landslide hazard zonation with flow path and deposit area.

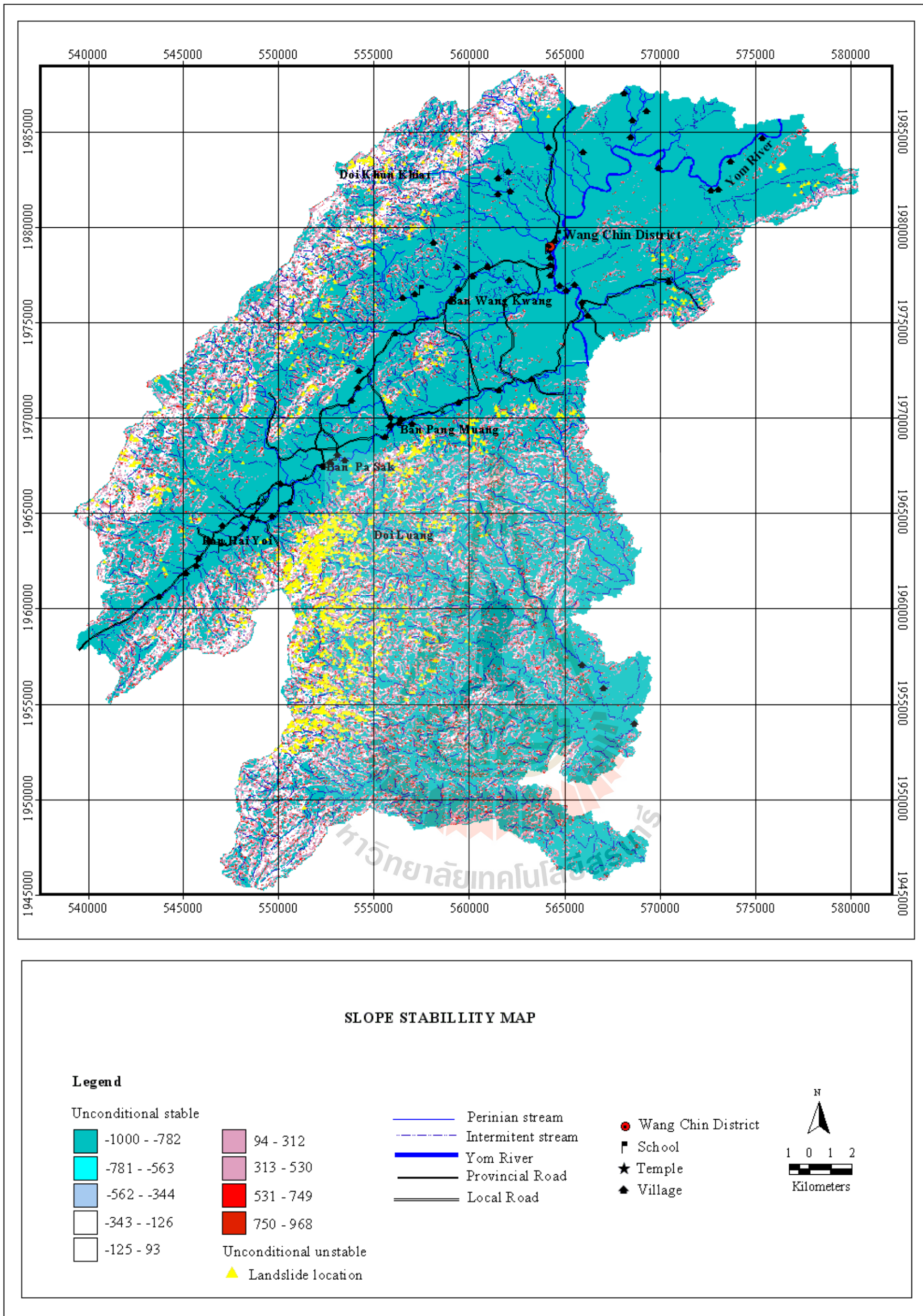


Figure 4.32 Slope stability map shows the stability of the Wang Chin area, which is derived from RSS model (from Guenther, 2005).

4.4 Landslide Prediction Model based on Band Math Tool in ENVI

In this study, the Band Math Tool in ENVI is used to construct landslide prediction model: It was developed from data obtained from the result of probability analysis and weighting of the study area (cf. table 4.4 and tables B1- B9). This landslide prediction model can be used as an automatic assessment for future landslide-prone ground in the area that has similar condition factors (e.g. lithology, elevation, slope, aspect etc) with the Wang Chin area.

The relation and basic arithmetic operations were used to custom the band math equation as follow:

For example Band Math equation of Lineament = (b1 eq 1) * 48 + (b1 eq 2) * 24 + (b1 eq 3) * 8 + (b1 eq 4) * 5 + (b1 eq 5) * 3 + (b1 eq 6) * 5 + (b1 eq 7) * 2 + (b1 eq 8) * 1 + (b1 eq 9) * 1 + (b1 eq 10) * 1

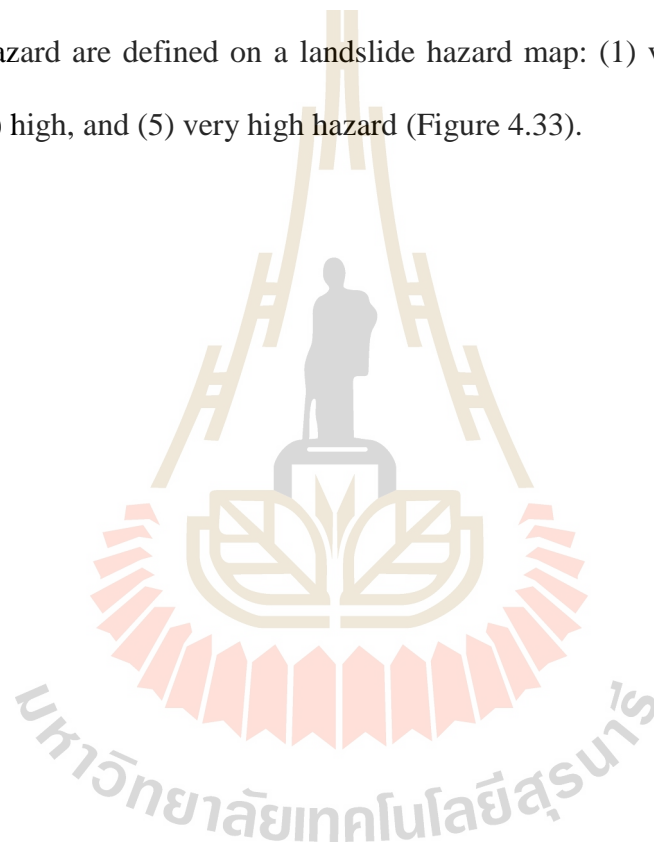
(b1 = band number of lineament, eq = equal, * = multiply, (b1 eq 1) * 48 means the lineament class 1(the distance 100 m from lineament line) will be replace by 48 (probability ratio of each class of lineaments multiply by the combination weights of reliability and accountability weight.)

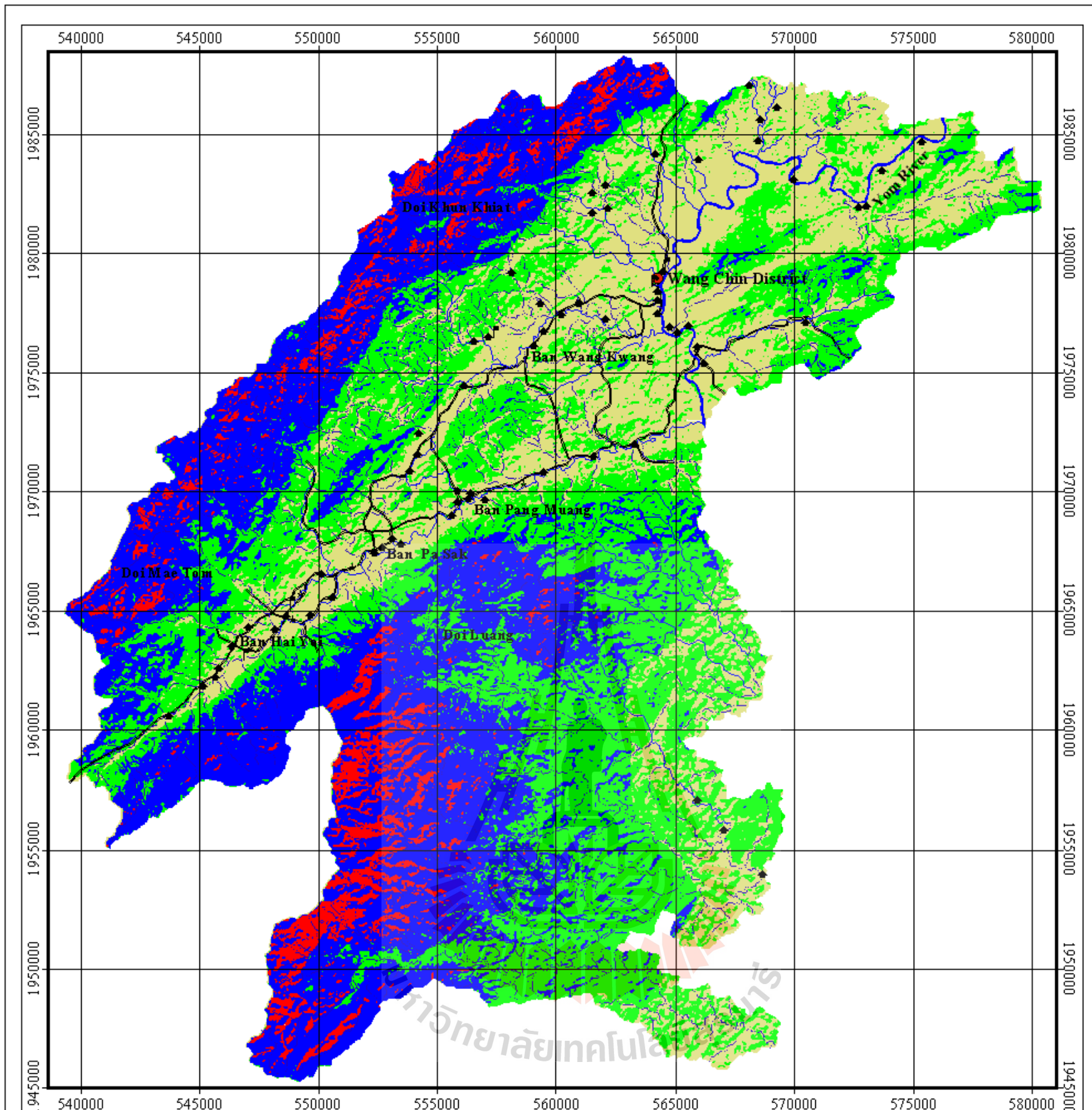
All band math equations are represented by the equations shown in Table 4.8. They are used to evaluate the landslide probability index of each factor. The out put file of each factor represents landslide probability index of attribute classes of the factor and will be used to produce landslide hazard zonation map in the next step of band math tool.

The landslide hazard zonation map was produced by summing the landslide probability index map of each factor. The band math equation was customized to construct the landslide hazard zonation map using addition operation (equation 4.2).

$$\text{Landslide Hazard Map} = B1 + B2 + B3 + B4 + B5 + B6 + B7 + B8 + B9 \dots \dots \dots (4.2)$$

Enter this band math equation that is used to evaluate landslide hazard zonation map in the expression text box and add to list. The process was the same as the step of evaluating landslide probability index map of each factor. The result is the landslide hazard map. This map was classified into five levels of relative landslide hazard zonation using the density slice in overlay function of ENVI. Then, five levels of relative hazard are defined on a landslide hazard map: (1) very low, (2) low, (3) moderate, (4) high, and (5) very high hazard (Figure 4.33).





LANDSLIDE SUSCEPTIBILITY MAP BASED ON BAND MATH PREDICTION MODEL

Legend

- High
- Moderate
- Low
- Very Low

- Perennial stream
- Intermittent stream
- Yom River
- Provincial Road
- Local Road

- Wang Chin District
- School
- Temple
- Village



Figure 4.33 Landslide susceptibility map based on Band Math prediction model.

Table 4.8 Band math expressions for evaluating the landslide probability index of each factor image.

Factors layers	Band math equations
Lineament	$(b1 \text{ eq } 1) * 48 + (b1 \text{ eq } 2) * 24 + (b1 \text{ eq } 3) * 8 + (b1 \text{ eq } 4) * 5 + (b1 \text{ eq } 5) * 3 + (b1 \text{ eq } 6) * 5 + (b1 \text{ eq } 7) * 2 + (b1 \text{ eq } 8) * 1 + (b1 \text{ eq } 9) * 1 + (b1 \text{ eq } 10) * 1$
Elevation	$(b2 \text{ eq } 1) * 1 + (b2 \text{ eq } 2) * 6 + (b2 \text{ eq } 3) * 9 + (b2 \text{ eq } 4) * 18 + (b2 \text{ eq } 5) * 26 + (b2 \text{ eq } 6) * 50 + (b2 \text{ eq } 7) * 66 + (b2 \text{ eq } 8) * 65 + (b2 \text{ eq } 9) * 56 + (b2 \text{ eq } 10) * 43 + (b2 \text{ eq } 11) * 40 + (b2 \text{ eq } 12) * 41 + (b2 \text{ eq } 13) * 39 + (b2 \text{ eq } 14) * 19 + (b2 \text{ eq } 15) * 19 + (b2 \text{ eq } 16) * 19 + (b2 \text{ eq } 17) * 0 + (b2 \text{ eq } 18) * 0 + (b2 \text{ eq } 19) * 0 + (b2 \text{ eq } 20) * 0 + (b2 \text{ eq } 21) * 0 + (b2 \text{ eq } 22) * 0 + (b2 \text{ eq } 23) * 0 + (b2 \text{ eq } 24) * 0 + (b2 \text{ eq } 25) * 0 + (b2 \text{ eq } 26) * 0 + (b2 \text{ eq } 27) * 0 + (b2 \text{ eq } 28) * 0 + (b2 \text{ eq } 29) * 0 + (b2 \text{ eq } 30) * 0$
Land use	$(b3 \text{ eq } 1) * 28 + (b3 \text{ eq } 2) * 27 + (b3 \text{ eq } 3) * 0 + (b3 \text{ eq } 4) * 6 + (b3 \text{ eq } 5) * 1 + (b3 \text{ eq } 6) * 0 + (b3 \text{ eq } 7) * 1 + (b3 \text{ eq } 8) * 2 + (b3 \text{ eq } 9) * 0 + (b3 \text{ eq } 10) * 0 + (b3 \text{ eq } 11) * 0 + (b3 \text{ eq } 12) * 0 + (b3 \text{ eq } 13) * 24 + (b3 \text{ eq } 14) * 0 + (b3 \text{ eq } 15) * 1$
Soil unit	$(b4 \text{ eq } 1) * 15 + (b4 \text{ eq } 2) * 8 + (b4 \text{ eq } 3) * 0 + (b4 \text{ eq } 4) * 6 + (b4 \text{ eq } 5) * 17 + (b4 \text{ eq } 6) * 0 + (b4 \text{ eq } 7) * 0 + (b4 \text{ eq } 8) * 0 + (b4 \text{ eq } 9) * 0 + (b4 \text{ eq } 10) * 0 + (b4 \text{ eq } 11) * 1 + (b4 \text{ eq } 12) * 2 + (b4 \text{ eq } 13) * 0 + (b4 \text{ eq } 14) * 0 + (b4 \text{ eq } 15) * 2 + (b4 \text{ eq } 16) * 0 + (b4 \text{ eq } 17) * 0 + (b4 \text{ eq } 18) * 0 + (b4 \text{ eq } 19) * 0 + (b4 \text{ eq } 20) * 0 + (b4 \text{ eq } 21) * 6 + (b4 \text{ eq } 22) * 0 + (b4 \text{ eq } 23) * 0 + (b4 \text{ eq } 24) * 0 + (b4 \text{ eq } 25) * 2 + (b4 \text{ eq } 26) * 5 + (b4 \text{ eq } 27) * 0 + (b4 \text{ eq } 28) * 15 + (b4 \text{ eq } 29) * 0 + (b4 \text{ eq } 30) * 0 + (b4 \text{ eq } 32) * 11 + (b4 \text{ eq } 33) * 0 + (b4 \text{ eq } 34) * 3 + (b4 \text{ eq } 35) * 22 + (b4 \text{ eq } 36) * 0 + (b4 \text{ eq } 37) * 0 + (b4 \text{ eq } 38) * 0 + (b4 \text{ eq } 39) * 0$
NDVI	$(b5 \text{ eq } 1) * 2 + (b5 \text{ eq } 2) * 2 + (b5 \text{ eq } 3) * 2 + (b5 \text{ eq } 4) * 4 + (b5 \text{ eq } 5) * 6 + (b5 \text{ eq } 6) * 9 + (b5 \text{ eq } 7) * 14 + (b5 \text{ eq } 8) * 26$
Aspect	$(b6 \text{ eq } 1) * 20 + (b6 \text{ eq } 2) * 9 + (b6 \text{ eq } 3) * 17 + (b6 \text{ eq } 4) * 16 + (b6 \text{ eq } 5) * 12 + (b6 \text{ eq } 6) * 8 + (b6 \text{ eq } 7) * 4 + (b6 \text{ eq } 8) * 2$
Lithology	$(b7 \text{ eq } 1) * 1 + (b7 \text{ eq } 2) * 6 + (b7 \text{ eq } 3) * 1 + (b7 \text{ eq } 4) * 1 + (b7 \text{ eq } 5) * 0 + (b7 \text{ eq } 6) * 0 + (b7 \text{ eq } 7) * 0 + (b7 \text{ eq } 8) * 4 + (b7 \text{ eq } 9) * 3 + (b7 \text{ eq } 10) * 3 + (b7 \text{ eq } 11) * 8 + (b7 \text{ eq } 12) * 13 + (b7 \text{ eq } 13) * 16$
Flow direction	$(b8 \text{ eq } 1) * 8 + (b8 \text{ eq } 2) * 14 + (b8 \text{ eq } 3) * 10 + (b8 \text{ eq } 4) * 8 + (b8 \text{ eq } 5) * 3 + (b8 \text{ eq } 6) * 3 + (b8 \text{ eq } 7) * 2 + (b8 \text{ eq } 8) * 5$
Slope	$(b9 \text{ eq } 1) * 1 + (b9 \text{ eq } 2) * 3 + (b9 \text{ eq } 3) * 6 + (b9 \text{ eq } 4) * 8 + (b4 \text{ eq } 5) * 10 + (b9 \text{ eq } 6) * 13 + (b9 \text{ eq } 7) * 13 + (b9 \text{ eq } 8) * 19 + (b9 \text{ eq } 9) * 24 + (b9 \text{ eq } 10) * 27 + (b9 \text{ eq } 11) * 0 + (b9 \text{ eq } 12) * 0 + (b9 \text{ eq } 13) * 0$

4.5 Verification of the Result

The verification method is performed by comparison of existing landslide Data with landslide hazard maps by cross tabulation in GIS environment. The validation results show satisfactory agreement between the landslide hazard map based on combination of reliability and accountability weighted and existing landslide location data.

The verification of probability analysis result is shown in Table 4.9. At a landslide probability index value below 1.08, the occurrence ratio(Ls/a) is very low and low with a value of 0 to 0.23. A landslide probability index value above 1.57, the occurrence ratio is high and very high, with a value of 2.55 to 7.31. The index value between 1.08-1.56 is equal to the occurrence ratio of 1. It represents the mean landslide incidence value for the whole area. In this case, the probability indexes of dependent hazard level output are conformed to the method of probability analysis, so the method can be applied well to the landslide occurrence analysis.

This verification method is also performed on both landslide hazard maps, which based on reliability, and accountability weighted. The validation results show unsatisfactory agreement between the landslide hazard map based on reliability, and accountability weighted and existing landslide location data derived from remote sensing data and fieldcheck (Tables 4.10-4.11).

The landslide occurrence ratio (Ls/a) value of landslide hazard map based on accountability weighted (0.69) is lower than the mean average value of landslide occurrence for the whole area (1). The landslide occurrence ratio (Ls/a) value of landslide hazard map based on reliability weighted (1.31) is higher than the mean average value of landslide occurrence for the whole area (1). In both cases, the results

of verification at moderate hazard level are not represents to the average landslide incidence value for the area, so the method can be applied to the landslide occurrence analysis. But there are less reliability than the landslide hazard analysis based on the combination of reliability and accountability weighted.

Table 4.9 Comparison of landslide occurrence and landslide hazard map based on combination of reliability and accountability weighted using probability method.

Class	Hazard level	Landslide probability index	Landslide (point)	% Point of Landslide (Ls)	% of Area (a)	Ls/a=Pr
1	Very Low	0.9-0.58	3	0.18	28.03	0.00
2	Low	0.59-1.07	113	6.93	30.24	0.23
3	Moderate	1.08-1.56	327	20.06	20.40	1.00
4	High	1.57-2.05	725	44.48	17.44	2.55
5	Very High	2.06-2.55	462	28.35	3.88	7.31
		Total	1630	100	100	1

Table 4.10 Comparison of landslide occurrence and landslide hazard map based on accountability weighted using probability method.

Class	Hazard level	Landslide probability index	Landslide (point)	% Point of Landslide (Ls)	% of Area (a)	Ls/a=Pr
1	Very Low	0.08-0.52	2	0.13	19.88	0.00
2	Low	0.53-0.97	45	2.76	30.16	0.09
3	Moderate	0.97-1.41	254	15.58	22.61	0.69
4	High	1.42-1.85	668	40.98	19.67	2.08
5	Very High	1.86-2.30	661	40.55	7.66	5.29
Total			1630	100	100	1

Table 4.11 Comparison of landslide occurrence and landslide hazard map based on reliability weighted using probability method.

Class	Hazard level	Landslide probability index	Landslide (point)	% Point of Landslide (Ls)	% of Area (a)	Ls/a=Pr
1	Very Low	0.08-0.62	8	0.49	35.19	0.01
2	Low	0.63-1.17	182	11.17	28.01	0.40
3	Moderate	1.18-1.71	416	25.52	19.44	1.31
4	High	1.72-2.26	706	43.31	14.87	2.91
5	Very High	2.27-2.81	318	19.51	2.49	7.83
Total			1630	100	100	1

CHAPTER V

DISCUSSION AND CONCLUSION

The methodology and result of landslide hazard assessment of this study in early chapters are discussed in this chapter. Additional discussion on further study and conclusion are also included.

5.1 Discussion

Based on the available, remote sensing and field data, a conceptual landslide hazard or susceptibility map was produced using GIS technique. The remote sensing techniques of interpretation and classification provide information about landslide causes and occurrences. According to this study, it has been found that high spatial resolution satellite image merged with product of IRS 1D PAN and ASTER are quite useful for landslide feature extraction and lineament interpretation as well as lithology. The digital elevation model is extracted from ASTER satellite image bands 3N and 3B. Many types of topographic condition i.e slope angle, slope aspect, watershed boundary, and flow direction are derived from DEM data. The land use/land cover map, lithology and NDVI are classified from Landsat ETM satellite image. The GIS has been demonstrated to be a convenient tool for sorting and displaying data, analysing relationship between landslides and factors, and generating landslide susceptibility map.

The basis of this research focuses on the distribution of past landslides, which can indicate the likelihood of future landslide events. The rationale involves establishing relationship of landslide occurrence with several independent factors (lithology, slope angle and slope aspect etc.). For the landslide susceptibility analysis, the statistic method was applied and validated for the study area based on probability analysis and weights of evidence approach using spatial database. The probability analysis of this study is bases on the form of bivariate analysis of physical characteristics that have led to landslide occurrence in the past.

The spatial data analysis and integration of factors can be divided in to three steps approaches that are used to prepare a landslide hazard zonation map of the study area. The first step is to overlay the landslide distribution map with the factor maps. The second is to perform the probability analysis. The third is to perform ranking and weighting for assessing the importance of factors as a predictor of landslide occurrences. Finally, the landslide hazard map was produced from the result of spatial data analysis and intergration.

For the step of performing ranking and weighting, the importances of each factor affected on landslide occurrence were considered in different way. The measures of reliability and accountability methods are provided for assessing the importance of factors to landslides. The reliability importance is calculated as the percentage area of factors corresponding to landslides. The accountability is calculated the total landslide population accounted for each factors compared with the total landslide points over the entire area. In both performance measures, only probability index values of attributes ≥ 1 are considered. The probability index 1 is called the regional average incidence of landslide for the whole area. The result of

two performance indicators do not provide the same information, but it is impossible to say which is the better indicator. Nevertheless, each of these measures provides useful information for the landslide hazard mapping.

The landslide hazard zonation map was produced by multiplying probability ratio value of classes with the weights of the factors, and then summing up all weights of each pixel. The susceptibility map was eventually divided into five hazard levels: very low, low, moderate, high, and very high. Although there are a lot of causing factors to landslides, this study cautiously selects nine factors for producing a conceptual landslide susceptibility map. The chosen factors are slope angle, slope aspect, elevation, flow direction, NDVI, land use/land cover, soil unit, lithology, and lineament. According to the importance of assessing factors, the major cause of landslide may be attributed to the presence of weak lineament planes and their relation to topographic condition and other factors.

The landslide susceptibility map was produced in a regional scale. The landslide prediction model for the future landslide occurrence was produced based on the result of the probability analysis. This model can be applied to the other areas that have similar condition to the study area such as lithology, slope, and soil unit.

The validation result shows satisfied agreement between the susceptibility map and the existing data on landslide locations. Most of the locations of the identified landslide actually fall into moderate to very high-class levels of the produced susceptibility map. This validates the applicability of the proposed methods, the conducted approaches and the classification scheme. However, the reliability of this study is directly dependent on the quality and quantity of the collected data as well as the methods and skill for conceptual landslide prediction.

These can be improved by applying other methods of analysis and comparing the results between each method.

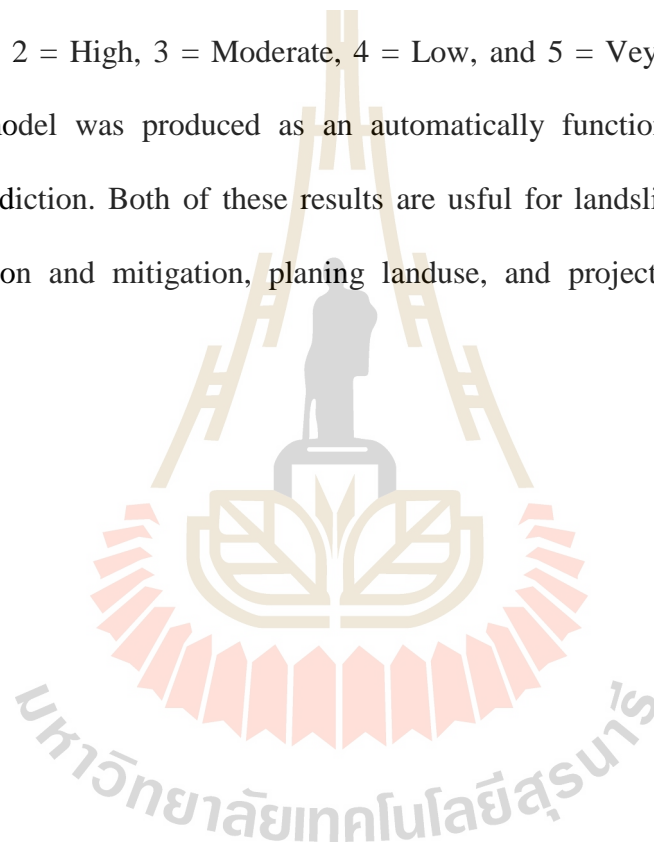
Having considered the relative importance of each factors, it can be seen that the two performance do not provide the same information. For example, soil type is ranked the highest on the basis of accoutability (96%), but has the lowest reliability value (1.36). However, lineament scores highly on both. The reason why the two measures give different results can be explained that within each catagory the landslides are not evently distributed but from clusters. For instant, the area where elevation A corresponded to landslide occurrence is particulary prone to landsliding. Bur such condition of high importance does not apply over most of the region. Therefore, it should consider their combined relationship for landslide analysis. Actually, the two factors are individually related to landsliding, then the two taken together should provide a better indicator. For example, elevation A accounts for 965 of all landslide but only 20% of the unit is corresponded to landslides. Slope B accounts for 68% of total landslides, but here 25% of the factor is responsible for landslides. The combination of elevation A and slope B accounts for 55% of the region's landslides and 45% of this catagory corresponds to landslides. Thus, the use of two combination of factors for the importance measure is considered to be more reliability.

5.2 Conclusions

This research has demonstrated that the considered factors have had a strong influence on the landslide occurrence in the study area. The method of probability analysis and the weights of evidence in conjunction with the application of GIS-

assisted indirect bi-variable evaluation techniques have applied for the landslide hazard analysis of the study area.

The landslide hazard map shows the high probability index for landslide incidence on the mountainous area of Wang Chin District. The higher the landslide probability index is the more instability of the slope. The landslide probability index map is grouped into five classes of hazard levels from very low to very high hazard (1 = Very high, 2 = High, 3 = Moderate, 4 = Low, and 5 = Very low). The landslide prediction model was produced as an automatically function of Band Math for landslide prediction. Both of these results are useful for landslide hazard prediction, risk prevention and mitigation, planning landuse, and project development in the future.



REFERENCES

- Abele, G. (1974). Bergsturze in den Alpen. Wiss. **Alpenvereinshefte No. 25, Munich (in German)**. Acres International Ltd. 1993. Greater Vancouver Regional District watershed ecological inventory pilot study. Quoted in Resources Inventory Committee. Government of British Columbia. (1996). Terrain stability mapping in British Columbia: A review and suggested methods for landslide hazard and risk mapping <http://srmwww.gov.ca/terrain/inventory/Stability/index.html>
- Agostina, V.D., and Marchi, L. (2001). Debrish flow magnitude in the Eastern italian Alps : Data collection and analysis. **Jour. Phys. Chem. Earth.** (C) 26 (9): 657-663.
- Akbar, T.A. (1998). Integration of GPS, GIS and remote sensing technology for landslide hazard analysis: A case study of western Himalayan Kaghan valley, Pakistan. **Master degree in engineering thesis**. Asian Institute of Technology. Bangkok. Thailand: 123 p.
- Aleotti, P., and Chowdhury. (1999). Landslide hazard assessmennt: Summary review and new perspectives. **Bull Eng Geol Env.** 58: pp. 21-44.
- Alfoldi, T. (1996). **Fundamentals of Remote Sensing**. Canada Centre for Remote Sensing. Natural Resources Canada. Ottawa. Canada. 258 p.
- Antoine, P. (1977). Reflexions sur la cartographie ZERMOS et bilan des experiences en cours. BRGM Bull, Sect III. 1-2 : 9-20. Quoted in Aleotti, P., and

- Chowdhury (1999). Landslide hazard assessment: Summary review and new perspectives. **Bull Eng Geol Env.** 58: pp. 21-44.
- BGR-DMR. (2001). Landslide risk map in Surat Thani Province. **Technical report.** Coastal Resources Institute. Prince of Songkla University. Songkla. Thailand: 77 p.
- Bonnard, C.H., Noverraz, F. (1984). Instability risk maps. **In proc. 4th Inter. Sym. on Landslides.** Toronto. Canada. J. Seychuk (editor). pp. 511-516.
- Bosi, C., Dramis, F., Gentili, B. (1982). Carte geomorfologiche di dettaglio e carte di stabilita: esempi nel territorio marcvhigiano. **Geol Appl ed Idrogeol.** 20: 53-62. Quoted in Aleotti, P., and Chowdhury. (1999). Landslide hazard assessment: Summary review and new perspectives. **Bull Eng Geol Env.** 58: pp. 21-44.
- Bunopas, S. (1981). Paleogeographic history of western Thailand and adjacent part of South-East Asia. A plate tectonics interpretation. **Geological Survey Paper., 5** (Spec. Iss.): 810 pp.
- By, R.A., Knippers, R.A., Sun Y., and Ellis, M.C. (2000). Principles of geographic information systems. **ITC Educational Textbooks.** International Institute for Aerospace Survey and Earth Sciences. Enschede. The Netherlands: 230 p.
- Carrara, A. (1983). Multivariate model for landslide hazard evaluation. **Mathematical Geology.** 15 (3): pp 403-427.
- Carrara, A., Cardinali, M., Detti, R., Guzzetti, F., Pasquol, V., and Reichenbach, P. (1991). GIS techniques and statistical models in evaluating landslide hazard. **Earth Surface processes and Landforms.** 16: 427-445.

- Carrara, A., Cardinali, M., Guzzetti, F., and Reichenbach, P. (1995). GIS technology in mapping landslide hazard. **Geographic Information Systems in Assessing Natural Hazards**. Kluwer, Dordrecht: pp. 125-175.
- Carrara, A., Merenda, L. (1976). Landslide inventory in northern Calabria, southern Italy. *Geological Society of America Bulletin*. 87: 1153-1162.
- Chadumrong, P., (1992). Stratigraphy, Sedimentology and Tectonic Setting of the Lampang Group, Central North Thailand. **Ph.D. Dissertation**, University of Tasmania, 230 p.
- Chang, K.T. (2000). **Introduction to geographic information systems**. Tata McGraw-Hill Publishing Company limited. New Delhi. India: 348 p.
- Charoenpravat, A. (1968). **Geology of Amphoe Wang Chin and Ban Bo Kaeo area**, with geologic maps 1:50,000, sheet 4944-I and 4964-I, Geological Survey Division., Department of Mineral Resources, Bangkok. (Unpubl. Map. And Rep.)
- Charoenpravat, A. Sripongpan, P., Thammadusadee, V. and Wolfart, R. (1987). **Geology of Amphoe Sop Prap (Sheet 1:50,000 No. 4844-I) and Amphoe Wang Chin (Sheet 1:50,000 No. 4944-IV)**, Thailand.
- Chung, C.F., Fabbri, A.G., Van Westen, C.J. (1995). Multivariate regression analysis for landslide hazard zonation. **Geographic Information Systems in Assessing Natural Hazards**. Kluwer, Dordrecht: pp. 107-133.
- Clerci, A., Perego, S., Tellini, C., and Vescovi, P. (2001). A procedure for landslide susceptibility zonation by conditional analysis method. **Journal of Geomorphology**. 48: 349-364.

- Cruden, D.M., Ematon, T.M. and Hu, X.Q. (1988). Rockslide hazard in Kananaskis Country, Alberta, Canada. **In Proc. 5th Inter. Sym. On Landslides**. C. Bonnard (editor). Lausanne, Switzerland. pp. 1147-1152.
- Cruden, D.M. (1991). A simple definition of a landslide. **Bulletin of the international Association of Engineering Geology**. 43: 27-29.
- Cruden, D.M. and Varnes, D.J. (1996). Landslide types and processes. In landslides investigation and mitigation. Transportation Research Board, US National Research Council, Turner, A.K. and Schuster, R.L. (editors). **Special Report 247**, Washington, DC 1996, Chapter 3, pp. 36-75.
- Dai, J.J., Lorenzato, S., and Rabe, D.M. (2004). A knowledge - based model of watershed assessment for sediment. **Journal of Environmental Modeling & Software**. 19: 423-433 pp.
- DeGraff, J.V., Canuti, P. (1988). Using isopleth mapping to evaluate landslide activity in relation to agricultural practices. **Bulletin of International Assoc. Engineering Geology**. 38: 61-71.
- DeGraff, J.V., Romesburg, H.C. (1984). Regional landslide susceptibility assessment for wildland management: a matrix approach. **In thresholds in geomorphology**. D.R. Coates and J. Vitak (editor). Allen and Unwin, Boston. pp. 401-414.
- Detley, D.N., Crick, W., Hart, A.B. (2000). **The use of satellite imagery in landslide studies in high mountain areas**. University of Durham. United Kingdom: 7 p.
- Donati, L., Turrini, M.C. (2002). An objective method to rank the importance of the Factors predisposing to landslide with the GIS methodology: Application to an

- area of the Apennines (Valnerina: Perugia, Italy). **Engineering Geology**. 63: 277-289.
- Fenti, V., Silvano, S., Soangna, V. (1979). Methodological proposal for engineering geomorphological map. Forecasting rock falls in the Alps. **Bull of the Int Assoc Eng Geol**. 19: 134-138. Quoted in Aleotti, P., and Chowdhury. (1999). Landslide hazard assessment: Summary review and new perspectives. **Bull Eng Geol Env**. 58: pp. 21-44.
- Fell, R. (1994). Landslide risk assessment and acceptable risk. **Geotech Journal**. 31: 261-272.
- Fotheringham, A.S., Brunston, C., and Charlton, M. (2000). **Quantitative geography: perspectives on spatial data analysis**. The Cromwell Press Ltd. Trowbridge. Wiltshire. Great Britain: 270 p.
- Gee, M.D. (1992). **Classification of hazard zonation methods and a test of predictive capability**. In Environmental planning and Geology, US Dept. of Housing and Urban Dev., Washington, DC.: pp. 154-169.
- Geoscience Australia. (2005). **Landslides**. http://www.ga.gov.au/urban/factsheets/landslide_causes.jsp
- Geoscience Australia. (2005). **Landslides – Slope processes**. http://www.ga.gov.au/Urban/factsheets/landslide_types_processes.jsp
- Geoscience Australia. (2005). **Landslide prone areas**. http://www.ga.gov.au/urban/Factsheets/landslide_areas.jsp
- Greenbaum, D. (1995). Project summary report: Rapid methods of landslide hazard mapping. **Technical Report WC/95/30**. International Division. British Geological Survey. Keyworth Nottingham. United Kingdom: 12 p.

- Greenbaum, D., Tutton, M., Bowker, M.R., Browne, T.J., Buleka, J., Grally, K.B., Kuna, G., McDonald, A.J.W., Marsh, S.H., Northmorre, K.J., O’Konnor. E.A., and Tragheim, D.G. (1995). Rapid methods of landslide hazard mapping : Papua New Guinea Case Study. **Technical Report WC/95/27 Overseas Geology Series**. Keyworth Nottingham. United Kingdom: 112 p.
- Guerricchio, A., Melidoro, G. (1979). Fenomeni franoci e neotetonici nelle argille grigio-azzurre calabriane di Pisticci (lucania). **Geol Appl e Idrogeol**. 14: 105-138. Quoted in Aleotti, P., and Chowdhury. (1999). Landslide hazard assessment: Summary review and new perspectives. **Bull Eng Geol Env**. 58: pp. 21-44.
- Günther, A. (2003). Slopemap: programs for automated mapping of geometrical and Kinematical properties of hard rock hill slopes. **Computers & Geosciences**. 29: pp. 865-875.
- Günther, A., Carstensen, A., and Pohl, W. (2003). The RSS-GIS (Rock Slope Stability GIS): **Tools for automated regional sliding-susceptibility assessments to hard-rock hill slope**. Institute for Geosciences. Technical University Braunschweig. Germany: 8 p.
- Günther, A., Carstensen, A., and Pohl, W. (2004). Automated sliding susceptibility mapping of rock slopes. **Natural Hazards and Earth System Sciences**. 4: pp. 95-102.
- Gupta, J., and Saha, A. (2001). Mapping debris flows in Himalayas. Natural resources management. **GIS development net**. 4 p.
- Gupta, P.R. (2002). **Remote Sensing geology**. 2nd Edition. Springer-Verlag Berlin Heidelberg New York, Germany.

- Hervas, J., Barredo, J., Pasuto, A., Montovani, F., and Silvano, S. (2003). Monitoring landslides from optical remotely sensed imagery: The case story of Tessina landslide, Italy. **Journal of Geomorphology**. 54. 63-75.
- Hick, B.G., and Smith, R.D. (1981). Management of steeplands impacts by landslide hazard zonation and risk evaluation. **Journal of Hydrology**. 20: 63-70.
- Howes, D.E. (1987). A terrain evaluation method for predicting terrain susceptible to post-logging landslide activity. **MOEP Technical Report 28**. Quoted in Resources Inventory Committee. Government of British Columbia. (1996). Terrain stability mapping in British Columbia: A review and suggested methods for landslide hazard and risk mapping. <http://srmwww.gov.bc.ca/terrain/inventory/Stability/index.html>
- Humbert, M. (1977). Risk mapping of area exposed to movements of soil and sub-soil: French “Zermos” maps **Bulletin of International Association of Engineering Geology**.16: 80-82.
- Ives, J.D., Messerli, B. (1981). Mountain hazard mapping in Nepal: Introduction to an Applied Mountain Research Project. **Mountain Research and Development**. 10: 185-212.
- Jibson, R.W., harp, E.L., and Michael, J.A. (1998). A method to produce probabilistic seismic landslide hazard maps. **Proceeding of International Association for Mathematical Geology 1998 Annual Meeting (IAMG'98)**. Ischia, Italy: pp. 35-51.
- John, A.R., and Jia X. (1999). **Remote Sensing digital image analysis-An introduction**. 3rd Edition. Springer-Verlag Berlin Heidelberg New York, Germany.

- John, R.D., Marry, R.J., and Leyton, R.L. (1999). Computer simulation of shallow landsliding in New Zealand hill country. **JAG**. 1. (2): 122-131.
- Kienholz, H. (1978). **Maps of Geomorphology and Natural Hazard of Griendewald. Switzerland**. Scale 1:10,000. Article and Alpime Research. 10: 169-184.
- Lee, S., Min, K. (2001). Statistic analysis of landslide susceptibility at Yougin Korea. **Journal of Environmental Geology**. 40: 1095-1113.
- Lee, S. (2004). Landslide hazard analysis using GIS and remote sensing. **Training Note**. Korea Institute of Geosciences and Mineral Resources (KIGAM). Korea: 194 p.
- Li, P., Zhou, Z., Li, Jianghai., Zhang, C., He, W., and Suh, M. (2003). Structural framework and its formation of the Kalpin thrust belt Tarim basin Northwest China from Landsat TM data. **International Journal of Remote Sensing**. 24 (18): 3535-3546.
- Lin, P.S., Lin, J.Y., Hung, H.C., and Yang, M.D. (2002). Assessing debris flow hazard in a watershed in Taiwan. **Engineering Geology**. 66: 295-313.
- Lincback Gritzner, M., Marcus, W., Aspinall, R., and Custer, S. (2001). Assessing landslide potential using GIS, soil wetness modeling and topographic attributes, Payette River, Idaho. **Geomorphology**. 37: 149-165.
- Lorente, A., Garcia-Ruiz, J., Begueria, S., and Arnaez. J. (2002). Factors explaining the spatial distribution of hillslope debris flows. **Mountain Research and Development**. 22: 32-39.

- Malczewski, J. (1999). GIS and multicriteria decision analysis. Department of Geography. University of Western Ontario. John Willey&Sons Inc. Canada: 392 p.
- Meneround, J.P., Calvino, A. (1976). **Carte ZERMOS, Zones Exposees a des Risques lies aux Mouvements. Region de la Moyenne Vesubie (Alpes Maritimes)**. Bureau de recherches Geologiques et Minieres, Orleans, France. Quoted in Aleotti, P., and Chowdhury. (1999). Landslide hazard assessment: Summary review and new perspectives. **Bull Eng Geol Env.** 58: pp. 21-44.
- Metternicht, G., Hurni, L., and Gogu, R. (2005). Remote sensing of landslides: An analysis of the potential contribution to geo-spatial systems for hazard assessment in mountainous environments. **Remote Sensing of Environment.** 98: pp. 284-303.
- Ministry of Energy, Mines and Petroleum Resources. (2005). **Landslide types** [On-line]. Available:<http://www.em.gov.bc.ca/Mining/Geolsurv/Surficial/landslide/ls2.html>
- Montavani, F., Soeters, R., and Westen, V., (1996). Remote sensing techniques for landslide studies and hazard zonation in Europe. **Journal of Geomorphology.** 15: pp. 213-225.
- Musaoglu, N., Kaya, S., Sekel, D.Z., Gokzel, C. (2002). A case study of using remote sensing data and GIS for land management: Cataca Region. **XXII FIG International Congress, April 19-23.** Washington DC. USA.
- Nationalatlas of the United States. (2005). **Landslide types and processes.** http://nationalatlas.gov/articles/geology/a_landslide.html

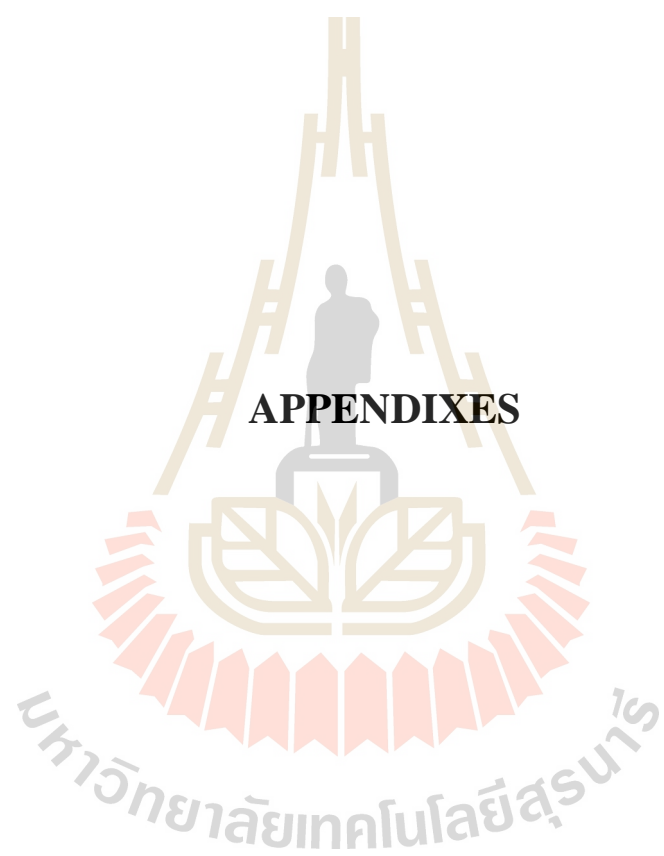
- Ngugen Quoc, P., Bui Hoang, B. (2004). Landslide hazard mapping using Bayesian approach in GIS: Case study in Yangsan area, Korea. **International Symposium on Geoinformatics for spatial Infrastructure Development in Earth and Allied Sciences**. Korea: 7 p.
- Nilaweera, N.S. (1994). Effects of tree roots on slope stability: The case of Khao Luang Mountain area, Southern Thailand. **Ph.D Dissertation**. Asian Institute of Technology. Bangkok. Thailand: 452 p.
- O'Loughlin, C.L. (1972). The stability of steepland forest soils in the Coast Mountains, southwestern British Columbia. **Ph.D Dissertation**. Department of Geology. University of British Columbia. Quoted in Resources Inventory Committee. Government of British Columbia. (1996). Terrain stability mapping in British Columbia: A review and suggested methods for landslide hazard and risk mapping. <http://srmwww.gov.bc.ca/terrain/inventory/Stability/index.html>
- Ostir, K., Veljanovski, T., Podobnikar, T., and Stancic, Z. (2003). Application of satellite remote sensing in natural hazard management: the Mount Mangart landslide case study. **International Journal of Remote Sensing**. 24 (20): 3983-4002.
- Pack, R.T. (1985). Multivariate analysis of landslide-related variables in Davis Conty, Utah. In delineation of landslide, Flash flood and debris flow hazards in Utha. Utah State University: pp. 50-58.
- Pantanahiran, W. (1994). The use of Landsat imagery and digital terrain models to assess and predict landslide activity in tropical areas. **Ph.D. Thesis**. University of Rhode Island. United State of America: 56 p.

- Patanakanog, B. (2001). **Landslide hazard potential area in 3 dimensions by remote sensing and GIS technique**. Land Development Department. Bangkok. Thailand: 5p.
- Piyasin, S. (1971). **Marine Triassic sediments of northern Thailand**. Newsl. Geol. Soc. Thailand, 4, 4-6, Bangkok.
- Piyasin, S. (1972). **Geological Map of Thailand**, 1:250,000, sheet Lampang (NE47-7), Bangkok.
- Piyasin, S. (1974). **Geological Map of Thailand**, 1:250,000, sheet Uttaradit (NE47-11), Bangkok.
- Rajbhandri, P.C.L. (1995). Application of GIS and remote sensing for landslide hazard zonation and mapping disaster prone area: A case study of the Kulekhari. **Ph.D Dissertation**. Asian Institute of Technology. Bangkok. Thailand: 136 p.
- Resources Inventory Committee. Government of British Columbia. (1996). **Terrain stability mapping in British Columbia: A review and suggested methods for landslide hazard and risk mapping**. <http://srmwww.gov.bc.ca/terrain/inventory/Stability/index.html>
- Rood, K.M. (1984). An aerial photograph inventory of the frequency of yield of mass wasting on the Queen Charlotte Islands, **Land Management Report No. 34**. Quoted in Resources Inventory Committee. Government of British Columbia. (1996). Terrain stability mapping in British Columbia: A review and suggested methods for landslide hazard and risk mapping. <http://srmwww.gov.bc.ca/terrain/inventory/Stability/index.html>

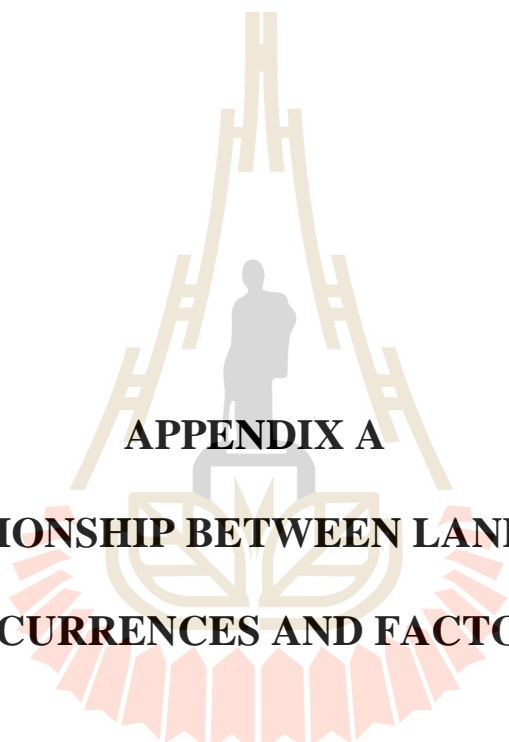
- Rupke, J., Cammeraat, E., Seijmonsbergen, A.C., Van Westen, C.J. (1988). Engineering geomorphology of Widentobel Catchment, Appenzell and Sankt Gallen, Switzerland: A geomorphological inventory system applied to geotechnical appraisal of slope stability. **Engineering Geology**. 26: 33-68.
- Sabin, FF. (1997) **Remote Sensing-Principles and interpretation**. 2nd Edition. Freeman, San Francisco, USA.
- Sarkar, S., Kanungo, D.P. (2004). An integrated approach for landslide susceptibility mapping using remote sensing and GIS. **Photogrammetric Engineering & Remote Sensing**. 70 (5): pp. 617-625.
- Schleiss, V.G. (1989). **Rogers Pass snow avalanche atlas**. Quoted in Resources Inventory Committee. Government of British Columbia. (1996). Terrain stability mapping in British Columbia: A review and suggested methods for landslide hazard and risk mapping. <http://srmwww.gov.bc.ca/terrain/inventory/Stability/index.html>
- Seker, D.Z., Altan, M.O., Duran, Z., Shrestha, M.B., Yuasa, A., Kawamura, K. (2004). **Producing landslide risk map of Sebinkarahisan by means of remote sensing and GIS techniques**. Civil Engineering Faculty, Istanbul University, Maslak, Istanbul, Turkey.
- Singhroy, V., and Molch, K. (2004). Characterizing and monitoring rockslides from SAR techniques. **Advances in Space Research**. 33: 290-295.
- Soeters, R., Van Westen, C.J. (1996). Slope stability: recognition, analysis and zonation. In: A.K. Turner, R.L. Shuster (editor) "Landslides: investigation and mitigation". **Transportation research Board - National Research Council, Special Report 247**: pp. 129-177.

- Sten, B. (1999). A digital elevation model for estimating flooding scenarios at the Falsterbo peninsular. **Journal of Environmental Modelling & Software**. 14: 579-587.
- Swanson, F.J., Janda, R.J., Dunne, T., and Swanston, D.N. (1982). Sediment budgets and routing in steep forested drainage basins. **Technical Report PNW-141**. Quoted in Resources Inventory Committee. Government of British Columbia. (1996). Terrain stability mapping in British Columbia: A review and suggested methods for landslide hazard and risk mapping. <http://srmwww.gov.bc.ca/terrain/inventory/Stability/index.html>
- Temesgen, B., Mohammed, M.U., and Korme, T. (2001). Natural hazard assessment using GIS and remote sensing methods with particular reference to the landslides in the Wondgenet area Ethiopia. **Journal of Phys. Chem. Earth (C)**. 26 (9):665-675.
- Thitisawarn, V. (2003). **Terrain characterization for landslide susceptibility analysis along Sillong-Silchen highway in northeastern India**. Geosciences division. Indian Institute of remote sensing. Dehra Dun. India: 66 p.
- Varnes, D.J. (1978). Slope movement types and processes. In landslide analysis and control. **Special Report 176** (Washington, DC.: transportation Research Board, 1978): pp. 12-33.
- Varnes, D.J. (1984). Landslide hazard zonation: A review of principles and practice, Natural hazard 3. **Commission on landslides of the IAGE**. UNESCO. Paris. France: 63 p.
- Van Westen, C.J. (1993). **Training Package for Geographic Information Systems in Slope Instability Zonation**. ITC-Publication n. 15. Part I. Enschede. The

- Netherlands. 245 p.
- Wang, S.Q. and Unwin, D.J., (1992). Modeling landslide distribution on loess soils in China: an investigation. **International journal of Geographic Information Systems**. 6-5: 319-405.
- Wang, S.Q. (2001). Landslide on natural terrain. **Journal of Mountain Research and Development**. 12: 40-47.
- Wright, R.H., cambell, R.H., and Nielsen, T.H. (1974). Preparation and use of isopleth maps of landslide deposits. **Geology**. 2: 483-485.
- Yamakawa, T. and Negishi, Y. (1998). OPS image processing II. **MMAJ-AOTS-MITI joint Seminar on Application of Satellite Image Analysis in Mineral Exploration in Tokyo, '98**. Mitsubishi Materials Natural Resources Development Corp. Tokyo. Japan. 213 p.
- Yamakuchi, Y., Tanaka, S., Odajima, T., Kamai, T., and Tsuchida, S. (2003). Detection of landslide movement as geometric missregistration in image matching of SPOT HRV data of two different dates. **International Journal of Remote Sensing**. 24. (18): 3523-3534.
- Zinck, A.J., and Lopez, J., Metternicht, G.I., Shrestha, D.P., and Vazques-Selem, L. (2001). Mapping and modeling mass movement and gullies in mountainous areas using remote sensing and GIS techniques. **JAG**. 3 (1): 43-53.
- Zomer, R., Ustin, S., and Ives, J., (2002). Using satellite remote sensing for DEM extraction in complex mountainous terrain : landscape analysis of the Makalu Barun National Park of Eastern Nepal. **International Journal of Remote Sensing**. 23 (1): 125-143.



APPENDIXES



APPENDIX A
RELATIONSHIP BETWEEN LANDSLIDE
OCCURRENCES AND FACTORS

มหาวิทยาลัยเทคโนโลยีสุรนารี

Table 1A. Landslide occurrence related with lithology.

Class	Lithologic Units	Area (Pixel)	% Area of Lithology (a)	Point of Landslide	% Point of Landslide (Ls)
1	Qt	78,464	7.79	20	1.23
2	Tr3	218,628	21.71	286	17.55
3	Qa	59,416	5.90	16	0.98
4	Pm2	16,071	1.60	4	0.24
5	CP	82,464	8.19	0	0.00
6	Pm3	4,814	0.48	0	0.00
7	Rht2	20,625	2.05	15	0.92
8	TR3-2	12,537	1.24	8	0.49
9	TR3-1	43,693	4.34	23	1.41
10	Rht1	155,054	15.39	250	15.34
11	TR3-3	8,386	0.83	22	1.35
12	Pm1	307,016	30.48	986	60.49
	Total	1,007,197	100	1630	100

Table 2A. Landslide occurrence related with distance from lineament.

Class	Dist. From Lineament	Area (Pixel)	% Area of distance from lineament (a)	Point of Landslide	% Point of Landslide (Ls)
1	Non Lineament	330,399	32.80	0	0.00
2	0-100	279,319	27.73	1194	73.57
3	100-200	157,361	15.62	342	20.67
4	200-300	75,499	7.50	56	3.49
5	300-400	45,219	4.49	22	1.35
6	400-500	31,431	3.13	7	0.44
7	500-600	24,235	2.41	1	0.06
8	600-700	19,579	1.94	3	0.18
9	700-800	16,844	1.67	2	0.12
10	800-900	14,516	1.44	1	0.06
11	900-1000	12,795	1.27	1	0.06
	Total	1,007,197	100	1,630	100

Table 3A. Landslide occurrence related with slope steepness.

Class	Slope Units	Area (Pixel)	% Area of Slope (a)	Point of Landslide	%Point of Landslide (Ls)
1	0-5	318,802	31.65	158	9.60
2	5-9	176,503	17.52	163	10.01
3	9-14	150,462	14.94	228	14.00
4	14-19	131,559	13.06	278	17.06
5	19-23	96,471	9.58	259	16.00
6	23-28	61,388	6.09	210	12.89
7	28-32	36,378	3.61	132	8.10
8	32-37	20,069	1.99	101	6.20
9	37-42	9,828	0.98	58	3.56
10	42-46	4,021	0.40	29	1.78
11	46-51	1,402	0.14	11	0.68
12	51-56	282	0.03	2	0.12
13	56-63	32	0.01	0	0
	Total	1,007,197	100	1,630	100

Table 4A. Landslide occurrence related with land use/land cover.

Class	Land use/Land cover Units	Area (Pixel)	% Area of Land use (a)	Point of Landslide	% Point of Landslide (Ls)
1	Open forest	340,760	33.83	1,114	68.34
2	Teak plantation	7,738	0.77	24	1.47
3	Crop_Orchard	11,197	1.11	0	0
4	Deforestation	263,316	26.14	187	11.47
5	Crop	14,642	1.45	2	0.13
6	Village	11,196	1.11	0	0
7	Rain paddy field	47,723	4.74	4	0.25
8	Teak_Crop	204,370	20.29	52	3.19
9	Water body	2,236	0.22	0	0
10	Orchard	112	0.02	0	0
11	Waste land	131	0.02	0	0
12	Teak_Orchard	5,183	0.51	0	0
13	Densely open forest	88,559	8.79	246	15.09
14	Reservoir	484	0.05	0	0
15	Deforestation_Orchard	9,604	0.95	1	0.06
	Total	1,007,197	100	1,630	100

Table 5A. Landslide occurrence related with NDVI.

Class	NDVI Units	Area (Pixel)	% Area of NDVI (a)	Point of Landslide	% Point of Landslide (Ls)
1	-1 to -0.75	84,686	8.41	28	1.72
2	-0.75 to -0.50	74,632	7.41	23	1.41
3	-0.50 to -0.25	92,132	9.15	23	1.41
4	-0.25 to 0.00	109,262	10.85	66	4.05
5	0.00 to 0.25	130,781	12.99	121	7.42
6	0.25 to 0.50	164,561	16.34	244	14.97
7	0.50 to 0.75	182,376	18.11	422	25.89
8	0.75 to 1.00	168,596	16.74	703	43.13
	Total	1,007,026	100	1,630	100

Table 6A. Landslide occurrence related with slope aspect.

Class	Aspect Units	Area (Pixel)	% Area of Aspect (a)	Point of Landslide	% Point of Landslide (Ls)
1	North	176,844	17.56	79	4.85
2	Northeast	129,765	12.88	209	12.82
3	East	138,709	13.77	427	26.20
4	Southeast	155,237	15.41	446	27.36
5	South	104,748	10.40	221	13.56
6	Southwest	90,234	8.96	134	8.22
7	West	87,485	8.69	64	3.93
8	Northwest	124,177	12.33	50	3.06
	Total	1,007,197	100	1630	100

Table 7A. Landslide occurrence related with soil type.

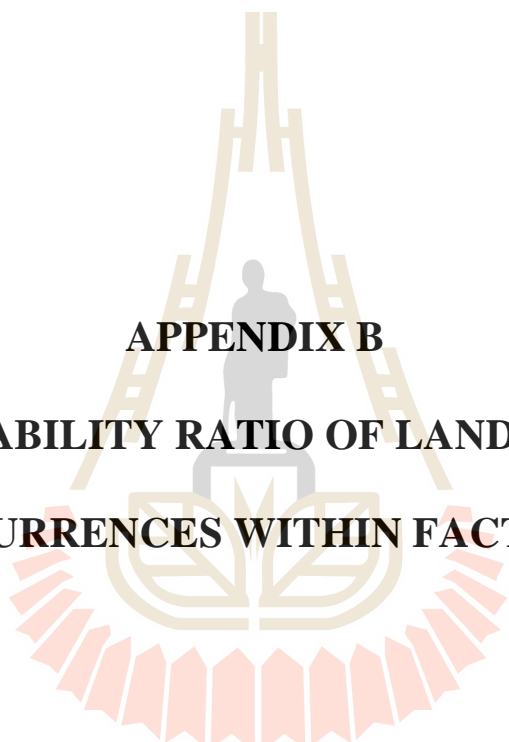
Class	Soil Units	Area (Pixel)	% Area of soil unit (a)	Point of Landslide	% Point of Landslide (Ls)
1	62	671,194	66.64	1,502	92.15
2	47E	3,354	0.33	3	0.18
3	47D/55C	2,453	0.24	0	0
4	47C	39,093	3.88	27	1.66
5	47B/29B	8,183	0.81	15	0.92
6	47B/55B	13,537	1.34	0	0
7	33	27,456	2.73	0	0
8	18/5	2,698	0.27	0	0
9	48C/55C	1,747	0.17	0	0
10	29B/46B	5,001	0.50	0	0
11	47D	13,403	1.33	2	0.12
12	35B/61B	4,302	0.43	1	0.06
13	48B	1,012	0.10	0	0
14	18	1,746	0.17	0	0
15	47B	86,904	8.63	22	1.35
16	18/18B	6,201	0.62	0	0
17	46B	6,444	0.64	0	0
18	59B(59)	423	0.04	0	0
19	15	31,468	3.13	0	0
20	55B/61B	2,371	0.24	0	0
21	59	3,076	0.31	2	0.12
22	47C/49C	871	0.09	0	0
23	47B/31B	1,544	0.15	0	0
24	7/15	13,798	1.37	0	0
25	47D/47E	7,886	0.78	2	0.12
26	47B/447C	8,189	0.81	4	0.25
27	7	3,054	0.30	0	0
28	47C/47D	27,609	2.74	45	2.77
29	47E/47D	2,113	0.21	0	0
30	33B	937	0.09	0	0
32	15/61B	1,251	0.12	2	0.12
33	15/59	1,056	0.10	0	0
34	59/61B	2,765	0.28	1	0.06
35	61B	552	0.06	2	0.12
36	15/33B	860	0.09	0	0
37	47C/55C	217	0.02	0	0
38	47B/56B	595	0.06	0	0
39	47D/56D	1,832	0.18	0	0
Total		1,007,204	100	1,630	100

Table 8A. Landslide occurrence related with flow direction.

Class	Flow_Direction Units	Area (Pixel)	% Area of Flow direction (a)	Point of Landslide	%Point of Landslide (Ls)
1	N to NE	177,578	17.63	324	19.88
2	NE to E	130,516	12.96	435	26.68
3	E to SE	167,091	16.58	400	24.54
4	SE to S	78,566	7.80	144	8.83
5	S to SW	120,132	11.93	90	5.52
6	SW to W	88,416	8.98	59	3.63
7	W to NW	142,094	14.11	70	4.29
8	NW to N	102,876	10.21	108	6.63
Total		1,007,197	100	1630	100

Table 9A. Landslide occurrence related with elevation.

Class	Elevation Units	Area (Pixel)	% Area of Elevation	Point of Landslide	% Point of Landslide
1	71-122	244,711	24.30	25	1.53
2	122-173	222,275	22.07	126	7.73
3	173-224	154,782	15.37	148	9.08
4	224-275	94,816	9.41	162	9.94
5	275-326	59,599	5.92	150	9.20
6	326-377	41,267	4.10	197	12.09
7	377-428	30,545	3.03	193	11.84
8	428-479	24,196	2.40	149	9.14
9	479-530	20,732	2.06	127	7.80
10	530-581	18,260	1.81	75	4.60
11	581-632	16,306	1.62	62	3.80
12	632-683	15,693	1.55	61	3.74
13	683-734	14,505	1.44	54	3.32
14	734-785	13,478	1.34	24	1.47
15	785-736	11,738	1.17	21	1.29
16	836-887	9,296	0.92	17	1.04
17	887-938	6,232	0.62	9	0.55
18	938-989	3,298	0.33	2	0.12
19	989-1040	1,880	0.19	6	0.37
20	1,040-1,091	1,240	0.12	2	0.12
21	1,091-1,142	629	0.06	2	0.12
22	1,142-1,193	312	0.03	6	0.37
23	1,193-1,244	244	0.02	2	0.12
24	1,244-1,295	208	0.02	1	0.06
25	1,295-1,346	166	0.02	1	0.06
26	1,346-1,397	189	0.02	4	0.25
27	1,397-1,448	324	0.03	4	0.25
28	1,448-1,499	259	0.023	0	0
29	1,499-1,550	58	0.006	0	0
30	1,550-1,602	13	0.001	0	0
Total		1,007,197	100	1630	100



APPENDIX B
PROBABILITY RATIO OF LANDSLIDE
OCCURRENCES WITHIN FACTORS

มหาวิทยาลัยเทคโนโลยีสุรนารี

Table 1B. Probability ratio of landslide occurrence within lithology.

Attribute	LithologicUnits	% Area of Lithology (a)	Point of Landslide	% Point of Landslide (Ls)	Ls/a=Pr (Probability Ratio)
1	Qt	7.79	20	1.23	0.16
2	Tr3	21.71	286	17.55	0.81
3	Qa	5.90	16	0.98	0.17
4	Pm2	1.60	4	0.24	0.15
5	SD	0.00	0	0.00	0.00
6	CP	8.19	0	0.00	0.00
7	Pm3	0.48	0	0.00	0.00
8	Rht2	2.05	15	0.92	0.45
9	TR3-2	1.24	8	0.49	0.40
10	TR3-1	4.34	23	1.41	0.32
11	Rht1	15.39	250	15.34	1.00
12	TR3-3	0.83	22	1.35	1.62
13	Pm1	30.48	986	60.49	1.98
	Total	100	1630	100	1

Table 2B. Probability ratio of landslide occurrence within buffered lineament.

Attribute	Dist. From Lineament	% Area of distance from lineament (a)	Point of Landslide	% Point of Landslide (Ls)	Ls/a=Pr (Probability ratio)
1	Non	32.80	0	0.00	0
2	0-100	27.73	1194	73.57	2.65
3	100-200	15.62	342	20.67	1.32
4	200-300	7.50	56	3.49	0.56
5	300-400	4.49	22	1.35	0.30
6	400-500	3.13	7	0.44	0.14
7	500-600	2.41	1	0.06	0.25
8	600-700	1.94	3	0.18	0.09
9	700-800	1.67	2	0.12	0.07
10	800-900	1.44	1	0.06	0.04
11	900-1000	1.27	1	0.06	0.05
	Total	100	1,630	100	1

Table 3B. Probability ratio of landslide occurrence within land use/land cover.

Attribute	Land use/Land cover Units	%Area of Landuse (a)	Point of Landslide	% Point of Landslide (Ls)	Ls/a=Pr (Probability ratio)
1	Disturbed open forest	33.83	1,114	68.34	2.02
2	Teak plantation	0.77	24	1.47	1.19
3	Crop_Orchard	1.11	0	0	0
4	Deforestation	26.14	187	11.47	0.44
5	Crop	1.45	2	0.13	0.09
6	Village	1.11	0	0	0
7	Rain paddy field	4.74	4	0.25	0.05
8	Teak_Crop	20.29	52	3.19	0.16
9	Water body	0.22	0	0	0
10	Orchard	0.02	0	0	0
11	Waste land	0.02	0	0	0
12	Teak_Orchard	0.51	0	0	0
13	Open forest	8.79	246	15.09	1.72
14	Reservoir	0.05	0	0	0
15	Deforestation_Orchard	0.95	1	0.06	0.06
	Total	100	1,630	100	1

Table 4B. Probability ratio of landslide occurrence within NDVI.

Class	NDVI Units	% Area of NDVI (a)	Point of Landslide	% Point of Landslide (Ls)	Ls/a=Pr (Probability ratio)
1	-1 to -0.75	8.41	28	1.72	0.20
2	-0.75 to -0.50	7.41	23	1.41	0.19
3	-0.50 to -0.25	9.15	23	1.41	0.15
4	-0.25 to 0.00	10.85	66	4.05	0.37
5	0.00 to 0.25	12.99	121	7.42	0.57
6	0.25 to 0.50	16.34	244	14.97	0.92
7	0.50 to 0.75	18.11	422	25.89	1.43
8	0.75 to 1.00	16.74	703	43.13	2.58
	Total	100	1,630	100	1

Table 5B. Probability ratio of landslide occurrence within land use/land cover.

Attribute	Slope Units	% Area of Slope (a)	Landslide (point)	%Point of Landslide (Ls)	Ls/a=Pr (Probability ratio)
1	0-5	31.65	158	9.60	0.09
2	5-9	17.52	163	10.01	0.57
3	9-14	14.94	228	14.00	0.94
4	14-19	13.06	278	17.06	1.31
5	19-23	9.58	259	16.00	1.67
6	23-28	6.09	210	12.89	2.11
7	28-32	3.61	132	8.10	2.24
8	32-37	1.99	134	8.22	4.13
9	37-42	0.98	58	3.56	3.62
10	42-46	0.40	29	1.78	4.45
11	46-51	0.14	0	0.00	0.00
12	51-56	0.03	0	0.00	0.00
13	56-63	0.01	0	0	0.00
	Total	100	1,630	100	1

Table 6B. Probability ratio of landslide occurrence within slope aspect.

Attribute	Aspect Units	% Area of Aspect (a)	Landslide (point)	% Point of Landslide (Ls)	Ls/a=Pr (Probability ratio)
1	North	17.56	79	4.85	0.28
2	Northeast	12.88	209	12.82	0.99
3	East	13.77	427	26.20	1.90
4	Southeast	15.41	446	27.36	1.78
5	South	10.40	221	13.56	1.30
6	Southwest	8.96	134	8.22	0.92
7	West	8.69	64	3.93	0.45
8	Northwest	12.33	50	3.06	0.25
	Total	100	1630	100	1

Table 7B. Probability ratio of landslide occurrence within flow direction.

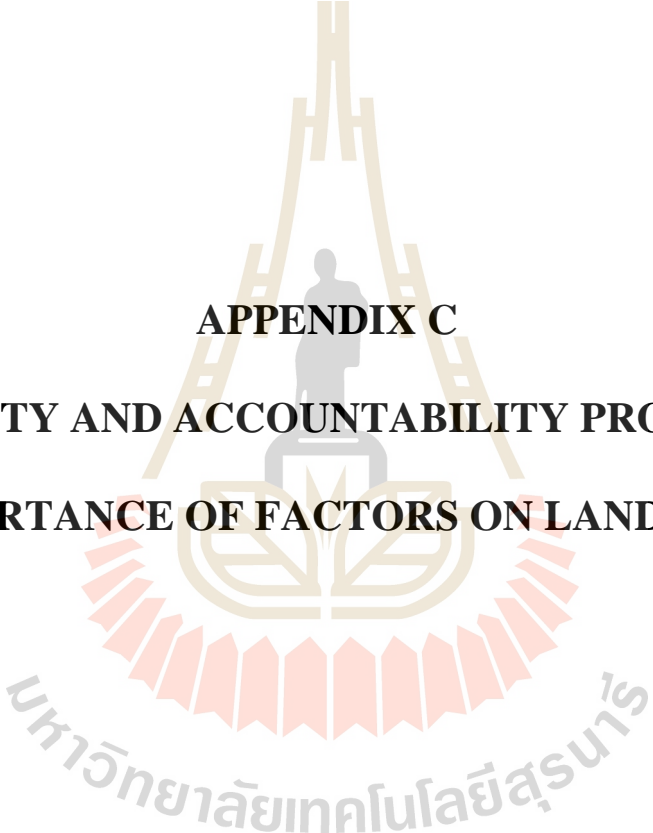
Attribute	Aspect Units	% Area of Aspect (a)	Landslide (point)	% Point of Landslide (Ls)	Ls/a=Pr (Probability ratio)
1	North	17.56	79	4.85	0.28
2	Northeast	12.88	209	12.82	0.99
3	East	13.77	427	26.20	1.90
4	Southeast	15.41	446	27.36	1.78
5	South	10.40	221	13.56	1.30
6	Southwest	8.96	134	8.22	0.92
7	West	8.69	64	3.93	0.45
8	Northwest	12.33	50	3.06	0.25
	Total	100	1630	100	1

Table 8B. Probability ratio of landslide occurrence within soil unit.

Attribute	Soil Units	% Area of soil unit (a)	Point of Landslide	% Point of Landslide (Ls)	Ls/a=Pr (Probability ratio)
1	62	66.64	1,502	92.15	1.38
2	47E	0.33	3	0.18	0.54
3	47D/55C	0.24	0	0	0
4	47C	3.88	27	1.66	0.43
5	47B/29B	0.81	15	0.92	1.14
6	47B/55B	1.34	0	0	0
7	33	2.73	0	0	0
8	18/5	0.27	0	0	0
9	48C/55C	0.17	0	0	0
10	29B/46B	0.50	0	0	0
11	47D	1.33	2	0.12	0.09
12	35B/61B	0.43	1	0.06	0.14
13	48B	0.10	0	0	0
14	18	0.17	0	0	0
15	47B	8.63	22	1.35	0.16
16	18/18B	0.62	0	0	0
17	46B	0.64	0	0	0
18	59B(59)	0.04	0	0	0
19	15	3.13	0	0	0
20	55B/61B	0.24	0	0	0
21	59	0.31	2	0.12	0.39
22	47C/49C	0.09	0	0	0
23	47B/31B	0.15	0	0	0
24	7/15	1.37	0	0	0
25	47D/47E	0.78	2	0.12	0.15
26	47B/447C	0.81	4	0.25	0.31
27	7	0.30	0	0	0
28	47C/47D	2.74	45	2.77	1.01
29	47E/47D	0.21	0	0	0
30	33B	0.09	0	0	0
32	15/61B	0.12	2	0.12	1
33	15/59	0.10	0	0	0
34	59/61B	0.28	1	0.06	0.21
35	61B	0.06	2	0.12	2
36	15/33B	0.09	0	0	0
37	47C/55C	0.02	0	0	0
38	47B/56B	0.06	0	0	0
39	47D/56D	0.18	0	0	0
	Total	100	1,630	100	1

Table 9B. Probability ratio of landslide occurrence within elevation.

Attribute	Elevation Units	% Area of Elevation	Point of Landslide	% Point of Landslide	Ls/a=Pr (Probability ratio)
1	71-122	24.30	25	1.53	0.06
2	122-173	22.07	126	7.73	0.35
3	173-224	15.37	148	9.08	0.59
4	224-275	9.41	162	9.94	1.06
5	275-326	5.92	150	9.20	1.55
6	326-377	4.10	197	12.09	2.95
7	377-428	3.03	193	11.84	3.91
8	428-479	2.40	149	9.14	3.81
9	479-530	2.06	127	7.80	3.77
10	530-581	1.81	75	4.60	2.54
11	581-632	1.62	62	3.80	2.35
12	632-683	1.55	61	3.74	2.41
13	683-734	1.44	54	3.32	2.31
14	734-785	1.34	24	1.47	1.10
15	785-736	1.17	21	1.29	1.10
16	836-887	0.92	17	1.04	1.13
17	887-938	0.62	9	0.55	0.89
18	938-989	0.33	2	0.12	0.36
19	989-1040	0.19	6	0.37	1.95
20	1,040-1,091	0.12	2	0.12	1.00
21	1,091-1,142	0.06	2	0.12	2.00
22	1,142-1,193	0.03	6	0.37	12.33
23	1,193-1,244	0.02	2	0.12	6.00
24	1,244-1,295	0.02	1	0.06	3.00
25	1,295-1,346	0.02	1	0.06	3.00
26	1,346-1,397	0.02	4	0.25	12.50
27	1,397-1,448	0.03	4	0.25	8.33
28	1,448-1,499	0.023	0	0	0
29	1,499-1,550	0.006	0	0	0
30	1,550-1,602	0.001	0	0	0
	Total	100	1630	100	1



APPENDIX C
RELIABILITY AND ACCOUNTABILITY PROBABILITY
OF IMPORTANCE OF FACTORS ON LANDSLIDING

มหาวิทยาลัยเทคโนโลยีสุรนารี

Table 1C. The reliability probability of lithology as a predictor of landsliding

Class	Lithologic units	Ls/a=Pr	% Point of Landslide	% Area of lithologic units	Reliability of lithology
1	Rht1	1.00	15.34	15.39	77.18/46.71
2	TR3-3	1.62	1.35	0.84	
3	Pm1	1.98	60.49	30.47	
Total			77.18	46.71	1.65

Table 2C. The reliability probability of slope aspect as a predictor of landsliding.

Class	Aspect unit	Ls/a=Pr	% Point of Landslide	% Area of Aspect unit	Reliability of Aspect
1	Northeast	1.00	12.82	12.88	79.94/52.46
2	East	1.90	26.20	13.77	
3	Southeast	1.78	27.36	15.41	
4	South	1.30	13.56	10.40	
Total			79.94	52.46	1.52

Table 3C. The reliability probability of land use as a predictor of landsliding.

Class	Land use unit	Ls/a=Pr	% Point of Landslide	% Area of Land use unit	Reliability of Land use
1	Open forest	2.02	68.34	33.83	84.90/43.39
2	Teak plantation	1.19	1.47	0.77	
3	Densely Open forest	1.72	15.09	8.79	
Total			84.9	43.39	1.96

Table 4C. The reliability probability of NDVI as a predictor of landsliding

Class	NDVI unit	Ls/a=Pr	% Point of Landslide	% Area of NDVI unit	Reliability of NDVI
1	0.50 to 0.75	1.43	25.89	18.11	69.02/34.85
2	0.75 to 1.00	2.58	43.13	16.74	
Total			69.02	34.85	1.98

Table 5C. The reliability probability of slope steepness as a predictor of landsliding.

Class	Slope unit	Ls/a=Pr	% Point of Landslide	% Area of Slope unit	Reliability of Slope
1	14-19	1.31	17.06	13.06	66.39/35.88
2	19-23	1.67	16.00	9.58	
3	23-28	2.11	12.89	6.09	
4	28-32	2.24	8.10	3.61	
5	32-37	4.13	8.22	1.99	
6	37-42	3.62	3.56	0.98	
7	42-46	4.45	1.78	0.4	
Total			66.39	35.88	1.85

Table 6C. The reliability probability of elevation as a predictor of landsliding.

Class	Elevation unit	Ls/a=Pr	% Point of Landslide	% Area of Elevation unit	Reliability of Elevation
1	224-275	1.06	9.94	9.41	80.88/36.38
2	275-326	1.55	9.20	5.92	
3	326-377	2.95	12.09	4.10	
4	377-428	3.91	11.84	3.03	
5	428-479	3.81	9.14	2.40	
6	479-530	3.77	7.80	2.06	
7	530-581	2.54	4.60	1.81	
8	581-632	2.35	3.80	1.62	
9	632-683	2.41	3.74	1.55	
10	683-734	2.31	3.31	1.44	
11	734-785	1.10	1.47	1.34	
12	785-836	1.10	1.29	1.17	
13	836-887	1.13	1.04	0.19	
Total			79.26	35.94	2.21

Table 7C. The reliability probability of soil type as a predictor of landsliding.

Class	Soil type unit	Ls/a=Pr	% Point of Landslide	% Area of Soil type unit	Reliability of Soil type
1	Unit 62	1.38	92.15	66.64	95.84/70.19
2	Unit47B/29B	1.14	0.92	0.81	
3	Unit47C/47D	1.01	2.77	2.74	
Total			96.08	70.37	1.36

Table 8C. The reliability probability of flow direction as a predictor of landsliding.

Class	Flow direction unit	Ls/a=Pr	% Point of Landslide	% Area of Flow direction unit	Reliability of Flow direction
1	N to NE	1.13	19.88	17.63	79.93/54.97
2	NE to E	2.06	26.68	12.96	
3	E to SE	1.48	24.54	16.58	
4	SE to S	1.13	8.83	7.80	
Total			79.93	54.97	1.45

Table 9C. The reliability probability of lineament as a predictor of landsliding.

Class	Dis_Lineament unit	Ls/a=Pr	% Point of Landslide	% Area Dis_lineament	Reliability of Dis_lineament
1	0-100	2.65	73.57	27.73	94.24/43.35
2	100-200	1.32	20.67	15.62	
Total			94.24	43.35	2.17

Table 10C. The accountability probability of lithology as a predictor of landsliding.

Attribute	Lithologic units	Ls/a=Pr	% Point of Landslide	% Total landslide of area	Accountability of lithology
1	Rht1	1.00	15.34	100	77.18/100
2	TR3-3	1.62	1.35		
3	Pm1	1.98	60.49		
Total			77.18		

Table 11C. The accountability probability of slope aspect as a predictor of landsliding.

Attribute	Aspect unit	Ls/a=Pr	% Point of Landslide	% Total landslide of area	Accountability of Aspect
1	Northeast	1.00	12.82	100	79.94/100
2	East	1.90	26.20		
3	Southeast	1.78	27.36		
4	South	1.30	13.56		
Total			79.94	0.80	

Table 12C. The accountability probability of land use/land cover as a predictor of landsliding.

Attribute	Land use unit	Ls/a=Pr	% Point of Landslide	% Total landslide of area	Accountability of Land use
1	Open forest	2.02	68.34	100	84.90/100
2	Teak plantation	1.19	1.47		
3	Densely Open forest	1.72	15.09		
Total			84.9		

Table 13C. The accountability probability of NDVI as a predictor of landsliding.

Attribute	NDVI unit	Ls/a=Pr	% Point of Landslide	% Total landslide of area	Accountability of NDVI
1	0.50 to 0.75	1.43	25.89	100	69.02/100
2	0.75 to 1.00	2.58	43.13		
Total			69.02		

Table 14C. The accountability probability of slope steepness as a predictor of landsliding.

Attribute	Slope unit	Ls/a=Pr	% Point of Landslide	% Total landslide of area	Accountability of Slope
1	14-19	1.31	17.06	100	67.61/100
2	19-23	1.67	16.00		
3	23-28	2.11	12.89		
4	28-32	2.24	8.10		
5	32-37	4.13	8.22		
6	37-42	3.62	3.56		
7	42-46	4.45	1.78		
Total			67.61	0.68	

Table 15C. The accountability probability of flow direction as a predictor of landsliding.

Attribute	Flow direction unit	Ls/a=Pr	% Point of Landslide	% Total landslide of area	Accountability of Flow direction
1	N to NE	1.13	19.88	100	79.93/100
2	NE to E	2.06	26.68		
3	E to SE	1.48	24.54		
4	SE to S	1.13	8.83		
Total		Total	79.93		0.80

Table 16C. The accountability probability of lineament as a predictor of landsliding.

Attribute	Dis_Lineament unit	Ls/a=Pr	% Point of Landslide	% Total landslide of area	Accountability of Dis_lineament
1	0-100	2.65	73.57	100	94.24/100
2	100-200	1.32	20.67		
Total		Total	94.24		0.94

Table 17C. The accountability probability of soil type as a predictor of landsliding.

Attribute	Soil type unit	Ls/a=Pr	% Point of Landslide	% Total landslide of area	Accountability of Soil type
1	Unit 62	1.38	92.15	100	95.84/100
2	Unit47B/29B	1.14	0.92		
3	Unit47C/47D	1.01	2.77		
Total		Total	95.84		0.96

Table 18C. The accountability probability of elevation as a predictor of landsliding.

Attribute	Elevation unit	Ls/a=Pr	% Point of Landslide	% Total landslide of area	Accountability of Elevation
1	224-275	1.06	9.94	100	79.26/100
2	275-326	1.55	9.20		
3	326-377	2.95	12.09		
4	377-428	3.91	11.84		
5	428-479	3.81	9.14		
6	479-530	3.77	7.80		
7	530-581	2.54	4.60		
8	581-632	2.35	3.80		
9	632-683	2.41	3.74		
10	683-734	2.31	3.31		
11	734-785	1.10	1.47		
12	785-836	1.10	1.29		
13	836-887	1.13	1.04		
Total		Total	79.26		0.79

BIOGRAPHY

Mrs. Suree Teerarungsigul was born in Singburi, Thailand on November 05, 1961. In 1981, she entered Faculty of Science, Khon Kaen University and decided to be majored in geology. After having degree of B.Sc. in 1984, she had worked in the field of groundwater mapping, for the Groundwater Division, Department of Mineral Resources during 1988 to 1990. In 1991, she had worked in the field of remote sensing and aerial photo interpretation for geological mapping with the Geological Survey Division, Department of Mineral Resources. Later on, she had decided to continue his post-graduate study leading to the Master Degree in the field of environmental geology at Chulalongkorn University and graduated in 2000. She joined a project with Thai-German technical cooperation project (DMR/BGR) during 2000 to 2002. Her interest is landslide assessment analysis using remote sensing, GIS technique and field geology as she has attended Ph.D. degree at Suranaree University of Technology.